Analysis of DOCK2 and SENP2 mutations on the immune system and CD8 T cell survival

Yan (Angela) Mei

A thesis submitted for the degree of Doctor of Philosophy of the Australian National University

Statement of declaration

The experimental work presented in this thesis constitutes original work by myself carried out at the John Curtin School of Medical Research under the supervision of Prof Chris Goodnow and Dr Edward Bertram unless otherwise stated in the methods, text or figures.

This thesis conforms to the Australian National University guidelines and regulations. The work contained within has not been submitted for the purpose of obtaining any other degree at this or other universities.

Yan (Angela) Mei

Professor Christopher Goodnow

Dr Edward Bertram

Associate Professor Anselm Enders

Acknowlegements

Professor Chris Goodnow: Thank you for giving me the opportunity to work on this project and your continual support, guidance and encouragement during my PhD. Thank you for sharing your tremendous wealth of knowledge with me. It has been an invaluable journey.

Dr Edward Bertram: Thank you for your time and patience, support and encouragement throughout my program.

Supervisory panel member - associate Professor Anselm Enders: Thank you for your assistance and helpful suggestions

All members of the Immunogenomics Laboratory, past and present: In particular I like to thank Lisa Miosge for her guidance and invaluable advice. Michelle Townsend, our lab manager, for keeping our lab running smoothly. I would like to acknowledge Debbie Howard for her help with all the bone marrow chimeras experiments. All technicians for their assistance.

Genotyping team and animal technicians at the Australian Phenomics Facility: for the effort in taking care and genotyping all the mice for this project

JCSMR resource team: Harpreet Vohra, Mick Devoy and Cathy Gillespie for their assistance with FACS machine and microscopes

My family and friends: for their understanding and support. Also, to Shunyi, a special thank you for your love, patience and support.

List of Abbreviations

α	alpha
APC	Allophycocyanin
APCs	antigen presenting cells
β	beta
Bim	Bcl-2 interaction molecule
Bcl-2	B-cell CLL/lymphoma 2
CD	cluster of differentiation
cDNA	complimentary deoxyribonucleic acid
CFSE	carboxylfluorecein succinamide ester
Cy	cyanine
DHR	Dock homology region
DN	double negative
DNA	deoxyribonucleic acid
Dock 2	dedicator of cytokinesis 2
Dock 8	dedicator of cytokinesis 8
DP	double positive
ELISA	enzyme linked immunoassay
ENU	N-ethyl N-nitrosurea
FACS	fluorescent activated cell sorting
FCS	fetal calf serum
FITC	fluorescein isothiocyannate
GEF	guanine exchange factor
GFP	green fluorescent protein
hnRNPs	heterogeneous nuclear ribonucleoproteins
Hnrpll	heterogeneous nuclear ribonucleoprotein L-like
IL-7/IL-7R	interleukin-7/interleukin-7 receptor
KO	knock-out
MFI	mean fluorescent intensity
MHC	major histocompatibility complex

MZ	marginal zone
NK	nature killer
NP	nucleoprotein
OVA	ovalbumin
PBS	phosphate buffered saline
PCR	polymerase chain reaction
PE	phycoerythrin
PerCP	peridinin chlorophyll protein
PI3K	phosphoinositide 3-kinase
PIP3	phosphatidylinositol (3,4,5)-triphosphate
PKC	protein kinase C
pri	primurus allele of *Dock8*
RAG	recombination activating gene
RBC	red blood cells
RNA	ribonucleic acid
Senp2	sentrin-specific protease 2
SP	single positive
TCR	T cell receptor
Tg	transgenic
thu	thunder allele of *Hnrpll*

Conference Presentations:

'The CD8 T cell deficiency in *Duan* mice' Australian Society for Immunology NSW/ACT Branch Retreat, Bowral, NSW, Australia, 2013 (Oral presentation).

Abstract

The discovery of genes essential for normal T cell numbers and T cell-mediated immune responses provides valuable insights into the adaptive immune system and targets for modulating disorders of immunity in cancer, transplantation, infection and autoimmunity. The studies presented in this thesis investigate two novel gene mutations that diminish the number of circulating T cells. The mutations were discovered by genome-wide ENU-mutagenesis in mice by flow cytometric screening of lymphocyte subsets in splenocytes and in peripheral blood. Genetic mapping and sequencing identified the two mutations. The first was a premature stop-gain mutation in *Dock2*, encoding a GTP exchange factor for the Rac family of cytoplasmic small G proteins, which has previously been found to be critical for T cells and immunity in mice and humans. The second mutation was a synonymous exonic nucleotide substitution in *Senp2*, encoding a specific protease for cleaving the ubiquitin-like SUMO protein from its conjugates with other proteins, whose critical role in T cells had not previously been shown.

Mice homozygous for the '*dockland'* E775X mutation in DOCK2 (*doc/doc*) had 80% fewer naïve ($CD44^{low}$) CD8 and CD4 T cells, 70% fewer NKT cells, 50% fewer B cells in the blood and 80% fewer B cells in the spleen, and absence of splenic marginal zone B cells. Mutant T cells nevertheless divided normally to anti-CD3 in vitro, consistent with intact TCR signaling, and peripheral $CD44^{high}$ activated memory T cells were present in normal or increased numbers consistent with homeostatic proliferation. Thymocytes showed evidence of developmental defects, including 50% decreased CD4+CD8+ double positive (DP) cells with lower CD5 expression and greatly decreased NKT cells. The percentage of CD4+ or CD8+ single positive (SP) thymocytes lacking CD69 was increased, consistent with delayed egress of fully mature cells. In competitive bone marrow transplantation experiments, mutant hematopoietic stem cells engrafted efficiently based on their contribution to granulocytes, but failed to contribute to peripheral T

cells due to progressive under-representation at the DP and SP thymocyte stages of development. Mutant B cells contributed poorly to the follicular and germinal centre subsets, and were completely absent from the marginal zone subset. These results establish that DOCK2 is essential within T and B lymphocytes.

Despite decreased circulating naïve T cells, *Dock2* mutant *doc/doc* mice exposed sequentially to H3N2 and H1N1 influenza viruses formed normal numbers of memory CD8 T cells binding H2-D^b MHC tetramers bearing the dominant influenza NP peptide epitope, NP366-374 (NP+), in contrast to *Dock8* mutant mice analysed in parallel which had greatly diminished memory T cells. Dock2 mutant mice nevertheless formed fewer NP-binding effector CD8 cells than wild-type at the peak of the primary and recall response. During acute lung infection with PR8-strain H1N1 influenza virus, Dock2 mutant mice were protected from weight loss and morbidity occurring between days 5 and 7 in wild-type mice. Mice with combined homozygous mutations in *Dock2* and Dock8 tended to have fewer circulating naïve T cells and NKT cells than either single mutant, although this did not achieve statistical significance in the cohort available. Collectively, these results extend earlier published findings in *Dock2* knockout mice, and provide new insights into the effects of DOCK2 deficiency on the anti-viral immune response that are relevant to the fatal infections and T cell lymphopenia in DOCK2-deficient children.

In the second mutant strain, *duan*, a 70% decrease selectively in circulating naïve CD8 T cells mapped as a recessive trait to a synonymous A>G substitution at Ch16:22,036,478 in exon 11 of *Senp2*. The mutation was +9 nucleotides from the exon 11 splice acceptor and diminished splicing of exon 10 to this acceptor. Of spliced mRNA that was produced, 55% skipped exon 11 to create an in-frame deletion of 15 amino acids. Upon expression of GFP-tagged SENP2, the internally deleted protein nevertheless exhibited normal intracellular localization to the nuclear membrane. While $Senp2^{-/-}$ null mutation in mice is homozygous lethal prior to blastocyst implantation, a complementation cross with the *duan* point mutant revealed that compound heterozygous $Senp2^{dua/-}$ mice were viable and

recapitulated the CD8 T cell deficiency of *Senp2*$^{dua/dua}$ homozygotes, confirming that partial deficiency of SENP2 causes a selective T cell deficit.

Thymic T cells subsets were unaffected in *Senp2*$^{dua/dua}$ mice, and the basis for the decreased number of naïve CD8 T cells was shown to be diminished survival in the periphery. This was most clearly shown by comparing the persistence of ovalbumin-specific OT-I CD8 T cells with normal or mutant *Senp2* after the T cells were "parked" in wild-type mice without antigenic stimulation. In this setting, mutant OT-I T cells transduced with a retroviral vector expressing wild-type SENP2 preferentially survived, further confirming that SENP2 deficiency was responsible. Competitive bone marrow transplantation also showed a cell autonomous requirement for normal splicing of *Senp2* to maintain peripheral CD8 T cell numbers but not for CD4 T cells or B cells. Upon sequential exposure to recombinant H3N2 and H1N1 influenza viruses expressing ovalbumin peptide, OT-I T cells bearing the *Senp2*$^{dua/dua}$ mutation formed an equally large population of effector CD8 T cells 7 days after primary or recall challenge, but persistence of memory CD8 T cells was decreased more than 90%. *Senp2* mutant CD8 T cells responded normally to CD3 stimulation *in vitro* as measured by cell division. They also responded normally to IL-7 *in vitro* as measured by STAT5 phosphorylation, despite a cell autonomous 25% decrease in IL7Rα/CD127 on their cell surface. Collectively, these results define a key role for controlling SUMO conjugation by SENP2 in the survival of naïve and memory CD8 T cells, apparently involving a pathway independent of the established TCR and IL-7 signalling mechanisms.

Table of Contents

Chapter 1: Introduction

Background

The immune system is important for eliminating pathogens and preventing diseases. The immune system consists of two arms: immunity and adaptive immunity. Innate immunity provides the first line of defense against infection and a hierarchy of support mechanisms for the acquired immune response. Macrophages, neutrophils, dendritic cells and NK cells all play important roles in this system. The adaptive immune system can induce antigen-specific immune response by recognizing antigens through specific receptors on lymphocytes. In addition, it also exhibits a 'memory' function enabling a rapid response when re-exposed to a previous encountered antigen. Lymphocytes are the cells involved in adaptive immunity they can be classified into T lymphocytes that express T cell receptors (TCRs) and B lymphocytes that express B cell receptors (BCRs). Both T and B lymphocytes arise in bone marrow, but unlike B cells which mature in the bone marrow and spleen, T cells migrate to the thymus gland to mature. T cells can be further divided to two subpopulations - T helper (Th) and T cytotoxic (Tc) cells, which can be distinguished from each other by the presence of either CD4 (Th cells) or CD8 (Tc cells) co-receptors on the cell surface. Th cells can be further delineated based on their cytokine profile (for example, Th1, Th2, Th17) and regulatory T cells (Treg's). This thesis focuses on T cells, mostly CD8 T cells, which have an astounding capacity to react to pathogens by differentiation into effector cells to clear the infection in the host.

T cell development

The immunological function of the thymus was first demonstrated in early 1960's, when skin grafts were not rejected in mice thymectomized at birth (Miller, 1961, 1962). Like other haematopoietic cells, T cells originate from haematopoietic stem cells (HSC) in bone marrow. Although T and B cells arise from the common lymphoid progenitors (CLPs), they have different maturation processes and develop in distinct locations. Unlike B cells that can mature in the bone marrow, T

cell progenitors are required to migrate to the thymus gland to undergo further maturation (Wu et al., 1991; Godfrey et al., 1993)

The thymus has two main regions: cortex and medulla. Immature cells mostly develop in the cortex and migrate to medulla when they become mature single-positive thymocytes. Thymic progenitors, after migrating to the thymus from the bone marrow, undergo differentiation to express a unique T-cell receptor (TCR). The TCR is a disulfide-bonded heterodimer of either TCRα (alpha) and TCRβ (beta) or TCR δ (delta) and TCR γ (gamma) chains expressed on the cell surface and noncovalently associated with the CD3 protein complex (Davis and Bjorkman, 1988). The T cells studied in this thesis are TCRαβ cells.

When progenitor cells enter the thymus, they don't express TCR, CD3, CD4 or CD8. The immature T cells start from the $CD4^-CD8^-$ double negative (DN) stage, progress to the $CD4^+CD8^+$ double positive (DP) stage and finally mature into $CD4^+CD8^-$ or $CD4^-CD8^+$ single positive (SP) T cells (Godfrey et al., 1993; Godfrey and Zlotnik, 1993; Shortman and Wu, 1996). The DN stage can be further divided to 4 different stages based on the expression of CD44 and CD25: DN1 ($CD25^-CD44^+$), DN2 ($CD25^+CD44^+$), DN3 ($CD25^+CD44^-$) and DN4 ($CD25^-CD44^-$) (Godfrey et al., 1993). The DN1 thymocytes (or early thymic precursor (ETP)) seed in thymus and lose their pluripotency to generate other cell lineages. In mouse, the DN1 population shows heterogeneity for Thy-1, HSA and c-kit expression. The cells in DN2 stage become physically larger (based upon forward scatter) and are $Thy\text{-}1^+$, HSA^+ and $c\text{-}kit^{hi}$ and start their D_β to J_β rearrangement in the T cell receptor β–chain locus (Godfrey et al., 1993). DN3 thymocytes are smaller than DN2 and become $c\text{-}kit^{lo}$ and continue V_β to DJ_β rearrangement. In DN4 stage, cells express the β-chain and have high expression in Thy-1, HSA but down-regulate c-kit. Notch-mediated signals delivered by binding of Delta ligands have been shown to promote both commitment to the T cell lineage and the early development of thymocytes (Radtke et al., 1999). IL-7 and the signals derived from cortical thymic epithelial cells (cTECs) are also indispensable to support the

initial thymocytes development (Peschon et al., 1994; Von Freeden-Jeffry et al., 1995).

The cells now enter CD4 and CD8 double-positive stage. These cells are required to go through positive and negative selection to become mature T cell. Only the DP thymocytes that can recognize self peptide-MHC molecule receive survival signal in a process named 'positive selection'. To allow self-tolerance, these cells also undergo negative selection to eliminate cells that have strong affinity for self antigens. Transcription factor Helios, an Ikaros family member, is preferentially expressed in regulatory T cells (Treg's). Its expression has been first suggested to discriminate thymic-derived from peripherally induced $Foxp3^+$ T regulatory cells (Thornton et al., 2010). Soon after, a study showed that Helios can also be peripherally induced in $Foxp3^+$ T cells (Gottschalk et al., 2012). Recently, Helios has been discovered to be a unique molecular marker to be induced in strongly self-reactive thymocytes and can qualitatively measure the thymocytes bearing strongly self-reactive TCR at two waves of thymic negative selection (Daley et al., 2013). Helios enhances induced Treg cell function in cooperation with FoxP3 (Takatori et al., 2015). Helios can control Treg-suppressive function, differentiation and survival in certain aspects (Sebastian et al., 2015). Thymocytes down-modulate CD4 or CD8 co-receptor molecules to commit to either the mature cytotoxic CD8SP or helper CD4SP T-cell lineages respectively. Zinc-finger transcription factor gene Th-POK (T helper inducing POZ/Kruppel factor or Zbhtb7) specific induced in developing class II-restricted thymocytes is a crucial regulator of CD4 lineage commitment (He et al., 2005; Kappes et al., 2006). RUNX (runt-related transcription factor) protein, particularly Runx3, is essential for the generation of cytotoxic T cell lineage. Runx3 and Th-POK forms a negative regulatory loop that regulate T-cell lineage commitment (Egawa, 2009; Collins et al., 2009). Only a small fraction of DP cells successfully proceed through positive and negative selection to become mature single-positive thymocytes ready to emigrate from the thymus and enter the circulation.

The maturation of thymic T cells also requires the expression of a CD4 or CD8 co-receptor. CD4 is a single-chain molecule consisting of four immunoglobulin-like extracellular domains, binding with low affinity to a nonpolymorphic part of MHC II molecules. CD8 is a disulfide linked α and β chain each consisting of a single immunoglobulin-like domain, binding with low affinity to a nonpolymorphic part of MHC I molecules (Babbitt et al., 1985). When a mature T cell binds to its specific peptide-MHC, the coreceptor CD4 or CD8 interacts with the lymphocyte-specific protein tyrosine kinase (Lck) through their cytoplasmic domain to initiate TCR signaling (Zamoyska et al., 2003; Salmond et al., 2009).

Adaptive immunity requires mature T-cells to exit from the thymus and travel between secondary lymphoid organs to survey for foreign antigens. Sphingosine-1-phosphate (S1P) and its receptor sphingosine 1-phosphate receptor-1 ($S1P_1$), a widely distributed G protein-coupled receptor, has been shown as the central mediator of lymphocyte egress from the thymus (Matloubian et al., 2004). Starting with studies using FTY720, an agonist ligand for $S1P_1$, $S1P_3$, $S1P_4$ and $S1P_5$ receptor (Brinkmann et al., 2002), the $S1P_1$ receptor has been shown to mediate and regulate lymphocyte recirculation and egress from the thymus and from secondary lymphoid organs (Matloubian et al., 2004). With T-cell specific deletion of $S1P_1$ receptor, the egress of mature T cell from thymus into periphery was blocked (Allende et al., 2004).

In transgenic overexpression studies, the cell surface activation marker CD69 has been shown to inhibit T cell egress from the thymus (Feng et al., 2002; Nakayama et al., 2002) Later, endogenous CD69 has been shown to inhibit the cell surface display and function of $S1P_1$ receptors in T and B cells (Shiow et al., 2006). By chemical agonism of S1P1 receptor, CD69 was down-modulated and thymic egress was inhibited (Alfonso et al., 2006).

By the end of their thymic development, newly mature CD4SP and CD8SP thymocytes need to lose the thymic putative retention signal CD69 and gain expression of the $S1P_1$ receptors, and respond to blood-borne chemotactic S1P to

promote them to exit the thymus and enter the periphery to encounter foreign antigens (Weinreich et al., 2009).

Peripheral survival of naïve CD8 T cells

It is important for an immunocompetent adult to maintain a constant number of T cells. Circulating T cell numbers remain remarkably fixed despite large changes of naïve T cell input from the thymus. In young animals, recent thymic emigrants make up a large proportion of the peripheral T cell population (Scollay et al., 1980). The T cell pool in adults is dependent on the division of mature T cells in the periphery. In an intact animal, the generation of new lymphocytes and the loss of cells are well balanced as the overall number of mature T cells is tightly regulated (Freitas and Rocha, 1993; Bell and Sparshott, 1997; Freitas and Rocha, 2000; Surh and Sprent, 2000; Sprent et al., 2008)

The newly matured CD8 T cells exiting the thymus are maintained in cell cycle interphase in the periphery for weeks or months (Jameson, 2002; Almeida et al., 2005; Surh and Sprent, 2008; Takada and Jameson, 2009). This long-lived pool of naïve CD8 T cells is regulated by a homeostatic mechanism governing their survival and proliferation depending upon the total number of peripheral T cells (Freitas and Rocha, 1993; Surh and Sprent, 2000). Survival of naïve $CD8^+$ T cells when there is a full complement of peripheral T cells, and proliferation of naïve cells in states of T-lymphopenia, depend upon signaling from the interaction of T-cell receptor (TCR) and self-peptide major histocompatibility complex (self-pMHC) as well as interleukin-7 (IL-7) binding to the IL-7 receptor (IL-7R), as summarized in more detail below.

TCR:MHC-peptide recognition in T cell survival

T cells recognize foreign antigen presented by MHC molecules during an immune response. Naive CD4 T cells require constitutive signalling from transient contact between TCRs and self-pMHC-II molecules (Takeda et al., 1996). Similarly, the adoptive transfer of naïve CD8 T cell into recipients with different or no MHC class I molecules caused the reduction in the number of donor cells. Naïve CD8 T cells were then shown to require interaction with host MHC molecule for long-term survival in periphery (Tanchot et al., 1997). More studies suggested that recognition of self-pMHC complex was required for naive T cells survival and homeostasis. (Kirberg, et al., 1997; Beutner and MacDonald, 1998; Kieper and Jameson, 1999; Nesic and Vukmanovic, 1998; Murali-krishna et al., 1999). However, comparable studies were more complicated for naïve CD4 T cells. As lymphopenic hosts were used in most of above studies, arguments were raised about the requirement of MHC complex in naïve T cell survival in lymphoreplete hosts. Some groups failed to found a role of MHC in naïve CD4 T cell survival (Dorfman et al., 2000; Grandjean et al., 2003; Clarke and Rudensky, 2000). More evidence has strongly supported the requirement of TCR signalling for naïve T cells survival. Abrogation of TCR expression or downstream molecules Fyn and Lck expression cause a survival defect in both CD4 and CD8 T cells (Labrecque et al., 2001; Polic et al., 2001; Seddon and Zamoyska, 2002). Unlike the polyclonal naïve T cell repertoire, there is no observation of competition for survival between TCR transgenic T cells (Kieper et al., 2004; Moses et al., 2003). The failure of survival when there was a high precursor frequency of one TCR clone further confirmed that the naïve T cell survival requires contacting self-pMHC ligands that are limiting (Hataye et al., 2006; Moon et al., 2007; Obar et al., 2008)

IL-7 signalling

IL-7 was originally discovered as a novel growth factor that stimulated proliferation of murine B cell progenitors *in vitro* (Namen et al., 1988). The murine IL-7 gene encodes a secreted protein of 154 amino acids produced by stromal cells in lymphoid organs. IL-7 was then shown to induce dramatic increases in the total number of T and B cells when administered to mice (Morrissey et al., 1991). In IL-7 transgenic mice, increased number of thymocytes and peripheral T lymphocytes were observed (Samaridis et al., 1991). IL-7 was first shown to be indispensible for murine B and T lymphopoiesis by injection of anti-IL-7 antibody (Grabstein et al., 1993) which was further affirmed by the severe peripheral and lymphoid organ lymphopenia phenotype in IL-7 knockout (-/-) mice (Von Freeden-jeffry et al., 1995). IL-7 was reported as a key factor for survival and persistence of naïve T cells in the periphery and the availability of IL-7 in the periphery determines the size of the naïve T cell pool (Boise et al., 1995; Vella et al., 1997; Rathmell et al., 2001, Schluns et al., 2000). IL-7 has also been shown to induce homeostatic expansion and restore the T cell homeostasis in a lymphopaenic environment by lymphopenia-induced proliferation (LIP) (Fry, T., et al., 2001; Tan et al., 2001; Surh and Sprent, 2008). In normal animals, naive T cells do not expand or proliferate due to restriction of cytokine and space. However, in T-cell-depleted hosts, increased availability of IL-7 could induce expansion of naïve T cells and restore the T cell homeostasis.

The IL-7 receptor consists of two subunits: the IL-7Rα chain (CD127) and the common γ chain (γ_c) (CD132) (Park et al., 1990; Noguchi et al., 1993). The common γ chain is also shared by receptors for IL-2, IL-4, IL-9, IL-15 and IL-21 (Takeshita et al., 1992; Kondo et al., 1993; Russell et al., 1993; Giri et al., 1994; Asao et al., 2001). Mice deficient in either IL-7Rα or γ_c chain displayed similar phenotypes of diminished total number of T cell and impaired lymphocyte development (Peschon et al., 1994; He and Malek, 1996; Cao et al., 1995; Di Santo and Rodewald, 1998). In humans, γ_c chain mutations result in X-linked severe combined immunodeficiency (SCID) with very few circulating T cells

(Noguchi et al., 1993). A similar T cell deficiency occurs in rare individuals with inactivating mutations in IL7RA (Puel, et al., 1998). In contrast to relatively constant level of IL-7, IL-7Rα expression is up and down during the development of both T and B cells. During thymopoiesis, IL-7Rα is highly expressed on DN stage, absent for DP stage but up again on thymocytes undergoing positive selection (Munitic et al., 2004; Mazzucchelli and Durum, 2007).

IL-7 signalling is transmitted through the intracellular portion of its cognate receptor IL-7R by inducing the tyrosine phosphorylation of downstream tyrosine kinases Janus kinase1 (JAK1) and JAK3 which are associated with CD127 and γ_c chain, respectively (Foxwell et al., 1995; Suzuki et al., 2000). The activated JAK proteins phosphorylate the cytoplasmic protein, Signal Transducer and Activator of Transcription 5 (STAT5), and the phosphorylated STAT5 forms heterodimers (STAT5a and STAT5b) and translocate into the nucleus to activate transcription (reviewed in Jiang et al., 2005). Mice deficient for both STAT5a and STAT5b have defective lymphoid development similar to IL-7R or Jak3 deficiency (Yao et al., 2006). JAK3 deficiency in humans also results in T-lymphopenia and SCID (Russell et al., 1995; Macchi et al., 1995) T cell specific deletion of STAT5 demonstrated that STAT5 was indispensible for naïve CD4 and CD8 T cell survival (Yao et al., 2006; Seki et al., 2007). Through these downstream signalling molecules and transcriptional factors, IL-7 maintains T cell survival by promoting the expression of anti-apoptotic B-cell lymphoma 2 (Bcl-2) family members BCL-2 and myeloid-cell leukaemia sequence 1 (MCL1) and redistributing the cell-death protein BCL-2-associated X (BAX) and BCL-2-antagonist of cell death (BAD) to inhibit the mitochondrial apoptotic pathway (Boise et al., 1995; Vella et al., 1997).

Combined blocking of IL-7R and TCR signalling results in more dramatic decline of T cell number than either single deficiency (Seddon and Zamoyska, 2002) raising the question whether they are distinct signals or additively to the same pathway. Recent studies have shown that there is co-operation between IL-7 and TCR signal in naïve CD8 T cells (Park et al., 2007). Signals from both IL-7

signalling pathway and self-peptide-MHC complex negatively feed back on their own receptor but promote the other receptor's expression (Park et al., 2007). In addition to inhibiting transcription of IL-7Ra, IL-7 signalling can transcriptionally enhance CD8α coreceptor expression and TCR-CD8 encounter with self-peptide-MHC complexes (Park et al., 2007). On the other hand, TCR signalling impairs IL-7 signalling and promotes the increase of *Il7ra* transcription (Park et al., 2007).

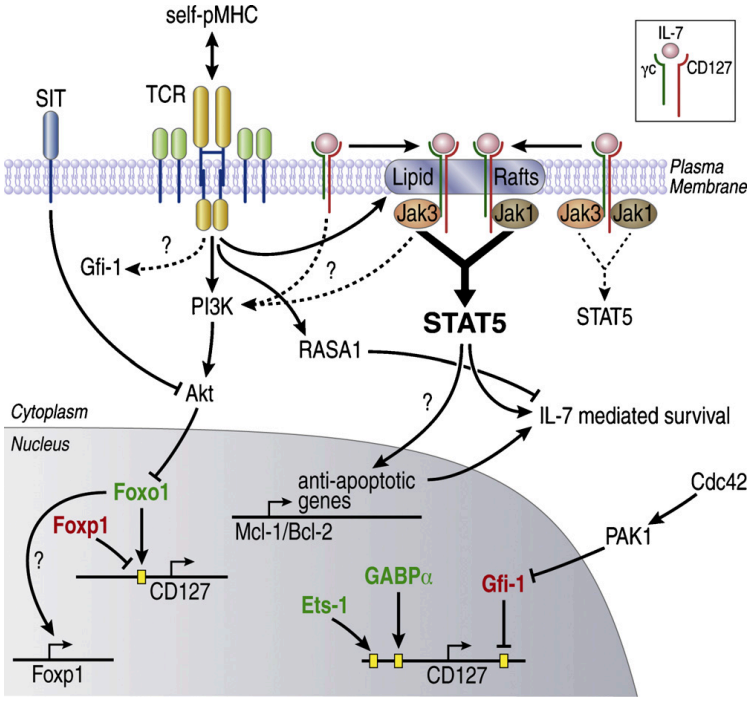

Figure 1. Cross-talk between TCR and IL-7 signaling. Survival of naïve CD8 T cells in the periphery requires signals from the interaction between TCR and self-peptide-MHC complex and IL-7 (Reprinted from Carrette and Surh, 2012). Transcription factors down streams of TCR that control CD127 expression: transcription factors inducing CD127 transcription (in green) and transcription factors repressing CD127 transcription (in red).

T cell activation

When naïve T cells encounter specific foreign antigen (Ag) presented by self-MHC on antigen presenting cells (APC), they are activated and start to proliferate. The first signal of cell activation comes from the binding of the TCR to its cognate peptide:MHC complex, Ag must be presented as short peptide fragments bound to MHC molecules on the surface of APC for T cell recognition (Townsend et al., 1985; Townsend et al., 1986). Cytotoxic CD8 T cells recognize peptides derived from protein in the cytosol and fragments of viral proteins on the surface by MHC-I molecules (human leukocyte antigen (HLA) in human) (Bjorkman et al., 1987a; Bjorkman et al., 1987b). CD4 T cells can recognize peptides derived from exogenous proteins processed within intracellular vesicles of macrophages and B cells presented by MHC-II molecules (Babbitt et al., 1985; reviewed by Unanue, 2002).

Proliferation is additively enhanced by costimulatory signals mediated by CD28 and CD86/CD80 and many other costimulatory receptors to prevent self attacking for a full activation (Gonzalo et al., 2001). Upon receiving TCR and co-stimulatory signals, a clone of progeny cells with same antigen specificity is generated and many of these differentiate into effector T cells. A memory commitment theory of sequential differentiation from naïve T cells to memory T cells was suggested in 1999 (Opferman et al., 1999). Opferman et al. proposed that naïve T cells activated by Ag stimulation differentiate into effectors and clear pathogens through clonal expansion. After clearance of Ag, most effector cells die (contraction phase) and only a tiny proportion of Ag specific cells survive to become long-lived memory T cells (Summarized in Figure 2).

Recent studies have reported that T cells require a third signal-inflammatory cytokines such as IL-2, IL-12, type I IFNs or IFN-γ for their optimal activation (Curtsinger et al., 1999; Kolumam et al., 2005; Cui et al., 2009). Therefore, signals from TCR, costimulation, and cytokines are critical for T cell activation

(Curtsinger et al., 1999; Zehn et al., 1999; Bertram, et al., 2004) and they can sum linearly to amplify the T cell response (Marchingo et al., 2014).

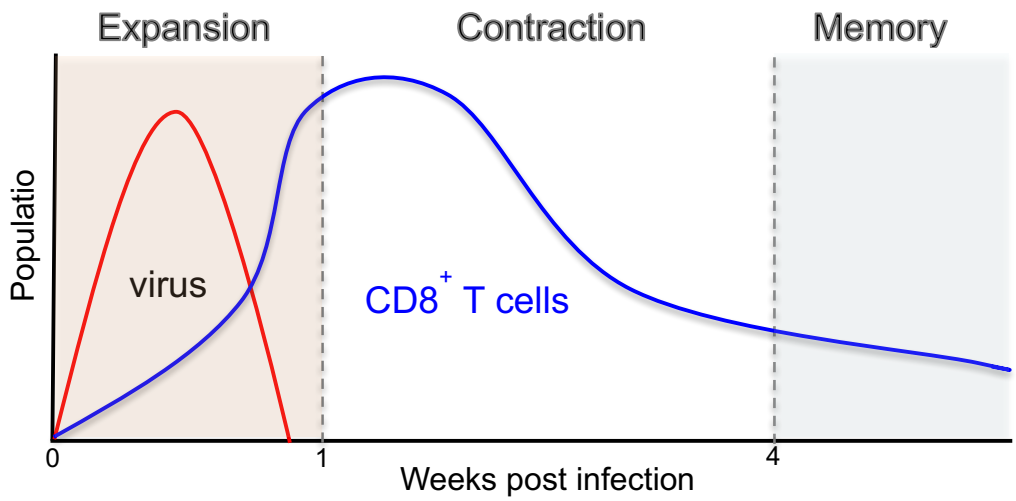

Figure 2: Kinetics of a CD8 T cell response. 1) Expansion phase: antigen specific CD8 T cells proliferation. 2) Contraction phase: most of effector CD8 T cells die after the elimination of pathogen. 3) Memory phase: a small population survive and differentiate to memory CD8 T cells.

Characteristics of T cell memory formation

After pathogen has been cleared, most of antigen-specific effector cells are eliminated by apoptosis. Only a tiny proportion of cells can survive and mature into long-term memory CD8 T cells (Lau et al., 1994; reviewed by Sprent and Surh, 2002). There are a number of different models to explain how effector T cells are selected to give rise to memory T cells. Effector CD8 T cells with increased expression of CD127, CD27 and Bcl-2 and decreased expression of killer cell lectin-like receptor G1 (KLRG1) were identified as early memory precursor cells in lymphocytic choriomeningitis virus (LCMV) infection experiments (Murali-Krishna, K. et al., 1998; Kaech, et al., 2003; Joshi et al., 2007; Joshi et al., 2008; Sarkar et al., 2008). However, these phenotypic markers

that defines the memory precursors at effector stages are not exclusive and the selection gets complicated with other studies (Croom et al., 2011; Obar et al., 2011).

Despite extensive heterogeneity, memory T cells can be broadly categorised into two functional subsets by surface markers CCR7 and CD62L (Sallusto, F.et al., 1999). Central memory T cells (T_{CM}) express CCR7 and CD62L ($CD62L^{hi}CCR7^{hi}$) and have homing receptors to secondary lymphoid organs and bone marrow (Mazo et al., 2005; Sallusto et al., 1999; Kaech and Wherry, 2007). On the other hand, effector memory T cells (T_{EM}) that do not express CCR7 ($CD62L^{low}CCR7^{low}$) are normally found in non-lymphoid tissues and can enter to inflamed tissue to have immediate effector functions (Masopust et al., 2001; Sallusto et al., 1999; Kaech and Wherry, 2007). T_{CM} lack immediate effector functions but they are sensitive to TCR simulation to mount a robust recall response and produce IL-2 after priming (Sallusto et al., 2004; Jameson and Masopust, 2009). T_{EM} have effector functions and can produce cytotoxic proteins (Sallusto et al., 1999; Kaech and Wherry, 2007). Although T_{CM} and T_{EM} have different locations and functional properties, there is evidence that they could interconvert to each other (Kaech and Wherry, 2007; Bouneaud et al., 2005; Wherry and Ahmed, 2004).

In addition, a third subset of memory T cells has been characterized as $CD103^{hi}CD69^{hi}CD27^{low}$ referred as tissue-resident memory T (T_{RM}) cells (Masopust et al., 2001; Gebhardt et al., 2009; Sheridan and Lefrancois, 2011; Carbone, 2015). These nonrecirculating tissue-resident memory T cells provide protective local immunity against pathogen (Gebhardt et al., 2009; Carbone, 2015).

There are more accumulating data showing that ‘Memory-like phenotype’ CD8 T cells can also rise without effector differentiation when naïve T cells are adoptively transferred into lymphopenic hosts through a process named homeostatic-driven proliferation (Goldrath et al., 2000). In this process, excess availability of self-pMHC and IL-7 induce naïve T cells to quickly undergo

homeostatic expansion and acquire phenotypes and functional characteristics similar to memory T cells (Goldrath et al., 2000; Schluns et al., 2000; Tan et al, 2001). This process was appropriated named as lymphopenia-induced proliferation (Min et al., 2003) and is dependent on MHC or IL-7 (Ernst et al., 1999; Goldrath and Bevan, 1999; Schluns et al., 2000; Tan et al., 2001). These homeostatic proliferation memory T cells display similar memory phenotypic markers as antigen-driven memory cells (Jameson, 2005; Surh and Sprent, 2005; Goldrath et al., 2000). Like antigen-specific memory T cells, homeostatic proliferation memory T cells display rapid proliferative response and enhanced cytotoxic function, and increased effector cytokine production compared with naïve T cells (Jameson, 2005; Surh and Sprent, 2005; Goldrath et al., 2000). Haluszczak et al demonstrated the existence of memory-like T cells in nonimmunized animal which are termed 'virtual memory' (VM) to describe this antigen-specific T cells within the unprimed T cell population (Haluszczak et al., 2009)

Homeostasis of memory CD8 T cell

The survival signals required by memory CD4 and CD8 T cells are still under investigation. Unlike naïve T cells, antigen and MHC molecules are not essential to sustain both CD4 and CD8 T cells (Surh and Sprent, 2005). It has been shown that the expression of common γ chain is not required for the survival of memory CD4 T cells (Lantz et al., 2000). However, IL-7 is essential to support the survival of CD4 T memory cells (Seddon et al., 2003).

The survival of memory CD8 T cells is antigen-independent and is dependent on the cytokines IL-7 and IL-15 (Surh and Sprent, 2008). IL-7 is not necessary for antigen-induced expansion of CD8 T cells but is critical for generation of T cell memory (Schluns et al., 2000). In IL-7R$^{-/-}$ CD8 T cells, they have normal activation but are poor producer of memory CD8 T cells (Schluns et al., 2002). Selective expression of the IL-7Rα identifies the effector CD8 T cells that will

differentiate into memory T cell after infection or immunization (Kaech et al., 2003). However, Hand et al., suggested that constitutive IL-7Rα expression has minimal effect the formation of memory CD8 T cell and is not sufficient to promote memory CD8 T cell development (Hand et al., 2007). These results implied that the generation and maintenance of memory CD8 T cells is a complicated process involving various cytokines and pathways. Memory CD8 T cells can also be formed in the absence of IL-7 suggesting that the precursor of memory CD8 T cells are not dependent on the interaction of IL-7/IL-7Rα interaction (Klonowski et al., 2006).

IL-15 together with IL-2, IL-4, IL-7, IL-9, and IL-21 stimulate receptors that all contain a common γ receptor subunit (Takeshita et al., 1992; Kondo et al., 1993; Russell et al., 1993; Giri et al., 1994; Asao et al., 2001). However, unlike other γ_C family members, IL-15 is presented on the cell surface and tightly bound to IL-15Rα chain to induce signalling at the contact site between APC and CD8 T or Natural Killer (NK) cells (Reviewed by Ma et al., 2006). IL-15 can bind to the IL-2/IL-15Rβ complex to mediate a response without IL-15Rα and this binding affinity is not further augment by IL-15Rα (Giri et al., 1994; Giri et al., 1995; Anderson et al., 1995). The IL-15 receptors are heterotrimeric and contain the γ_C, IL-2/IL-15Rβ (CD122) and IL-15Rα chain (Grabstein et al., 1994; Giri et al., 1995). The up-regulation of IL-15Rα expression on effector CD8 T cells and sustaining of expression on memory CD8 T cells suggested that IL-15 is crucial for the generation and maintenance of memory CD8 T cells (Schluns et al., 2002). IL-15 has been first reported to have an important role in stimulating proliferation of memory CD8 T cells (Zhang et al., 1998). By studying IL-15 transgenic and deficient mice, IL-15 has been shown to be essential in survival and homeostatic proliferation of memory CD8 T cells. The generation of antigen specific memory CD8 T cells was impaired in IL-15 deficient mice and it correlated with decreased turnover in memory CD8 T cells (Schluns et al., 2002). Moreover, overexpression of IL-15 leads to increase persistence of antigen-specific CD8 T cells by preventing apoptosis during contraction phase of primary infection (Yajima et al., 2002; Yajima et al., 2006).

Following the previous discussion, both IL-7 and IL-15 are important for memory CD8 T cells homeostasis. IL-7 is important for memory CD8 T cell survival, whereas basal homeostatic proliferation is largely depended on IL-15. Memory CD8 cells can utilize either IL-7 or IL-15 to undergo homeostatic proliferation, however, homeostatic proliferation fails to occur in the absence of both IL-7 and IL-15. (Tan et al., 2002). Kieper et al. demonstrated that normal memory precursor CD8 T cell number can be observed in the absence of IL-15 by overexpression of IL-7 using IL-7 TG mice (Schluns et al., 2000; Kieper et al., 2002). Lymphopenia-induced proliferation of memory phenotype CD8 T cells was induced by excess amounts of IL-7 in lymphopenic mice with absence of IL-15 (Goldrath, et al., 2002; Tan, et al., 2002). Antigen-specific CD8 T cells failed to undergo proliferative renewal and disappeared after infection in IL-$15^{-/-}$ mice (Becker et al., 2002). Therefore, IL-15 is required for homeostatic proliferation (Becker et al., 2002). In conclusion, long-term survival of memory CD8 T cells is dependent and regulated by both IL-7 and IL-15 with different roles supporting survival and inducing homeostatic renewal, respectively.

Other factors or cytokines also contribute to the long lifespan of memory CD8 T cells. Autophagy is an intracellular degradation system that delivers cytosolic contents to the lysosome for cell degradation. Autophagy has been shown to dynamically regulate the survival of effector CD8 T cells and formation of memory T cells during LCMV infection in mice (Xu et al., 2014). The IL-10/IL-21/STAT3 pathway has also been shown to be critical for the differentiation of virus-specific CD8 T cells to memory T cells in mice with acute LCMV infection (Cui et al., 2011). Consistent with the mouse findings, STAT3 has also been suggested to play a critical role in formation of human T cell memory and control of some chronic viruses (Siegel et al., 2011). Recently, IL-7 was discovered to induce glycerol channel aquaporin 9 (AQP9) expression which has an important role in supporting glycerol import for triglyceride (TAG) synthesis and storage in memory CD8 T cells (Cui et al., 2015). This study uncovers new mechanisms of memory CD8 T cells metabolism in long-term survival.

Thesis aims

In this thesis, I analyse two mouse strains discovered by ENU-mutagenesis, with mutations in *Dock2* and *Senp2* named '*dockland*' and '*duan*', respectively, to define the role of these genes in the immune system. *Dockland* was identified through a splenocyte screen and *duan* was identified through a peripheral blood screen and both strains were analyzed by flow cytometry.

The aim of *dockland* strain:

To characterize the cellular phenotype of the *dockland* mice

To map and identify the ENU variant gene responsible for the T cell lymphopenia

The aim of *duan* strain:

To characterize the cellular phenotype of the *duan* mice

To map and identify the ENU variant gene responsible for the loss of peripheral CD8 T cell

To investigate the effect of the Duan *Senp2* mutation on T cell homeostasis in vivo

Chapter 2: Mice, materials and methods

2.1 Mice and procedures

2.1.1 Mice

All mice used for this work were housed in specific pathogen-free conditions. All procedures were approved by the Australian National University Animal Ethics and Experimentation Committee.

The following mouse strains were used for the work detailed in this thesis:

C57BL/6: in-bred mouse strain originally obtained from the Jackson Laboratory.

C57BL/6.SJL-CD45.1: C57BL/6 strain congenic for CD45.1 derived from the SJL/J mouse strain

CBA.H: in-bred mouse strain

Dockland (*Dock2*$^{doc/doc}$): ENU-derived mouse strain carrying a missense mutation in *Dock2* gene on the C57BL/6 background. This allele was nicknamed '*dockland'* (*doc*).

Duan (*Senp2*$^{dua/dua}$): ENU-derived mouse strain carrying a missense mutation in *Senp2* gene on the C57BL/6 background. This allele was nicknamed '*duan*' (*dua*).

Senp2 knockout mice (Chiu et al, 2008) were obtained from RIKEN BioResource Center.

OT-I: Transgenic mouse strain produced on the C57BL/6 background expressing T cell receptor that recognises the OVA peptide SIINFEKL in association with MHC I protein H-2K^{b} (Hogquist et al., 1994).

Primurus (*Dock8*$^{pri/pri}$): ENU-derived mouse strain carrying a missense mutation in *Dock8* gene on the C57BL/6 background (Randall et al., 2009). This allele was nicknamed '*primurus*' (*pri*).

Thunder (*HnRNPLL*$^{thu/thu}$): ENU-derived mouse strain carrying a missense mutation in *Hnrpll* gene on the C57BL/6 background (Wu et al., 2008). This allele was nicknamed '*thunder*' (*Thu*).

Rag1-/-: This strain, B6.129-*Rag1*^{tm1Mom}, lacks all B and T cells (Mombaerts et al., 1992) and was originally obtained from the Animal Resources Centre, Canning Vale, Western Australia, and maintained as a breeding colony at the Australian Phenomics Facility.

2.1.2 Procedures

2.1.2.1 ENU mutagenesis and breeding strategy

100mg/kg ENU was injected into the intraperitoneal cavity to male C57BL/6 mice (Generation (G) 0) 3 times 1 week apart. These male mice were then used to start pedigrees by crossing to wild-type female C57BL/6 mice and inter-crossing their G 1 offspring.

2.1.2.2 Bone marrow chimeras

To test whether cellular phenotypes were of hematopoietic origin and cell intrinsic, bone marrow chimeras were generated by irradiating B6.SJL-CD45.1 mice or *Rag1*$^{-/-}$ mice with 10 Gy and reconstituting with $2x10^6$ donor bone marrow cells (50:50 mixture of wild-type (WT) B6.SJL-CD45.1 bone marrow and either mutant or WT B6 (CD45.2) bone marrow) or 100% mutant or WT (CD45.2). The recipient mice were analysed 8-10 weeks post reconstitution.

2.2 In vitro cell stimulation assays

2.2.1 Buffers and reagents

Sample collection media	RPMI 1640 (GibcoBRL) HI-FCS (sigma) 10% (v/v)
Complete cell culture media (cRPMI)	RPMI 1640 (GibcoBRL) HI-FCS (sigma) 10% (v/v) 10 mM HEPES, pH7.4 (GibcoBRL) 1 mM sodium pyruvate (sigma) 50uM beta-mercaptoethanol (GibcoBRL) 0.1 mM non-essential amino-acid solution (GibcoBRL) 10mL L-glutamate and penicillin/streptomycin (GibcoBRL)

2.2.2 Proliferation and overnight activation

Proliferation and overnight activation of 2 x 10^6 lymphocytes was carried out in 200uL complete media and stimulated with 5μg/mL anti-CD3 (0.5 mg/mL, clone: 500A2, BD pharmingen) and 5μg/mL anti-CD28 (0.5mg/mL, clone: 37.51, BD pharmingen).

2.2.3 IL-7 stimulation

Splenocytes were resuspended in cRPMI at room temperature. 2 x10^6 cells (50:50 mixtures of wild-type and mutant cells) were cultured in 1mL complete medium with 1μg/mL IL-7 (407-ML-005, R&D systems) at 37°C overnight.

2.3 Flow cytometry

2.3.1 Buffers and reagents

FACS wash	2 L phosphate buffer saline (PBS) 50 ml bovine serum albumin 2.5% (v/v) 20 ml sodium azide 1% (v/v)
Red blood cell (RBC) lysis buffer (10X) (pH 7.3)	8.99 g ammonium chloride 1 g potassium bicarbonate 37 mg EDTA 100 mL H_2O

2.3.2 Preparation of cells

100-200 µL blood samples were collected from the retro-orbital sinus of mice into tubes containing 10-20ul heparin or EDTA. 50 µL of anti-coagulated blood was lysed with 200µL red blood cell (RBC) lysis buffer (made up to 1X with dH_2O and adjusted pH to 7). After 5 minute incubation at room temperature, the lysed cells were centrifuged for 4 minutes at 1240 rpm at 12°C. The supernatant was discarded by flicking the plate and the pellets were resuspended in 200 µL RBC lysis buffer. The incubation and centrifugation steps were repeated. The pellet was washed twice with ice cold 200 µL FACS buffer and kept on ice.

Mouse spleen and thymus were collected in 5 mL of RPMI1640 + 10 % FCS. Bone marrow cells were flushed from tibias and femurs in 3 mL of RPMI1640 + 10 % FCS. Single cell suspensions of splenocytes, thymocytes and bone marrow cells were prepared by passing through a cell strainer and kept on ice. Cells were pelleted by centrifugation for 4 minutes at 1340 rpm at 4°C. Splenocytes were

lysed with RBC lysis buffer for 5 minutes and washed twice with 5mL RPMI1640 + 10% FCS.

2.3.3 Surface staining of lymphocytes

2 x 10^6 cells were added into each well of 96-well round-bottom plate (Nunc). 40 µL of a cocktail of premixed fluorochrome-conjugated antibodies (Table 2) was added to each well and incubated at 4°C for 30 minutes in the dark. After incubation, the cells were washed twice with FACS buffer and resuspended in 70 µL FACS buffer and transferred into cluster tubes. The samples were analysed on LSR II flow cytometer (BD Biosciences).

Table 2.: Antibodies used for flow cytometry.

Antibodies	**Clone**	**Conjugate**	**Vendor**
Anti-mouse CD122	TM-β1	Biotin	BD pharmingen
Anti-mouse CD127	A7R34	PE Cy5	eBioscience
	A7R34	PE	eBioscience
Anti-mouse CD19	eBio1D3	Alexa Fluor® 700	eBioscience
Anti-mouse CD21	7E9	PerCP	Biolegend
Anti-mouse CD23	B3B4	Pacific Blue	Biolegend
Anti-mouse CD24	M1/69	Pacific Blue	Biolegend
Anti-mouse CD25	7D4	FITC	BD pharmingen
	PC61.5	PE	eBioscience
Anti-mouse CD3	145-2C11	PE	BD pharmingen
Anti-mouse CD4	RM4-5	Alexa Fluor® 700	BD pharmingen
	RM4-5	APC	BD pharmingen
Anti-mouse CD43	S7	PE	BD pharmingen
Anti-mouse CD44	IM7	Pacific Blue	Biolegend
	IM7	A700	Biolegend
Anti-mouse CD45.1	A20	APC	eBioscience

	A20	FITC	BD pharmingen
	A20	Pacific Blue	Biolegend
	A20	PE	BD pharmingen
Anti-mouse CD45.2	104	Pacific Blue	Biolegend
	104	FITC	BD pharmingen
Anti-mouse CD45R (B220)	RA3-6B2	APC Cy7	BD pharmingen
	RA3-6B2	Biotin	eBioscience
	RA3-6B2	PE Cy7	BD pharmingen
	RA3-6B2	PerCP	BD pharmingen
Anti-mouse CD5 (Ly-1)	53-7.3	APC	eBioscience
Anti-mouse CD62L	MEL-14	APC Cy7	Biolegend
Anti-mouse CD69	H1.2F3	PE Cy7	eBioscience
Anti-mouse CD8	53-6.7	APC	eBioscience
	53-6.7	APC Cy7	Biolegend
	53-6.7	PE	Biolegend
Anti-mouse CD93	AA4.1	APC	eBioscience
Anti-mouse CD95		PE	BD pharmingen
Anti-mouse KLRG1	2F1	PE Cy7	eBioscience
	2F1	APC	eBioscience
Anti-mouse IgD	11-26	Biotin	eBioscience
Anti-mouse IgM	11/41	PE Cy7	eBioscience
Anti-mouse NK1.1	PK136	APC	BD pharmingen
	PK136	FITC	BD pharmingen
Anti-mouse Vα2 TCR	B20.1	PE	BD pharmingen

2.3.4 Data acquisition and analysis

Data were acquired using LSRII or Fortessa flow cytometers (BD Biosciences) and were analysed using flowJo software (Treestar).

2.4 Adoptive transfer experiments

2.4.1 Adoptive transfer of OT-I $CD8^+$ T cells

Mice were sacrificed by cervical dislocation. Splenocytes were collected in 5 mL of RPMI1640 + 10% fetal calf serum (FCS). Single cell suspensions were prepared by mashing and filter through nylon mesh filter (BD Bioscience). Cells were diluted with trypan blue and counted using a haemacytometer. 200 uL of 10 $x10^6$ WT OT-I or mutant OT-I cells were mixed at a 50:50 ratio in RPMI + 10% FCS. Recipient mice were immobilized in a restrainer and 200 μL of cell suspension were intravenously injected via the tail.

2.4.2 Adoptive transfer of OT-I CD8+ T cells and immunisation with recombinant influenza A viruses HKx31-SIINFEKL and PR8-SIINFEKL

Mice were sacrificed by cervical dislocation. Splenocytes were collected in 5 mL of RPMI1640 + 10% FCS. Single cell suspensions were prepared by mashing and filter through nylon mesh filter (BD Bioscience). Cells were diluted with trypan blue and counted using a haemocytometer. 1000 WT OT-I or mutant OT-I cells were mixed at a 50:50 ratio per 200 μL RPMI + 10% FCS for each recipient mouse. The recipient mice were immobilized in a restrainer and 200 μL of cell suspension were intravenously injected via the tail. The recipients were intraperitoneally injected with 200 HAU/μL influenza A virus HKx31-SIINFEKL on the same day. The second challenge was intraperitoneally injected on day 70 post first challenge with influenza A virus PR8-SIINFEKL. Recombinant viruses were a gift of Dr Stephen Turner (Jenkins et al., 2006) and virus stocks were prepared in chicken eggs by Dr Ed Bertram.

2.5 cloning and sequencing

2.5.1 cDNA preparation and primers

2.5.1.1 Preparation of RNA

Preparation of RNA was carried out in an RNA designated room and hood to avoid RNA degradation. Mouse spleen was collected in 5 mL of RPMI1640 + 10 % FCS. Single cell suspensions of splenocytes were prepared by mashing and sieving under sterile condition and kept on ice. Cells were pelleted by centrifugation for 4 minutes at 1340 rpm at 4°C. Splenocytes are lysed with RBC lysis buffer for 5 minutes and 5 mL RPMI1640 + 10 % FCS was added. The cells were resuspended with 5 mL PBS and the cells were counted. 5 x 10^6 cells were pelleted in 1.5 mL eppendorf tube and mixed in 1mL of TRIzol™ (Invitrogen). 200 ul chloroform was added to the tube and shaken vigorously for 30 seconds. The mixture was incubated at room temperature for 10 minutes and then centrifuged at 13000 g for 15 min at 4°C. The upper aqueous layer was transferred into new eppendorf tubes containing 500 µL isopropanol and incubated at room temperature (RT) for 10 -15 minutes. The samples were centrifuged at 13000 g for 15 minutes at 4°C to pellet RNA. The supernatant was removed and the pellet was washed with 1 mL of 75% ethanol. The samples were centrifuged at 7500 g for 5 minutes at 4°C and the ethanol supernatant was carefully removed. The pellet was air dried for 10-15 min and redissolved in 20 µL DEPC-treated water and stored at - 80°C. The concentration of RNA was determined by using Nanodrop spectrophometer (ND-1000, Nanodrop Technologies, USA)

2.5.1.2 Preparation of cDNA

This process was carried out by using SuperScript™ II Reverse Transcriptase kit (Invitrogen, Cat. #: 18064-022). 500 ng of RNA was added to 0.5 mL eppendorf tubes together with 1 µL oligo dT and dNTP (10mM). DEPC-treated water was added to make a total volume of 12 µL. Each sample was heated at 65°C for 5 minutes and quickly chilled on ice. A master mix of 4 µL 5X First-Strand buffer, 2 µL DTT (0.1 M) and 1 µL RNAse out was added to each sample and incubated at 37°C for 2 minutes. 1 µL of SuperScript II reverse transcriptase was added to each sample and incubated at 42°C for 50 minutes. The sample was heated to

70°C for 15 minutes to inactivate the reaction. 1 µL RNAse-H was added and samples were incubated at 37°C for 20 minutes. The synthesized cDNA was stored at -20 °C.

2.5.1.3 Oligonucleotide primers

All primers used in this study were obtained from Gene Works:

Senp2 **Forward:**	5' CTCAAGCTTACCATGTACAGATGGCTGGCTAAGGTTC 3'
Senp2 **Reverse:**	5' GCAGTCGACGACAGCAACTGCTGGTGAAGGATC 3'

2.5.2 PCR Amplification

This process was carried out by using AccuPrime™ *Pfx* DNA polymerase (Invitrogen, Cat. #: 12344-024). Each reaction contained the following:

10x AccuPrime™ *Pfx* Reaction mix	5 µL
10mM forward primer	1.5 µL
10mM reverse primer	1.5 µL
AccuPrime™ *Pfx* DNA polymerase	1 µL
Template DNA	250 ng
dH2O	Make up to 50 µL

PCR program:

Denature the template at 95°C for 2min:

Denature	95°C for 15 seconds	
Anneal	52°C for 30 seconds	X 35 cycles
Extend	68°C for 2.5 minutes	

2.5.3 DNA Cloning

2.5.3.1 PCR product Purification and digestion

The PCR products were purified by using PureLink PCR purification kit (Invitrogen, Cat. #: K3100-01).

2.5.3.2 Digestion for PCR products (insert):

10x Buffer	3 µL
10x BSA	3 µL
Enzyme 1: HindIII	1.5 µL
Enzyme 2: SalI	1.5 µL
DNA	2 µg
MQ H2O	Make up to 20 µL

2.5.3.3 vector

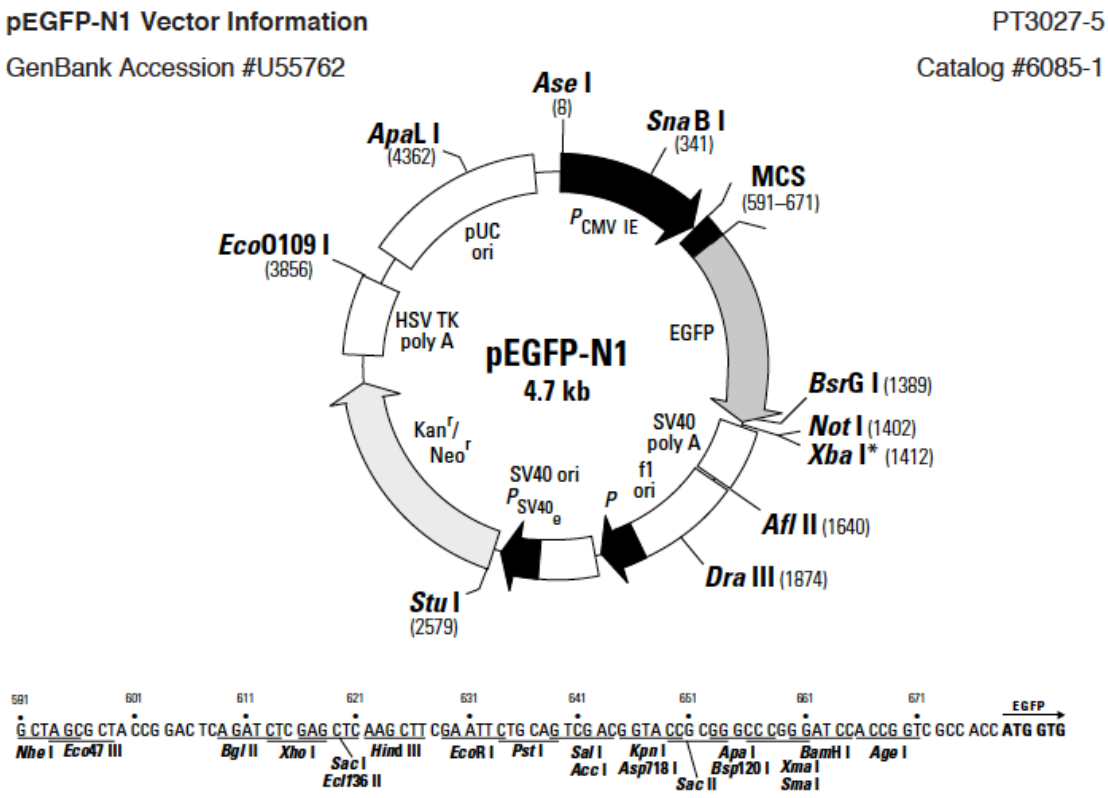

Figure 2.5.3: The plasmid for cloning with restriction sites shown

2.5.3.4 Digestion of plasmid:

10x Buffer	5 µL
10x BSA	5 µL
Enzyme 1: HindIII	2.5 µL
Enzyme 2: SalI	2.5 µL
Plasmid DNA	1-3 µg
MQ H2O	Make up to 50 µL

*following digestion, DNA was ran on an agarose gel.

2.5.4 Gel extraction

DNA samples were extracted from the gel using QIAEX II gel extraction Kit (QIAGEN, Cat. #: 20021)

2.5.5 Ligation and transformation

Ligation was carried out using LigaFast™ Rapid DNA ligation system (Promega, Cat. #: M8221).

Ligation Buffer	2.5 µL
Ligase (T4)	0.5 µL
Insert	1.5 µL
Vector (pEGFP-N1)	0.5 µL

Mix was incubated at room temperature for 10 min.

The ligation product was added to 500 µL competent cells and incubated on ice for 15 minutes. The competent cells and DNA mix was heat shock for 30 seconds using 37°C water bath and followed by cooling on ice for 2 minutes. The sample was added to 450 µL L-Broth (LB) and incubated in shaker at 37 for 60 min. The cells were centrifuged at 10,000 rpm for 1 min and resuspend in 100 µL LB. The transfected cells were plated on agar plates.

Molecular weight markers: 1Kb Plus DNA ladder (invitrogen)

2.5.6 Sequencing

Oligonucleotide Primers:

eGFP forward	5' CGT GTA CGG TGG GAG GTC TA 3’
Senp2 forward	5' CAG GAG CAA GGT GTG ACA GA 3’
eGFP reverse	5' CGT CGC CGT CCA GCT CGA CCA G 3’

Components of sequencing reaction:

5X sequencing buffer (BRF, JCSMR, ANU)	3.5 µL
Forward or reverse primer (10mM)	1 µL
Big dye (BRF, JCSMR, ANU)	1 µL
DNA template	100 – 300 ng (3 µL)
dH2O	Make up to 20 µL

2 µL 12.5 mM EDTA, 2 µL 3M NaOAC and 60 µL of 100% ethanol was added to each sample and centrifuged at 13000 rpm for 30 minutes. The supernatant was removed from each tube and 200 µL of 80% ethanol was added to wash the pellet. The sample was centrifuged at 13000 rpm for 5 min and vacuumed dried at room temperature. The samples were sequenced in The Australian Cancer Research Foundation (ACRF) Biomolecular Resource Facility (BRF), and the data was analysed using CodonCode aligner software.

2.6 Immunofluorescence

293T cells were grown to 90% confluence on slides in 6-well plate. The transfection was done by using Lipofectamine 2000 (Invitrogen, Cat. #: 11668-027). 12 uL Lipofectamine 2000 was added to tube #1 with 150 uL DMEM (GibcoBRL). 10 ug of plasmid was added to tube #2 with 150uL DMEM (GibcoBRL). Mix tube #1 and #2 and incubate for 5 min. The DNA-lipid complex was added to the cells. 2 days after transfection, the slides were taken out and put in a new 6-well plate and gently rinsed with 2mL PBS. The coverslips were immersed in 4% paraformaldehyde for 30 min and followed by rinse with PBS. The coverslips were incubated in 1% TritonX-100/PBS at RT for 5 min and followed by wash with PBS 2 times for 10 min. The coverslips were placed in a humid chamber and inverted over 25-50 µL of blocking buffer and incubated at

RT for 30 min. The coverslips were inverted onto a slide containing 3-5 µL of anti-fade solution (Molecular Probe) and air-dried. The GFP expression photographs were taken using confocal microscope (Imaging and Cytometry Facility (ICF), JCSMR).

2.7 Retroviral transduction

2.7.1 Buffers and reagents

Magnetic cell separation buffer (MACS buffer)	500 mL phosphate buffer saline (PBS) 2 mL 2mM EDTA 2.5 mL HI-FCS (sigma) 0.5% (v/v)
Complete DMEM (cDMEM)	DMEM (GibcoBRL) HI-FCS (sigma) 10% (v/v) 100 u/ml penicillin, 100 µg/ml streptomycin (GibcoBRL)

2.7.2 Retroviral – mediated primary T cell transduction

2.7.2.1 Transfection

Phoenix cells were maintained in NUNC T_{75} flasks (Thermo Scientific) in cDMEM media at 37°C until reaching confluence.

Experimental procedure:

Day	**Procedure**
1	$1x10^6$ cells/ 5 mL phoenix cells were plated in 60 mm petri dish
2	Cells were Transfected with Lipofectamine 2000 ((Invitrogen, Cat. #: 11668-027) as described above (For 60mm petri dish: 20 uL

Lipofectamine and 8 ug of plasmid DNA were used)

3 Media was changed with 3 mL of cRPMI

4 Viral supernatant was collected into 15 mL Falcon tubes and centrifuged at 1500 rpm to get rid of dead phoenix cells. 3 mL of fresh cRPMI was added (Viral supernatants were stored at 4˚C)

5 Viral supernatant was collected into 15 mL Falcon tubes and centrifuged at 1500 rpm to get rid of dead phoenix cells. GFP expression of phoenix cells was confirmed by FACS

2.7.2.2 Transduction

Primary murine T cells were isolated from the spleen. To do this, CD8 cells were enriched from splenocytes by depletion using anti-B220 and CD4 biotinylated antibodies and streptavidin MACS beads (130-048-102, Miltenyi Biotec). After washing with 5 mL MACS buffer, the cells were passed through a magnetic column (LS columns, 130-042-401, Miltenyi Biotec) according to manufacturer's instructions. The $B220^{-}CD4^{-}$ eluted cells were cultured for 24 hours at 37°C, 10 % CO2 in 6-well plate at 2 x 10^6 cells/mL in cRPMI. Cells were activated by plate bound αCD3 (5µg/mL) and soluble αCD28 (5µg/mL). 24 hours after activation, primary cells were pelleted and resuspend with 2ml viral supernatant. Cells were added to 6 - well plate with 20 µL/10 x 10^6 cells DOTAP and spinoculated for 90 minutes at 2800 rpm at 30°C.

2.7.3 Cell lines

2.7.3.1 293T cells

293T cells were maintained in NUNC T_{75} flasks (Thermo Scientific) in cDMEM media at 37°C until reaching confluence. For passage, the cells were washed with 10 mL PBS and then treated with 1.5 mL trypsin-EDTA at 37°C for 2-3 minutes to release the adherent cells. 8.5 mL cDMEM was added to inactivate the trypsin.

1 mL of cell suspension was seeded to a new flask containing 20 mL fresh cDMEM.

2.7.3.2 phoenix cells

Phoenix cells were maintained in NUNC T_{75} flasks (Thermo Scientific) in cDMEM media at 37°C until reaching confluence. For passage, the cells were washed with 10 mL PBS and then treated with 1.5 mL trypsin-EDTA at 37C for 2-3 minutes. 8.5 mL cDMEM was added to inactivate the trypsin. 1 mL of cell suspension was seeded to a new flask containing 20 mL fresh cDMEM.

Chapter 3: Identification of causative mutation in DOCK2

3.1 Aim

The aim of this research project was to identify new mutant mouse strains with T cell abnormalities produced by N-ethyl N-nitrosourea (ENU) mutagenesis. Identification of mutations in these strains could help to investigate pathways important to the immune system.

The production of novel mouse strains by ENU mutagenesis

Over last decades, the mouse has been a powerful model to study the mammalian genome not only because of its' short breeding period but also the mouse genome shares high similarity with the human genome sequence. Gene knock out (KO) techniques have been widely applied in biomedical research, but they require a priori knowledge in selecting which gene to mutate. As a complement to targeted gene knock-outs, genome-wide chemical mutagenesis coupled with a phenotypic screen is a powerful approach to identify novel genes and elucidate gene functions without requiring prior knowledge about specific genes of interest.

N-ethyl-N-nitrosourea (ENU) has been shown to be an effective chemical mutagen that causes random point mutation in mouse spermatogonia (Russell et al., 1979 and Russell et al., 1982). ENU can transfer the ethyl group to reactive oxygen or nitrogen radicals of purine or pyrimidine resulting in mispairing during DNA replication in both somatic and germ cells (Singer and Dosahjh, 1990). ENU-mutagenesis is a powerful tool to generate a variety of alleles for investigation of gene function (Quwailid, et al., 2004). T/A base pairs are the most preferential targets by ENU. AT to TA tranversions and AT to GC transitions comprise 82% of the total lesions sequenced (Noveroske, et al., 2000) which is possibly due to the mispairing of alkylated O4-thymine and O2-thymine respectively (Justice et al., 1999). ENU-induced gene mutations resulting in Mendelian phenotypes comprise 64% missense, 10% nonsense and 26% splicing errors (Justice et al. 1999). This range of alleles mirrors many of the inherited or

de novo mutations found in human Mendelian diseases, providing a source for human disease models (Justice et al., 1999).

My goal was to isolate new mouse models that might correspond to human immune disorders. The majority of ENU induced mutations produce recessive traits only detectable after three generations breeding to homozygosity. When injected to the founder "Generation 0" (G0) mice, ethylnitrosourea (ENU) produces single nucleotide substitutions in the DNA sequence of mouse spermatogonial stem cells (Beier, 2000).

In my studies, once the males have regained fertility, they can be bred with WT females to produce G1 mice carrying approximately 50 heterozygous mutations in protein-coding sequences. After two more generations of breeding some of these mutations can be brought to homozygosity and the mice (G3) can be screened for phenotypes of interest (Vinuesa and Goodnow, 2004, Vinuesa et al., 2005, and Wu et al., 2008). Causal mutations can then be identified through the use of exome or whole genome sequencing (Andrews et al., 2012). Whereas previous screens have only tested blood, in my studies G3 mice were sacrificed after flow cytometric screening of blood and their spleen screened by flow cytometry for heritable recessive mutations. This would detect mutations affecting sessile lymphocyte subsets like marginal zone B cells, which are not detectable in blood. Mutant strains were propagated from parents and additional siblings, and further confirmed by peripheral blood, thymus, and bone marrow flow cytometric analysis.

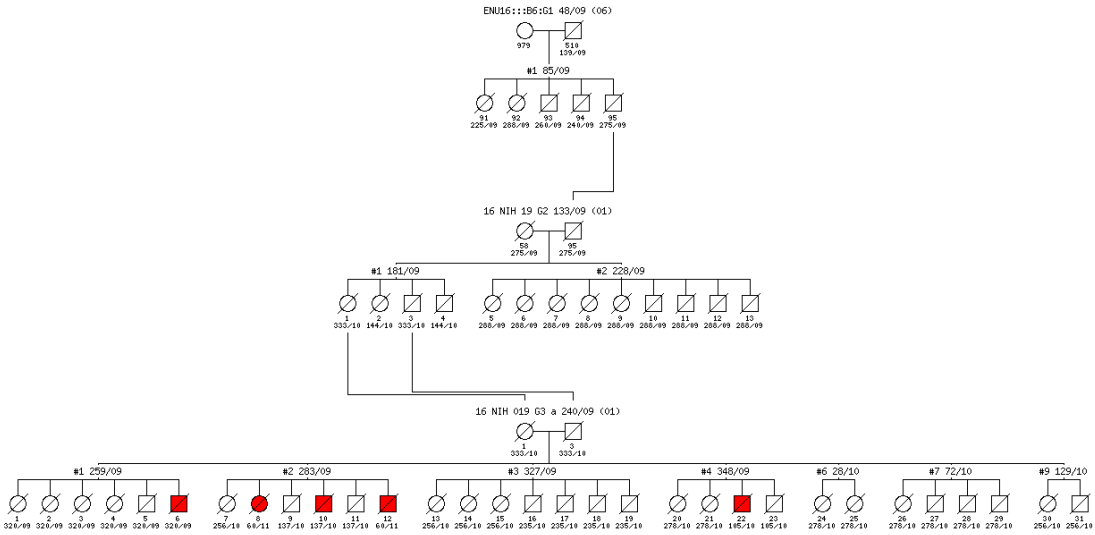

Figure 3.1 Pedigree of the ENU16NIH19a *'dockland'* strain. In the G3 generation, 1 female and 4 males had a significant reduction of lymphocytes in spleen. Male mice = squares, female mice = circles. Affected mice = red filled symbols; unaffected mice = open symbols.

3.2 Discovery of a mouse strain produced by ENU mutagenesis with absent marginal zone B cells and T cell lymphopenia

In Figure 3.1, pedigree ENU7B6039 was found at the G3 generation with B cell lymphopenia and reduced CD4:CD8 ratio. Analysis of spleen cells from one G3 mouse of this strain showed that it had higher CD44 expression on T cells (Figure 3.2) and a reduced marginal zone B cell population (about 1/10 of the wild type) compared to normal mice. By screening of all G3 mice from the pedigree, 4 out of 25 mice showed the same phenotype (Table 3.1). Following the Mendelian inheritance law, this strain was inferred to carry a recessive mutation.

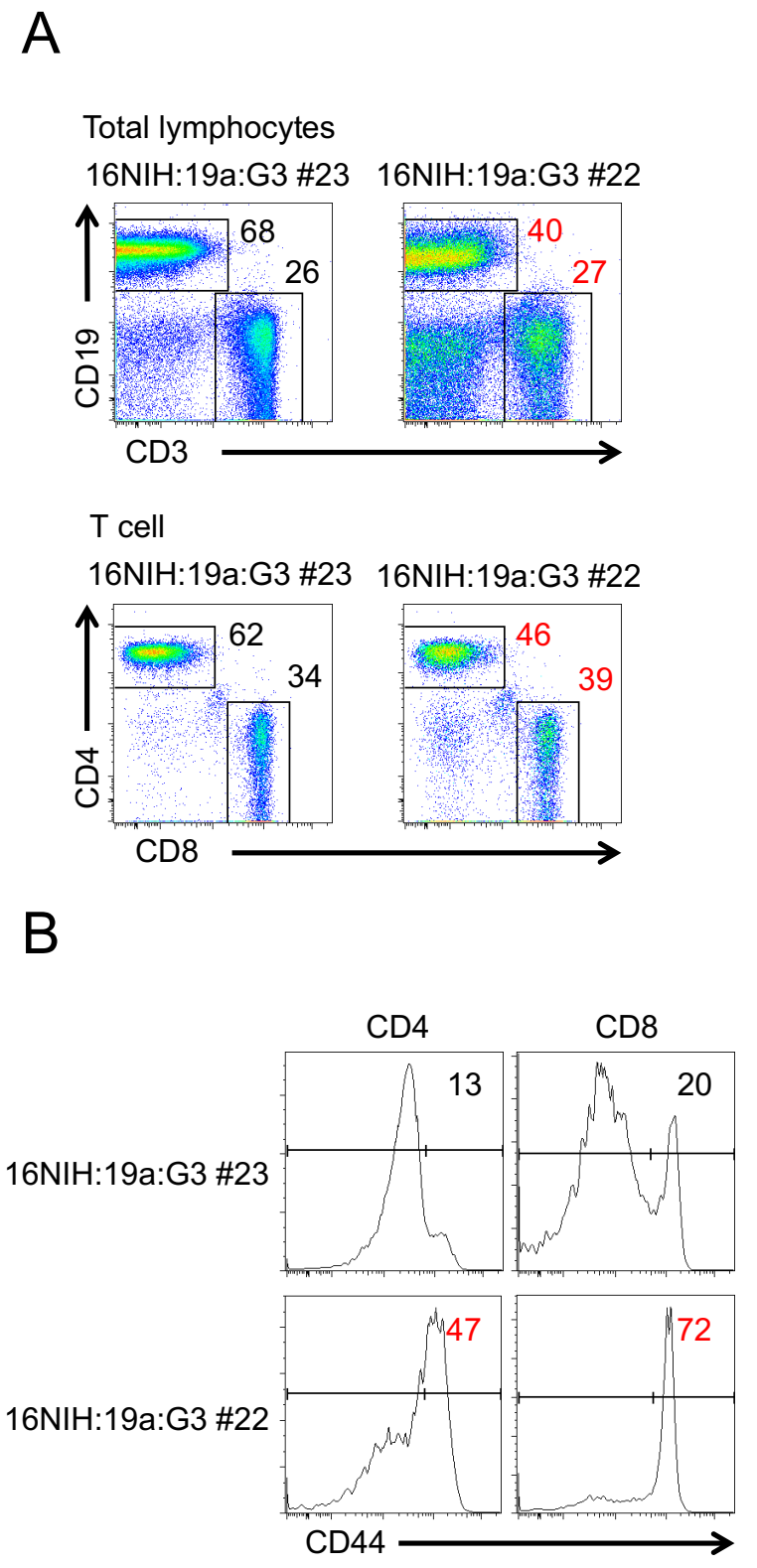

Figure 3.2 Splenic subsets in *dockland* mouse. (A) Representative flow cytometry plots of $B220^{+}$ and $CD3^{+}$ splenocytes for either wildtype (G3

#23) or *dockland* mutant mice (G3 #22, colored in red). (B) Representative flow cytometry plots of CD4 and CD8 T splenocytes and histogram of CD44 expression on CD4 and CD8 T splenocytes for either wildtype or *dockland* mice (colored in red). The percentage of CD4 or CD8 cells falling within the CD44hi gate is shown.

Total mouse number	phenotype: normal	phenotype: affected
25	21	4
100%	84%	16%

Table 3.1 The percentage of mice displaying the *dockland* lymphocyte trait (affected) in the ENU16NIH19a pedigree G3 generation.

The percentage of CD4 and CD8 in mice displaying the *dockland* trait (affected) and in unaffected littermates is plotted in Figure 3.3. As the mutant mice have lower CD4/CD8 ratio, and higher CD44 surface expression on CD4 and CD8 T cells, the affected mutant group could be separated from the normal littermates by using CD4% versus CD8%, and were best resolved by plotting CD44%$^{+}$CD8 versus CD8% (Figure 3.3).

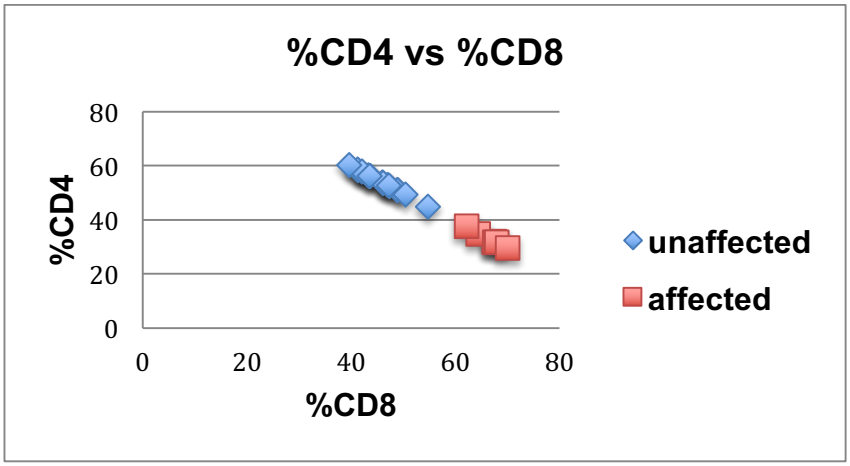

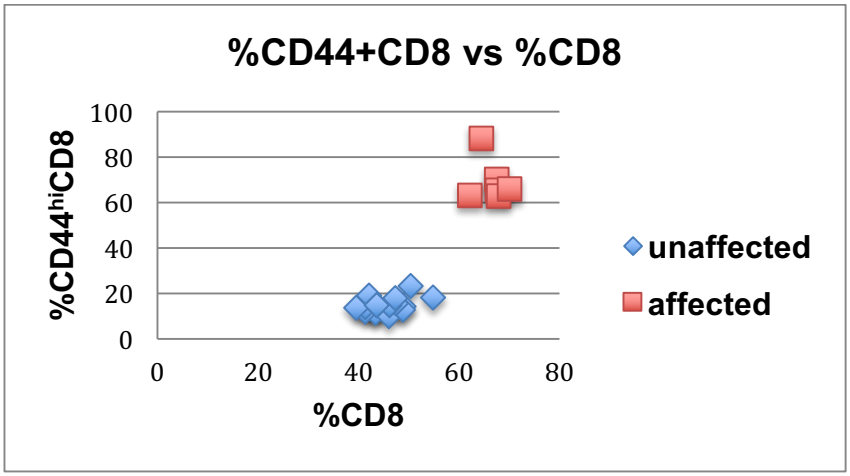

Figure 3.3 *dockland* mutation leads to altered CD4/CD8 ratio and increased of CD44 expression on T cells. Flow cytometric analysis of blood. A) The percentage of CD4 T cells versus CD8 T cells. B) The frequency of $CD44^{hi}$ CD8 T cells versus CD8 T cells. Each symbol represents a single animal: Red = affected and Blue = unaffected.

3.3 Mapping and sequencing to identify the causative *dockland* mutation

To identify the *dockland* mutation, one affected mouse was outcrossed to mice of the CBA/H strain to generate an F1 generation. After intercrossing F1s, blood from the F2 generation was analysed by flow cytometry to identify affected individuals using the traits above. DNA was collected from affected individuals and typed for single nucleotide polymorphic markers throughout the genomes between C57BL/6 and CBA/H strain by the mapping team at the Australian Phenomics Facility. The affected mice shared a single chromosomal interval homozygous for DNA of B6 origin on Chromosome 11, whereas the unaffected mice were either heterozygous or homozygous for DNA of CBA origin in this part of Chromosome 11. By these criteria, the *dockland* mutation was narrowed down to chromosome 11 with an interval from 4.4 Mb to 47.4 Mb (Figure 3.4A). The recombinant genotypes of affected and unaffected animals excluded

everything proximal to the marker at 4.4 Mb, and everything distal to the marker at 47 Mb, but there were no recombinants that excluded the interval between 4.4 and 23 Mb (Figure 3.4A). A search of the genes in this interval led to one strong candidate gene, *Dock2*. *Dock2* deficient mice have similar phenotypes such as T lymphopenia and loss of marginal zone B cells (Fukui, Y el al., 2001) therefore *Dock2* was a candidate gene for the *dockland* mutation. Sequencing the *Dock2* gene in affected and in normal B6 DNA revealed a homozygous G to T single nucleotide substitution in exon 23 that produced a premature stop codon (TAA) instead of Glutamic acid residue 775 (GAA) (Figure 3.4B). The *dockland* (*doc*) mutation was thus predicted to truncate and eliminate the C-terminal half of the DOCK2 protein.

A

4.403	* 23.035	47.224	70.331	
HET	B6	B6	HET	
B6	B6	HET	HET	
B6	B6	B6	HET	affected
B6	B6	B6	B6	
B6	B6	B6	B6	
B6	B6	B6	B6	
B6	B6	B6	HET	
HET	HET	HET	HET	
CBA	CBA	CBA	CBA	
HET	HET	HET	HET	
HET	HET	HET	HET	
CBA	CBA	B6	B6	
CBA	HET	HET	HET	unaffected
HET	HET	HET	HET	
CBA	CBA	CBA	CBA	
CBA	HET	HET	B6	
B6	HET	HET	HET	

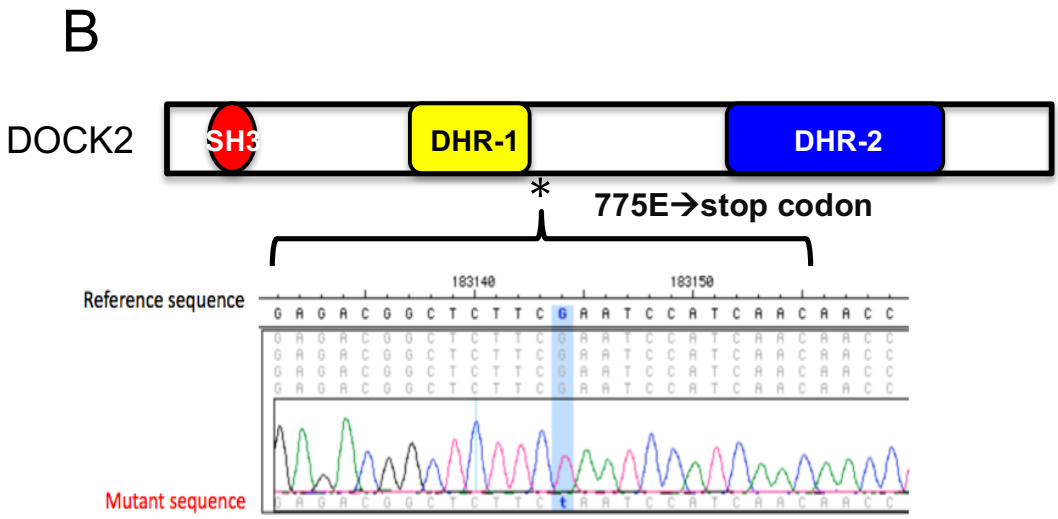

Figure 3.4 Mutation in *Dock2* in *dockland* mouse. (A) Results of DNA typing of individual affected and unaffected mice from *dockland* C57BL6/CBA F2 intercross showing linkage of the *dockland* mutation to a segment of chromosome 11 from 4.4MB to 47MB. . Each row is a single F2 mouse, and each column shows the genotype for a single nucleotide polymorphism at the indicated coordinate (megabasepair, mouse genome build 37) on Chromosome 11. (B) DNA sequence from C57BL/6 and *dockland* affected mice showed a G to T base change in exon 23, changing codon 775 from encoding Glutamic acid to a stop codon. The premature stop is downstream of DHR-1 domain of DOCK2 protein and upstream of the DHR-2 domain (schematically showed).

3.4 DOCK2 expression and protein structure

DOCK2 is a mammalian homolog of the *Caenorhabditis elegans* protein CED-5 and the *Drosophila melanogaster* protein myoblast city, and is a guanine nucleotide-exchange factor (GEF) expressed mainly in haematopoietic cells (Meller et al., 2005; Cote and Vuori, 2007; Figure 6). Mouse DOCK2 comprises 1828 amino acid residues, including an SH3 domain, a DOCK-homology region 1

(DHR-1) domain and a DHR-2 domain (Figure 3.5). DOCK2 protein can physically interact with ELMO1 through its SH3 domain. The DHR-1 domain binds phosphatidylinositol-3,4,5-triphosphate (PtdIns(3,4,5)P3) lipids generated by PI(3)K activity to promote localized membrane binding and activation. Moreover, DOCK2 can regulate cell migration, cytoskeletal dynamics and membrane polarization by activating Rac through its DHR-2 domain (Meller et al., 2005; Cote and Vuori, 2007). Rac is a one of the Rho family GTPases that regulate membrane polarization and cytoskeletal dynamics in various cells. Rac is transformed from a GDP-bound inactive state to a GTP-bound active state upon exchanging GDP for GTP, which is stimulated by GTP exchange factors including the DOCK proteins (Hall, 1998; Penninger and Crabree, 1999). Previous analysis of *Dock2* knock-out mice suggests that Dock2 functions as a central molecule that activates Rac and mediates cytoskeletal reorganization during lymphocyte migration (Sanui, et al., 2003; Terasawa et al., 2012). Dock2 has been demonstrated to link TCR signals to the degradation and downregulation of IL-4Rα through Rac activation and microtubule dynamics (Tanaka et al., 2007). In addition, Dock2 deficiency causes marked reduction of Vα14 NKT cells in the thymus, liver, and spleen by affecting the generation of Vα14 NKT cells (Kunisaki et al., 2006). The *dockland* mutant strain has acquired a stop codon immediately C-terminal to the DHR-1 domain, eliminating the DHR-2 Rac GTP-exchange factor domain. In mice, *Dock2* mRNA is primarily produced in hematopoietic cells (Figure 3.6).

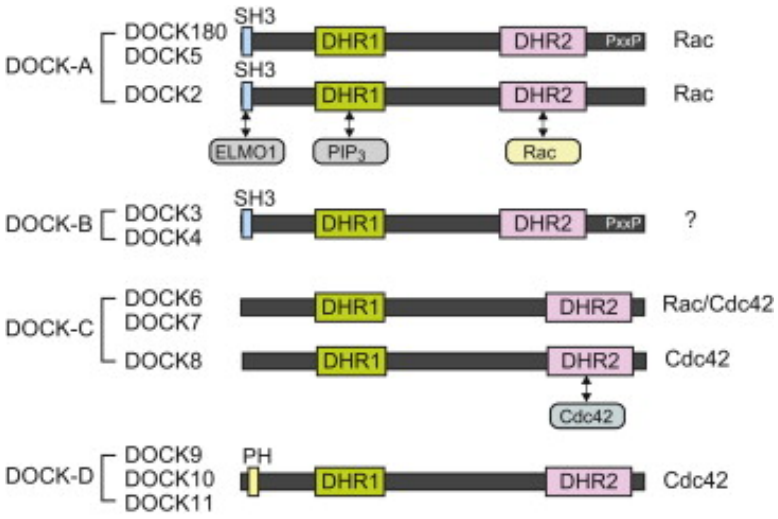

Figure 3.5 Dedicator of cytokinesis (DOCK) family proteins. The structure and domains of mammalian DOCK family proteins. (Adapted from Nishikimi et al., 2013)

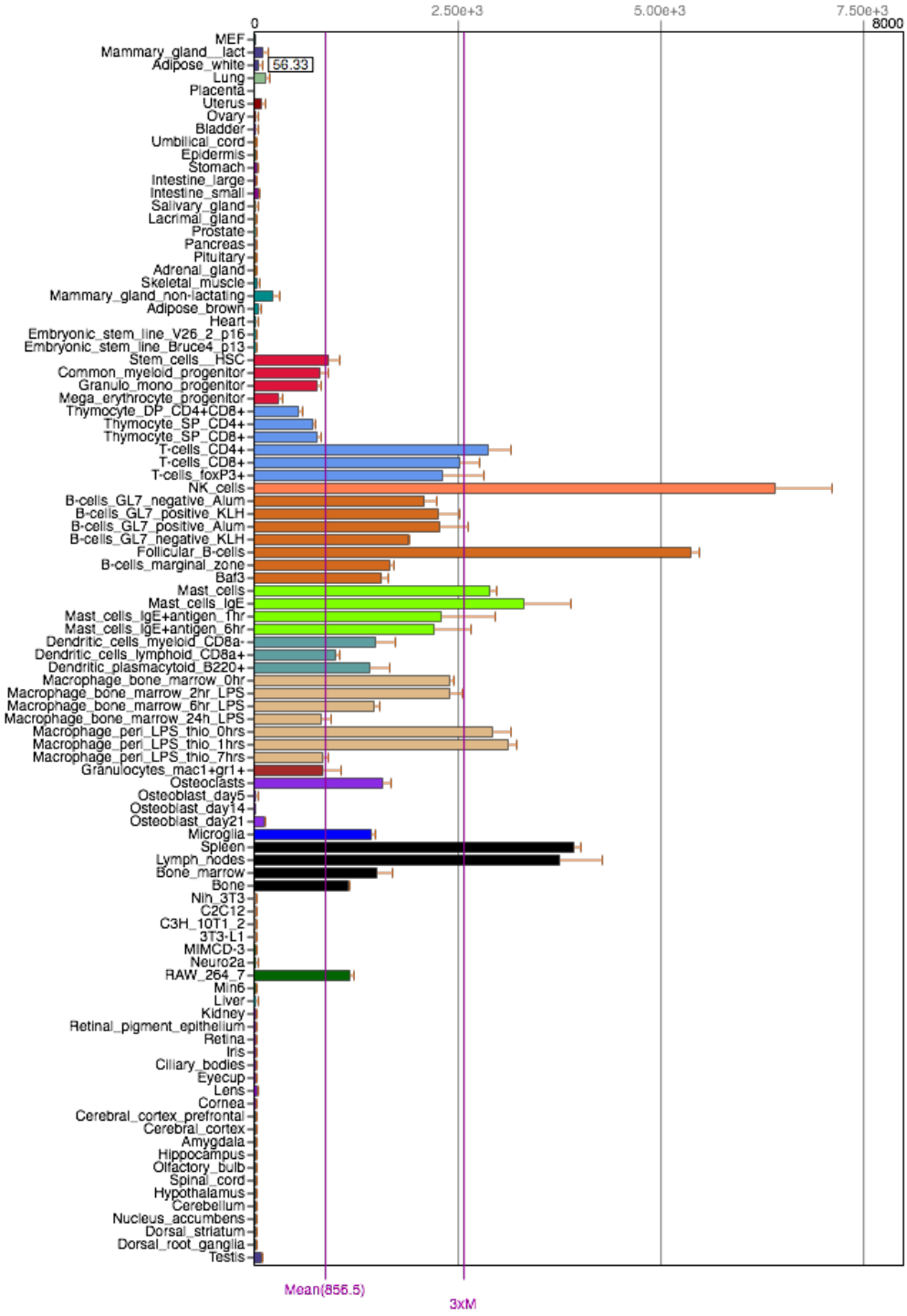

Figure 3.6 *Dock2* mRNA is highly expressed in immunological cells and tissues. Affymetrix microarray profiling data from BioGPS showing relative amount of *Dock2* mRNA in the indicated mouse tissues and cell types. (http://biogps.org/#goto=genereport&id=94176)

3.5 Lymphocyte deficiency in *dockland* mice

The *dockland* homozygous mice were compared with age-matched wild-type controls and heterozygous mice. Spleen cells were investigated by flow cytometric analysis using the gating strategy shown in Figure 3.7. B cells ($B220^{+}$) and T cells ($CD3^{+}$) were gated from total lymphocytes (Figure 3.7A). T cells were further divided into CD4 and CD8 T cells (Figure 3.8) and both populations were analysed for CD44 and KLRG1 expression (Figure 3.7B and C). In the spleen, wild-type and *doc/+* heterozygous mice had comparable percentages of lymphocytes (Figure 3.8A left). However, *doc/doc* homozygous mice had a significantly lower percentage of lymphocytes in the spleen compare to the other two groups ($p<0.001$), as well as significantly lower total lymphocyte numbers per spleen compared to wild-type ($p<0.01$) and *doc/+* mice ($p<0.05$) (Figure 3.8A right). The *doc/doc* mice had a significantly lower percentage of B cells compared to the other two groups ($p<0.001$) (Figure 3.8B left). The *doc/+* mice had an intermediate decrease in percentage of B cell compared to wild type mice ($p<0.05$). The absolute numbers of B cell were analysed (Figure 3.8B right). There was no significant difference between the wild type and *doc/+* mice, but the *doc/doc* homozygous mice had significantly less B cells compare to wild type ($p<0.001$) and the *doc/+* mice ($p<0.01$). Although there was no significant difference regarding the T cell percentage (Figure 3.8B left), the *doc/doc* mice had less T cells compared to the other two groups (Figure 3.8B right). CD4 and CD8 T cells were also analysed individually (Figure 3.8C). The *doc/doc* mice had a significantly lower percentage of CD4 T cells ($p<0.001$) and significantly lower numbers of CD4 T cells compared to wild type and *doc/+* mice ($p<0.01$). For CD8 T cells, *doc/doc* mice had a slightly lower number of CD8 T cells, but no difference in the percentage of CD8 T cells. It was also noted that *doc/doc* mice have higher percentage of $CD44^{hi}$ cells among CD4 and CD8 T cells compared with *doc/+* and +/+ mice and the typical FACS plots are shown in Figure 3.7B. KLRG1 was used to measure T cell differentiation into activated effector cells. The *doc/doc* mice had a higher percentage of $KLRG1^{hi}$ cells and more $KLRG1^{hi}CD44^{hi}$ cells among CD4 and CD8 T cells compared to the other two

groups (typical FACS plots were shown in Figure 3.7C; analysis were shown in Figure 3.8D). The percentage of subsets and surface marker expression between *dockland* heterozygous mice and wild-type mice were similar.

A

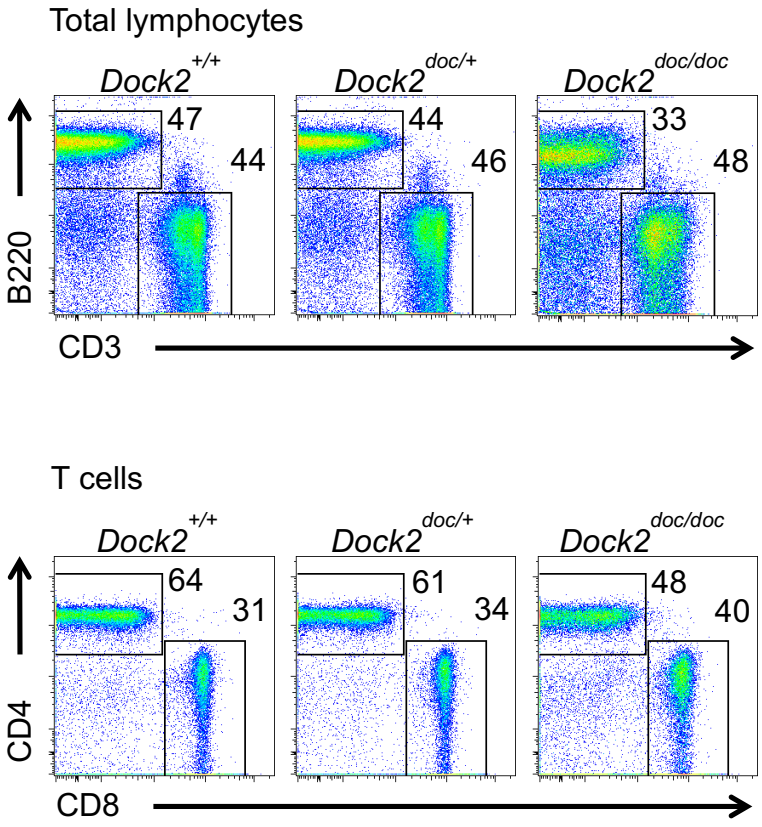

B

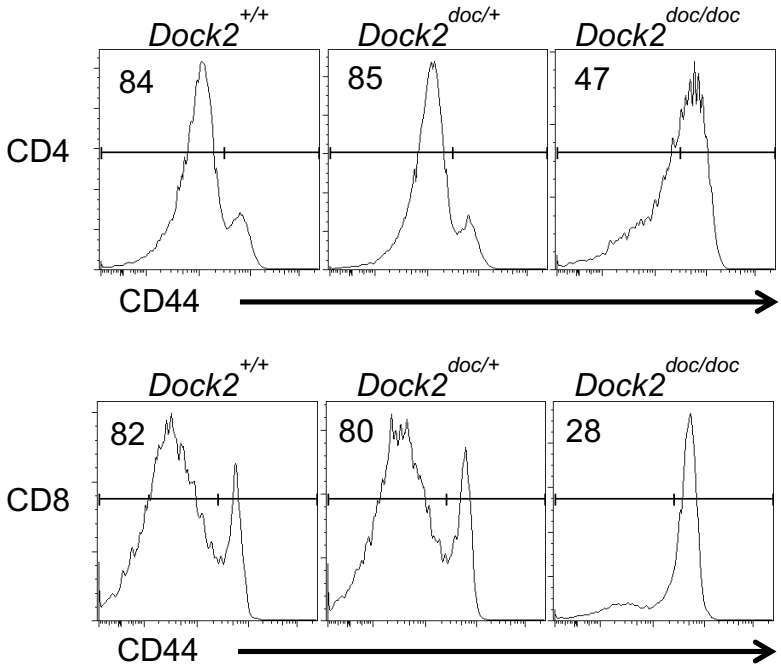
Dock2+/+
Dock2doc/+
Dock2doc/doc
84
85
47
CD4
CD44
Dock2+/+
Dock2doc/+
Dock2doc/doc
82
80
28
CD8
CD44

C

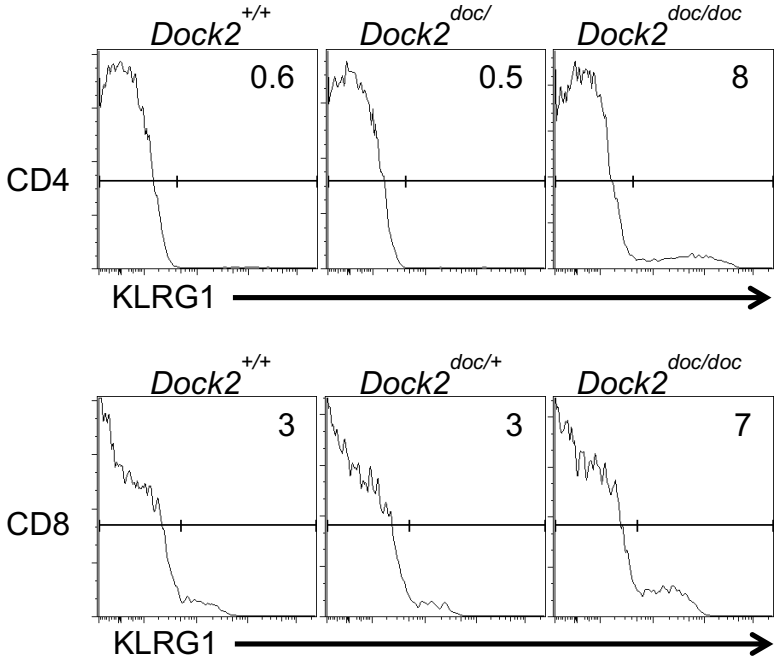
Dock2+/+
Dock2doc/
Dock2doc/doc
0.6
0.5
8
CD4
KLRG1
Dock2+/+
Dock2doc/+
Dock2doc/doc
3
3
7
CD8
KLRG1

Figure 3.7 Splenic T cell subsets in *dockland* mice. (A) Representative flow cytometry plots of splenic cells from wild-type (+/+), heterozygous (*doc/*+) and homozygous *dockland* (*doc/doc*) mice showing division of B cell ($B220^+$) and T cells ($CD3^+$) and percentage of CD4 T cells ($CD4^+$) and CD8 T cells ($CD8^+$) gated on T cells ($CD3^+$). (B) Representative histograms of CD44 expression on the CD4 and CD8 T cells, and % $CD44^{hi}$ cells. (C) Representative histograms of KLRG1 expression on the CD4 and CD8 T cells, and % KLRG1 positive cells.

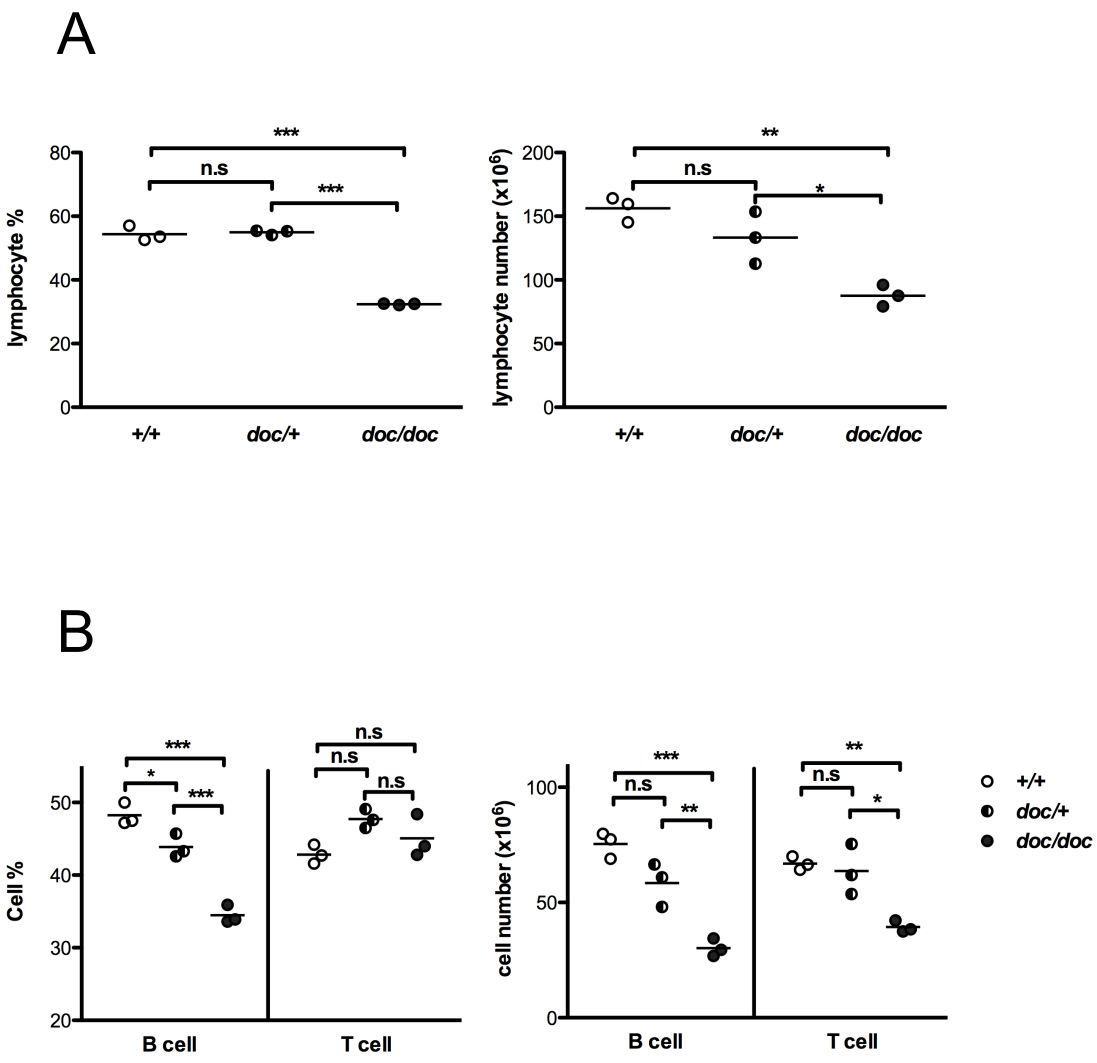

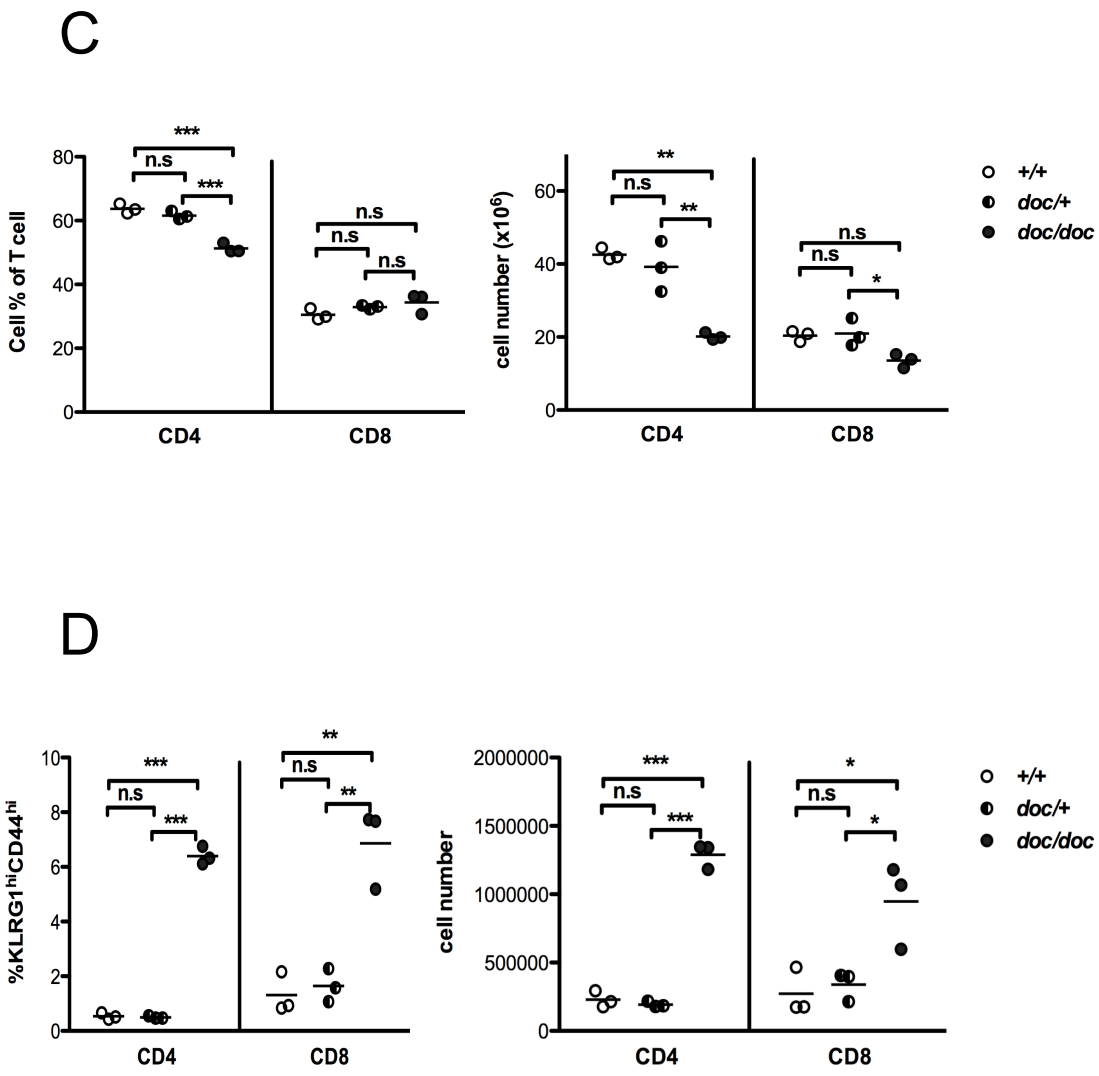

Figure 3.8 Analysis of lymphocyte subsets in the spleen. (A) Graph of percentage of lymphocytes (left) and absolute number of lymphocytes in spleen (right) of individual wild-type mice (white circles), heterozygous mice (half filled circles) and homozygous *dockland* mice (filled circles). (B) Graph of percentage of B and T cells (left) and absolute number of B and T cells in spleen. (C) Graph of percentage of CD4 and CD8 T cells (left) and absolute number of CD4 and CD8 T cells in spleen. (D) Graph of percentage of $KLRG1^{hi}CD44^{hi}$ CD4 and CD8 T cells (left) and absolute number of $KLRG1^{hi}CD44^{hi}$ CD4 and CD8 T cells in spleen. Dots represent

single mice and the bars represent the mean. Statistical analysis by one-way ANOVA and post analysis by Bonferroni test.

As shown in the previous section, *doc/+* heterozygous mice did not show any phenotype except a possible decrease in the percentage of B cells which was not seen in additional experiments. The absolute numbers were calculated for different splenic T cell subsets of *doc/doc* and wild-type mice with 4 mice in each group as a repeated experiment. As shown in Figure 3.9, the *doc/doc* mice had significantly reduced total number of lymphocytes in spleen compare to wild-type mice. Compared to wild-type mice, there were 3.7-fold fewer CD4 T cells and 3.3 fold fewer CD8 T cells in *doc/doc* animals (Figure 3.9B). The CD4 and CD8 T cell were further sub-divided by marker CD44. The *doc/doc* mice had comparable numbers of $CD44^{hi}$ (activated/effector) CD4 and CD8 T cells compared to +/+ mice (Figure 3.9C). However, there were dramatically reduced numbers of $CD44^{lo}$ (naïve) CD4 and CD8 T cells in doc/doc splenocytes, accounting for the overall decrease in T cell numbers.

A

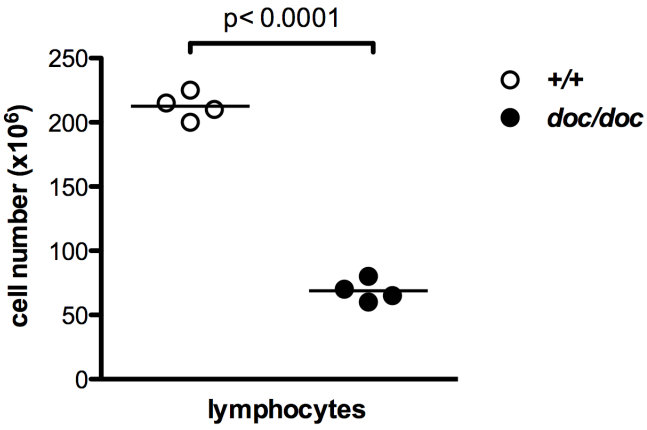

B

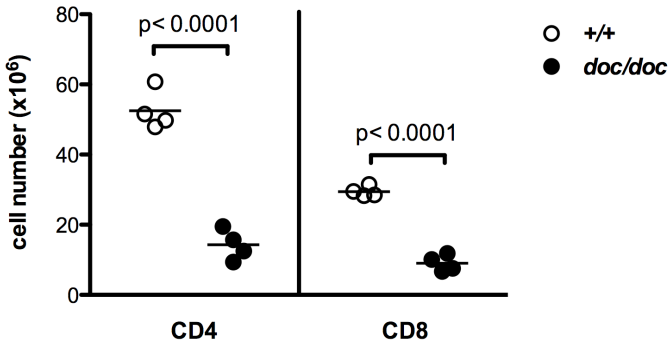

C

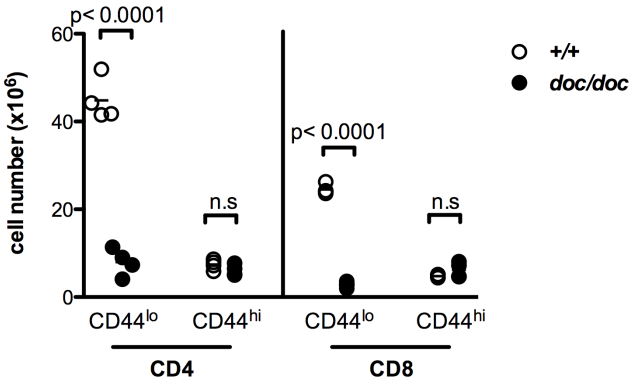

Figure 3.9 Quantitation of splenocyte subsets. (A) Number of lymphocytes per spleen in wild-type (+/+, white circles) and homozygous mutant mice (*doc/doc*, black circles). (B) Number of CD4 and CD8 T cells per spleen from wild-type (+/+, white circles) and homozygous mutants (*doc/doc*, black circles). (C) Number of naïve ($CD44^{lo}$) and activated ($CD44^{hi}$) CD4 and CD8 T cells in the spleen of wild-type (+/+, white circles) and homozygous mutant (*doc/doc*, black circles). Mean is shown as bar and statistical analysis by unpaired t-test.

3.6 Peripheral T cell defects in *dockland* mice

Analysis of the four subsets of peripheral T cells was also performed in blood (Figure 3.10). The *doc/doc* homozygotes had a lower percentage of blood T cells compared to wild type (8% vs 34%). The CD4 and CD8 T cells were sub-divided by CD44. Expressed as a percentage of blood lymphocytes, the mean percentage of CD4+ $CD44^{lo}$ was decreased 10-fold and the mean percentage of CD8+ $CD44^{lo}$ naïve T cells was decreased 7-fold in *doc/doc* mice, and these differences were reproducible and statistically significant (Figure 3.10B). By contrast, there was a similar mean percentage of $CD44^{hi}$CD4 T cells and significantly higher mean percentage of $CD44^{hi}$CD8 T cells in *doc/doc* mice compared to wild type mice.

A

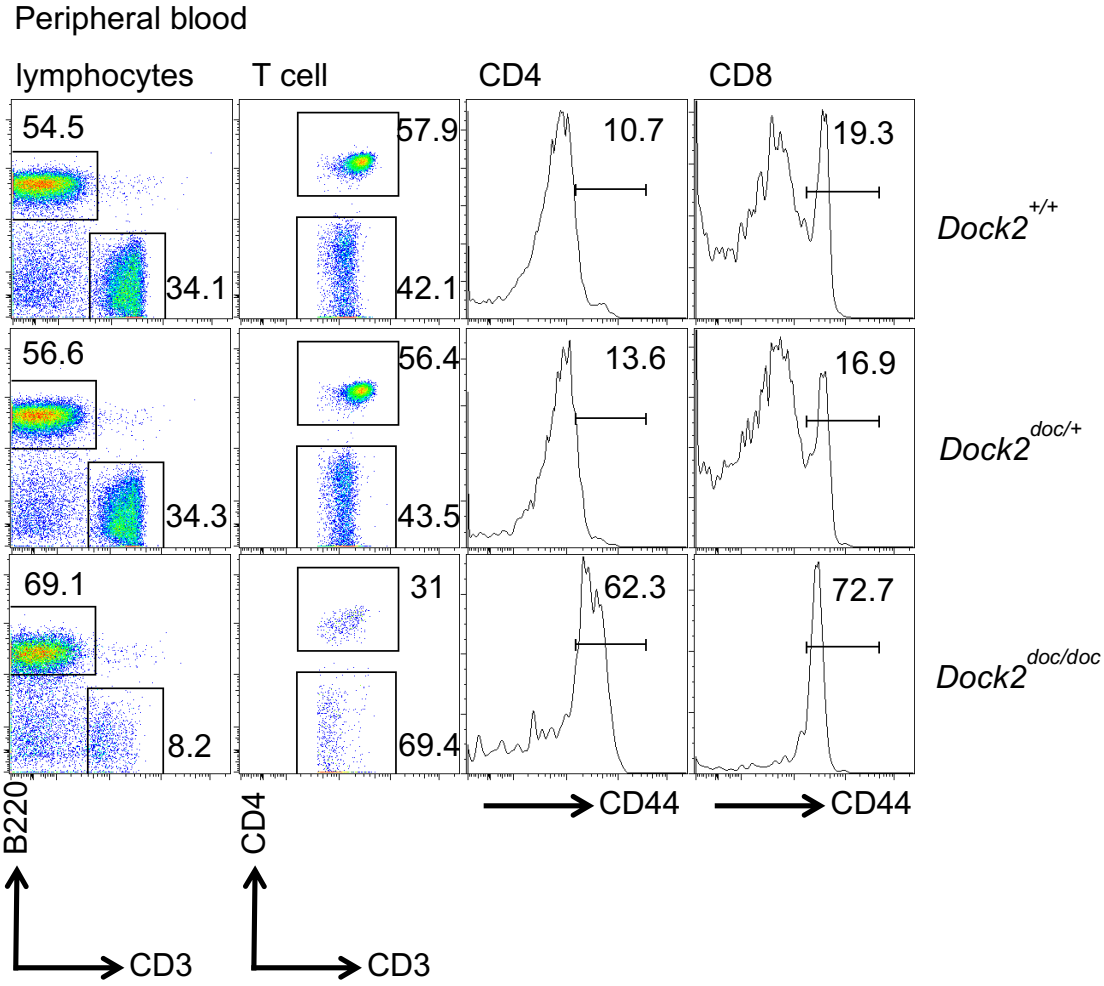
Peripheral blood
lymphocytes
T cell
CD4
CD8
54.5
34.1
57.9
42.1
10.7
19.3
Dock2+/+
56.6
34.3
56.4
43.5
13.6
16.9
Dock2doc/+
69.1
8.2
31
69.4
62.3
72.7
Dock2doc/doc
B220
CD3
CD4
CD3
CD44
CD44

B

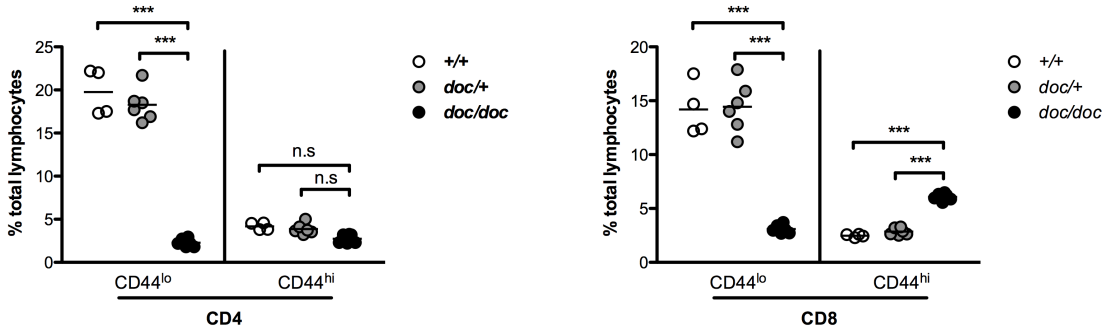
% total lymphocytes
CD44lo
CD44hi
CD4
n.s
CD8
+/+
doc/+
doc/doc

Figure 3.10 T cell subsets in peripheral blood. A. Representative flow cytometry plots of T subsets and representative histogram of CD44 expression on CD4 and CD8 T cells in blood from *Dock2* wild type (+/+), heterozygous (*doc/+*) and homozygous (*doc/doc*) mice. B. Quantitation of naïve ($CD44^{lo}$) and activated ($CD44^{hi}$) CD4 and CD8 T cells in blood in wild type (white circles), heterozygous (*doc/+*) and *doc/doc* homozygotes (black circles). Mean is shown as bar and statistical analysis by two-way ANOVA and Bonferroni post-test.

TCR-induced division of mutant and wild-type T cells was compared. $CD44^{lo}$ naïve T cells were sorted from the spleen of CD45.1 +/+ mice and from CD45.2 +/+ or *doc/doc* mice, and the CD45.1 and CD45.2 T cells were mixed at a 50:50 ratio, labelled with CFSE, co-cultured with 1ng/ml αCD3 antibody, and analysed for dilution of CFSE 3 days later. As shown in Figure 3.11, the unstimulated control had a single peak with no dilution of CFSE. In response to CD3 stimulation, CD45.2 doc/doc and +/+ naïve CD4 and CD8 T cells diluted CFSE comparably to their co-cultured CD45.1 +/+ internal control T cells. Therefore there was no apparent disadvantage of TCR-induced cell division caused by the *Dock2* mutation.

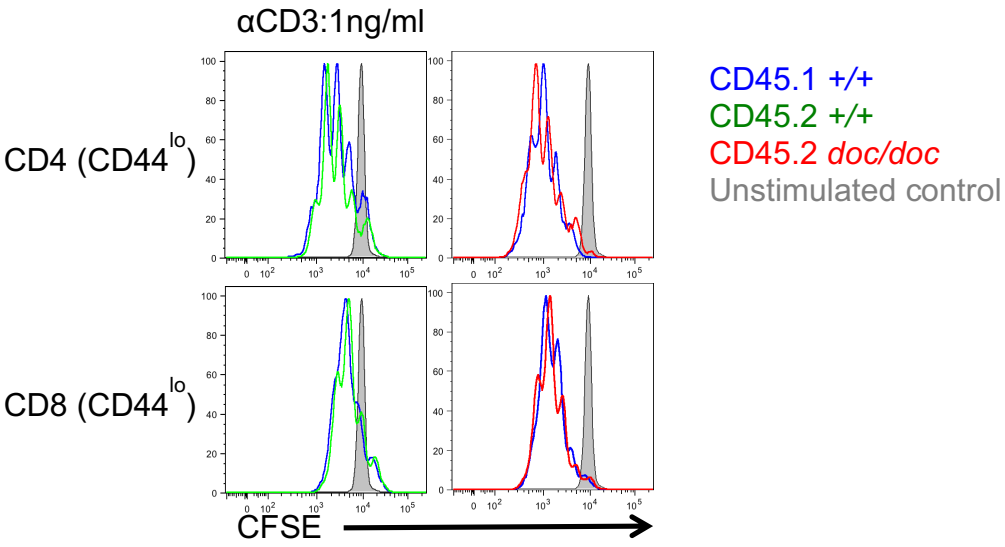

Figure 3.11 In vitro proliferation of wild type and *Dock2*$^{doc/doc}$ T cells. CD45.1 wild type and CD45.2 wild type or *doc/doc* naïve T cells were sorted from spleen and mixed in 50:50 ratio. They were CFSE labeled and stimulated with 1ng/ml of αCD3. Histograms show CFSE fluorescence after 3 days stimulation in CD45.1 wild type internal control T cells (blue histograms) superimposed on CFSE in co-cultured CD45.2 +/+ T cells (green histograms) or CD45.2 *doc/doc* T cells (red histograms) T cells, and CFSE fluorescence in unstimulated cells (shaded grey histogram). This experiment was performed twice.

3.7 DOCK2 deficiency in thymus

Thymocytes were analysed to investigate if the T lymphopenia in *dockland* homozygous mice was caused by a development deficiency in the thymus, as opposed to a survival or migration defect in the periphery. As shown in Figure 3.12A, the proportion of T cell subsets in DN, DP, CD4SP and CD8SP stages in *doc/doc* mice were comparable to wild type mice. The DN stage could be further divided by CD44 and CD25 into DN1, DN2, DN3 and DN4. The *doc/doc* mice had a lower percentage of cells in DN1 stage and higher percentage of cells in DN4 stage. The absolute number for each subset was also calculated (Figure 3.12B). The number of *doc/doc* thymocytes was reduced to 50% of the numbers in wild type mice. The *doc/doc* mice also had significantly less DP cells but there was no difference between *doc/doc* and wild type mice in DN cells. The number of CD4 SP cells in the thymus was also decreased in *doc/doc* mice ($p<0.05$). However, the mutation did not affect the number of CD8 SP cells. The surface expression of CD5 was also measured since its induction reports the strength of pre-TCR signaling in DP T cells and TCR signaling in SP T cells (Azzam et al, 1998) (Figure 3.12C). The expression of CD5 was significantly lower on *doc/doc* mice in DP stage which suggested a lower signaling strength on *doc/doc* mice (DP stage) (Figure 3.12E) but there was no difference in the expression of CD5 between *doc/doc* mice and wild type mice on CD4 and CD8 SP thymocytes.

CD69 is an activation marker that marks thymocytes undergoing positive or negative selection or having just been positively selected (Yamashita et al., 1993). In Figure 3.12C, the *doc/doc* mice had normal CD69 expression on DP stage thymocytes but proportionally more CD69-negative cells among CD4 SP and CD8 SP. CD69 downregulates surface expression of the $S1P_1$ receptor, a G-protein-coupled receptor (GPCR) (Shiow et al., 2006; Alfonso et al., 2006; Bankovich et al., 2010) and the latter is expressed on fully mature thymocytes and required for thymocyte egress to the blood (Allende et al., 2004). The percentage of CD69- CD4 and CD8 SP cells are both significantly higher than wild-type controls (Figure 3.12D left). Since the overall number of DP and SP cells per thymus is diminished, while the number of CD69lo SP cells is not diminished (Figure 3.12D right), this implies that the *doc/doc* SP cells accumulate at the CD69lo stage consistent with a defect in thymus egress. Collectively, these results indicate that the *dockland* mutation cause peripheral T cell lymphopenia at least partly because of decreased T cell formation and export from the thymus.

A

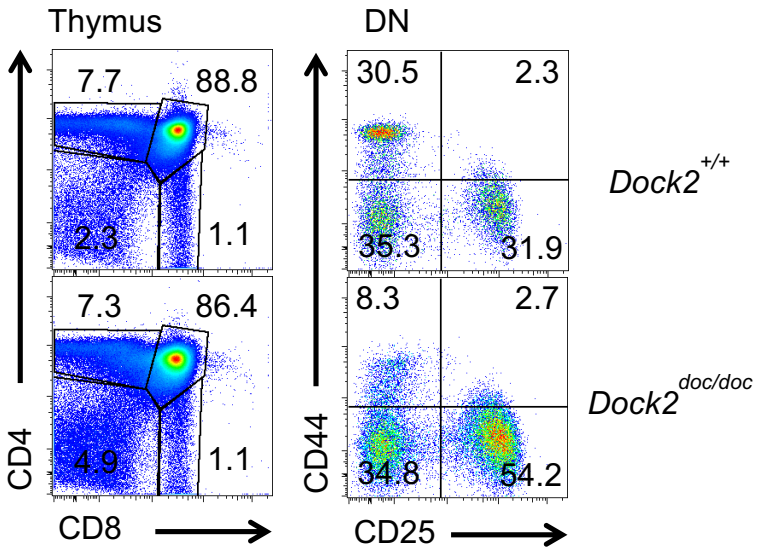
Thymus
DN
7.7
88.8
2.3
1.1
30.5
2.3
35.3
31.9
Dock2+/+
7.3
86.4
4.9
1.1
8.3
2.7
34.8
54.2
Dock2doc/doc
CD4
CD8
CD44
CD25

B

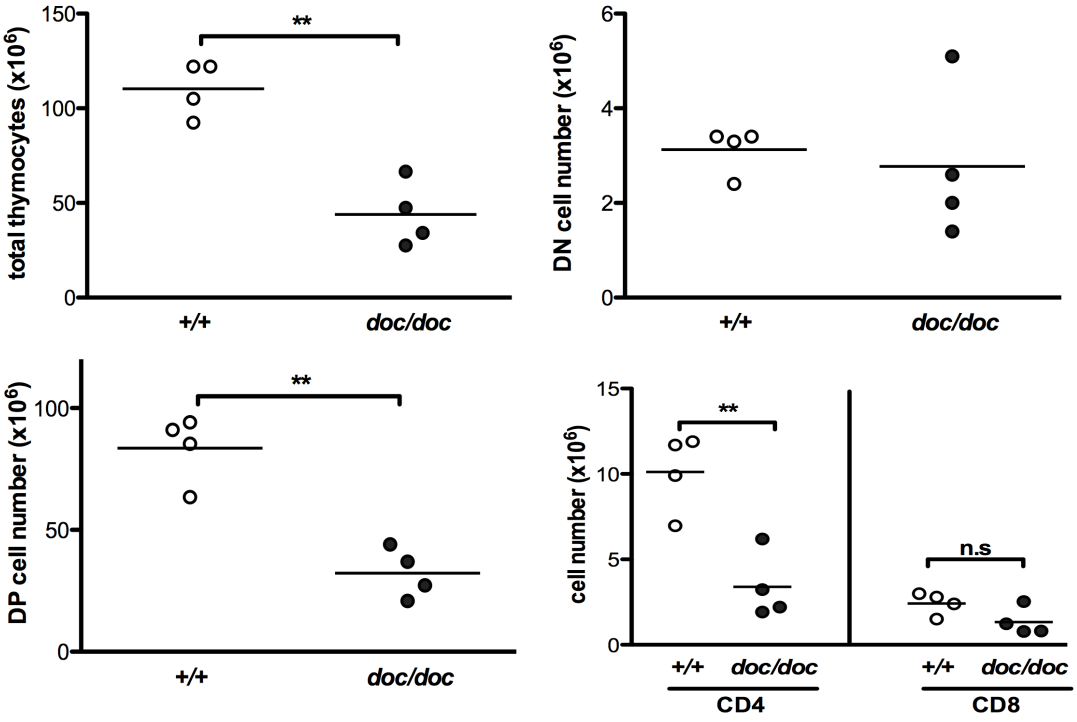
total thymocytes (x10⁶)
150
100
50
0
**
+/+
doc/doc
DN cell number (x10⁶)
6
4
2
0
+/+
doc/doc
DP cell number (x10⁶)
100
50
0
**
+/+
doc/doc
cell number (x10⁶)
15
10
5
0
**
n.s
+/+
doc/doc
CD4
+/+
doc/doc
CD8

C

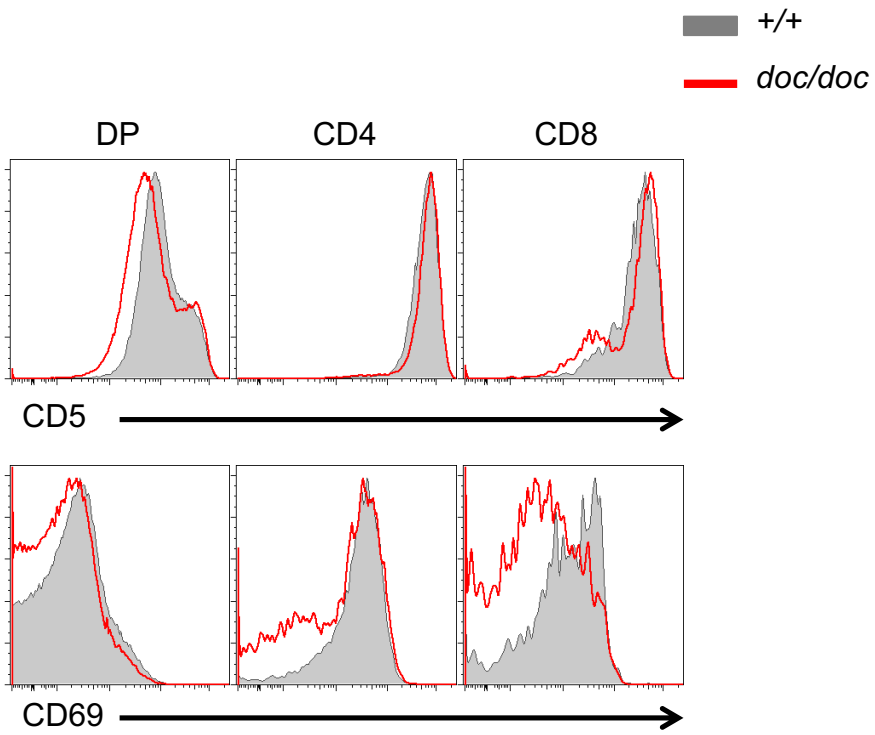
+/+
doc/doc
DP
CD4
CD8
CD5
CD69

D

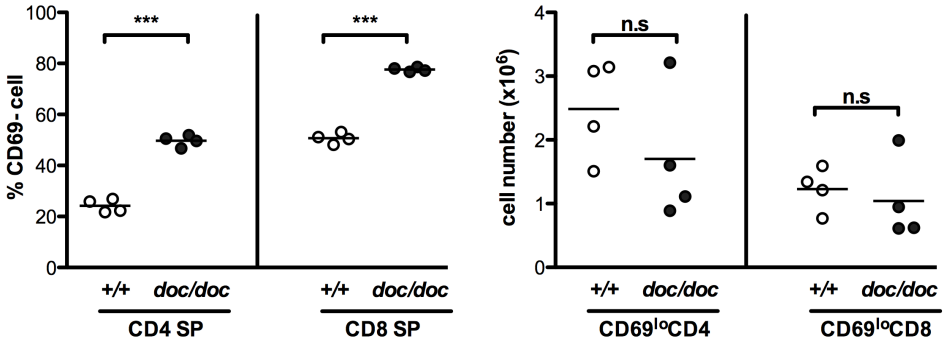
% CD69- cell
100
80
60
40
20
0
***
***
+/+
doc/doc
+/+
doc/doc
CD4 SP
CD8 SP
cell number (x10^6)
4
3
2
1
0
n.s
n.s
+/+
doc/doc
+/+
doc/doc
CD69loCD4
CD69loCD8

E

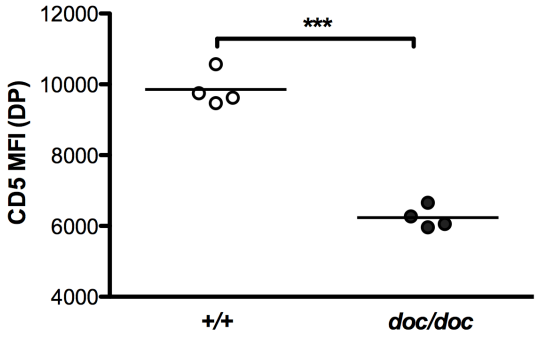

Figure 3.12 Thymic T cell subsets in *dockland* mice. (A) Representative flow cytometry plots of thymocytes from wildtype (+/+) and mutant (*doc/doc*) mice, showing expression of CD4 and CD8 and the percentage of DN ($CD4^-CD8^-$), DP ($CD4^+CD8^+$), CD4 SP ($CD4^+CD8^-$) and CD8 SP ($CD4^-CD8^+$) cells. (B) Quantitation of thymocyte subsets in *Dock2* wild-type (white circles) and *doc/doc* (black circles) C57BL/6J mice. Bar is shown as mean. Statistical analysis by unpaired t-test. This experiment was repeated twice with at least 3 mice in a group. C) Representative overlay histograms of CD5 or CD69 expression on the thymic cell subsets listed on *Dock2* wild-type (grey shaded) and *doc/doc* (red line) mice. D) Percentage of CD69 negative cells of CD4 and CD8 single positive cells (left) and quantitation of CD69 negative CD4 and CD8 single positive cells for *Dock2* wild-type (white circles) and *doc/doc* (black circles) C57BL/6J mice. Bar is shown as mean. Statistical analysis by unpaired t-test. E) CD5 mean fluorescence intensity (MFI) values for *Dock2* wild-type (white circles) and *doc/doc* (black circles) C57BL/6J mice. Statistical analysis by unpaired t-test.

3.8 B cell defects in *dockland* mice

B-cell development occurs primarily in fetal liver and transfers to bone marrow after birth. Originating from a common lymphoid progenitor (CLP), B cell differentiation progresses through pro-B, pre-B and immature B stages based on the different expression of B cell antigen receptor subunits. Hardy et al. identified pro-B cells by cell surface expression of B220, CD43 and c-kit. Four fractions of pro-B cells can be further distinguished by differential expression of heat-stable antigen (HSA) and BP-1 (Hardy, R. et al., 1991). DNA rearrangement begins at this stage in the immunoglobulin heavy chain locus to bring individual D_H and J_H gene segments together. V_H-D_HJ_H rearrangement completes the heavy chain gene to express IgM heavy chains in the endoplasmic reticulum of large pre-B cells (Abbas and Lichtman, 2003). Once light chain rearrangement completes successfully, the cell expresses a unique IgM antigen receptor on its surface as an immature B cell (Abbas and Lichtman, 2003). Immature B cells leave the bone morrow and continue their development into mature B cells in the periphery (Loder, F. et al., 1999).

B cell subsets in bone marrow of *dockland* mice were assessed by flow cytometry and divided into three stages based on their expression of IgD and IgM: Pre and pro B cells ($B220^+$ IgD^-IgM^-), immature B cells ($B220^+$ $IgD^{lo}IgM^{hi}$) and mature B cells ($B220^+$ $IgD^{hi}IgM^{int}$). As shown in Figure 3.13A, *doc/doc* mice had a lower percentage of $B220^+$ B cells compared to +/+ mice. From the bottom panel of Figure 3.13A, *doc/doc* mice had a higher proportion of pre and pro B cells ($IgD^{lo}IgM^{lo}$) (64%) compared to +/+ mice (54%). This might due to the reduction of circulating mature B cells ($IgD^{hi}IgM^{int}$) in *doc/doc* mice (6%) compared to +/+ mice (22%). Percentage of B cell was lower in mice with significant less B cells in *doc/doc* mice (Figure 3.13 B) When the percentage and absolute number of bone marrow B lineage subsets was calculated, there was lower percentage of mature B cells in the bone marrow between homozygous mutant and wildtype mice (Figure 3.13B). All the absolute cells numbers at pre/pro, immature, mature B stages were significant decreased in mutant mice (Figure 3.13B).

A

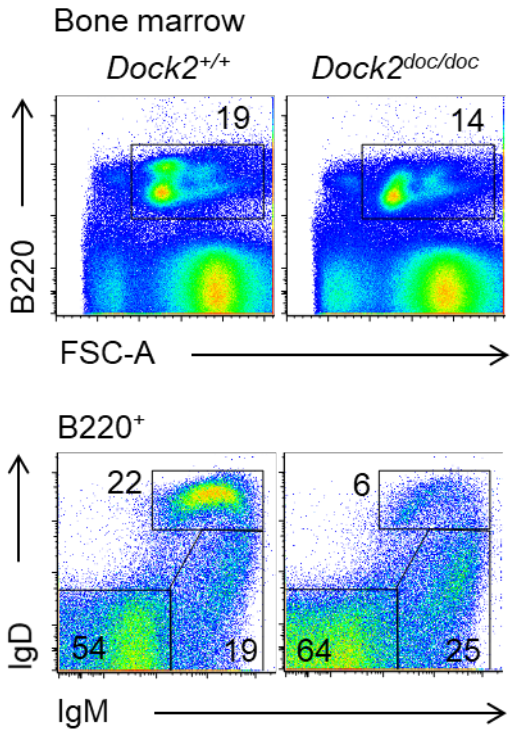
Bone marrow
Dock2+/+
Dock2doc/doc
19
14
B220
FSC-A
B220+
22
6
54
19
64
25
IgD
IgM

B

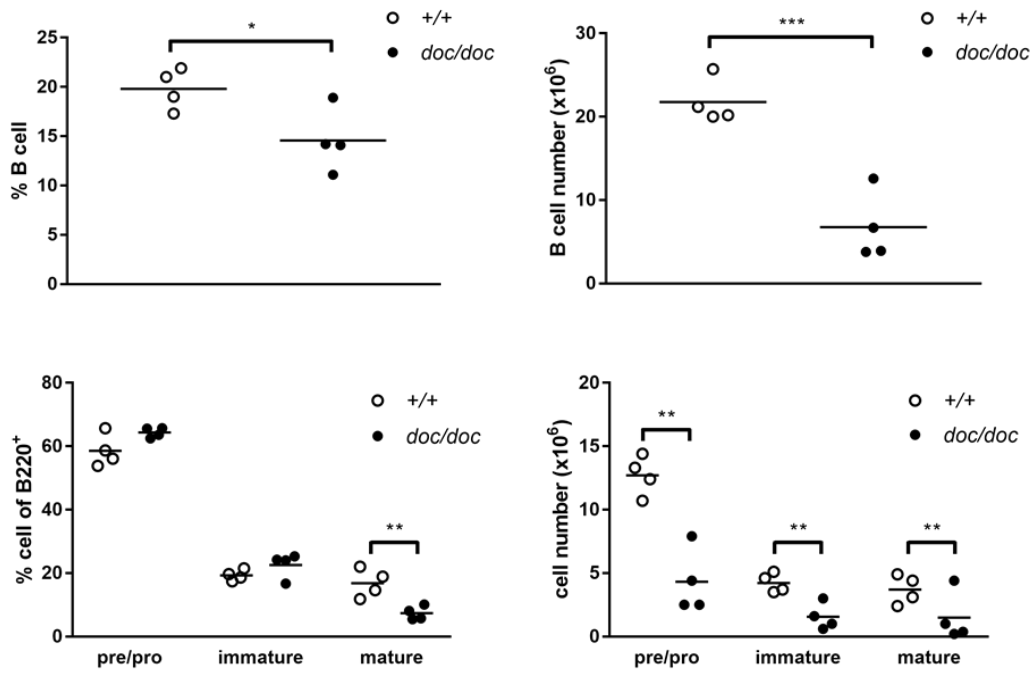
% B cell
B cell number (x10^6)
+/+
doc/doc
*
***
% cell of B220+
cell number (x10^6)
**
pre/pro
immature
mature

Figure 3.13 Bone marrow B cell subsets in *dockland* mice. (A) Representative flow cytometry plots of bone marrow lymphocytes showing the gating strategy to detect the various subsets of bone marrow B-lineage cells ($B220^{+}$): pre and pro B cells ($IgD^{lo}IgM^{lo}$), immature B cells ($IgD^{lo}IgM^{hi}$) and mature B cells ($IgD^{hi}IgM^{int}$). (B) Quantification of cells of the subsets defined in A. Statistical analysis by unpaired t-test and this experiment was repeated twice.

Analysis of subsets of peripheral B cells with wild type, *doc/+* and *doc/doc* mice in the blood is shown in Figure 3.14A. The *dockland* homozygotes had significantly higher percentage of B220+ B cells, which might be secondary to the reduction of T cell subsets shown above (Figure 3.14B left). The surface IgM and IgD expression was also examined on B cells in these three groups of mice (Figure 3.14B right). Among B220+ cells in blood, the percentage of IgD^{hi} mature B2-type B cells was significantly lower in *doc/doc* mice than in heterozygous or wild-type controls, whereas $IgD^{lo}IgM^{hi}$ transitional B cells were significantly higher in *doc/doc* mice. There was no difference observed between *dockland* heterozygous mice and wild type mice.

A

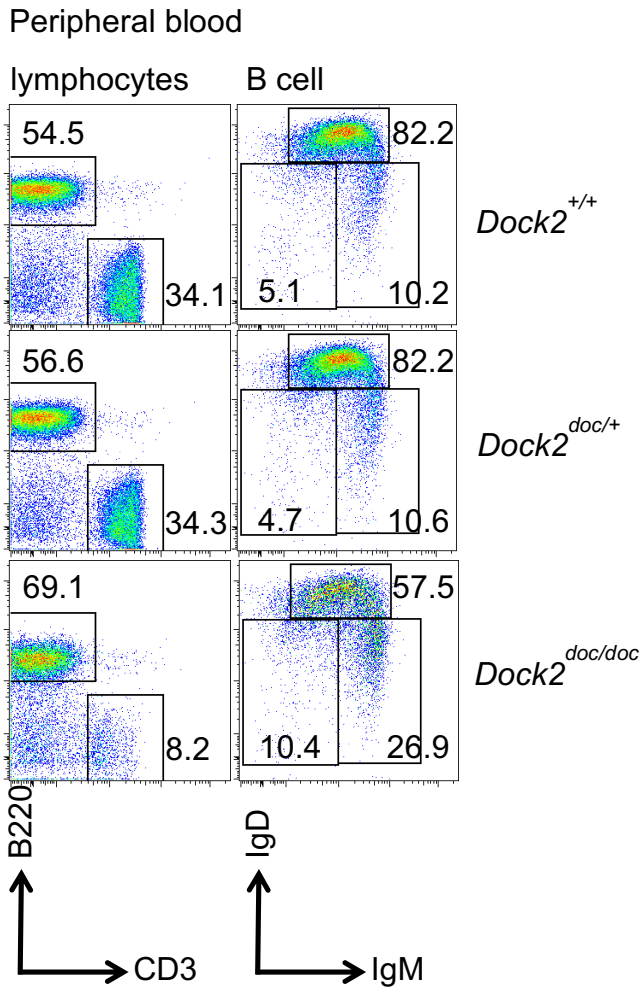
Peripheral blood
lymphocytes
B cell
54.5
34.1
82.2
5.1
10.2
Dock2+/+
56.6
34.3
82.2
4.7
10.6
Dock2doc/+
69.1
8.2
57.5
10.4
26.9
Dock2doc/doc
B220
CD3
IgD
IgM

B

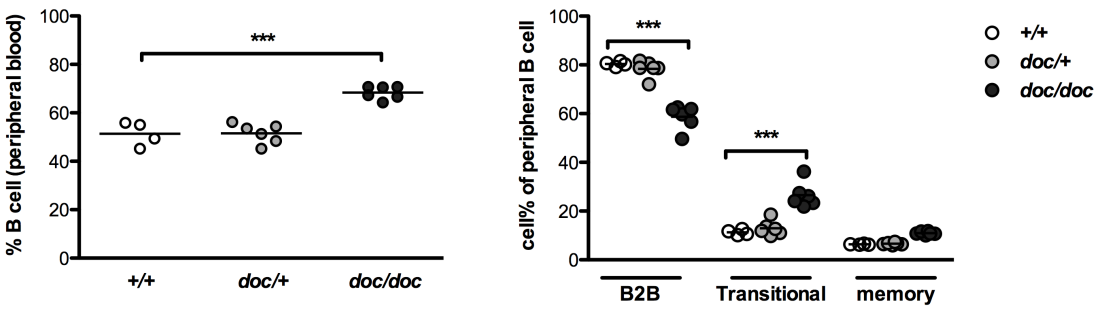
% B cell (peripheral blood)
100
80
60
40
20
0
***
+/+
doc/+
doc/doc
cell% of peripheral B cell
***
***
B2B
Transitional
memory
+/+
doc/+
doc/doc

Figure 3.14 B cell subsets in the blood of *dockland* mice. (A) Representative flow cytometry plots of *doc/doc*, *doc/+* and +/+ mice showing expression of IgD and IgM on $B220^{+}$ cells in the blood, and the percentage of B cells falling with the indicated gates representing mature B2-type B cells (IgD^{hi}), transitional B cells (IgD^{low} IgM^{high}) and switched memory B cells (IgD- IgM-). (B) Left panel: percentage of B cells in blood lymphocytes from wild type (white circles), heterozygous (*doc/+*) and *doc/doc* homozygotes (black circles). Right panel: percentage of B2 B cells, transitional B cells, and memory B cells among total B220+ B cells. Mean is shown as bar and statistical analysis by two-way ANOVA and Bonferroni post-test.

3.9 B subsets in spleen

After development in bone marrow, newly formed immature B cells emigrate initially to the spleen. In spleen, they go through transitional stages and mature into follicular B cells and marginal zone B cells (Vitetta, E.S. et al., 1975; Allman, D.M. et al., 1992; Oliver, A.M. et al., 1997; Cariappa, A. et al., 2007).

The marginal zone B cell subset is a unique population of B cells located in the marginal zone at the border of white and red pulp in the spleen, where blood percolates slowly through the marginal sinus. The marginal zone offers an ideal environment for the resident cells to encounter blood-borne microbes and antigens. Therefore, marginal zone B cells are critical for host immunity in early defense of blood–borne bacterial pathogens. Marginal zone B cells can be distinguished from follicular B cells by slightly larger cell volume, higher expression of CD21, CD1d, CD38, CD9 and CD25. They also express high level of IgM and very low levels of CD23 and IgD (Pillai et al., 2005). The exact developmental mechanisms of marginal zone B cell are still waiting to be elucidated. However, *Notch2* and NF-κB1 seem to play indispensable roles (Lopes-Carvalho and Kearney, 2004; Pillai et al., 2005).

Flow cytometric analysis of splenic B cell subsets in *dockland* mice was based on the Allman classification (Allman and Pillai, 2008). The marker CD93 was used to separate immature B cells ($CD93^{+}B220^{+}$) from mature B cells ($CD93^{-}B220^{+}$). The immature B cells were further divided into T1 ($IgM^{hi}CD23^{lo}$), T2 ($IgM^{hi}CD23^{hi}$), and T3 ($IgM^{lo}CD23^{hi}$). The mature B cells were further divided into follicular cells ($CD21^{int}$ IgM^{int}) and marginal zone B cells ($CD21^{hi}IgM^{hi}$) which can be subdivided into marginal zone cells ($CD23^{lo}B220^{+}$) and marginal zone precursor (MZP) cells ($CD23^{hi}B220^{+}$) by using the marker CD23.

Representative plots from a *doc/doc* homozygous mouse (16NIH19a:G3#22) compared with a wild-type littermate (16NIH19a:G3#23) are shown in Figure 3.15. Although *doc/doc* mice had a lower percentage of $B220^{+}CD19^{+}$ cells compared to wild-type littermates, there was no difference in the surface marker expression of T1, T2 or T3 B cell subsets. In the mature B cells, there was no difference in the marker of follicular or marginal zone precursors. However, there were significantly fewer marginal zone B cells in *doc/doc* mice.

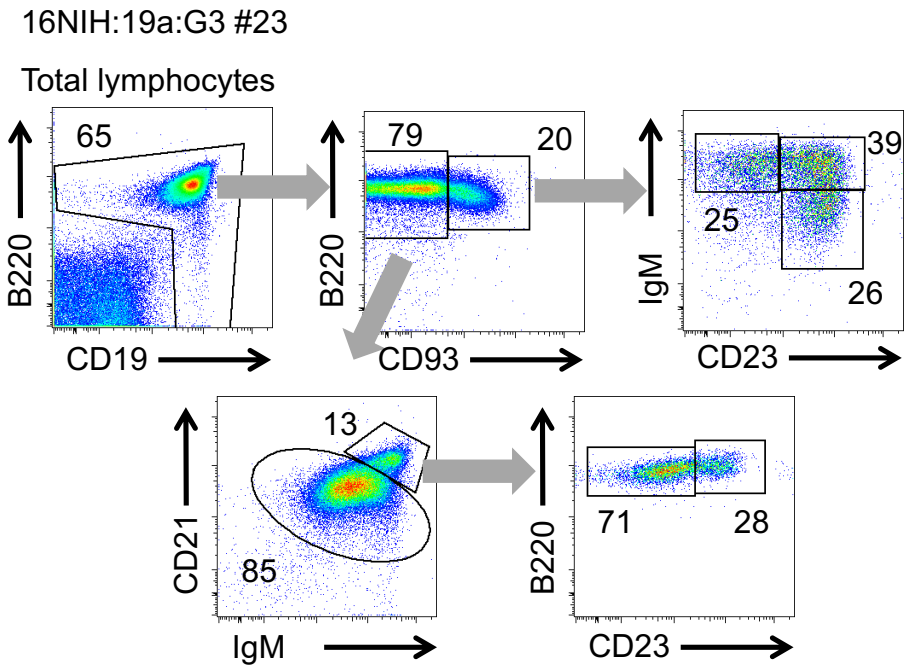

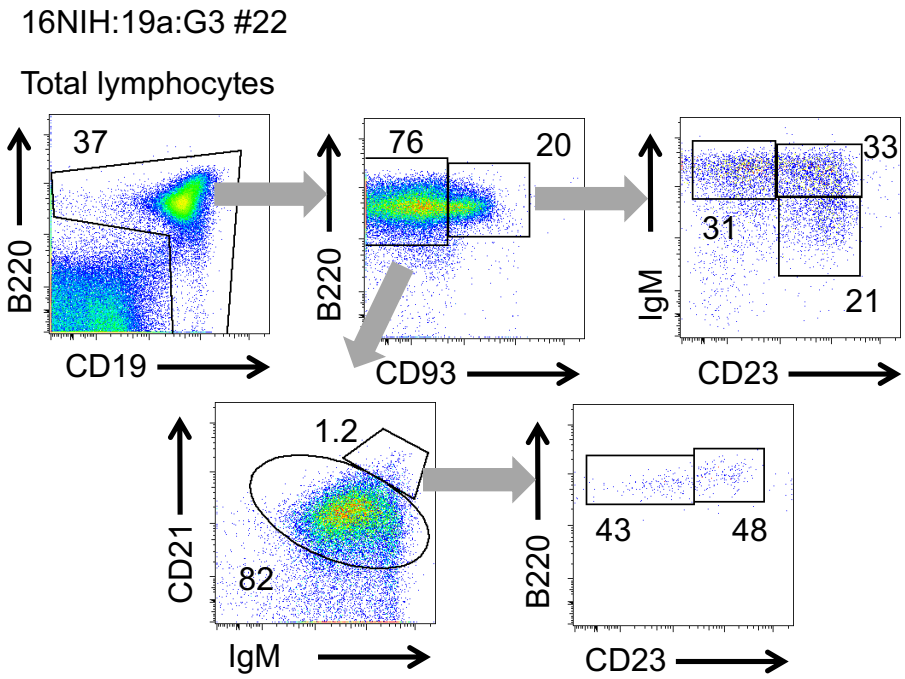

Figure 3.15 Splenic B cell subsets in *dockland* mice. A. Representative flow cytometry plots of $B220^{+}CD19^{+}$ splenocytes, subgated as $CD93^{+}$ and $CD93^{-}$. $CD93^{+}$ cells were subsequently subgated into T1 ($IgM^{hi}CD23^{lo}$), T2 ($IgM^{hi}CD23^{hi}$), and T3 ($IgM^{lo}CD23^{hi}$) subsets. The $CD93^{-}$ B cells were further divided into follicular cells ($CD21^{int}$ IgM^{int}) and marginal zone B cells ($CD21^{hi}IgM^{hi}$) which can be subdivided into marginal zone cells ($CD23^{lo}B220^{+}$) and marginal zone precursor (MZP) cells ($CD23^{hi}B220^{+}$) by using the marker CD23 for *Dock2* +/+ wildtype (upper panel) and *doc/doc* (lower panel) mice

When the absolute number of each splenic B cell subset was calculated in multiple animals of each genotype (Figure 3.16), *doc/doc* mice had a significantly lower B cell number per spleen compared to wild-type mice, with a 3.7-fold reduction in mean B cell number. Upon further subdivision, *doc/doc* mice had significantly less cells in T1, T2 and T3 subsets (T1: decreased 3.4-fold, $p=0.0003$; T2 decreased 6.3-fold, and T3 decreased 6-fold, $p<0.0001$). Compared

to wild-type mice, *doc/doc* animals also had 5-fold fewer mean number of follicular B cells ($p<0.0001$) and 59-fold fewer marginal zone B cells ($p=0.001$).

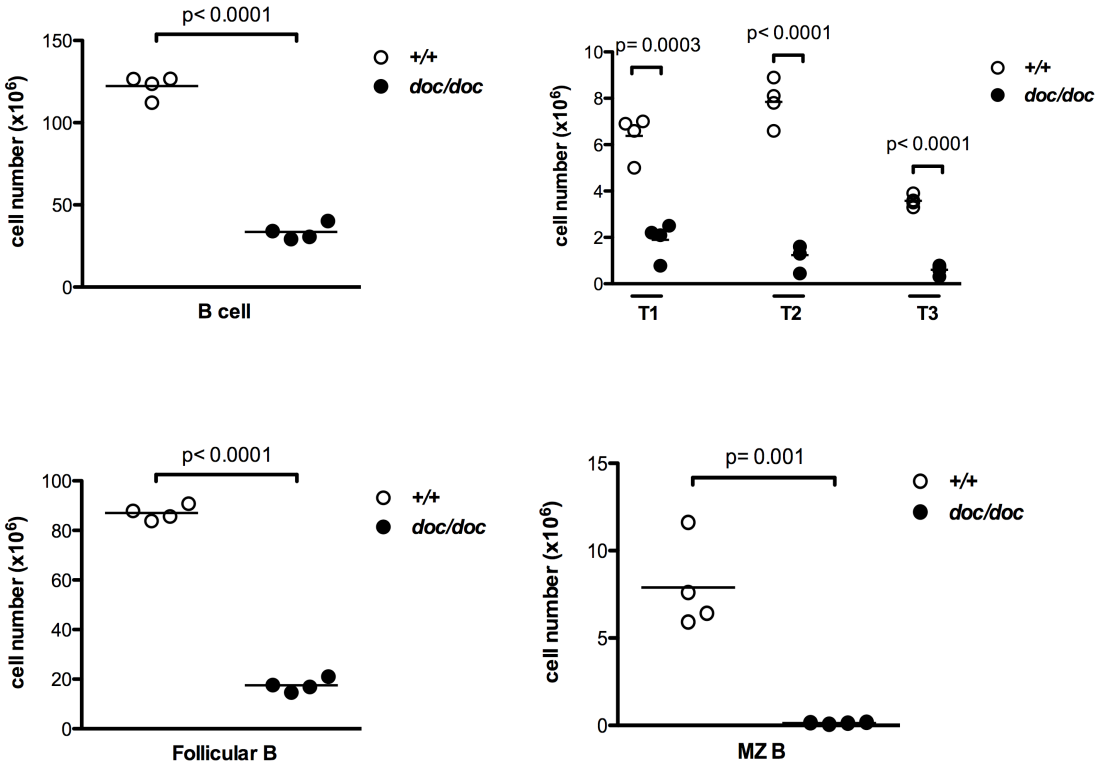

Figure 3.16 Absolute number of B cell subsets in spleen of individual *dockland* mice and wild-type controls. Absolute number of total B cells, T1-3 transitional, follicular and marginal zone B cells for *Dock2* wild type (white circles) and homozygous mutant (*doc/doc*, black circles) mice. Statistical analysis by unpaired t-test.

3.10 Analysis of mixed bone marrow chimeras

The results above were performed in animals with mutant DOCK2 in all cells and tissues. To establish which of these traits were due to DOCK2 deficiency within haematopoietic cell subsets, and to understand the behavior of *Dock2*$^{doc/doc}$ cells in a competitive environment alongside blood cells with wild type DOCK2, 50:50 mixed bone marrow chimeras were set up by transplanting mixtures of CD45.1 +/+ and CD45.2 +/+ or *doc/doc* bone marrow cells. The bone marrow cell mixtures were injected into irradiated CD45.1 B6 recipient mice and allowed 8 weeks for engraftment and reconstitution before they were bled, and mixed chimeras were sacrificed for spleen cell analysis at week 10 after marrow transplant (Figure 3.18A).

The irradiated recipients were bled after 8 weeks of reconstitution. Mice that received a mix of 50% wild type CD45.1 and 50% *doc/doc* CD45.2 bone marrow showed less CD45.2 peripheral B cells ranging between 7% to 40% in individual chimeric animals (numbered 1 through 10) (Figure 3.17A). For control mice reconstituted with 50% CD45.2 wild-type bone marrow, CD45.2 cells accounted for 30%-60% of total B cells (numbered 11 through 20). Less than 1% of T cells came from CD45.2 *doc/doc* bone marrow cells in recipient mice reconstituted with 50% wild type CD45.1 and 50% *doc/doc* CD45.2 bone marrow, whereas 20-40% of T cells were CD45.2 derived in control chimeras where the CD45.2 marrow has wild-type DOCK2. Blood granulocytes were also analysed to provide a measure for the composition of their hematopoietic stem cell precursors, since granulocyte lifespan is short and their composition is not distorted by the processes of proliferation in the thymus or secondary lymphoid tissues that affect T and B cells. The mean percentage of CD45.2 cells among granulocytes did not differ significantly between recipients of CD45.2 wild-type or *doc/doc* marrow (Figure 3.17B), establishing that the *doc/doc* marrow engrafted comparably to wild-type marrow.

A

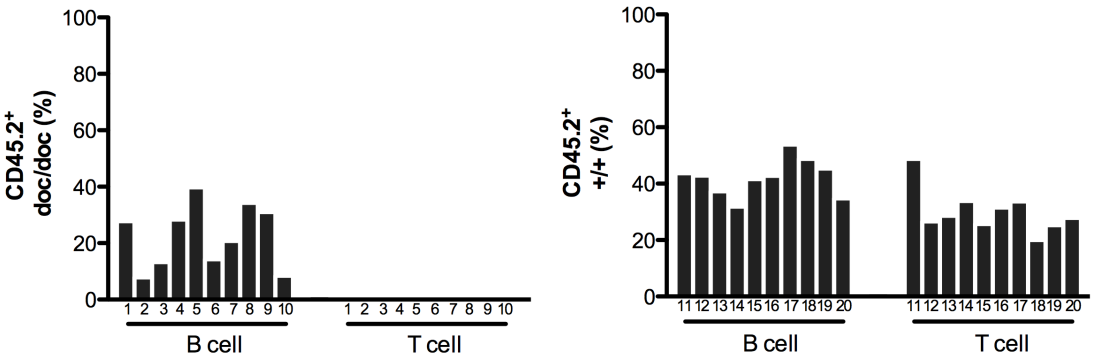
CD45.2+ doc/doc (%)
100
80
60
40
20
0
1 2 3 4 5 6 7 8 9 10
B cell
1 2 3 4 5 6 7 8 9 10
T cell
CD45.2+ +/+ (%)
11 12 13 14 15 16 17 18 19 20
B cell
11 12 13 14 15 16 17 18 19 20
T cell

B

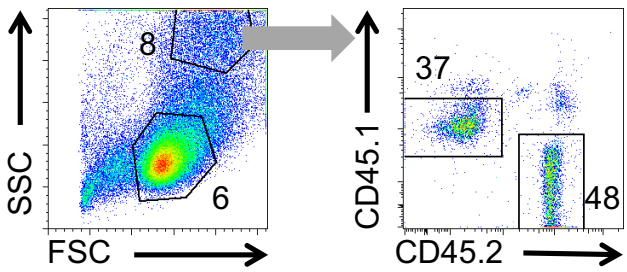
SSC
FSC
8
6
CD45.1
CD45.2
37
48

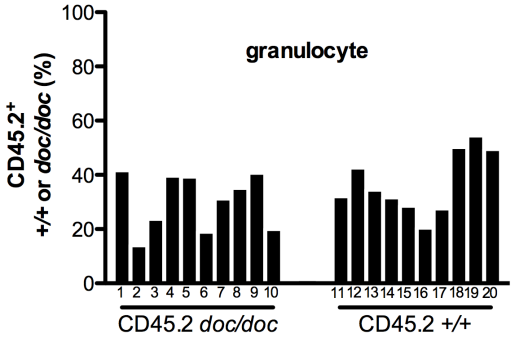
granulocyte
CD45.2+ +/+ or doc/doc (%)
100
80
60
40
20
0
1 2 3 4 5 6 7 8 9 10
CD45.2 doc/doc
11 12 13 14 15 16 17 18 19 20
CD45.2 +/+

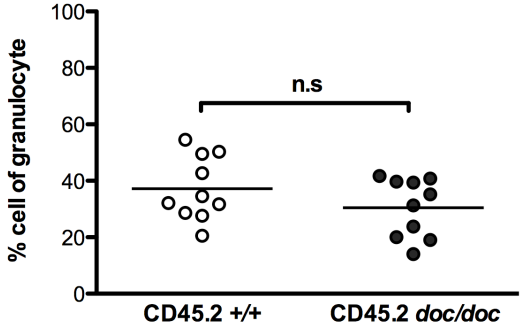

Figure 3.17 Analysis of peripheral blood from mixed bone marrow chimeras. A) Each column shows data for a single, numbered chimeric animal 8 weeks after irradiation and transplantation with a mixture of CD45.1 +/+ marrow and CD45.2 doc/doc or +/+ marrow. For each chimeric animal, the bar shows the percentage of CD45.2 *doc/doc* or CD45.2 +/+ cells within the B or T cell subsets. B) Each column shows data for a single, numbered chimeric animal 8 weeks after irradiation and transplantation with a mixture of CD45.1 +/+ marrow and CD45.2 doc/doc or +/+ marrow. For each chimeric animal, the bar shows the percentage of CD45.2 *doc/doc* or CD45.2 +/+ cells within the granulocyte subset (top). Relative percentage of CD45.2 wild type (+/+, white circles) and *dockland* (*doc/doc*, black circles) granulocytes in the recipient mice (bottom). Dots represent single mice and the bars represent the mean (statistical analysis by unpaired t-test).

Analysis of the spleen in each chimera is shown in Figure 3.18B. Less than 2% of CD4 or CD8 T cells were derived from the CD45.2 *doc/doc* donor, in contrast to 30% CD45.2 +/+ in control mixed chimeras (Figure 3.18B right panel). Naïve ($CD44^{lo}$) and activated ($CD44^{hi}$) CD4 and CD8 T cells were also analysed based on the expression of CD44 marker in Figure 3.18C. There were less than 1% of T cells in each of these subsets derived from the CD45.2 *doc/doc* bone marrow cells.

It was noticed that there were less than the expected mean of 50% CD45.2 +/+ cells in the T cell subset of the control mixed chimeras after 8 weeks' reconstitution. The likely reason for this is that memory T cells are known to be radioresistant and hence recipient-derived CD45.1+ memory T cells proliferate in response to lymphopenia during the reconstitution phase after irradiation and add to the CD45.1^{+} population derived from the donor marrow. For more accurate results, RAG1 deficient mice could be used as recipients. The effect of recipient T cell reconstitution was nevertheless controlled for in the experiments here by comparing the frequency of CD45.2+ donor derived T cells in control chimeras, where the CD45.2+ cells had wildtype *Dock2*, and test chimeras where the CD45.2+ cells had mutant *Dock2*. By this comparison, it was clear that the *Dock2* mutation acts cell autonomously in T cells to diminish either their production by the thymus or their accumulation in the periphery. To answer this question, thymus of in each chimera were analysed (Figure 3.19) The CD45.2^{+} *doc/doc* bone marrow cells only constituted less than 20% of total DN cells. The percentage was further reduced in DP stages and more mature CD4 and CD8 SP stages. It suggests that the mutant T cells were outcompeted at the DP stage.

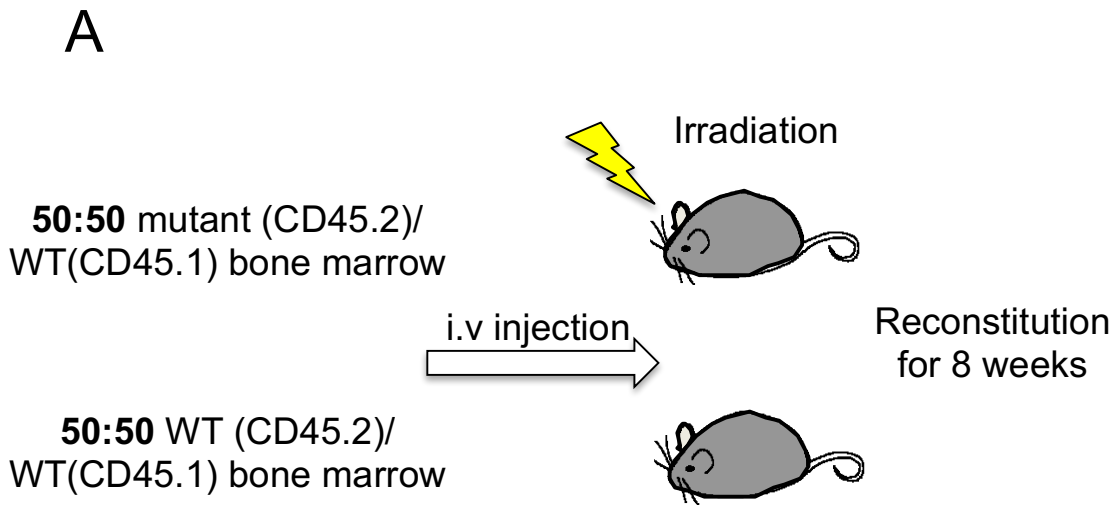

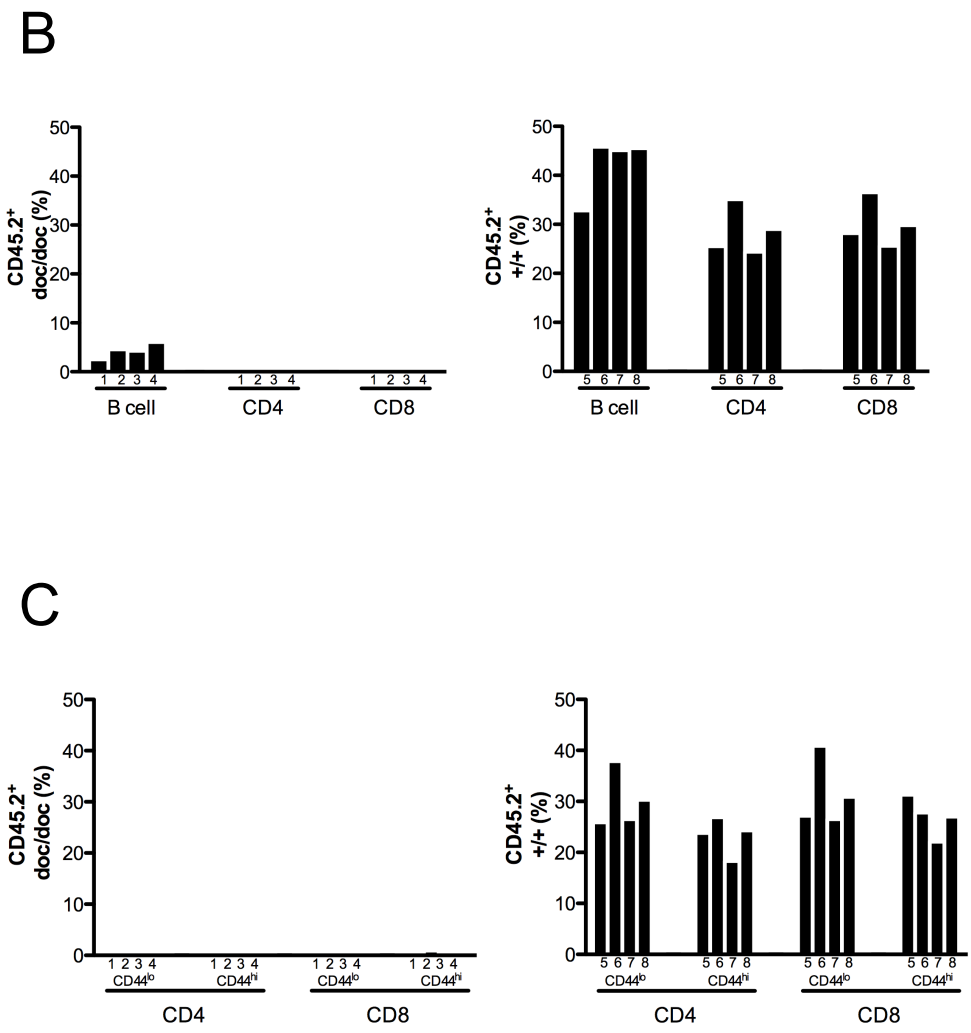

Figure 3.18 Bone marrow chimeras reveal profound T cell deficiency caused by *dockland* mutation during competitive repopulation. A) Schematic of 50:50 bone marrow chimera experiments. Bone marrow cells from CD45.1 WT and CD45.2 *doc/doc* or +/+ (WT) cells were injected into irradiated CD45.1 B6 recipient mice and the recipients were taken down after 10 weeks for spleen cell analysis. B) Each column corresponds to a single, numbered chimeric animal and shows the percentage of CD45.2 *doc/doc* or +/+ cells within the B, CD4 or CD8 T cell subsets (upper panel) and within the naïve ($CD44^{lo}$) and activated ($CD44^{hi}$) CD4 and CD8 T cell subsets (lower panel).

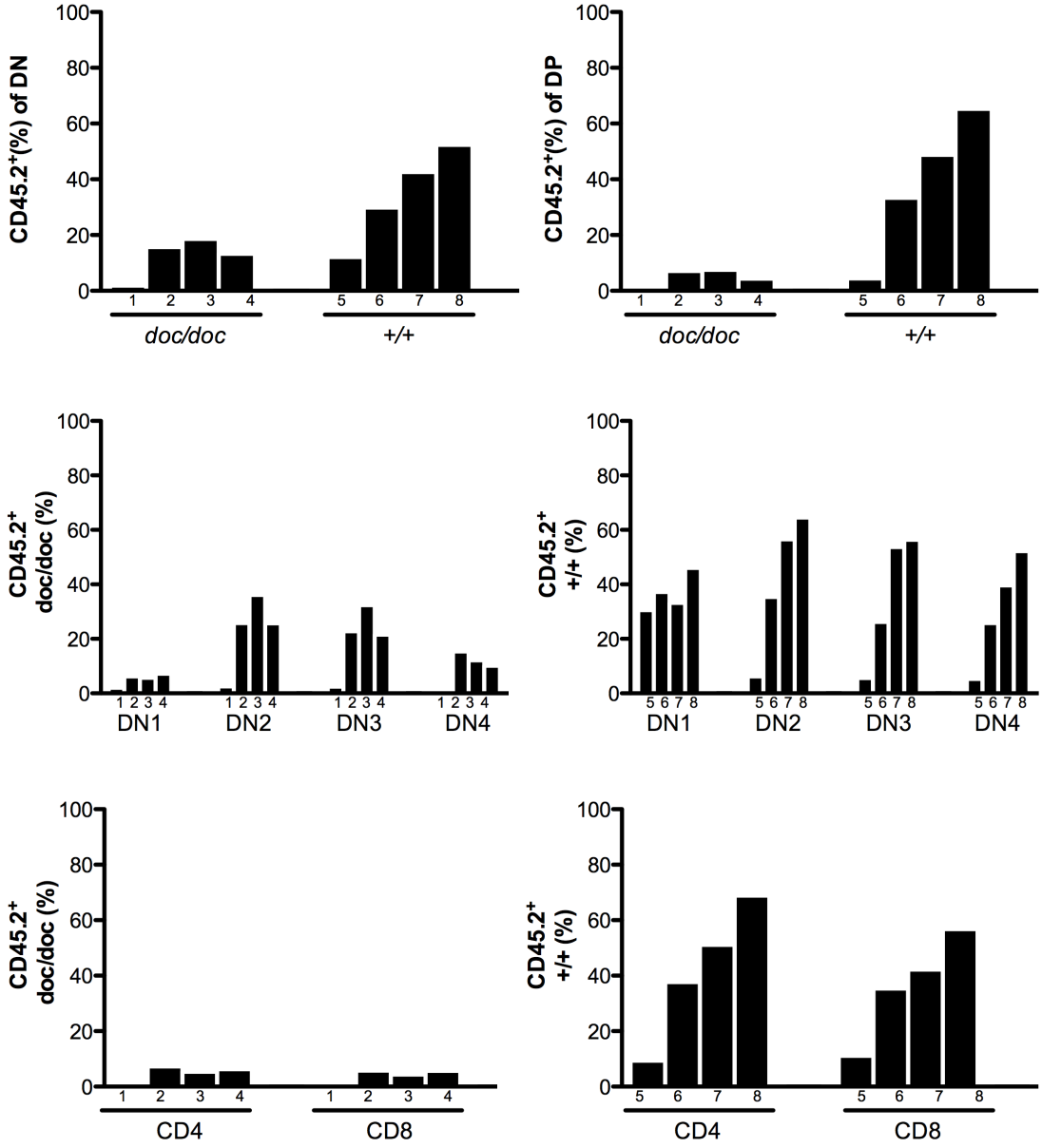

Figure 3.19 Bone marrow chimeras reveal profound T cell deficiency caused by *dockland* mutation under competitive environment. Each column corresponds to a single, numbered chimeric animal and shows the percentage of CD45.2 *doc/doc* or +/+ cells DN DP stages (upper panel), DN1-DN4 stages (middle panel) and CD4 and CD8 single positive stages (lower panel).

To investigate whether the reduction in B cell subsets in the spleen observed in Fig 3.8 was due to an intrinsic defect in the B cells, spleen cells from the same 50:50 mixed bone marrow chimeras were analysed. As shown in Figure 3.18B, 30-40% of splenic B cells ($B220^{+}$) were derived from $CD45.2^{+}$ cells with wild-type *Dock2* in the control chimeras. However, CD45.2 *doc/doc* bone marrow cells only constituted 2-6% of splenic B cells in each of the test chimeras. As shown in Figure 3.20, there were 3-10% CD45.2 *doc/doc* cells in T1; 1-3% in T2 and 1-5 in T3 stage compared to 20-80% of CD45.2 +/+ cells in T1, 20-65% in T2 and 20-65% in T3 stage in control chimeras. There was 2-7% of follicular B cells were contributed by *doc/doc* bone marrow cells compared to 35-50% came from CD45.2 +/+ in control group. There were even fewer (0.17-0.33%) CD45.2 *doc/doc* cells within the marginal zone B cell subset. From the data showing here, it seems clear that *doc/doc* cells have a development disadvantage in a competitive environment. But because of the absence of a reference cell population unaffected by the mutation in *Dock2*, it is impossible to demonstrate the expected percentage of CD45.2 +/+ cells in each population and to perform a statistical test against the reference populations.

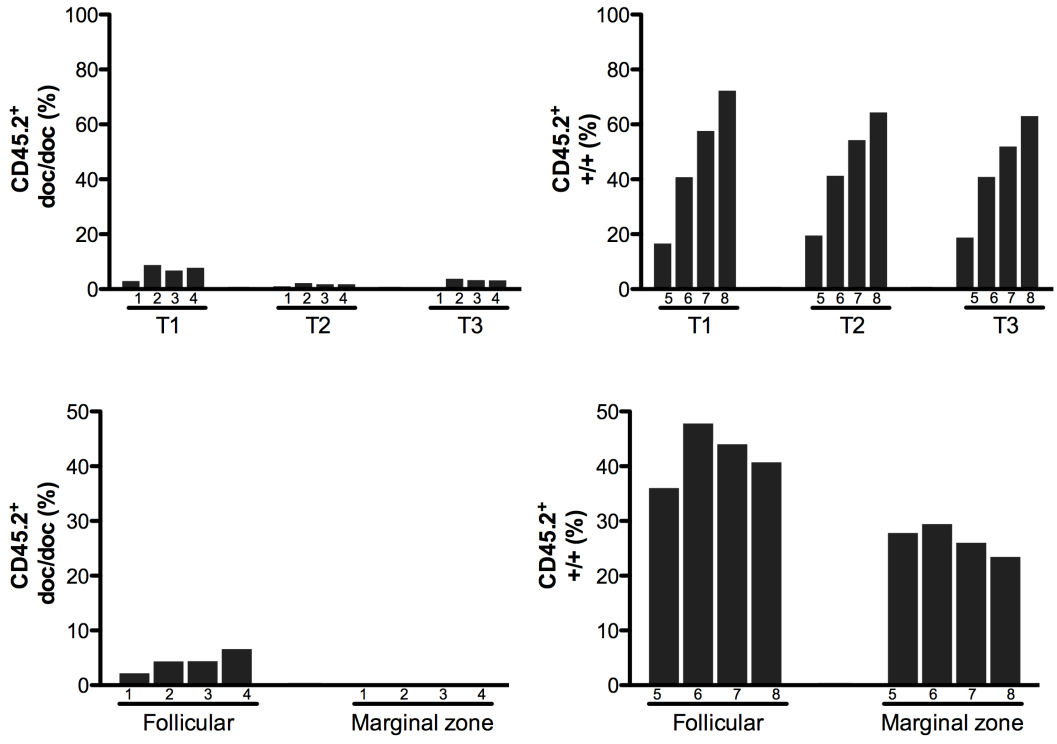

Figure 3.20 Bone marrow chimeras reveal B cell deficiency under competitive environment. Each column indicates the percentage of CD45.2 *doc/doc* or +/+ T1-3 transitional B cells (upper panel) and follicular and marginal zone B cells (lower panel) in an individual, numbered chimeric mouse after 10 weeks reconstitution.

To investigate if *dockland* mutant B cells have normal T cell-dependent antibody response, germinal centre reactions were also studied in the 50:50 mix bone marrow chimeras. Germinal centres (GC) develop within B cell follicles when B cells are activated by T follicular helper cells (MacLennan, 1994). The germinal centre B cells could be detected by flow cytometry as having high expression of the markers of GL7 and CD95 (Han et al., 1997). The reconstituted chimeric mice were immunized with sheep red blood cells (SRBCs), which elicits a rapid and reproducible germinal response.

The bone marrow chimeras were allowed to reconstitute for 8 weeks and were then immunized with SRBC and spleen cells analysed 7 or 10 days later. The contribution of CD45.2 *doc/doc* or +/+ cells to GC B cells 10 days after immunization is shown in Figure 3.21A. The immunization resulted in a clear population of GC B cells in each recipient mouse. Analysis of GC B cells (Figure 3.21B) revealed a mean of only 0.18% of GC cells at day 7 and 0.63 % of GC cells at day 10 were derived from CD45.2 *doc/doc* bone marrow. By comparison, in the wild-type control mixed chimeras, there was a mean of 23.2% (day 7) and 17.6% (day 10) of GC B cells derived from CD45.2 wild-type bone marrow. As CD45.2 *doc/doc* B cells have much lower overall frequency, their relative capacity to make GC cells was examined by measuring the percentage of GC cells among the CD45.2+ B cells in the spleen of each immunized chimera (Figure 3.21C). There was a small but significantly lower mean of 1.6% GC cells among CD45.2 *doc/doc* B cells compared with a mean of 3.4% GC cells among CD45.2 +/+ B cells on day 7. This apparent difference between CD45.2 +/+ and *doc/doc*

B cells in forming GC cells was not observed 10 days of immunization (Figure 3.21C right). More experiments (possibly in mice receiving 80% *doc/doc* BM cells) to increase the frequency of mutant GC B cells would be required.

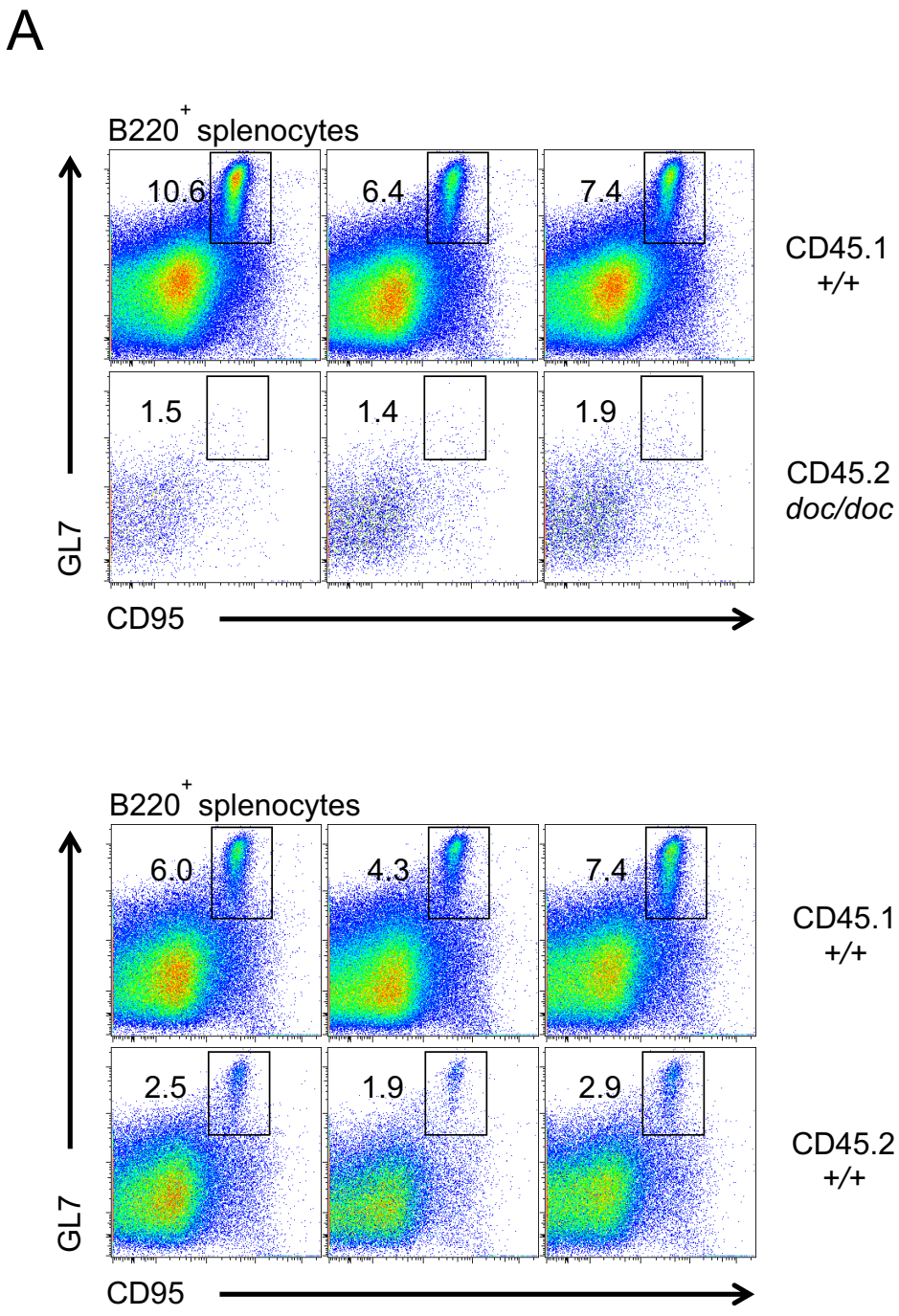

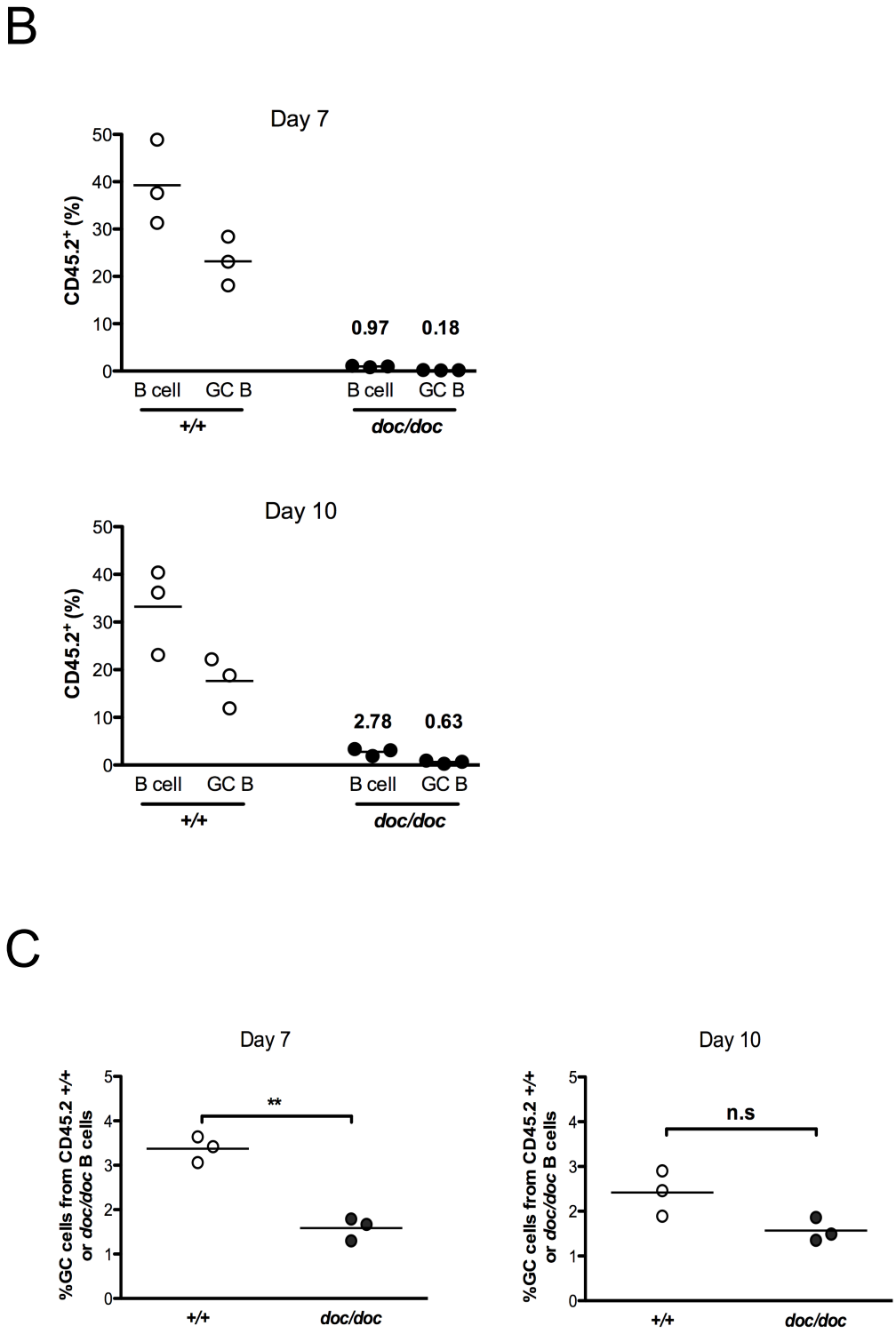

Figure 3.21 Effect of the *dockland* mutation on formation of germinal centre B cells after immunization of mixed chimeras with sheep red blood cells (SRBC). (A) Representative flow cytometry plots from three

mixed bone marrow chimeras receiving CD45.1 wild type (+/+) and CD45.2 *doc/doc* bone marrow (upper panel) and from three control chimeras reconstituted with CD45.1 wild type (+/+) and CD45.2 wild type (+/+) marrow (lower panel). Plots are gated on splenic B220+ CD45.1+ or CD45.2+ cells 7 days after immunization with sheep red blood cells, and numbers show the % of gated cells that are Fas+ GL7+ germinal centre B cells. (B) Relative percentage of CD45.2 wild type (+/+, white circles) and *dockland* (*doc/doc*, black circles) cells among all splenic B cells and among germinal centre B cells 7 days after immunization with sheep red blood cells (upper panel) and 10 days after immunization (lower panel) with mean shown for *doc/doc* mice. (C) Percentage of GL7+ Fas^{hi} GC cells among all CD45.2+ B cells 7 or 10 days after immunization of chimeras transplanted with CD45.2 wild type (+/+, white circles) or CD45.2 *dockland* (*doc/doc*, black circles) marrow. Dots represent single mice, and bars are arithmetic means. Statistical analysis by t-test.

3.11 NKT cells in the *dockland* mice

NKT cells were first described in 1995 as a subset of T cells expressing the NK1.1 marker (in mouse) and share some characteristics with natural killer (NK) cells (Makino, Y. et al., 1995). Type I NKT cells, or invariant NKT (iNKT) cells, are characterized by the expression of a particular TCR alpha chain formed by a canonical rearrangement of the Vα14 gene segment to the Jα18 gene segment in mice (Matsuda et al., 2008). NKT cells recognize glycolipids such as alpha-galactosylceramide (αGalCer) presented by the MHC class-I like molecule CD1d and are selected at the DP thymocyte stage by CD1d-expressing DP cells.

Splenic iNK T cells in the *dockland* mice were analysed by staining with CD1d tetramers (Figure 3.22). There were fewer tetramer binding ($CD1d^{+}$) $CD3^{+}$ cells in the spleen of *doc/doc* mice expressed as a percentage of total lymphocytes (Figure 3.22A). The absolute number of iNKT cells in spleen was also calculated. As

shown in Figure 3.22B, the *doc/doc* mice had significantly less iNKT cells compared to *doc*/+ (p=0.003) and +/+ (p<0.0001), whereas there was no difference between *doc*/+ and +/+ mice.

A

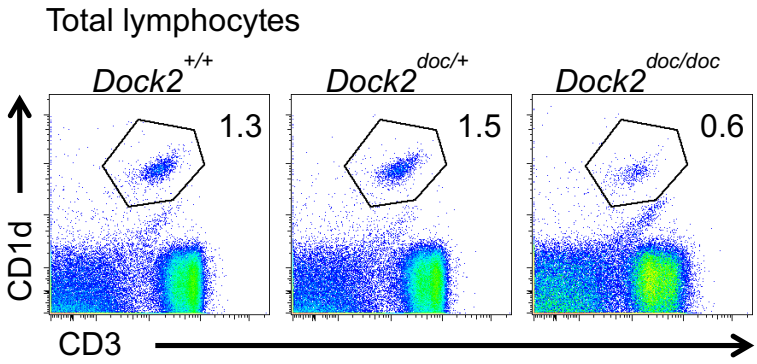

B

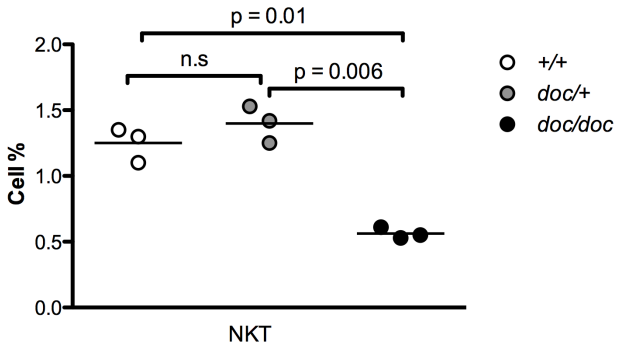

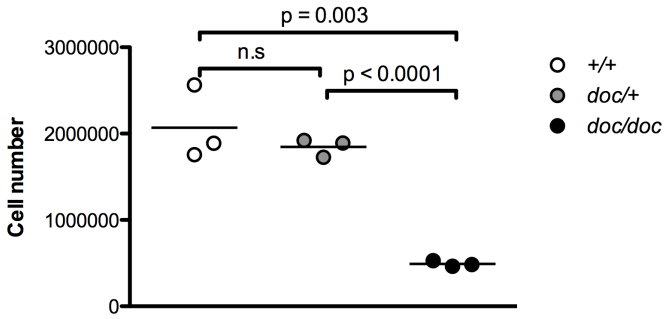

Figure 3.22 Analysis of NKT cells in the spleen. A. Representative flow cytometry plot of spleen from wild type (+/+) and *dockland* (*doc/doc*) mice, stained with fluorescent CD1d-αGalCer tetramers and antibody to CD3. B. Quantitation of spleen NKT cells in *Dock2* wild type (white circles) and homozygous *doc/doc* mutant (black circles) as percentage of the lymphocyte gate and as absolute numbers. Mean is shown in bar and statistical analysis by two-way ANOVA and followed by Bonferroni post-test. This experiment has been repeated twice.

To understand if the decreased numbers of splenic NKT cells in *doc/doc* mice was due to developmental deficiency or a defect in migration/survival, thymic NKT cells were also analysed (Figure 3.23). There were fewer $CD1d^{+}$ $CD3^{+}$ cells present in the thymus of *doc/doc* mice expressed as a percentage of lymphocytes (Figure 3.23A), and their absolute number was decreased 10-fold compared to wild type mice (p=0.0005) (Figure 3.23B).

A

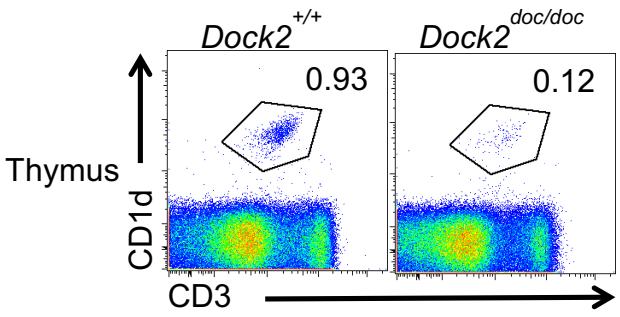

B

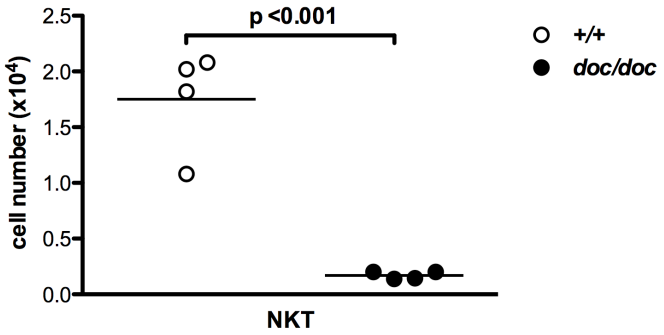

Figure 3.23: Analysis of NKT cells in the thymus. A. Representative flow cytometry plot of thymic NKT cells from wild type (+/+) and *dockland* (*doc/doc*) mice. B. Quantitation of thymic NKT cells in wild type (white) and *doc/doc* (black circles) as absolute numbers per thymus. Mean is shown in bar and statistical analysis by unpaired t-test. This experiment has been repeated twice.

3.12 Comparison of influenza CD8 T cells response in DOCK2 deficient and DOCK8 deficient mice

Previously, Katrina Randall discovered a novel mutation in mouse *Dock8* gene named *primurus*. DOCK8 is also a member of DOCK family proteins and in DOCK-C subgroup (Fig. 3.5). DOCK8 is guanine nucleotide exchange factor (GEF) for Cdc42 and involved in the cytoskeletal rearrangements (Harada et al., 2012 and Côté et al., 2007). The Dock8$^{pri/pri}$ mutation is a T-to-C substitution that changed codon 1827 from a highly conserved serine residue to a proline residue in its DHR2 domain (Randall et al., 2009). Dock8$^{pri/pri}$ B cells were unable to form marginal zone B cells or to persist in germinal centers and undergo affinity maturation. The Dock8$^{pri/pri}$ mice also have a cell autonomous reduction in peripheral naive T cells. The study of Dock8 in mouse is complemented by the independent discovery of DOCK8 mutations associated with immunodeficiency

in human. DOCK8 deficient patients have various viral infections and allergic diseases due to defects of different lymphocyte populations (Zhang et al., 2009).

DOCK2 and DOCK8 deficiency appear to have similar effects, causing a lack of marginal zone B cells and T lymphopenia. To study if DOCK2 and DOCK8 play a similar role in the survival of memory CD8 T cells in a polyclonal repertoire, groups of mutant or control mice were challenged with influenza virus to measure the primary and secondary immune response. *Dock2*$^{doc/doc}$, *Dock8*$^{pri/pri}$ and wild type C57BL/6 mice were intra-peritoneally challenged first with a modified H3N2 influenza A virus expressing SIINFEKL (HKx31-SIINFEKL) followed by a secondary challenge with a serologically non-crossreactive H1N1 strain of influenza A virus expressing the same nucleoprotein (NP) and SIINFEKL (PR8-SIINFEKL). The percentage of antigen-specific CD8 T cells that bound H2-D^{b} MHC tetramers bearing the dominant influenza NP peptide epitope, $NP_{366-374}$ (NP+), among blood lymphocytes was analysed over time points representing different stages of the antigen-specific immune response: expansion, contraction and recall response. Two independent experiments were performed with different time lengths between primary and secondary challenge (Expt 1, Figure 3.24; Expt 2, Figure 3.25). NP-tetramer binding CD8 cells were enumerated both as a percentage of all lymphocytes, and as a percentage of CD8 cells to normalize for the decreased overall numbers of CD8 T cells in *doc/doc* mice.

At day 7 post primary challenge with HKx31, NP^{+} CD8 T cells had undergone clonal expansion to comprise a mean of 1.9% in total lymphocytes of wild type mice. The *Dock2*$^{doc/doc}$ mice had 0.35% NP positive cells, which was significantly lower than +/+ in both experiments but higher than naïve mice which had 0.13% NP positive cells representing the background level of tetramer staining. *Dock8*$^{pri/pri}$ mice also had fewer NP positive CD8 cells, comprising 0.46% of total lymphocytes. A similar day 7 result was observed in the 2nd experiment.

After 35 days, NP positive CD8 T cells from mice in all groups dropped to just above the background level in naïve controls (Figure 3.24). To trigger a recall

proliferation of memory CD8 T cells, all experimental mice were re-challenged on day 42 with PR8 virus, which expresses the same NP antigen but a serologically distinct haemagglutinin and neuraminidase surface proteins to avoid neutralization by antibody against the first influenza exposure. All groups receiving the 2nd challenge elicited a recall NP positive CD8 T cell response. In wild type mice, NP positive CD8 T cells represented a mean of 4% of lymphocytes while both *Dock2*$^{doc/doc}$ (0.97%) and *Dock8*$^{pri/pri}$ (1.6%) mice had a significantly lower mean percentage of NP positive CD8 T cells of lymphocytes after secondary challenge ($p<0.0001$ and $p<0.01$ respectively). 35 days post secondary challenge, wild type and *Dock2*$^{doc/doc}$ mice had similar frequencies of NP positive CD8 T cells among blood lymphocytes while *Dock8*$^{pri/pri}$ mice had fewer ($p<0.05$) consistent with earlier evidence that DOCK8 is required for memory CD8 cells to persist (Randall et al. 2011).

A

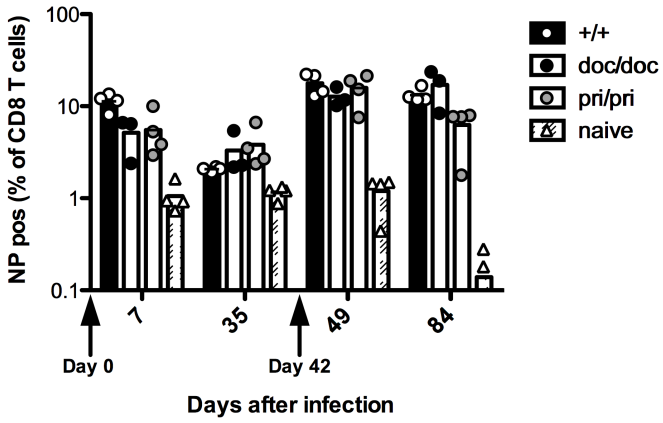

B

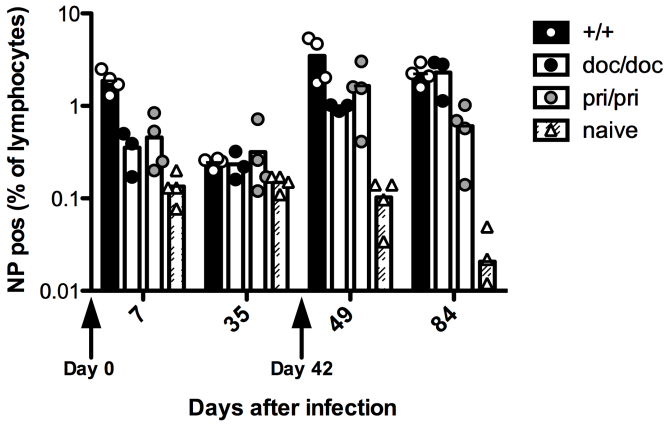

Figure 3.24 Frequency of influenza-specific CD8 T cells in wild type (*Dock2*$^{+/+}$ and *Dock8*$^{+/+}$), *Dock2*$^{doc/doc}$ and *Dock8*$^{pri/pri}$ C57BL/6 mice. Mice with the indicated genotypes were injected intraperitoneally with HKx31 influenza A virus at day 0, and boosted with PR8 influenza A virus on Day 42. An unchallenged group of wild type mice were also included as a naïve control. A) Frequency of NP tetramer positive CD8 T cells as a percentage of all CD8 T cells in blood at the indicated time points. B) The frequency of NP tetramer positive CD8 T cells as a percentage of total blood lymphocytes. 4 wild type mice, 3 *Dock2*$^{doc/doc}$ mice, 4 *Dock8*$^{pri/pri}$ mice and 4 naïve control mice were used in this experiment. Statistical analysis by two-way ANOVA (post-test by Bonferroni-test) showed a significant difference between challenged wild type +/+ and *Dock8*$^{pri/pri}$ NP-binding cells as a percentage of CD8 T cell at Day 84 ($p<0.05$); between +/+ and *Dock2*$^{doc/doc}$ NP positive CD8 T cells as total lymphocytes at Day 49 ($p<0.001$); and between +/+ and *Dock8*$^{pri/pri}$ NP positive CD8 T cells as percentage of total lymphocytes at Day 49 ($p<0.01$) and Day 84 ($p<0.05$).

The experiment shown above was repeated with increased time length before secondary challenge to reveal the behavior of true memory CD8 T cells. As shown in Figure 3.25, all challenge mice were kept until day 172 for generating memory CD8 T cells. Seven days after secondary challenge on day 179, wild type mice had significantly greater memory response (mean 6% of NP positive CD8 cells among lymphocytes). *Dock2*$^{doc/doc}$ (mean 1.2%) and *Dock8*$^{pri/pri}$ (mean 1.1%) mice exhibited a recall NP positive CD8 T cell response that was significantly less than wild type mice ($p<0.001$).

A

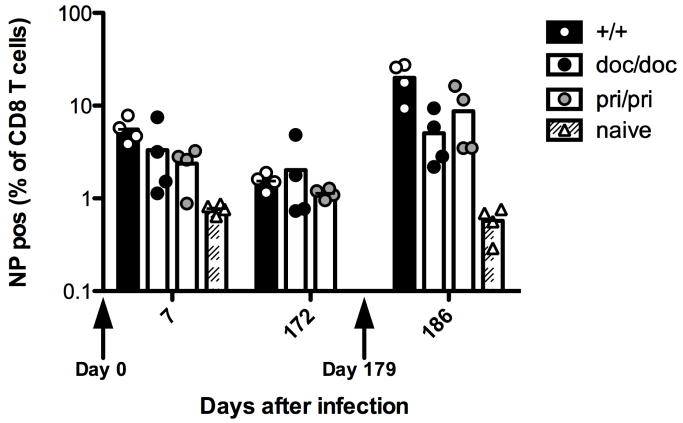

B

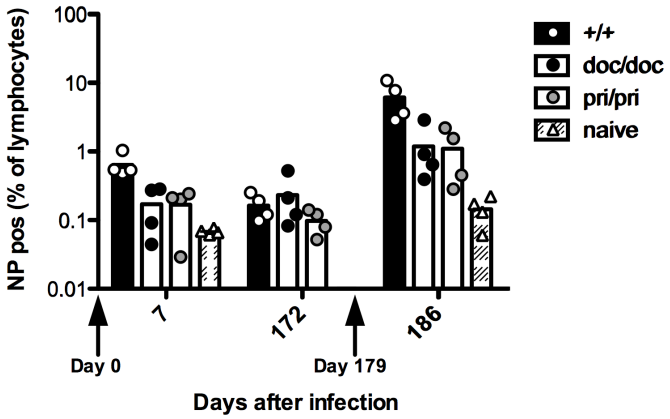

Figure 3.25 Frequency of influenza-specific CD8 T cells in wild type (*Dock2*$^{+/+}$ and *Dock8*$^{+/+}$), *Dock2*$^{doc/doc}$ and *Dock8*$^{pri/pri}$ C57BL/6 mice. Survival of polyclonal CD8 T cells in C57BL/6 (*Dock2*$^{+/+}$ and *Dock8*$^{+/+}$), *Dock2*$^{doc/doc}$ and *Dock8*$^{pri/pri}$ mice (long term). Wild type *Dock2*$^{doc/doc}$ and *Dock8*$^{pri/pri}$ mice were first challenge intraperitoneally with HKx31 at day 0, and rechallenged on Day 179 with PR8. An unchallenged group of C57BL/6 mice were also included as naïve control. A) Frequency of NP tetramer positive CD8 T cells at various time points as a percentage of CD8 T cells in blood. B) The frequency of NP tetramer positive CD8 T cells at various time points as a percentage of total lymphocytes in the blood. 4 wild type mice, 4 *Dock2*$^{doc/doc}$ mice, 4 *Dock8*$^{pri/pri}$ mice and 4 naïve control mice were used in this experiment. Statistical analysis: two-way ANOVA and Bonferroni post-test were performed and statistical analysis showed significant difference between wild type and *Dock8*$^{pri/pri}$ NP positive CD8 T cell as a percentage of CD8 T cell and total lymphocytes at Day 186 ($p<0.001$). The statistical analysis showed significant difference between wild type and *Dock2*$^{doc/doc}$ NP positive CD8 T cells as a percentage of CD8 T cells and total lymphocytes at Day 186 ($p<0.001$).

3.13 Comparison of influenza lung infection in DOCK2 deficient and DOCK8 deficient mice

DOCK2 was shown to be indispensable for TLR7 and TLR9 mediated IFN-α induction in plasmacytoid dendritic cells (pDCs) (Gotoh et al, 2010). To examine the effect of the *dockland* mutation on the response to influenza infection in the lung, which is dominated by innate immunity in the first 5 days, C57BL/6 *dockland* heterozygous and homozygous mice and wild-type controls were challenged intra-nasally with 0.01 HAU of PR8 influenza virus. The body weight of each mouse was recorded before the infection, and the percentage of starting body weight measured and calculated each day after infection. Mice were ethically culled if they lost >30% of original body weight. From Figure 3.26,

body weight of all mice started to drop 3 days post infection and continue to reduce until day 9, with trend for greater weight loss in the *Dock2* +/+ and *doc*/+ mice compared to *doc/doc*. Fewer *doc/doc* animals had to be ethically culled (4 *doc/doc* mice survived compared to 2 *doc*/+ mice and 1 C57BL6 mice). Further analysis performed on day 6 before any mouse was culled indicated that there was no significant effect of genotype on the survival of mice.

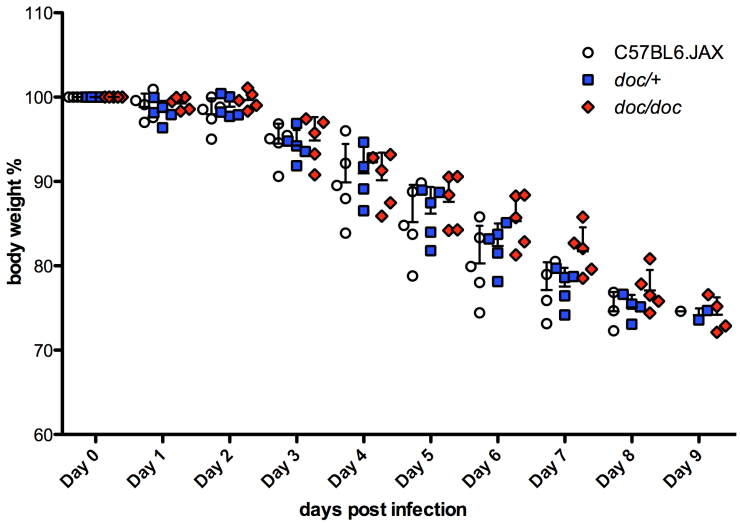

Figure 3.26 Weight loss of *dockland* mice after intra-nasally injected with flu virus. 5 *doc/doc* (red), 5 *doc*/+ (blue) and 5 C57BL6.JAX (white) mice were intra-nasally injected with 0.01 HAU PR8 virus and body weight for each mouse recorded each day and shown here as % of starting weight on Day 0.

The experiment was repeated with addition of DOCK8 *primurus* mutant mice. The 5 groups of mice were: *doc/doc*, *doc*/+, +/+, *pri/pri* and C57BL6 mice. As shown in Figure 3.27, the results of each group were variable and both *dockland* and *primurus* mice didn't show survival disadvantage with flu challenge. Combining the results of the two experiments (Table 3.2), a total of 8/10 *doc/doc*, 2/10 *doc*/+, and 2/10 C57BL/6 survived without requiring to be ethically culled.

The survival of these 3 groups were analysed by chi-squared test yielding a p value = 0.007, strongly suggesting that the DOCK2 *doc* mutation had a protective effect on morbidity following influenza lung infection.

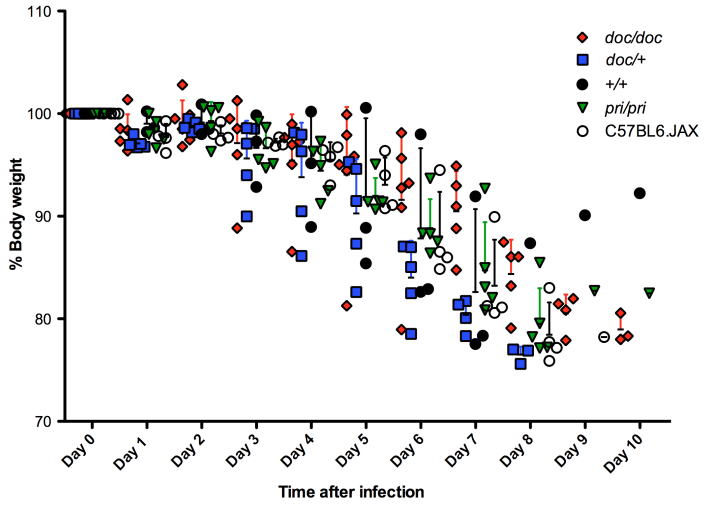

Figure 3.27 Weight loss of *dockland* and *primurus* mice after intra-nasally injected with flu virus. 5 *doc/doc* (red), 5 *doc/+* (blue) 5 +/+ (black), 5 pri/pri (green) and 5 C57BL6.JAX (white) mice were intra-nasally injected with 0.02 HAU PR8 virus and the loss of body weight were calculated.

	C57BL/6	*doc/+*	*doc/doc*
Ethically culled	8	8	2
Healthy	2	2	8

Table 3.2 Combined morbidity data from two individual influenza lung infection experiments. There are a total of 10 mice in each group.

3.14 Effects of combined DOCK2 and DOCK8 deficiency

To understand whether or not *Dock2* and *Dock8* serve overlapping roles in the immune system, the C57BL/6 *dockland* and *primurus* strains were intercrossed to generate double homozygous mice. As shown in Figure 3.28A, the double homozygous mice had lower T cells proportion and higher CD44 expression compared to either $Dock2^{doc/doc}$ or $Dock8^{pri/pri}$ single homozygous mice. There was no difference in the percentage of B cells and total cell number of B cells in all groups of mice (Figure 3.28B). The double homozygous mice has significantly lower percentage of T cells, higher percentage of CD4 T cells and lower percentage of CD8 T cells compared to $Dock2^{doc/doc}$ mice, although these differences did not achieve significance when expressed as absolute cell numbers per spleen (Figure 3.28C). The double homozygous tended to have a lower percentage of NKT cells and total NKT cell number compared to $Dock2^{doc/doc}$ mice, although this was not statistically significant in the small number of animals available (Figure 3.28D).

A

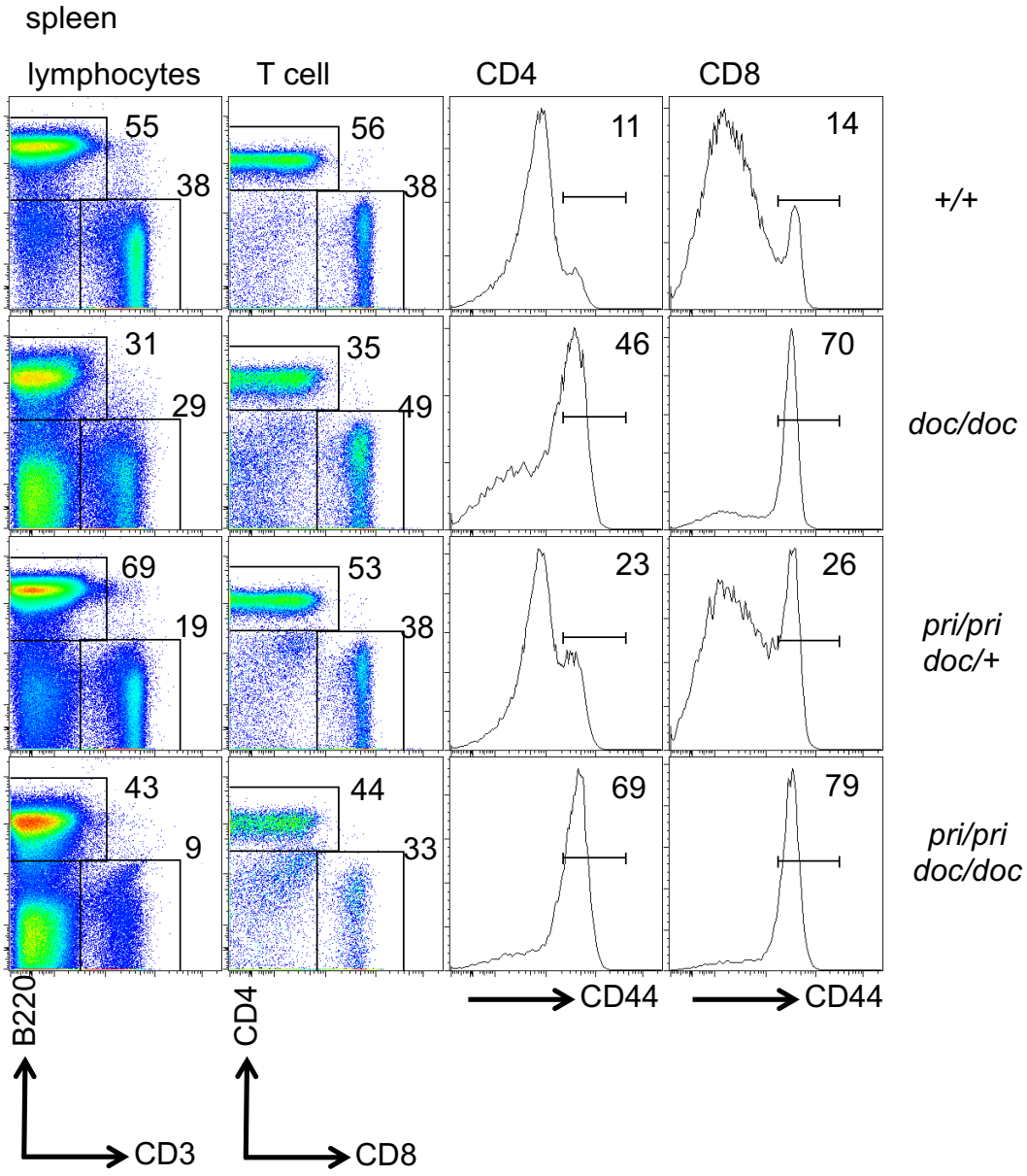
spleen
lymphocytes
T cell
CD4
CD8
55
38
56
38
11
14
+/+
31
29
35
49
46
70
doc/doc
69
19
53
38
23
26
pri/pri
doc/+
43
9
44
33
69
79
pri/pri
doc/doc
B220
CD3
CD4
CD8
CD44
CD44

B

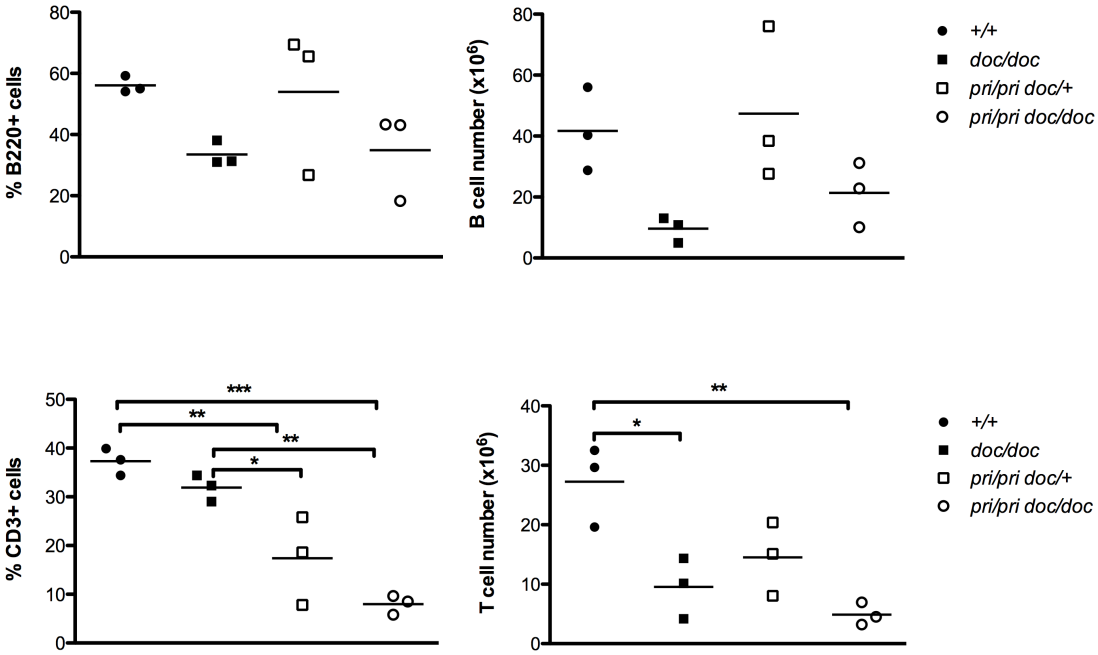
% B220+ cells
B cell number (x10^6)
% CD3+ cells
T cell number (x10^6)
+/+
doc/doc
pri/pri doc/+
pri/pri doc/doc

C

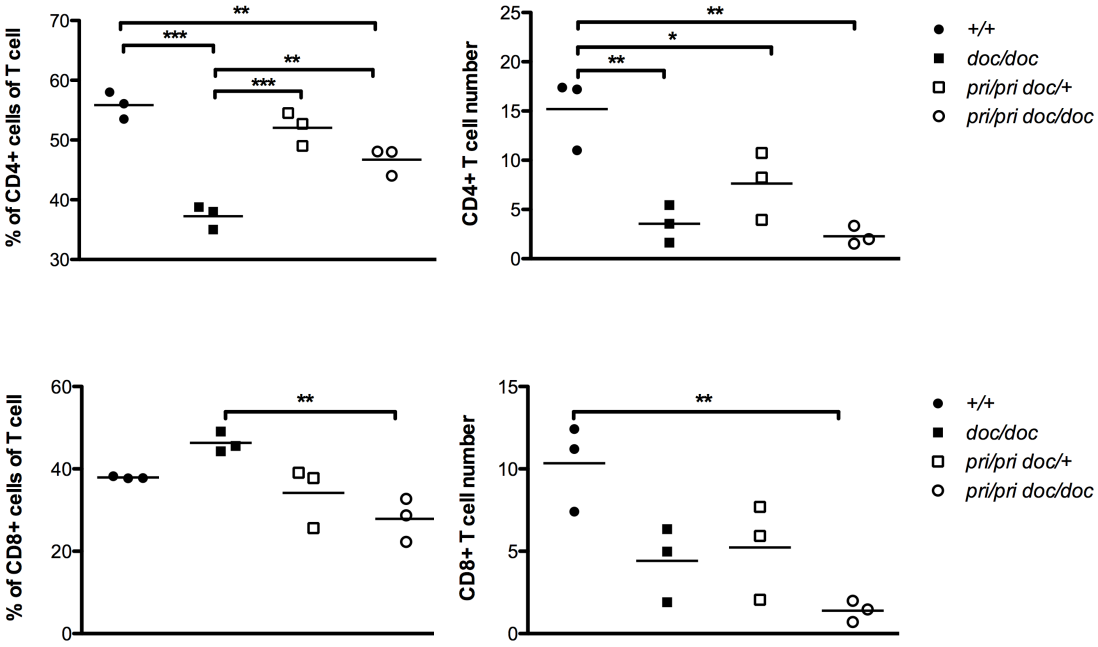
% of CD4+ cells of T cell
CD4+ T cell number
% of CD8+ cells of T cell
CD8+ T cell number
+/+
doc/doc
pri/pri doc/+
pri/pri doc/doc

D

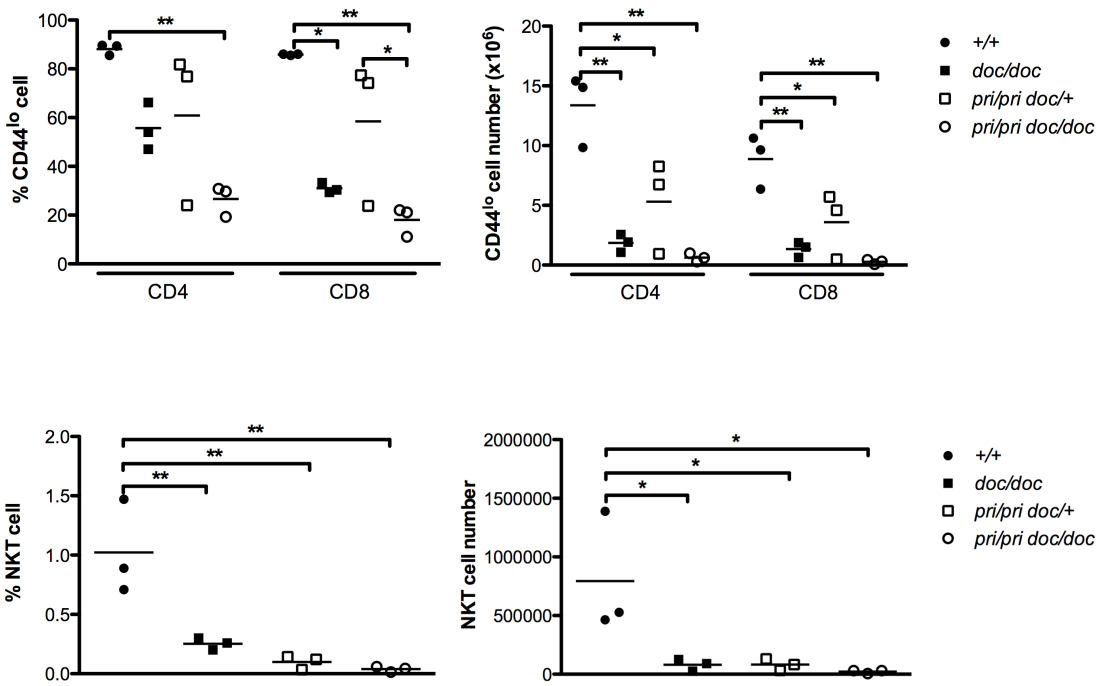

Figure 3.28 Analysis of *Dock2*$^{doc/doc}$ *Dock8*$^{pri/pri}$ double deficient mice. A. Representative flow cytometry plot splenocytes from wild type (+/+), *dockland* homozygous (*doc/doc*), *dockland* heterozygous *primurus* homozygous (doc/+ pri/pri) and *dockland:primurus* double homozygous (doc/doc pri/pri) mice. B. Quantitation of lymph subsets for all 4 groups of mice. 3 mice were included in each group. Mean is shown as bar and statistical analysis by one-way ANOVA followed by Tukey's test. * = $p<0.05$; ** = $p<0.01$.

3.15 Discussion

A search for novel mouse strains with lymphocyte defects in spleen led to the identification of the *dockland* mutant mouse strain in the ENU16:019a pedigree with T cell lymphopenia and absent marginal zone B cells in homozygous

mutants. The mutation was mapped to a large interval on chromosome 11 and identified as a G to T single nucleotide change in *Dock2* gene introducing a premature stop codon instead of glutamic acid at codon 775 in the middle of the DOCK2 protein. Since this eliminates the DH2 domain responsible for GTP exchange factor activity, the E775X *doc* allele is likely to be a complete loss of function allele. The mutation may also trigger nonsense mediated decay of the mutant mRNA, although this was not tested.

My analysis revealed *doc* homozygotes had fewer total lymphocytes and total T cells (both CD4 and CD8), but normal numbers of activated/memory ($CD44^{hi}$) T cells in the spleen and blood. Homozygotes also had 2.5-fold fewer thymocytes and thymic DP and 3-fold fewer CD4 SP T cells. The lower CD5 expression on *doc/doc* thymic DP cells indicating lower pre-TCR signaling strength results lower SP T cells due to lack of efficient positive selection at DP stage. The fewer SP T cells indicated that the peripheral T lymphopenia was at least partly explained by diminished T cell formation in the thymus. The percentage of SP CD8 and CD4 T cells that were CD69-negative, representing the mature subset that normally express the S1P1R for thymic egress, was nevertheless increased in the thymus of homozygotes suggesting diminished thymus egress. A greater decrease in naïve ($CD44^{lo}$) CD4 and CD8 T cells was observed in the peripheral blood and spleen of *doc/doc* mice (6-10 fold), implying either less thymic egress or diminished accumulation/survival in the periphery. By contrast, $CD44^{hi}$ T cells were present in normal or increased numbers in homozygotes, consistent with lymphopenia-induced homeostatic proliferation to replace the depleted pool of naïve T cells. In mixed bone marrow chimeras, where numerical deficiency of Dock2 mutant T cells could be replaced by competing wild-type T cells, a mean of only 0.3% of blood T cells were derived from *doc/doc* mutant bone marrow, in contrast to 22.6% *doc/doc* mutant cells within the blood B cells and 30.5% within granulocytes in the blood of the same chimeric animals. Therefore, DOCK2 is required within T cells for normal accumulation of naïve T cells in the periphery.

DOCK2-deficient mice were first generated by homologous recombination in embryonic stem (ES) cells to produce a null allele encoding a DOCK2 protein truncated after 42 amino-acid residues which was undetectable in thymus and spleen (Fukui et al., 2001). DOCK2$^{-/-}$ mice were viable and born at the expected Mendelian ratio with no apparent physical abnormality. The loss of DOCK2 gave rise to an absence of marginal B cells and reduced total number of T and B cells in spleen and lymph nodes mainly due to impaired lymphocyte migration. Rac, a member of the Rho GTPase family, is known to regulate cell migration, membrane polarization, and cytoskeletal dynamics in various cells (Hall, A., 1998; Penninger, J.M., and Crabree, G.R., 1999). DOCK2 has been shown to bind Rac protein through its DHR2 domain and mediates Rac2 activation, measured by GTP loading, following CXCL12 stimulation or T cell receptor stimulation. DOCK2 can regulate the TCR polarization and lipid raft clustering during immunological synapse (IS) and lymphocyte migration through inducing Rac activation in response to chemokine receptor signaling (Nombela-arrieta et al., 2004; Sanui et al., 2003). There was no detectable chemokine-induced Rac activation in DOCK2-deficient mice and DOCK2-deficient lymphocytes migrated poorly to the lymphoid chemokines CXCL12/SDF1, CXCL13/BLC, CCL19/ELC and CCL21/SLC (Fukui et al., 2001). More functional roles of DOCK2 have been revealed by other studies. Although DOCK2 mediates most T and B cell migration, integrin activation is defective in DOCK2$^{-/-}$ B cells but was not affected in DOCK2$^{-/-}$ T cells (Nombela-arrieta et al., 2004). DOCK2 deficient mice spontaneously develop high serum IgE onto an allergy-prone genetic background due to impaired antigen-driven downregulation of IL-4Rα expression (Tanaka, Y. et al., 2007).

Consistent with the findings above, homozygous *doc* mutation caused absence of marginal zone B cells. DOCK2$^{-/-}$ mice have normal B lymphopoiesis or myelopoiesis (Fukui et al., 2001). The *doc* mutation does not change the amount of pro-B, pre-B, immature B and myeloid cells in bone marrow. Consistent with DOCK2's guanine exchange factor activity for the hematopoietic-specific Rac isoform RAC2, *Rac2*-deficient mice have marked reductions in marginal zone B

cells and peritoneal cavity B-1a lymphocytes (Croker et al., 2002). Mice lacking DOCK8 also lack marginal zone B cells (Randall et al., 2009). Fewer marginal zone B cells are present in mice genetically deficient for *Lsc,* encoding the murine homolog of human p115 Rho GEF and a member of Dbl-homology family of Rho GTP exchange factors (Girkontaite, I., et al., 2001). Formation or maintainance of marginal zone B cells thus requires multiple GTP-exchange factors that are not critical for mature follicular B cells.

In 50:50 bone marrow chimeras, *doc/doc* homozygous haematopoietic progenitors contributed to the blood B cell compartment almost as well as they contributed to the blood granulocyte compartment, but the mutant B cells were ten-fold less well represented in the corresponding B cell subsets within the spleen. Since there is a smaller decrease in B cell numbers in the spleen of unmanipulated *doc/doc* mice, the competitive disadvantage of *doc/doc* B cells in the mixed bone marrow chimeras is likely to reflect their diminished responsiveness to CXCL12/SDF1, CXCL13/BLC, CCL19/ELC and CCL21/SLC (Fukui et al., 2001), which promote migration of blood B cells into the splenic white pulp (Arnon and Cyster, 2014). In addition to the diminished contribution to B cells, there appeared to be a small further decrease in the formation of GC B cells by *doc/doc* cells, which again may reflect diminished responsiveness to CXCL12 and CXCL13 that attract B cells into germinal centres (Arnon and Cyster, 2014). To further investigate whether the cell intrinsic defect in *dockland* GC B cells was due to a failure of production or sustaining germinal center B cells, SW_{HEL} mice could be an ideal model to study the GC response. By adoptive transfer of comparable numbers of SW_{HEL} cells with normal or mutant DOCK2, the antigen-specific B cells could be followed through the immune response.

DOCK8 in DOCK-C subgroup and DOCK11 in DOCK-D subgroup are known and suspected, respectively, to have a role in the germinal centre. DOCK8 was shown to have a role within germinal centre B cells in sustaining antibody responses after immunization, which could be used as an important model to investigate the mechanisms of antibody persistence and affinity maturation

(Randall et al., 2009). DOCK11 was discovered for its high expression on germinal centre cells. It has been shown to bind Cdc42 but its role in GC has not been elucidated (Nishikimi et al., 2005).

Vav2 and SWAP-70 are other guanine exchange factors implicated in GC formation. Vav2 is a Dbl-type guanine exchange factor for Rho-family GTPases. Although the *Vav2* gene is expressed in T and B cells, loss of *Vav2* does not have a prominent effect on the development of B and T cells. However, *Vav2* deficient mice have defects in B cell activation and T-dependent and T-independent antibody responses and GC formation despite normal splenic architecture (Doody et al., 2001; Tedford et al., 2001). SWAP-70 is a Rac-interacting protein with a domain weakly homologous to the Dbl (DH) domain. SWAP-70 deficient mice have fewer and smaller GC upon immunisation with SRBCs or NP-KLH but increased antigen-specific antibody and antibody-forming B cells (Quemeneur et al., 2008).

The findings here are consistent with published evidence that DOCK2 is required for early development of Vα14 NKT cells in thymus (Kunisaki et al., 2006). Kunisaki et al showed that DOCK2 deficiency caused severe reduction of Vα14 NKT cells in the thymus, liver and spleen with no effect on NK cells in thymus and liver. Homozygotes for the *dockland* mutation had severely reduced numbers of NKT cells in both thymus and spleen. Similar as DOCK2 deficient mice, DOCK8-deficient mice have impaired development and survival of NKT cells (Crawford, G., et al., 2013). Failure of NKT cell formation is thought to be due to effects on the strength of TCR signalling and the threshold for positive selection (Kunisaki et al., 2006).

Previously, DOCK2 has been shown to be involved in antiviral immunity. pDC can respond rapidly to viral exposure by secreting IFN-I for an efficient antiviral immune response. DOCK2 deficiency diminished TLR7- and TLR9-mediated INF-I induction through a requirement for DOCK2 in Rac activation following exposure to TLR nucleic acid ligands in pDCs (Gotoh et al, 2010). In this chapter, the *doc* mutation was shown to protect mice from morbidity during the early

phases of lung infection by influenza virus. One hypothesis to explain this protective effect of DOCK2 deficiency *in vivo* is that local production of interferon by infected lung epithelium, which expresses little DOCK2, occurs normally to control viral replication. By contrast, diminished production of systemic interferon by pDCs decreases morbidity. Future studies will need to test this possibility by measuring virus RNA and interferon RNA in fractionated cells from lung and by measuring interferon in blood plasma.

Recently, five children with early onset invasive bacterial and systemic viral infections, including two fatal cases of systemic varicella and Klebsiella infection, were found to have bi-allelic inactivating *DOCK2* mutations (Dobbs K et al NEJM 2015 PMID 26083206). One of the deceased patients inherited a homozygous frameshift truncating mutation at codon 744, p.F744Cfs*27, near to the *dockland* mutation at codon 775, which when expressed as a cDNA (obviating nonsense mediated decay) produced a truncated protein lacking the DH2 domain. Consistent with the mouse results here and published previously, all five cases had greatly decreased T cell numbers in the blood. Newborn blood spots from the p.F744Cfs*27 patient and one other patient were shown to have low T cell receptor excision circles below the normal cutoff, consistent with diminished thymic output. These results are also in line with the diminished thymocyte numbers and evidence of egress deficits observed in DOCK2 deficient mice. There was also diminished interferon alpha production by pDCs from the patients. Three of the five patients successfully underwent bone marrow transplantation and this corrected their recurrent infections and allowed cessation of intravenous gammaglobulin. These results are consistent with the evidence here that the T cell and B cell deficits are cell autonomous.

Whereas systemic viral and bacterial infections dominate the clinical picture of human DOCK2 deficiency, human DOCK8 immunodeficiency is characterised by persistent and recurrent cutaneous infections with human papilloma viruses, molluscum contagiosum, and herpes simplex virus (Zhang, Q. et al., 2009 and Engelhardt, KR et al., 2009). Most DOCK8-deficient patients exhibit T cell

lymphopenia, albeit milder than DOCK2 deficiency, and high serum IgE and eosinophilia and CVID-like antibody and memory B cell abnormalities.

DOCK8 has been shown to be critical for the survival of peripheral CD8 T cells in both human and mice (Randall et al., 2011 and Lambe et al., 2011). CD8 T cells in DOCK8-deficient human patients displayed exhausted $CD45RA^{+}CCR7^{-}$ phenotype and fail to active, divide and expand in vitro. In mice, although DOCK8-deficient CD8 T cells are able to generate a comparatively normal primary clonal expansion after immunisation with Modified Vaccinia Ankara (MVA) or recombinant influenza virus, the memory recall response is greatly reduced (Randall et al., 2011 and Lambe, 2011). It remains unclear why cutaneous viral infections dominate DOCK8 deficiency in mice, whereas a more typical picture of severe combined immunodeficiency with systemic viral infections occurs in DOCK2 deficiency. The simplest interpretation is that T cell lymphopenia is more severe in DOCK2 deficiency, both in humans and in the side-by-side comparison of unchallenged T cell numbers in mice with DOCK2 or DOCK8 deficiency performed here. However, it is interesting that when I performed a side-by-side comparison of influenza NP-specific CD8 cells in the two mutant mouse strains, there was a similar decrease in effector CD8 cells after primary and secondary challenge in both mutant relative to wild-type controls.

The observation here that the circulating naïve T cell frequency was further decreased in double mutant mice with homozygous mutations in DOCK2 and DOCK8 has two equally simple interpretations. First, both proteins may serve identical functions in T cell formation, thymic egress, and peripheral T cell survival with partial redundancy and DOCK2 bearing a much greater load for T cell chemotaxis. Alternatively, the two proteins may serve parallel functions that contribute to the efficiency of filling the T cell repertoire. This would be consistent with the presence of an SH3 domain in DOCK2 and not DOCK8, and the much greater defect in migration to chemokines observed in DOCK2 deficient lymphocytes.

Chapter 4: Identification of the causative mutation in SENP2

4.1 Introduction

Since ubiquitin was first discovered in the late 80's, its role has been well established: covalent ligation of ubiquitin to amino acid side-chains of other proteins triggers either protein degradation in the proteasome or assembly of large macromolecular signaling (Hershko and Ciechanover, 1998). During the last decade, a number of ubiquitin-like proteins have been isolated without clear functional role. The significance of these ubiquitin-related proteins was first elucidated by showing that a novel protein, SUMO (small ubiquitin-like modifier)-1, can be covalently conjugated to RanGAP1 and regulate its subcellular localization (Matunis et al., 1996; Mahajan et al., 1997). As the best-characterized member of the family of ubiquitin-related proteins, SUMO has been shown to have other roles and does not mark proteins for degradation.

The ubiquitin-like protein SMT3 from *Saccharomyces cerevisiae* was the first identified member of SUMO family (Meluh and Koshland, 1995). Subsequently, other SUMO members in human and mouse were reported by serveral groups with different names: sentrin, PIC1, SMT3, UBl1 (Mannen et al., 1996; Boddy et al., 1996; Mahajan et al., 1997; Matunis et al., 1996; Okura et al., 1996; Shen et al., 1997; Lapenta et al., 1997 Chen et al., 1998). In mouse and human, there are 5 different SUMO proteins: SUMO1, SUMO2, SUMO3, SUMO4 and SUMO5. SUMO2 and SUMO3 share 86% sequence identity but both have lower identity (44%) to SUMO1 in humans (Su and Li, 2002). All 3 isoforms are ubiquitously expressed in the human and mouse (Chen et al., 1998;). SUMO1, SUMO2 and SUMO3 are localized at the nuclear membrane, nuclear bodies and cytoplasm, respectively (Su and Li, 2002). SUMO4 and SUMO5 are expressed in selective tissues (Rabellino et al., 2017).

SUMO, like ubiquitin, is post-translationally attached by covalent linkage to other proteins. Unlike ubiquitination that has a pivotal role in marking proteins for degradation, SUMOylation affects activity, stability, and subcellular localization of the target proteins. SUMO is ~10 kDa in size and synthesized in an

inactive/precursor form with 2-11 amino acids adjacent to 2 invariable glycine residues at the carboxyl terminus (Figure 1). The C-terminal residues are cleaved to reveal the carboxy-terminal Gly-Gly motif before SUMO can be covalently conjugated to the target protein: a process that is mediated by sentrin-specific proteases (SENPs). Then the conjugation reaction is catalyzed by E1 heterodimer enzyme (AOS1-UBA2) and results in formation of a thioester bond between the C-terminal glycine and cysteine of E1 enzyme (Johnson et al., 1997; Desterro et al., 1999; Okuma et al., 1999; Gong et al., 1999). The SUMO group is then transferred to the cysteine of the E2 enzyme (UBC9) (Desterro et al., 1997; Johnson and Blobel, 1997; Lee et al., 1998; Okuma et al., 1999). Finally, the SUMO molecule is conjugated to the target protein by the formation of an isopeptide bond between the C-terminal glycine and the ε-amino group of a lysine side chain in the target protein. The last step is mostly catalyzed by a SUMO protein ligase (E3) (Hay, 2005; Johnson and Gupta, 2001; Takahashi et al., 2001). The best characterized E3 ligases are members of the Protein Inhibitor of Activated STAT (PIAS) family, which are encoded by four genes in mammals (Rabellino et al., 2017).

SUMOylation is highly dynamic and reversible, with the deconjugation process mediated by a family of sentrin specific proteases (SENPs). The first member, SENP1, was first described to remove SUMO1 from RanGAP1 *in vitro* (Gong et al, 2000). There are 6 members in the SENP family. They can be further divided to 3 subgroups based on sequence homology and subcellular localization (Mukhopadhyay and Dasso, 2007):

Group I - SENP1 and SENP2: both localize at the nuclear envelope and associate to the nuclear pore complex (NPC)
Group II – SENP3 and SENP5: have the highest degree of homology and both localize to nucleoplasm
Group III – SENP6 and SENP7: both localize to the nucleoplasm

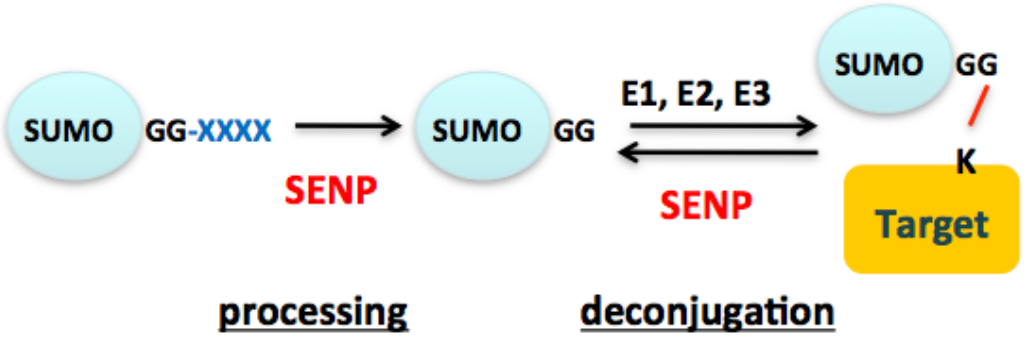

Figure 4.1: The SUMOylation and deSUMOylation processs

The human *Senp2* gene encodes a 589 amino acid protein (588 in mouse). Although SENPs share homology in their catalytic domain, they have a wide diversity in N- and C- terminal primary sequence. The divergent regions in SUMO proteases have an important role in spatial regulation to their specific subcellular localization. Human SENP2 has been shown to associate with the nuclear pore through the N-terminal 70 amino acids. SENP2 binds Nup153, which is a constituent of the nuclear basket and is localized to the nucleoplasmic side of the nuclear pore complex (Pante et al, 1994). Removal of N-terminal sequences causes SENP2 to relocalize to other compartments in the cell and to increase its activity in promoting deconjugation of SUMO-1 conjugated species (Hang and Dasso, 2002). Later studies have shown that SENP2 has the KRRR-X-KR sequence that constitutes a bipartite nuclear localization signal (NLS) and a CRM1-dependent nuclear export sequence (NES) (Itahana et al., 2006). By using SENP2 mutants, SENP2 was shown to shuttle between the nucleus and cytoplasm.

The aim of this project was to use a genome wide N-ethyl N-nitrosurea (ENU) mutagenetic screen screen in mice to identify novel genes involved in CD8 T cell development or function. This chapter describes the discovery and initial analysis of a *Senp2* mutation affecting CD8 T cell accumulation.

4.2 Screening and identification of the *duan* strain

Male B6 mice were injected with ENU and bred with wild-type female B6 mice to generate G1 offspring carrying multiple mutations. Each G1 mouse was bred with wild-type females to generate G2 offspring carrying heterozygous mutations. Sibling G2 mice were intercrossed to generate G3 mice, which had a 25% chance of being homozygous for any mutation carried by both of the G2 parents. The G3 mice were bled around 8 weeks of age and the peripheral blood analysed by flow cytometry for abnormal frequencies of the T cell population.

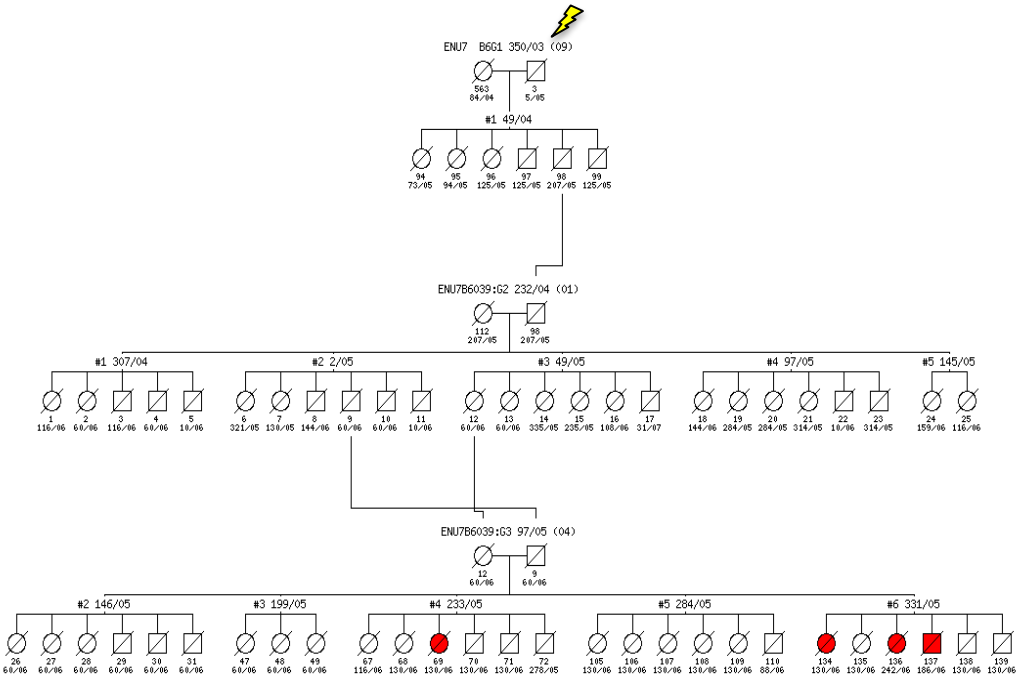

Figure 4.2 ENU7B6:039 pedigree segregating the *duan* mutation affecting CD8 T cell frequency. In the 27 offspring in the G3 generation, 3 females and 1 male had a lower frequency of peripheral blood CD8 T cells. Male mice = squares, female mice = circles. Affected mice = red filled symbols; unaffected mice = open symbols.

In the ENU7B6:039 pedigree, 4 out of 27 G3 mice had a decreased percentage of CD8 T cells (Figure 4.2), which suggested that it is a homozygous recessive mutation. The affected animals had 6-10% CD8 T cells among blood lymphocytes, compared to 15% in wild type. Most mutant mice also had an increased fraction of CD8 T cells displaying high levels of CD44, corresponding to the subset of activated memory or effector CD8 T cells (Fig 4.3A). Breeding of affected G3 mice with unaffected carrier G3 siblings yielded approximately 50% of G4 offspring affected by the trait of low CD8 T cell frequency, while breeding of two unaffected carrier mice yielded ~25% affected offspring with no discernable physical abnormality. Scatter plots comparing the percentage of CD4 versus CD8 T cells in the blood of individual animals (Figure 4.3A), or the percentage of $CD44^{hi}$ cells among CD8 T cells versus the frequency of all CD8 T cells (Figure 4.3B), showed a clear separation between affected and unaffected mice, consistent with a single mutation causing a fully penetrant, recessive Mendelian trait.

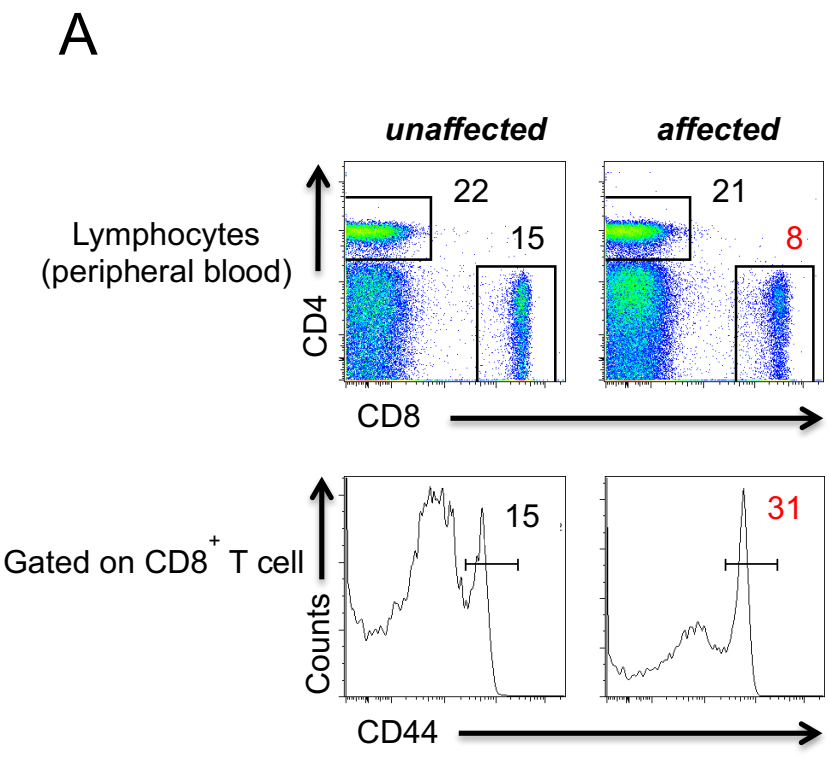

B

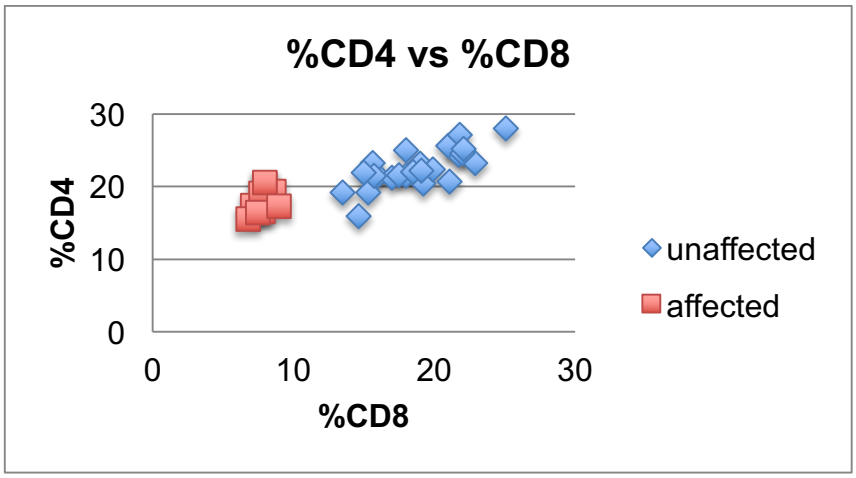

C

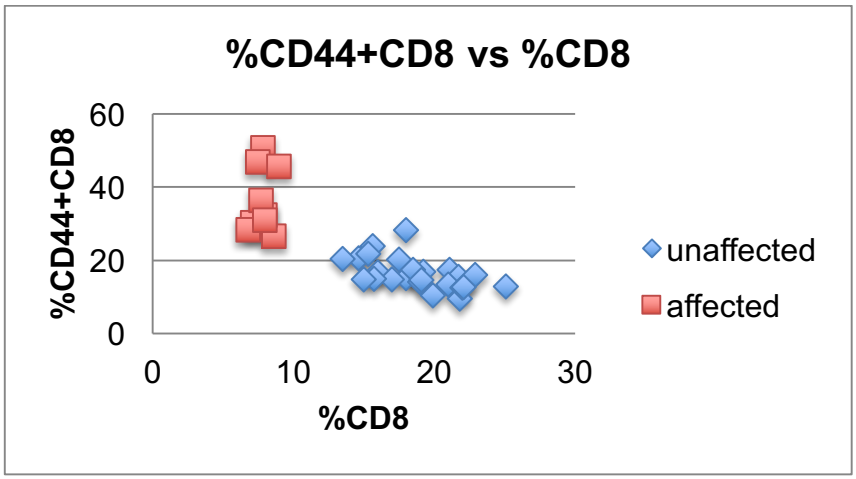

Figure 4.3 *duan* mutation leads to a loss of peripheral naive CD44^{low} CD8 T cells. A. Representative FACS plots of lymphocytes in peripheral blood. The upper panel shows the percentage of CD4 and CD8 cells. The lower panel shows the expression of CD44 on CD8^{+} T cells, and the gates and percentage of CD44^{hi} activated/memory CD8 cells resolved from CD44^{low} naïve CD8 cells. B) The percentage of CD4 T cells versus CD8 T cells in individual mice. C) The frequency of CD44^{hi} CD8 T cells versus

CD8 T cells in individual mice. Each symbol represents a single animal from G3 and G4 generations: Red = affected and Blue = unaffected.

4.3 Meiotic mapping of the *duan* mutation to an interval on Chromosome 16

The *duan* mutation was mapped and identified by Dr Lina Tze and Belinda Whittle prior to my PhD studies. Homozygous *dua/dua* B6 mice were crossed with C57BL/10 (B10) mice, and the F1 offspring intercrossed to produce an F2IC generation. In these animals the mutation-bearing C57BL/6 chromosomal segment could be distinguished from the corresponding wild-type chromosome from the B10 mapping partner strain using a genome-wide panel of single nucleotide polymorphisms. The flow cytometric traits above were used to identify the 25% of F2IC animals that were affected homozygotes for the mutation-bearing B6 chromosome.

In F2IC mice, the low CD8 T cell trait mapped to chromosome 16 in a 3.9 Mb interval bounded by two SNPs: rs4165081 at Ch16:19,883,079 and rs4165422 at Ch16: 23,794,202 (GRCm38 coordinates). This interval contained 70 annotated protein coding genes. Using DNA from a homozygous affected mouse, each exon of the 70 genes was PCR amplified with custom oligonucleotides, Sanger sequenced, and compared to the reference B6 genome sequence (these experiments were designed, performed and analysed by Belinda Whittle). Only one exonic mutation was present: a synonymous A>G substitution at Ch16:22,036,478 in exon 11 of *Senp2*. Allele-specific PCR primers were then used to establish an Amplifluor genotyping assay for the $Senp2^{dua}$ mutation.

Once the mutation was identified, the flow cytometric difference between homozygous *dua/dua* animals and *dua/+* heterozygous or +/+ siblings could be further analysed (Figure 4.4). The homozygous mice had a statistically significant decrease in the percentage of CD8 and CD4 T cells in peripheral blood compared to wild type or heterozygous littermates. Mutant mice had significantly higher

percentage of B cells as a reflection of lower percentage of both CD4 and CD8 T cells.

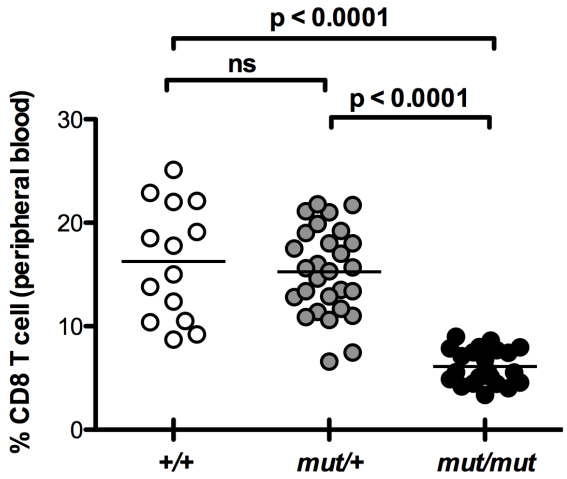

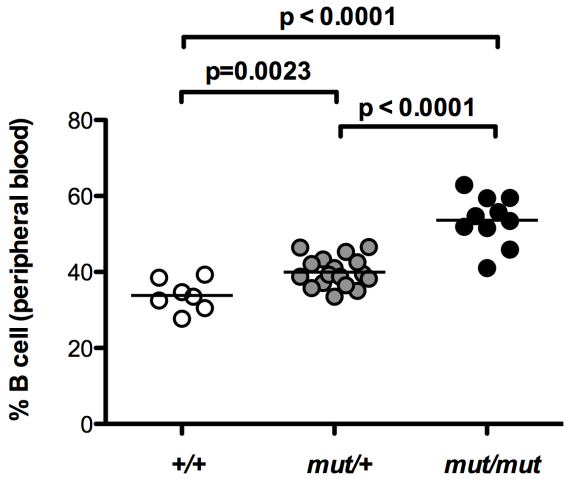

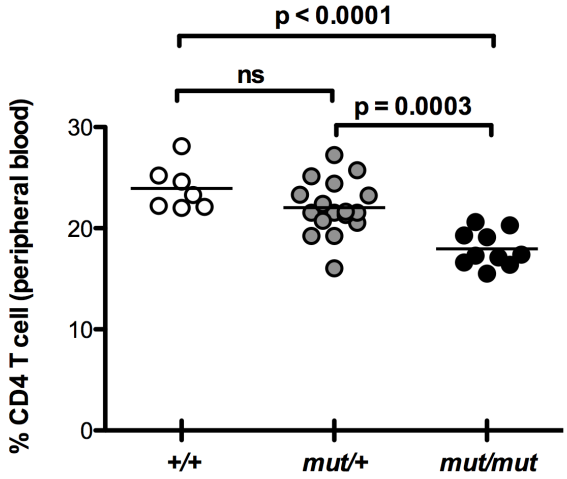

Figure 4.4 Lower percentage of CD8$^+$ T cells in mice homozygous for the *duan* mutation in *Senp2*. Percentage of B220$^+$, CD4$^+$ and CD8$^+$ T cells in blood lymphocytes of mice genotyped for the *Senp2^{dua}* exon 11 mutation, with either wild-type (white circles), heterozygous (grey circles) or homozygous mutant genotypes (black circles). Dots represent single mice and the bars represent the arithmetic mean. Statistical analysis by one-way ANOVA followed by Bonferroni post-test.

4.4 Lower CD127 expression on naïve *Senp2$^{dua/dua}$* mice

As reviewed in Chapter 1, CD127 (IL-7Rα) is expressed on and transmits IL-7 survival signals into naïve CD8 T cells. The expression of CD127 on the surface of naïve (CD44^{lo}) and effector/memory (CD44^{hi}) CD8 T cells from wild type, heterozygous and homozygous mice in the peripheral blood was compared. The results from Figure 4.4 showed that naïve CD8 T cells from homozygous *Senp2* mutant mice had significantly lower expression of CD127 compared to naïve CD8 T cells from wild type or heterozygous mice (Figure 4.5A). However, no difference in CD127 expression was seen in the effector/memory CD8 T cells (Figure 4.5B).

A

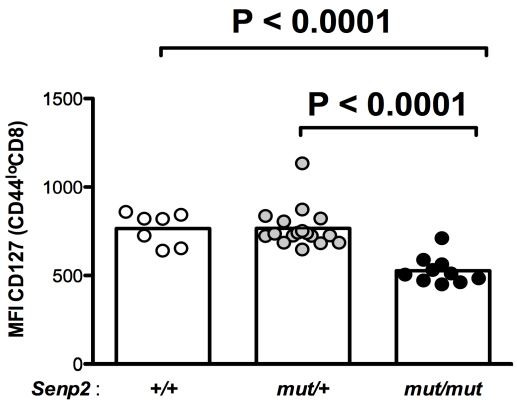

B

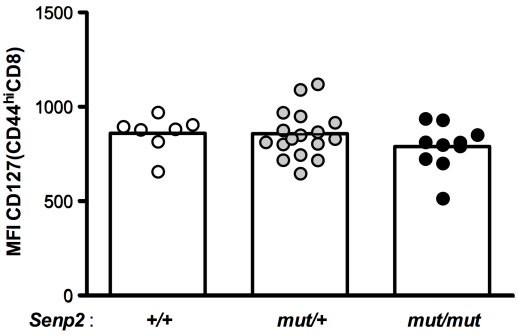

Figure 4.5 Lower expression of CD127 (IL-7Rα) on *Senp2*$^{dua/dua}$ naïve CD8 T cells. Graph of geometric mean of CD127 expressed on naïve (CD44^{lo}) CD8 T cells (A) and effector/memory (CD44^{hi}) CD8 T cells (B) in the blood of wild-type *Senp2*$^{+/+}$(white circles), heterozygous *Senp2*$^{dua/+}$ (grey circles) and homozygous *Senp2*$^{dua/dua}$ mice (black circles). Dots represent single mice and the bars represent the arithmetic mean. Statistical analysis by one-way ANOVA followed by Bonferroni post-test.

4.5 Splicing consequences of the synonymous coding mutation in *Senp2* exon 11

As described above, mapping and sequencing revealed a single A to G base change in exon 11 of the *Senp2* gene. This synonymous mutation did not alter the encoded amino acid, Glycine 313 (Figure 4.6A), but its location 9 bp downstream from the splice acceptor site of exon 11 (Figure 4.6B) raised the possibility that it might affect mRNA splicing. Reverse transcriptase PCR (RT-PCR) was performed with primers in exons flanking exon 11. This revealed two different size products in approximately equal amounts in cDNA from homozygous mutants (Figure 4.6C and D): a large product corresponding to the predominant species in cDNA from wild type mice and a smaller sized band corresponding to a trace species accounting for a mean of 5% of amplified Senp2 cDNA in wild-type (+/+) mice. The percentage of the smaller product among the two amplified cDNA bands was significantly increased to a mean of 30% in $Senp2^{dua/+}$ heterozygotes and 55% in homozygous $Senp2^{dua/dua}$ mutants (Figure 4.6C, D). Belinda Whittle excised both bands from wildtype and homozygous mutant mice and performed Sanger sequencing, finding the smaller product results from skipping exon 11 in mutant and wild-type mice, while the larger product retains normal splicing of exon 10 to exon 11 and of exon 11 to exon 12 in mutant mice. Thus, the exon 11 mutation appears to interfere with an exonic splicing enhancer in exon 11, decreasing the fraction of mRNA where exon 10 is spliced to exon 11 to encode full-length SENP2 protein.

A

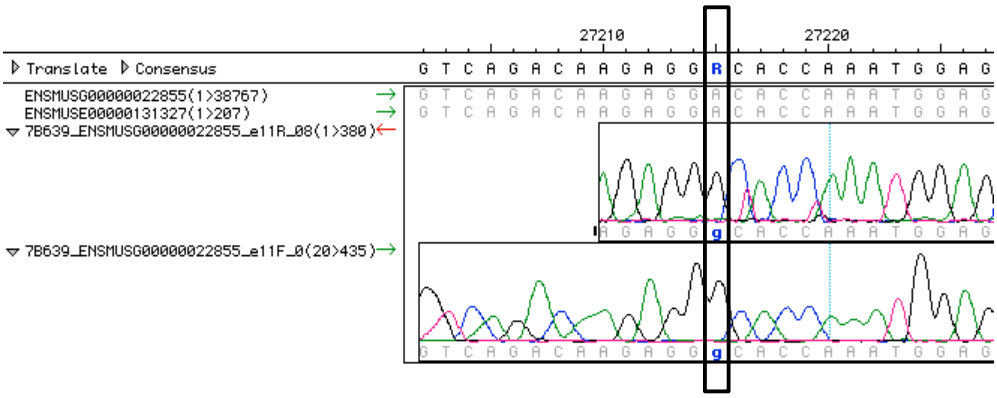
27210
27220
Translate
Consensus
ENSMUSG00000022855(1>38767)
ENSMUSE00000131327(1>207)
7B639_ENSMUSG00000022855_e11R_08(1>380)
7B639_ENSMUSG00000022855_e11F_0(20>435)

B

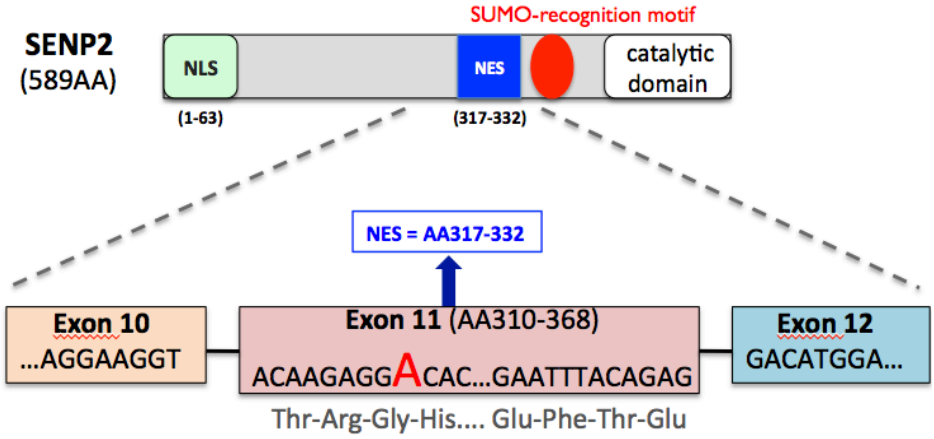
SENP2
(589AA)
SUMO-recognition motif
NLS
NES
catalytic domain
(1-63)
(317-332)
NES = AA317-332
Exon 10
...AGGAAGGT
Exon 11 (AA310-368)
ACAAGAGGACAC...GAATTTACAGAG
Exon 12
GACATGGA...
Thr-Arg-Gly-His.... Glu-Phe-Thr-Glu

C

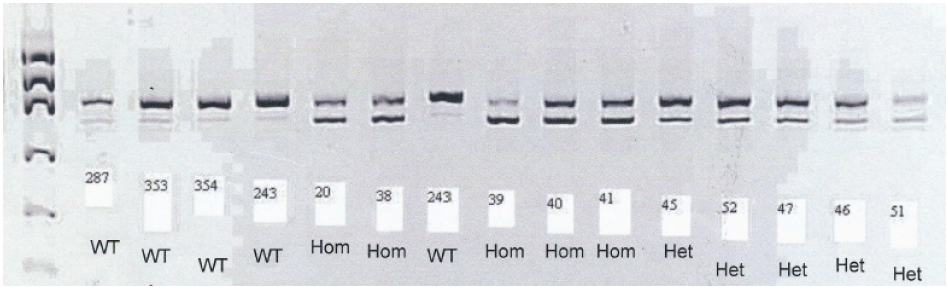
287
353
354
243
20
38
243
39
40
41
45
52
47
46
51
WT
WT
WT
WT
Hom
Hom
WT
Hom
Hom
Hom
Het
Het
Het
Het
Het

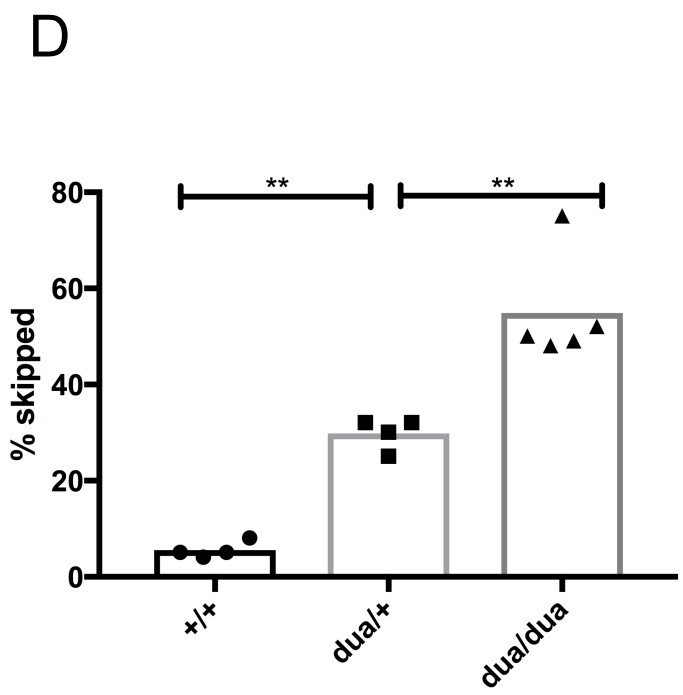

Figure 4.6 Mutation in *Senp2* in *duan* mice causing exon skipping. A) DNA sequence traces for forward and reverse strands of exon 11 from *dua/dua* mice, aligned to the reference B6 mouse genome sequence above, showing the A to G base change. B) Schematic showing location of the mutation in the wobble position of the Glycine 313 codon in exon 11, and the location of annotated domains in the SENP2 protein including a nuclear export signal (NES) encoded by exon 11. C) RT-PCR analysis with primers in exons 9 and 13 from spleen cDNA of mice with the indicated *Senp2*^{duan} genotypes. (Forward primer: GCGTCAGAACAACCCATTTT and reverse primer: CACAGATCCTGTG GCCTTTT). This experiment was performed by Belinda Whittle. (D) ImageJ quantitation of bands in panel C corresponding to correctly spliced and exon 11 skipped PCR products. Columns show arithmetic means, and each dot corresponds to a single sample showing the % skipped from the sum of the areas of both peaks. The lanes on far left and right were omitted from the analysis because of low total PCR product. Statistical analysis by ANOVA with Tukey's multiple comparison test. The difference between +/+ and dua/dua was also significant at $p<0.0001$.

4.6 SENP2 expression and protein structure

The mouse *Senp2* gene encodes a protein of 588 amino acids (589 AA in humans) and is classified as a member of the sentrin-specific proteases family. The SENP2 protein is involved in the processing and deconjugation steps of 'SUMOylation' which is the covalent conjugation of SUMO molecule to the target protein. SENP2 has both isopeptidase and hydrolase activities. However, the deconjugation step is shown to be more efficient (Zuccolo et al, 2007). SENP2 contains both NLS and NES sequences suggesting it undergoes nucleocytoplasmic shuttling.

SENP2 contains several functional domains (Figure 4.5B):
NLS: nuclear localization signal – region required for proper nuclear localization
NES: nuclear exporting signal
SUMO-recognition motif
CD: Catalytic domain

A

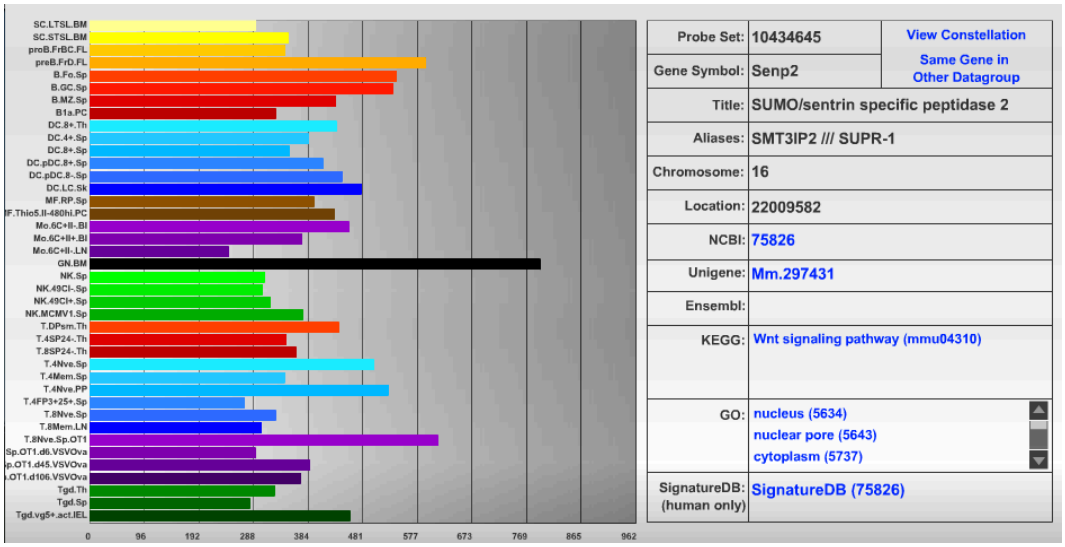

B

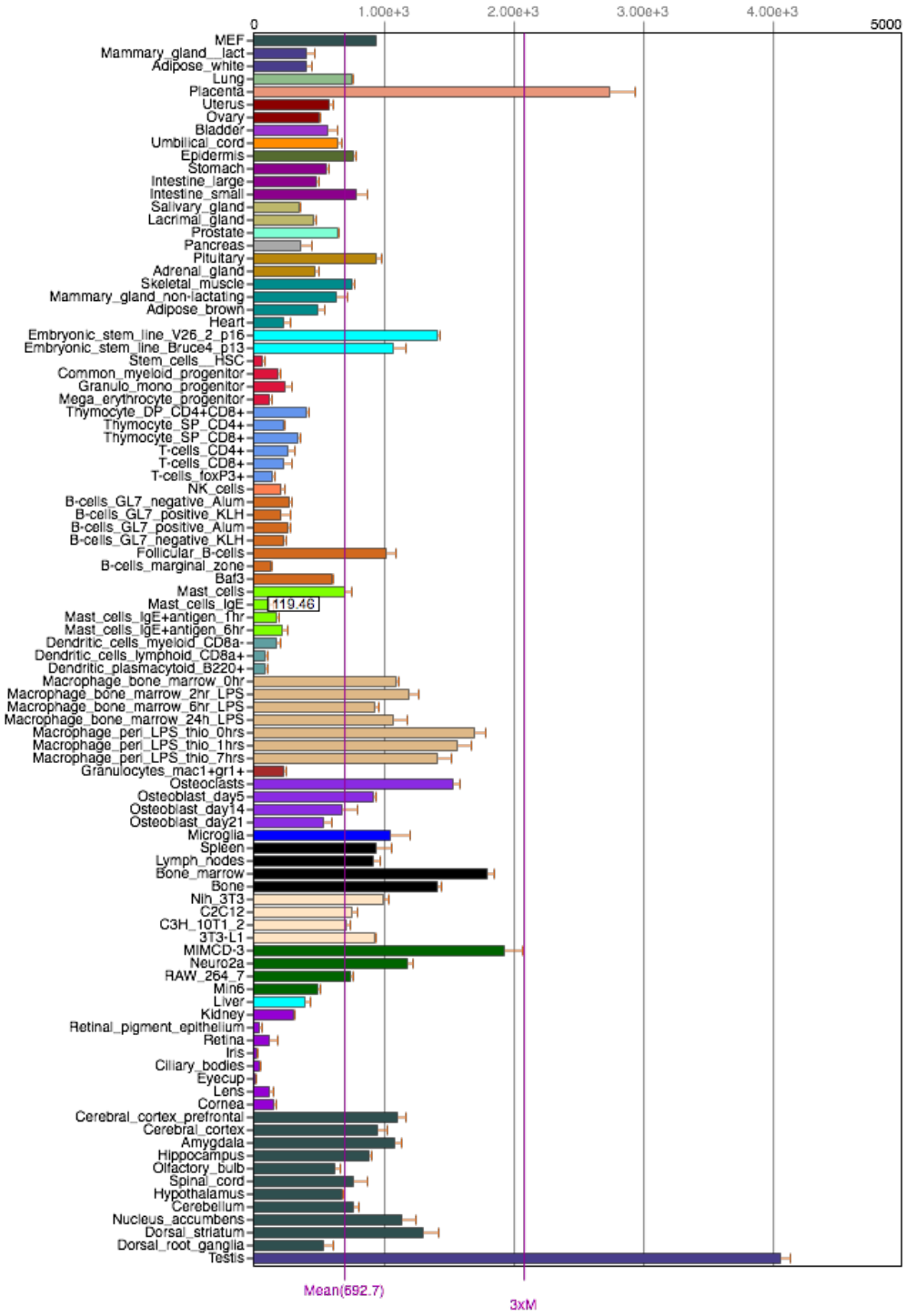

Figure 4.7 *Senp2* mRNA is expressed in immunological cells and tissues. A) *Senp2* expression in immune system, measured by Affymetrix

microarrays in the IMMGEN database (http://www.immgen.org/databrowser/index.html).
B) Affymetrix microarray profiling data from BioGPS showing tissue distribution of *Senp2* mRNA in various mouse tissues (http://biogps.org/#goto=genereport&id=75826).

SENP2 has previously been shown to be highly expressed in trophoblast cells and is indispensible for modulating the p53-Mdm2 pathway in trophoblast development (Chiu et al., 2008). Other studies have shown that SENP2 can colocalize and associate with SUMO conjugated MDM2 in PML bodies and catalyzed the desumoylation step of SUMO conjugated MDM2. The desumoylated MDM2 can bind to and promote p53 degradation, leading to the hypothesis that decreased SENP2 would decrease Mdm2 activity and thereby increase p53 to respond to genotoxic stresses (Jiang et al., 2010). *Senp2* mRNA is expressed widely in cells of the immune system (Figure 4.7A), with somewhat higher expression in naïve OT-I CD8 T cells than in WT naïve CD8 T cells. Interestingly, T cells express lower amounts of *Senp2* mRNA than most other tissues (Figure 4.7B), raising the possibility that they may be particularly sensitive to small decreases in SENP2 activity.

4.7 Investigating the subcellular localization of the mutant SENP2 protein

The *Senp2*$^{dua/dua}$ mutation caused exon 11 skipping in approximately half the amplified spleen cDNA, with the alternatively spliced product encoding a normally minor protein isoform lacking the nuclear export signal (NES). To determine if the alternative splicing affects the subcellular localization of the resulting protein, full-length (WT) and exon 11 deleted (ex11_del) SENP2-GFP fusion proteins were overexpressed in 293T cells. The localization of both proteins was examined 48 hours after transfection. Transiently expressed full-length GFP-SENP2 protein showed typical nuclear punctate localization in

HEK293T cells. (Figure 4.8) The mutant SENP2 displayed a similar localization to WT. Measured in this way, the lack of the NES had no discernable effect on the subcellular localization of SENP2.

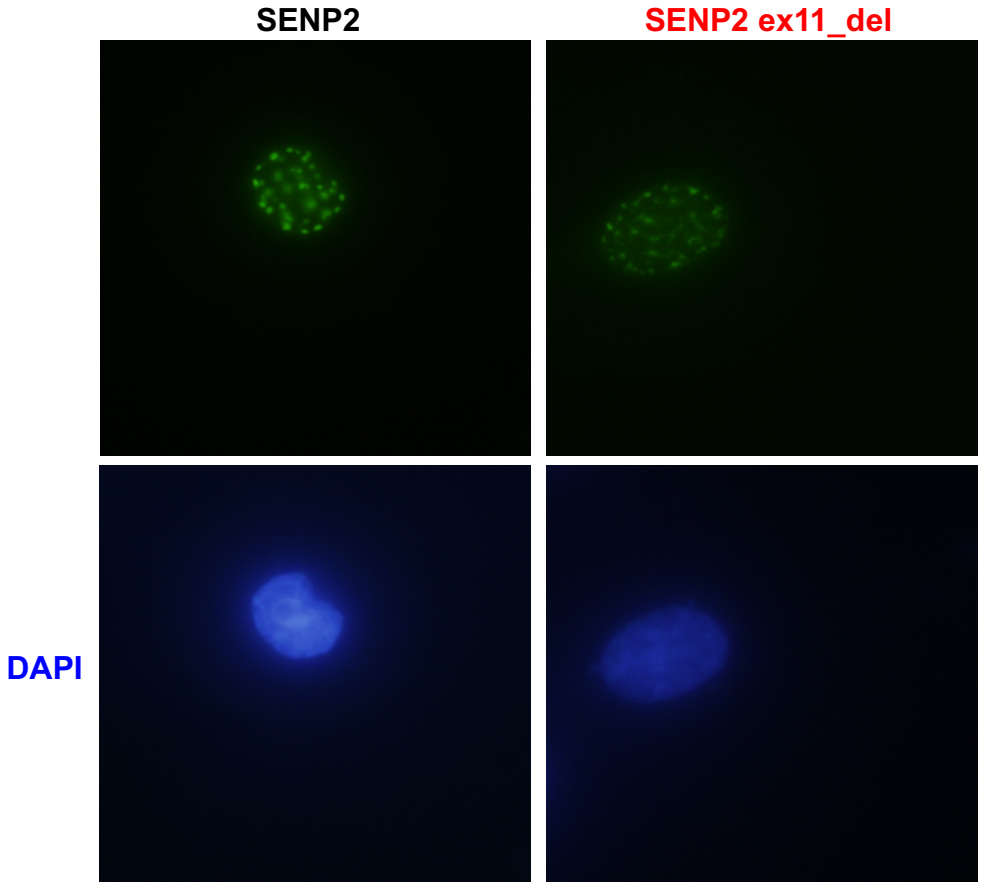

Figure 4.8 SENP2 localizes to the NPC. 293T cells were transiently transfected with cDNA high expression vectors (pEGFP-N1) encoding EGFP-SENP2 (left) or EGFP-SENP2^{ex11_del} (right), fixed and stained with DAPI, and examined by epifluorescence microscopy. Representative images showing EGFP fluorescence in green and DAPI staining in blue.

It has been reported that when expressed at low levels, SENP2 localized around the periphery of the nucleus (Zhang et al, 2002). To study if the *duan* mutation affects the expression of SENP2 when expressed at low level, cDNAs encoding

SENP2-GFP or SENP2^{ex11_del}-GFP fusion proteins were expressed from the retroviral vector pMX in transiently transfected 293T cells. The localization of protein was determined by direct immunofluorescence 48 hours after transfection. WT SENP2 signal localized as a ring around the nucleus. (Figure 4.9) The expression of the mutant SENP2 protein was similar as the WT SENP2 protein. Therefore, the mutation does not appear to affect the subcellular localization of SENP2 even when the protein is expressed at lower levels. It would be valuable to analyse localization in CD8 T cells, given the numbers of these cells were specifically diminished by the mutation, but time did not permit me to perform these follow up experiments.

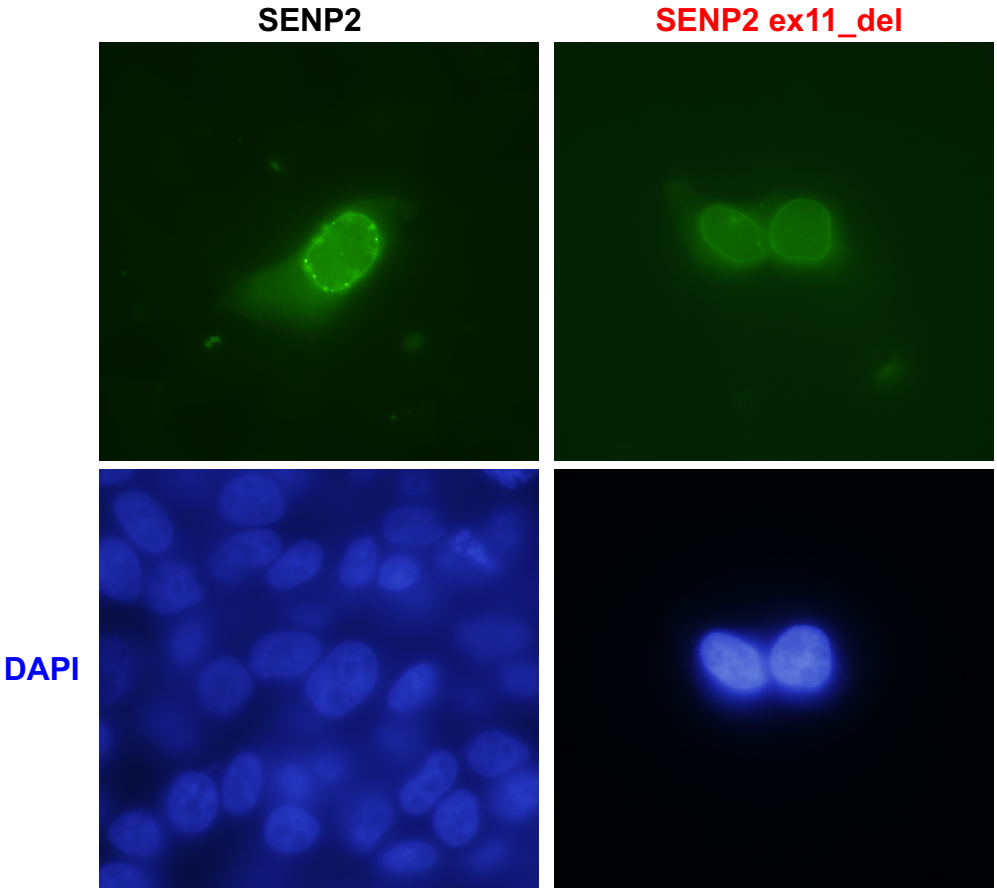

Figure 4.9 Lower expression of SENP2 reveals localization to a discontinuous ring around the nucleus. 293T cells were transiently transfected with pMX expressing EGFP-SENP2 and EGFP-SENP2$^{(ex11_del)}$,

fixed and stained for immunofluorescence. fixed and stained with DAPI, and examined by epifluorescence microscopy. Representative images showing EGFP fluorescence in green and DAPI staining in blue.

4.8 *Senp2*$^{dua/dua}$ OT-I TCR-transgenic mouse model

To study the effect of the *Senp2*^{dua} mutation in antigen specific CD8 T cells, *Senp2*$^{dua/dua}$ mice were bred to the OT-I TCR transgenic strain to generate a monoclonal population of OT-I CD8 T cells that recognize the ovalbumin (OVA) peptide in the context of H-2K^{b}. The percentage of CD8^{+}Vα2^{+} double positive cells was measured to indicate OVA-specific T cells (Fig. 4.10A). Interestingly, in the TCR transgenic setting the percentage of CD8 T cells was not decreased: OT-1 *Senp2*$^{dua/dua}$ mice had similar frequencies to OT-1 *Senp2*$^{+/+}$ mice (4.10A). There was also a similar proportion of CD44^{high} OT-I CD8 T cells in *Senp2*$^{dua/dua}$ mice and WT controls. (Fig. 4.10B). Thus, in OT-1 transgenic *Senp2*$^{dua/dua}$ mice the CD8 T cell lymphopenia was not observed as seen on the nontransgenic background. The particularly high TCR affinity for self peptide – MHC complexes conferred by the OT-I TCR may rescue this phenotype.

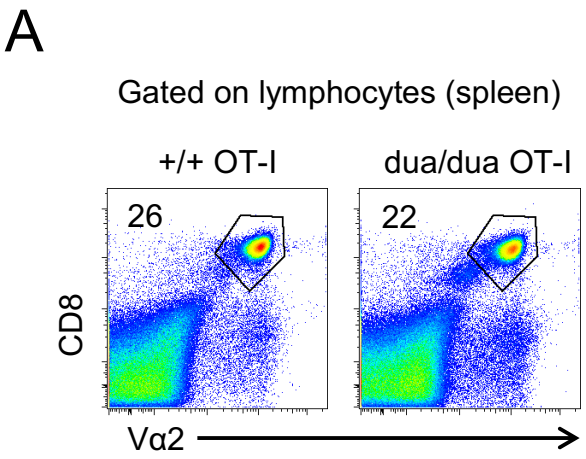

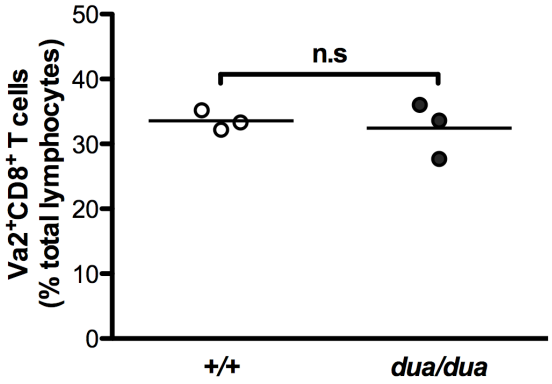

B

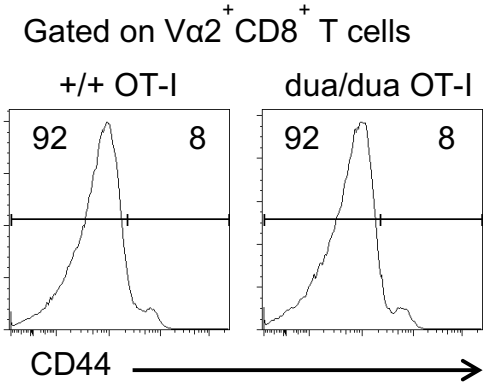

Figure 4.10 Comparison of OT-I CD8 T cell proportions in wild type (+/+) and *Senp2*$^{dua/dua}$ (*dua/dua*) OT-I mice. (A) Representative flow cytometry plots (top) and graph of the percentage of CD8$^+$ Vα2$^+$ cells among lymphocytes in the spleen of wild type (+/+) and *Senp2*$^{dua/dua}$ (*dua/dua*) OT-I mice. Statistical analysis by t-test. (B) Representative histograms show the expression profile of cell surface CD44 on gated CD8$^+$ Vα2$^+$ splenic OT-I CD8 T cells of wild type (+/+) and *Senp2*$^{dua/dua}$ (*dua/dua*) OT-I mice, and the percentage falling within the CD44^{low} and CD44^{hi} gates.

4.9 Poor survival of naïve *Senp2*$^{dua/dua}$ OT-I T cells in lympho-replete recipients

To compare the survival of mutant and wild-type OT-1 CD8 T cells, five million wild-type and *Senp2*$^{dua/dua}$ OT-I CD8 T cells were mixed and co-transferred into the lympho-replete wildtype recipients (Fig. 4.11). The two donor populations could be distinguished from one another and from recipient lymphocytes by their differential expression of the congenic marker CD45.1/CD45.2. The blood of recipients was analyzed at the indicated time points and the population of wild type or *Senp2*$^{dua/dua}$ OT-I CD8 T cells enumerated by flow cytometry along with surface expression of CD44 to assess their activation status.

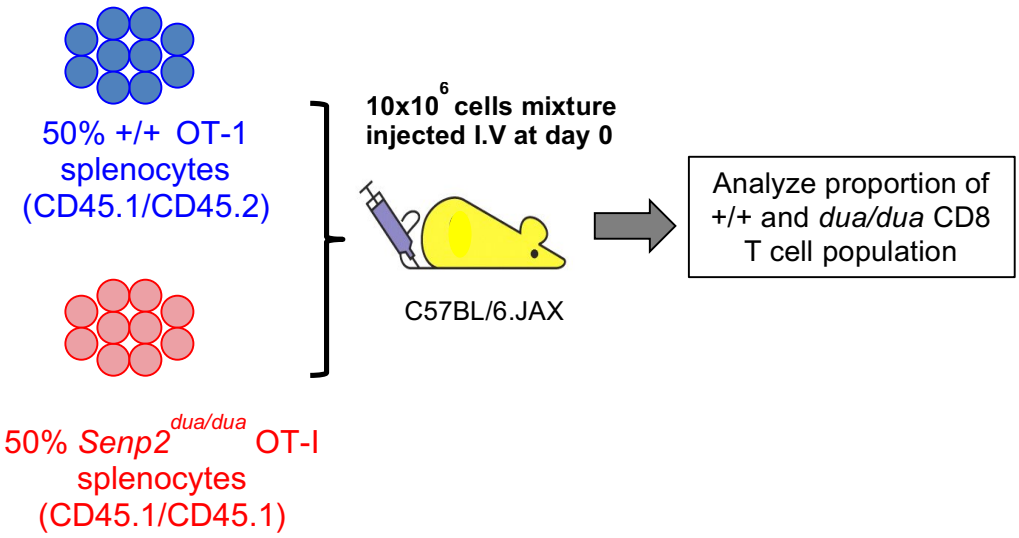

Figure 4.11 Experimental design to compare the survival and persistence of CD8 T cells bearing *Senp2*$^{dua/dua}$ mutation with control T cells bearing wild-type *Senp2*. Schematic diagram showing the experimental design to study whether the survival defect of *Senp2*$^{dua/dua}$ OT-I T cells is cell intrinsic. A 10 x 10^6 cells mixture comprising a ratio of 50:50 wild type (+/+) or *Senp2*$^{dua/dua}$ OT-I CD8 T cells were injected intravenously into the tail vein of each recipient wild type B6 mouse. Recipient mice were bled at various time points and the blood samples of animals were analyzed by flow cytometry.

As shown in Fig. 4.12A, representative flow cytometry plots show the gating strategy applied to identify donor-derived wild type or *Senp2*$^{dua/dua}$ OT-I CD8 T cells from recipient-derived T cells. The OT-I (donor) cells were first gated using CD8^{+} and Vα2^{+} markers and further distinguished using CD45.1, since the B6 recipient-derived CD8^{+}Vα2^{+} cells were homozygous CD45.2 whereas the donor cells were CD45.1 positive. The donor-derived OT1 cells were either heterozygous CD45.1/CD45.2 in the case of *Senp2*$^{+/+}$ wild type OT-I CD8 cells or homozygous CD45.1/CD45.1 in the case of *Senp2*$^{dua/dua}$ OT-I CD8 T cells.

On day 1 after transfer, *Senp2*$^{dua/dua}$ (*dua/dua)* OT-I CD8 T cells comprised 47% of all the OT-1 T cells in the blood, but steadily decreased to 30% by day 15 post transfer, 13% at day 30, and only 6% by day 50 (Figure 4.12B top panel). The surface expression of CD44 was nevertheless comparable on wild type and *Senp2*$^{dua/dua}$ OT-I CD8 T cells at each time point (Figure 4.12B bottom panel).

The survival of wild type and *Senp2*$^{dua/dua}$ OT-I CD8 T cells was analysed as a percentage of all blood lymphocytes in the recipient mice, where they comprised a small minority competing with a full repertoire of normal CD8 and CD4 T cells (Figure 4.13A). Wild type OT-I and *Senp2*$^{dua/dua}$ OT-I CD8 T cells started on Day 1 with similar percentages, between 0.05 and 0.1% of lymphocytes, but the *Senp2*$^{dua/dua}$ OT-I CD8 T cells were significantly reduced compared to wild type cells by day 15 post transfer and became more severe at days 30 and 50 post transfer. Wild-type OT-1 T cells declined slowly, reaching 50% of the day 1 percentage only after 50 days, whereas homozygous mutant OT-1 T cells decreased with a half-life of approximately 10 days.

To show the survival defect caused by the mutation in *Senp2* was not due to a minor histocompatibility rejection from the recipients, a control group of recipients received a mixture of CD45.1/CD45.1 *Senp2*$^{dua/+}$ (*dua/+)* heterozygous mutant OT-1 T cells (from litter mates of the *Senp2*$^{dua/dua}$ mice used in the experimental group) mixed with CD45.1/CD45.2 wild type (+/+) OT-I T cells .

As shown in Fig. 4.13B, there was no significant difference between the wild type and *Senp2*$^{dua/+}$ (*dua/+)* OT-I CD8 T cells as a percentage of all lymphocytes in the recipients at any time point post transfer.

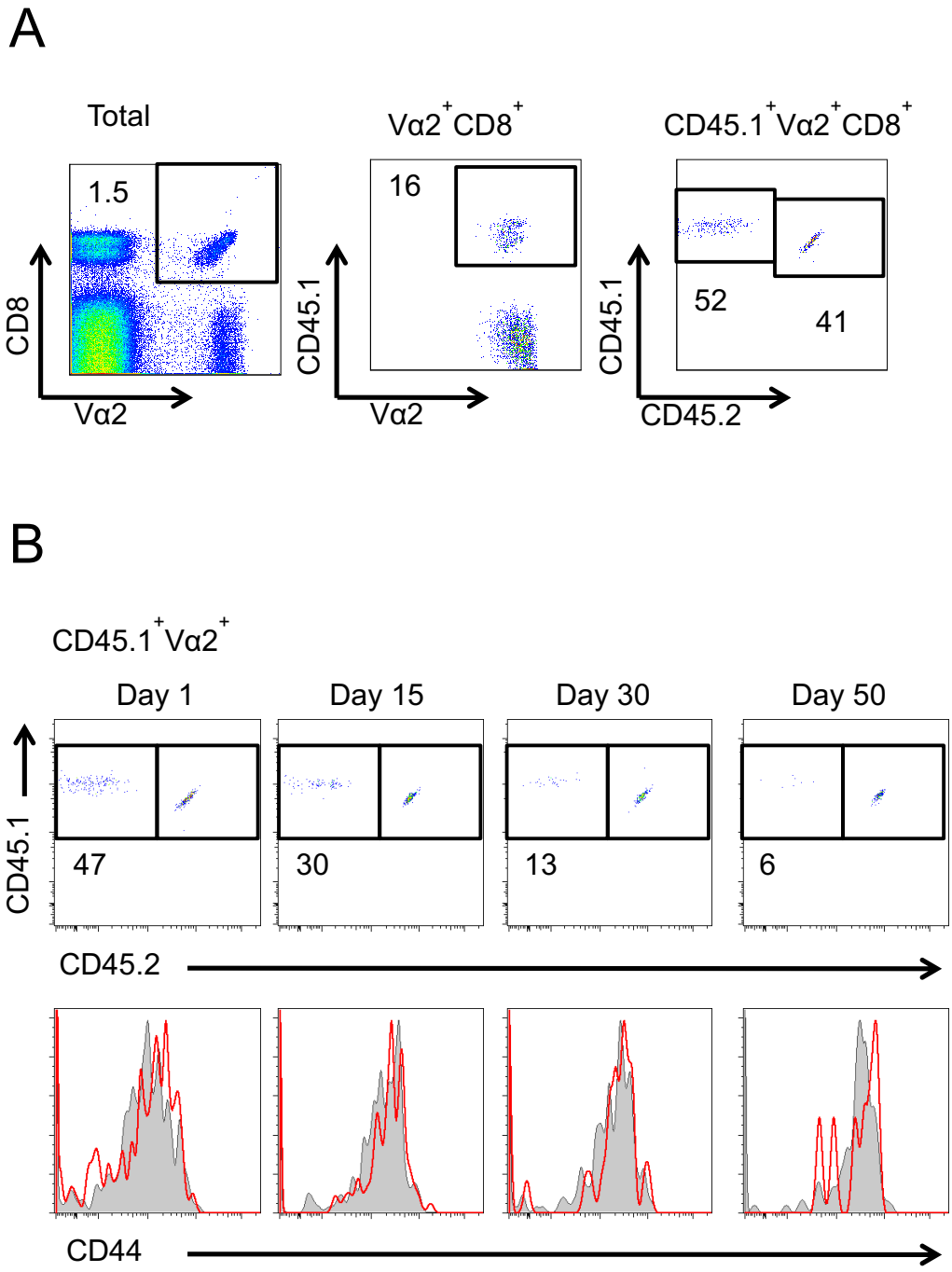

Figure 4.12 Comparison of the persistence of wild type and *Senp2*$^{dua/dua}$ OT-I CD8 T cells adoptively transferred into wild type

recipients. A total number of 10^7 cells, comprising wild type (CD45.1/CD45.2) and mutant (CD45.1) CD8 T cells mixed at a 50:50 ratio, were injected into the tail vein of each B6 wildtype (CD45.2) recipient. (A) Representative flow cytometry plots showing the gating strategy applied to identify the wild type (+/+) or *Senp2*$^{dua/dua}$ (*dua/dua*) OT-I CD8 T cells from the host-derived cells. (B) Representative flow cytometry plots show the survival of donor cells (wild type (+/+) or *Senp2*$^{dua/dua}$ (*dua/dua*) OT-I CD8 T cells) at day 1, day 15, day 30 and day 50. The number indicates the percentage of *Senp2*$^{dua/dua}$ OT-I CD8 T cells among donor OT-I CD8 T cells (top). Representative histograms show the expression profile of CD44 marker on wild type (grey) and *Senp2*$^{dua/dua}$ (solid red line) OT-I CD8 T cells at the same time points (bottom).

A

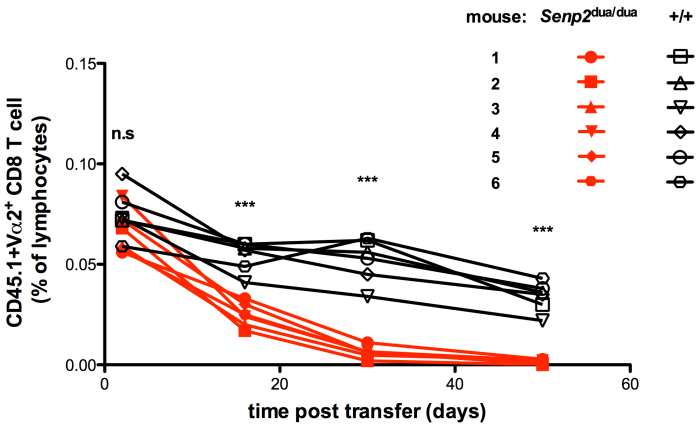

B

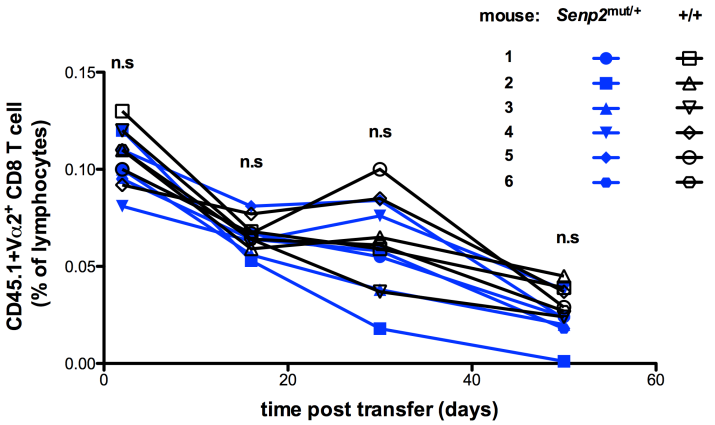

Figure 4.13 Comparison of the persistence of naïve wild type and *Senp2*$^{dua/dua}$ OT-I CD8 T cells in wild type recipients. (A) Frequency of wild type (+/+) OT-I CD8 T cells (black symbols) and *Senp2*$^{dua/dua}$ *(dua/dua)* OT-I CD8 T cells (red symbols) expressed as a percentage of total blood lymphocytes in individual recipients at the indicated days after co-transfer. Two-way ANOVA and Bonferroni post-tests were performed to compare statistical differences in +/+ and *dua/dua* at the indicated time points: at D2 (ns), D16 ($p<0.001$), D30 ($p<0.001$) and D50 ($p<0.001$). 5 animals analysed per time point. This experiment was performed three times. (B) Frequency of wild type (+/+) OT-I CD8 T cells (black symbols) and heterozygous *Senp2*$^{dua/+}$ *(dua/+)* OT-I CD8 T cells (blue symbols) expressed as a percentage of total recipient lymphocytes on the indicated days after co-transfer. Two-way ANOVA and Bonferroni post-tests were performed to compare statistical differences in +/+ and *dua/+* at the indicated time points: D2 (ns), D16 (ns), D30 (ns) and D50 (ns). 5 animals were analysed per time point.

4.10 Retroviral complementation to confirm *Senp2*^{dua} is responsible for diminished survival of T cells from *duan* mice

The data in the previous sections show that the synonymous *Senp2 duan* mutation decreased normal splicing of the mRNA but did not cause any obvious difference in subcellular localization of the short protein isoform. While the *Senp2* mutation was the only mutation detected by exon sequencing of the 70 annotated genes in the mapped chromosome 16 interval, it was necessary to confirm that the mutation found in the *Senp2* gene was responsible for the phenotype seen in the *duan* mice. To prove that the mutation in *Senp2* was responsible for the survival defect in CD8 T cells of *duan* mice, a retroviral based gene transfer experiment was carried out. The *dua/dua* OT-I cells were transduced with a retroviral vector encoding WT full-length SENP2 or a control retroviral vector (empty vector, EV), and then injected into B6 recipients and tracked for survival *in vivo* to determine if the survival of the *dua/dua* CD8 T cells could be restored.

The pMIG II bicistronic plasmids encoding either wildtype *Senp2* and enhanced green fluorescent protein (EGFP) or EGFP alone (empty vector, EV) were transfected into the Phoenix retroviral packaging cell line which expresses env, gag and Pol virus proteins. The supernatants containing infective retroviral particles were used to transduce mouse primary T cells from *Senp2*$^{dua/dua}$ or *Senp2*$^{+/+}$ CD45.1 OT-I TCR-transgenic mice that had first been activated with anti-CD3 and anti-CD28 and cultured for 3 days *in vitro*. Because there were limited numbers of transduced cells, these were injected into the tail vein of single C57BL/6J recipients which were followed longitudinally by flow cytometric analysis of GFP expression among the donor T cells in peripheral blood. To provide a staining control to distinguish the GFP^{+} and GFP^{-} population, non-transduced wild-type OT-I splenocytes were also injected into C57BL.6J mice. As shown in Figure 4.14A upper panel and C, donor OT-1 CD8 T cells (CD45.1^{+}CD8^{+}) were reliably separated from the rest CD8 T cells by using CD45.1 marker, and the GFP^{+} subset could be readily distinguished among them. Three days after transfer, 34% of *Senp2*$^{dua/dua}$ OT-I CD8 T cells were GFP+

expressing the Senp2-GFP vector, and 32% of WT OT-I CD8 T cells transduced with EV were GFP+ (Figure 4.14A upper panel). By day 97 after transfer, the percentage of GFP^+ cells increased to around 37% in the *Senp2*$^{dua/dua}$ OT-I CD8 T cells while the percentage of GFP^+ cells in the WT OT-I CD8 T cells remained at 22%. By day 140, the percentage of GFP^+ cells increased to 47% in the *Senp2*$^{dua/dua}$ OT-I CD8 T cells but remained at 20% for the WT OT-1 controls (Figure 4.14 lower panel).

The recipient mice were sacrificed 328 days after transfer and spleen cells analysed. As shown in Figure 4.14C, the WT OT-1 cells with no transduction lacked GFP+ cells while the WT OT-I CD8 T cells transduced with EV had 8% GFP^+ cells. By contrast, the GFP^+ cells had dramatically increased to 88% of the *Senp2*$^{dua/dua}$ OT-I CD8 T cells transduced with WT SENP2.

A

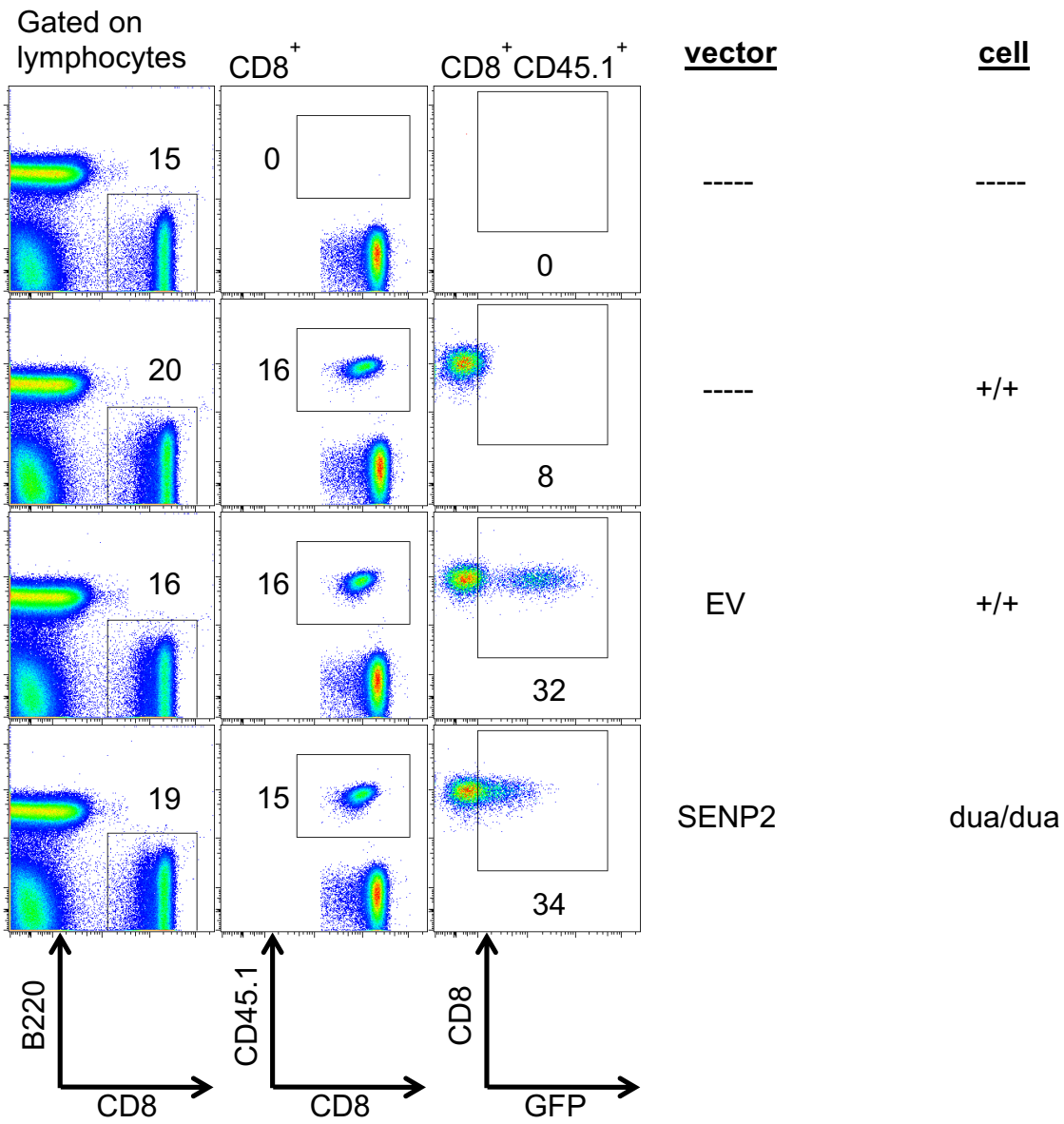
Gated on lymphocytes
CD8+
CD8+CD45.1+
vector
cell
15
0
0

20
16
8

+/+
16
16
32
EV
+/+
19
15
34
SENP2
dua/dua
B220
CD8
CD45.1
CD8
CD8
GFP

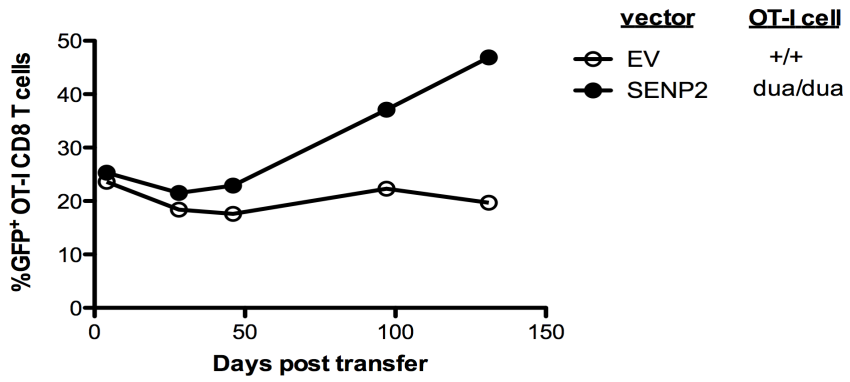
%GFP+ OT-I CD8 T cells
50
40
30
20
10
0
0
50
100
150
Days post transfer
vector
OT-I cell
EV
+/+
SENP2
dua/dua

B

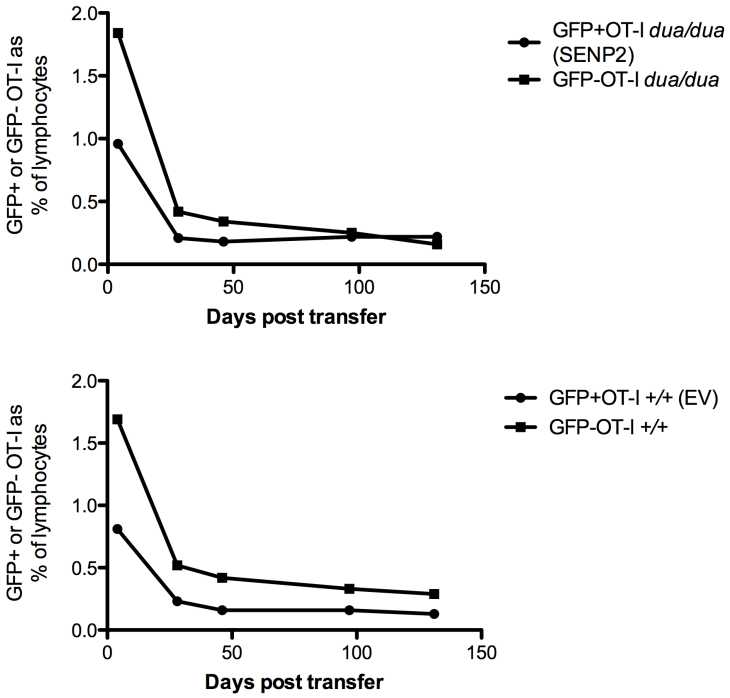
GFP+ or GFP- OT-I as % of lymphocytes
2.0
1.5
1.0
0.5
0.0
0
50
100
150
Days post transfer
GFP+OT-I dua/dua (SENP2)
GFP-OT-I dua/dua
GFP+ or GFP- OT-I as % of lymphocytes
2.0
1.5
1.0
0.5
0.0
0
50
100
150
Days post transfer
GFP+OT-I +/+ (EV)
GFP-OT-I +/+

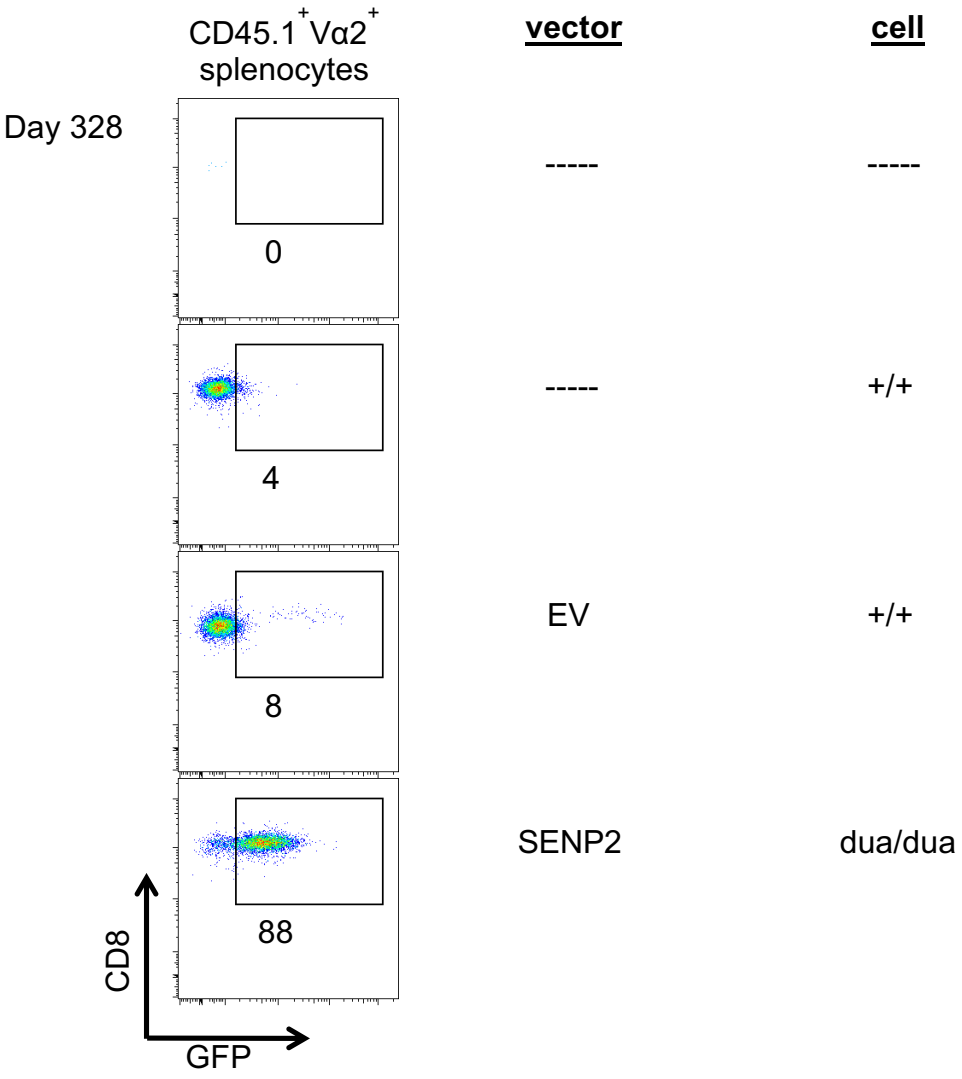

Figure 4.14 Preferential survival of *Senp2*$^{dua/dua}$ OT-1 CD8 T cells transduced with a retroviral vector encoding full length SENP2. (A) Representative flow cytometry plots show the gating strategy applied to identify the GFP^{+} cells on CD45.1^{+}CD8^{+} donor cells in blood 3 days after transfer into C57BL/6 recipients. (upper panel) Results of sequential flow cytometry testing of blood on the indicated days after transfer of OT-1 T cells into C57BL/6 mice, showing the percentage of GFP^{+} cells among CD45.1+ CD8+ *Senp2*$^{dua/dua}$ OT-I T cells transduced with WT SENP2

(close circles) and among WT OT-I CD8 T cells transduced with EV (open circles) (lower panel) (B) Results of decline of GFP+ or GFP- cells as % of lymphocytes. (C) Flow cytometry of spleen cells on day 328 after transfer, gated on CD45.1+ CD8+ lymphocytes, showing the % that were GFP^+ cells in recipients of no donor cells, non-transduced WT OT-I CD8 T cells, EV-transduced WT OT-I CD8 T cells, and WT SENP2-transduced *Senp2*$^{dua/dua}$ OT-I CD8 T cells.

The retroviral complementation experiment was then repeated with 2 recipient mice receiving the *Senp2*$^{dua/dua}$ OT-I splenocytes transduced with WT SENP2 and 1 recipient receiving the WT OT-I splenocytes transduced with EV. As shown in Figure 4.15A, at the first timepoint after transfer 5% of WT OT-I CD8 T cells were GFP+ and 10% of *Senp2*$^{dua/dua}$ OT-I CD8 T cells were GFP+. Similar to the previous experiment, the percentage of GFP^+ cells had increased to 23% in both recipients 88 days after transfer and more than 30% after 180 days in the SENP2 transduced *Senp2*$^{dua/dua}$ OT-I CD8 T cells. By contrast, there was little increase in the percentage of GFP^+ cells in EV-transduced WT OT-I CD8 T cells at the same timepoints. When the recipient mice were sacrificed at day 329 after transfer (Figure 4.15B), the percentage of GFP^+ cells in the *Senp2*$^{dua/dua}$ OT-I CD8 T cells transduced with WT SENP2 in individual recipients had increased to 45% and 65%.

A

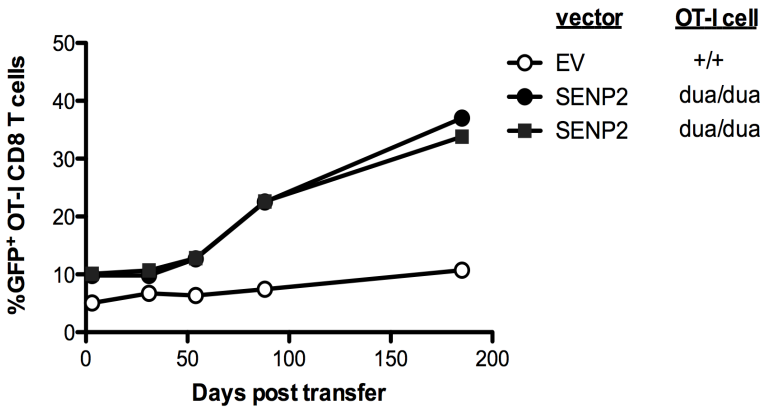

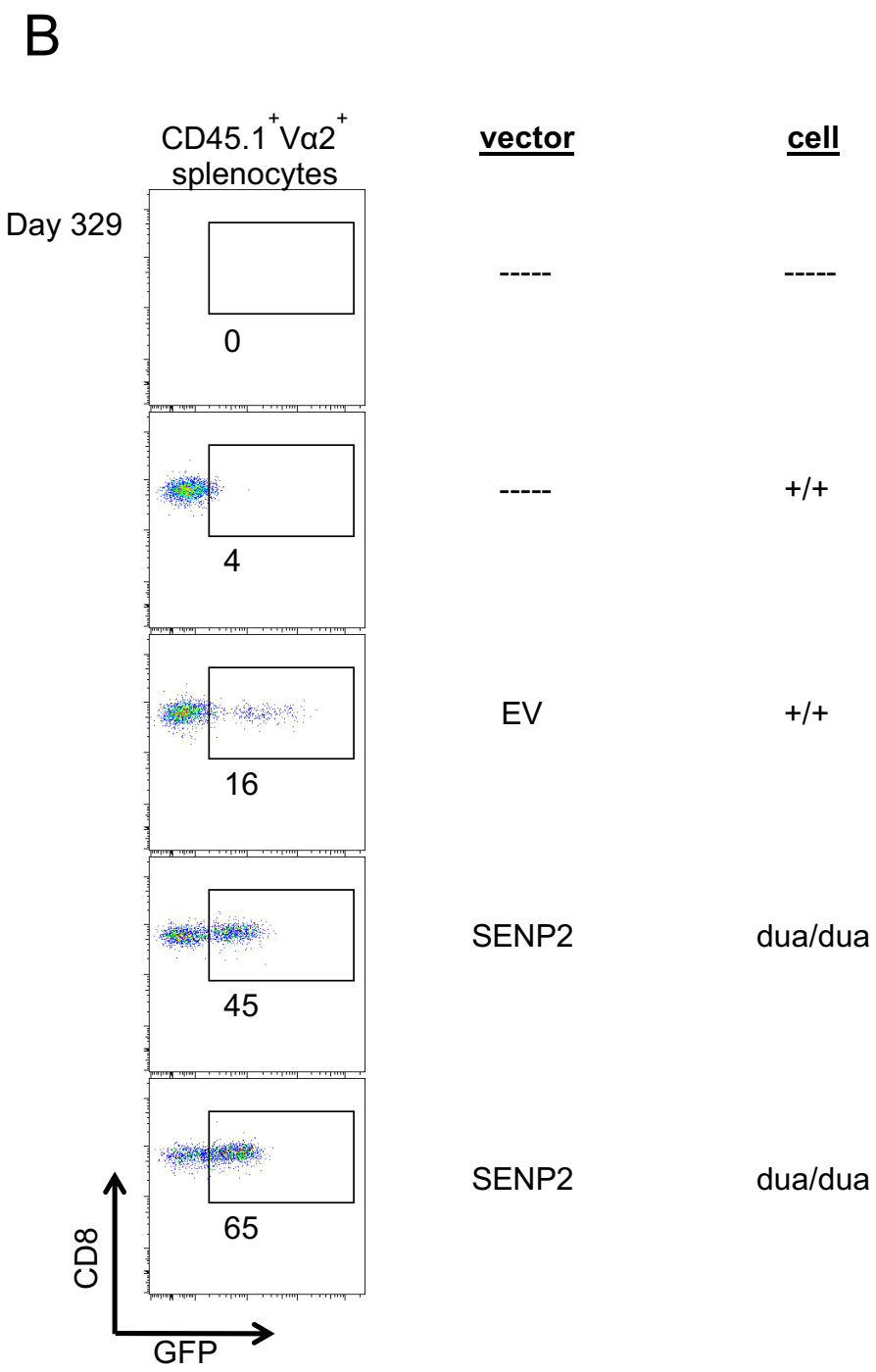

Figure 4.15 Preferential survival of *Senp2*$^{dua/dua}$ CD8 T cells with retroviral expression of full length SENP2. (A) Results of sequential flow cytometry testing of blood on the indicated days after transfer of OT-1 T cells into C57BL/6 mice, showing the percentage of GFP^{+} cells among

CD45.1+ CD8+ *Senp2*$^{dua/dua}$ OT-I T cells transduced with WT SENP2 (close circles) and among WT OT-I CD8 T cells transduced with EV (open circles). (B) Flow cytometry of spleen cells 329 days after transfer, gated on CD45.1+ CD8+ lymphocytes, showing the % that were GFP^{+} in recipients of no donor cells, non-transduced WT OT-I CD8 T cells, EV-transduced WT OT-I CD8 T cells, and WT SENP2-transduced *Senp2*$^{dua/dua}$ OT-I CD8 T cells.

The experiments above left open the possibility that overexpression of full length SENP2 might enhance survival of OT-1 cells generally, regardless of the *duan* mutation. To test this possibility, a separate experiment was designed. C57BL/6J mice were injected with WT OT-I splenocytes that had been transduced with the full length SENP2 EGFP vector or the empty EGFP vector. The recipient mice were bled at various time points to check if enforced SENP2 expression could increase the survival of WT OT-I CD8 T cells. As shown in Figure 4.16, at the first time after transfer there were 10-13% GFP^{+} cells among blood CD45.1+ CD8+ OT-I T cells transduced with WT SENP2 or EV, and these percentage remained steady between 10-16% from day 20 to day 125. The lack of any increase in GFP+ cells when SENP2 vector was introduced into OT1 cells with wildtype *Senp2* genes contrasted with two experiments above where the percentage of GFP^{+} cells progressively increased over time when the SENP2 vector was introduced into *Senp2*$^{dua/dua}$ OT1 cells. This gene complementation experiment supports the conclusion that the deficiency of full-length SENP2 protein is responsible for the survival defect of CD8 T cells in *duan* mice.

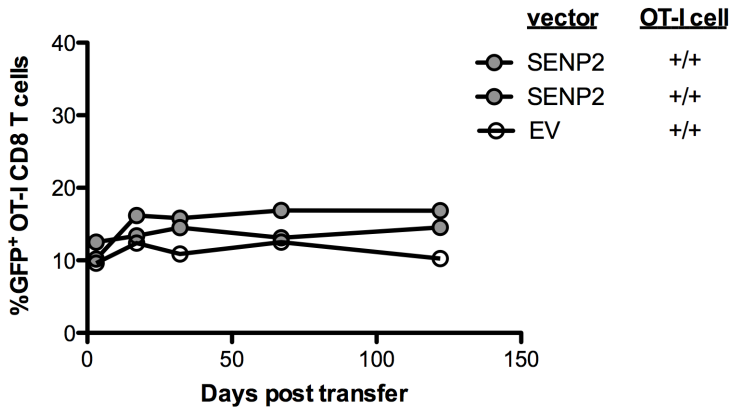

Figure 4.16 Retroviral expression of full length SENP2 does not give wild type OT-1 T cells an extra survival advantage. (A) The percentage of GFP^+ cells among CD45.1+ CD8+ WT OT-I cells transduced with WT SENP2 (grey circles) or among WT OT-I CD8 T cells transduced with EV (open circles), measured sequentially in blood lymphocytes of individual recipients on the indicated days.

4.11 Outcross to knockout strain shows that the *Senp2* gene is responsible for the *duan* phenotype

To further confirm that the *duan* mutation in *Senp2* causes the CD8 T cell phenotype, $Senp2^{dua/+}$ mice were crossed to $Senp2^{+/-}$ mice heterozygous for a targeted null allele that causes early embryonic lethality in homozygous state due to developmental defects in all three trophoblast layers (Chiu et al, 2008). As shown earlier (Fig 4.4), the *dua* mutation is recessive, so that *dua/+* animals with one wild type *Senp2* allele have normal frequencies of CD8 T cells. If the exon 11 variant in *Senp2* was the causative mutation, then inactivation of the wild type allele in *dua/-* compound heterozygotes should either yield the same T cell deficiency as observed in *dua/dua* homozygotes or a more severe phenotype (due to a further loss of full length SENP2). As shown in figure 4.17A and B, there was no discernable decrease in CD8 T cells comparing $Senp2^{+/+}$ and $Senp2^{+/-}$

mice heterozygous for the null allele whereas the number of CD8 cells was significantly lower in *Senp2*$^{dua/-}$ compound heterozygous mice, comparable to *dua/dua* homozygotes. Likewise, the percentage of CD44^{hi} cells among CD8 T cells was higher in compound heterozygous *Senp2*$^{dua/-}$ mice than in *Senp2*$^{+/+}$ and *Senp2*$^{+/-}$ controls (58% vs 25% and 21%) (Figure 4.17A) and the number of CD44^{low} CD8 T cells was diminished even more than the total number of CD8 cells (Figure 4.17B). *Senp2*$^{dua/-}$ compound heterozygous mice and *dua/dua* homozygotes were comparable in all analysis (Figure 4.17B). Thus, the *duan* mutation was not complemented by a null mutation in Senp2, confirming that the SENP2 loss of function is responsible for the diminished number of naïve CD8 T cells in the *duan* strain.

Interestingly, the *Senp2*$^{dua/-}$ compound heterozygous mice had significantly fewer B cells and CD4 T cells compared to *Senp2*$^{+/+}$ and *Senp2*$^{+/-}$ mice, whereas the decrease in these numbers was not statistically significantly in the *dua/dua* mice analysed alongside (Figure 4.17B) and no significant decrease in B cells or CD4 T cells was found in independent cohorts of *dua/dua* mice analysed in the next chapter. This raises the possibility that B cell and CD4 T cells are not affected by the reduced amount of correctly spliced *Senp2* mRNA in *dua/dua* homozygotes, but are affected when the normal mRNA is further decreased because one of the alleles carries the exon 11 *dua* mutation and the other is unable to make *Senp2* mRNA at all.

A

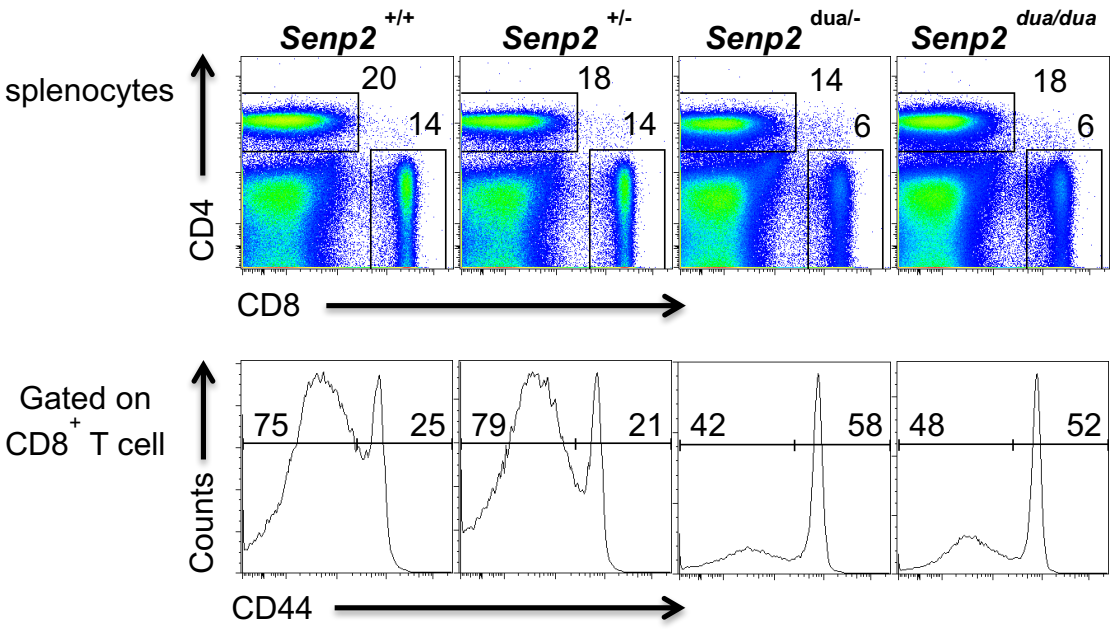
Senp2 +/+
Senp2 +/-
Senp2 dua/-
Senp2 dua/dua
splenocytes
20
14
18
14
14
6
18
6
CD4
CD8
Gated on
CD8+ T cell
75
25
79
21
42
58
48
52
Counts
CD44

B

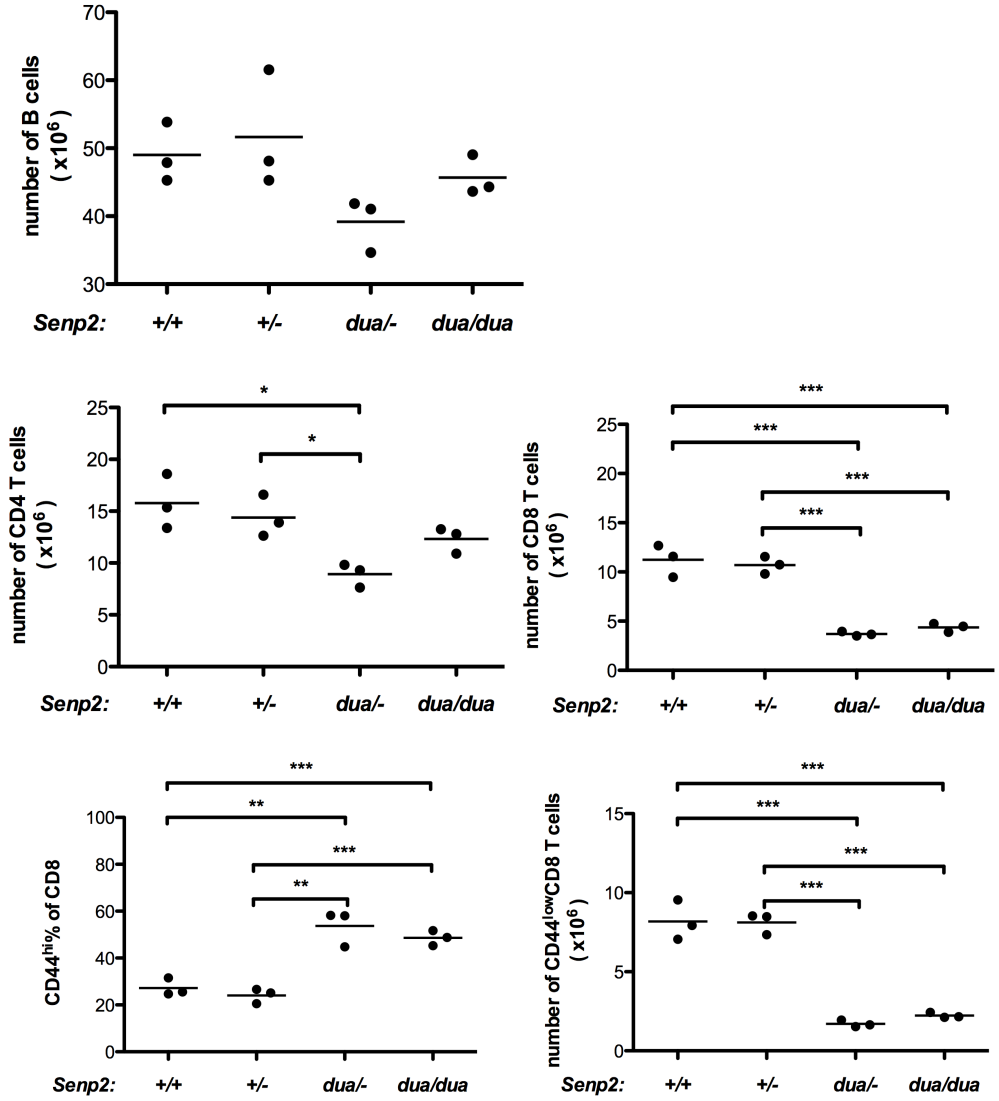

Figure 4.17: Lower percentage of CD8$^+$ T cells in *Senp2*$^{dua/-}$ compound heterozygotes like *Senp2*$^{dua/dua}$ homozygotes. (A) Representative FACS plots of peripheral blood lymphocytes, showing the percentage of CD4 and CD8 cells (upper panel) and %CD44^{low} and CD44^{hi} among CD8 cells in mice with the indicated genotypes. (B) Absolute number of B220+, CD4+, CD8+, CD8+CD44^{lo} and percentage of CD44^{hi}CD8 lymphocytes in the spleen of individual

mice of the indicated genotypes. Dots represent single mice and the bars represent the arithmetic mean. Statistical analysis by one-way ANOVA followed by Bonferroni post test: * p<0.5, ** p<0.005, ***p<0.0005.

4.12 Discussion

The findings presented in this chapter reveal a mouse strain, ENU7B6:039, with CD8 T cell lymphopenia caused by a recessive decrease-of-function mutation in *Senp2*. Homozygous mutant mice had decreased numbers of CD8 T cells and especially reduced number and percentage of naïve $CD44^{low}$ CD8 T cells, and shorter persistence of naïve $CD44^{low}$ CD8 T cells when transplanted into syngeneic wild-type mice. The mutation was mapped to a 3.9 Mb interval on chromosome 16 and identified as a synonymous mutation in exon 11 of the *Senp2* gene that decreased splicing of exon 10 to exon 11. Mice with a *Senp2* null allele fail to develop beyond the earliest stages of embryogenesis (Chiu et al, 2008), and an immunological role for SENP2 has not been previously reported.

From our RT-PCR data, the '*dua*' mutation decreased the percentage of amplified cDNA product splicing exon 10 to exon 11 from 95% to 45% (Figure 4.6D). While the remaining amplified PCR product skipped exon 11 and spliced exon 10 to the unmutated exon 12 acceptor, it is not possible from the PCR study to determine how much the mutation decreases the overall abundance of full-length *Senp2* mRNA. In wild-type mice, 5% of the PCR product skipped exon 11 and spliced to exon 12. If the exon 11 mutation does not enhance splicing to exon 12 but simply decreases splicing to exon 11, then the increase of the skipped product from 5% to 30% of the amplified material in the heterozygotes would imply an 8-fold decrease in the abundance of full-length mRNA from the mutant allele. In the homozygotes, where the skipped product comprises 55% of both products, this would represent a 23-fold decrease in full-length product assuming the rate of splicing to exon 12 is unaltered. However if there is competition between the exon

11 and exon 12 splice acceptors, the exon 11 mutation may increase the efficiency of the competing splicing reaction to exon 12 as much as it decreases splicing to exon 11. In this scenario there would be no decrease in overall Senp2 mRNA and the abundance of full-length mRNA would be decreased by 55%.

As shown here, heterozygosity for a null *Senp2* mutation on its own did not cause CD8 T cell deficiency, indicating that complete loss of half the normal gene dose is insufficient to recapitulate the homozygous *dua/dua* T cell phenotype. Conversely complete lack of normal SENP2 in homozygous knockouts is embryonic lethal (Chiu et al, 2008), indicating that the *duan* mutation preserves some normal SENP2. Based on the reasoning above and the intermediate proportion of skipped PCR product in heterozygotes, it was theoretically possible that T cell deficiency in *dua/dua* homozygotes was caused by increased production of the exon 11 skipped product above a threshold crossed in *dua/dua* homozygotes but not in *dua/+* mice with only one mutant allele. This possibility is nevertheless excluded by the finding that CD8 T cell deficiency was at least as severe in mice with a single *dua* mutant allele when the other *Senp2* allele was null. Thus it is likely that diminished CD8 T cells in *duan* mice results from a decrease in the production of normally spliced *Senp2* mRNA and protein by more than 55%, and potentially as much as 96% (23-fold), but less than 100%. Since the PCR experiments only examine one part of the mRNA, it is also possible the loss of normally spliced *Senp2* mRNA involves some transcripts from the gene and not others, for example originating at different promoters or using alternative exons 5' or 3' to exons 10-12. It would be useful in future studies to compare the total amount of *Senp2* mRNA in *dua/dua*, +/+ and +/- CD8 T cells by quantitative RT-PCR with primers from different regions of the cDNA, and to measure the amounts of different SENP2 protein species by western blotting of sorted CD8 T cells.

Inefficient splicing of *Senp2* exon10 to exon 11 has also been associated with another mutation causing diminished T cell survival and lower CD127 expression, involving a distinct gene, *Hnrpll,* which encodes an RNA-binding splicing

regulator (Cho et al., 2014). In that study, deep sequencing of oligo-dT primed cDNA from OT1 CD8 T cells revealed that splicing of *Senp2* exon 10 to exon 11 is normally delayed compared to the other exons, so that a substantial proportion of the sequence reads retained parts of the intron. In T cells with a destabilizing HNRPLL mutation a larger fraction of reads retained this intron and less mRNA encoding full-length protein was present. Poor survival of *Hnrpll* mutant OT1 CD8 T cells could be corrected by retroviral expression of cDNA encoding full length SENP2 (Cho et al.,2014). Hence the inefficient splicing of *Senp2* exon 11 appears to be an important rate-limiting step controlling CD8 T cell survival.

The nuclear export signal (NES) encoded by *Senp2* exon 11 is located in the nonhomologous domains of SENP2 and can be blocked by CRM1 inhibitor leptomycin B (LMB) (Itahana et al., 2006). We hypothesized that the mutation in SENP2 protein might affect the subcellular localization of the mutant protein. However, overexpression of the mutant in HEK293T cells revealed no difference in the subcellular localization compared to the WT SENP2 protein. The loss of NES was dispensable for proper subcellular localization. The phenotype is unlikely caused by the mislocalization of protein, or mislocalization might occur selectively in CD8 T cells. Alternatively, as appears to be the case in *Hnrpll* mutant CD8 T cells, a further decrease in an already slow splicing reaction between exon 10 and exon 11 may simply decrease the overall abundance of SENP2 mRNA and protein by more than 50% and as much as 90% as discussed above.

The results here showing that the NES skipped SENP2 product of the *duan* mutation has apparently normal subcellular localization is consistent with previous work showing that the localization of SENP2-GFP was not affected by mutating the essential leucine residues in the NES (Itahana et al., 2006). In that study, the NES mutation only had an effect when combined with NLS deletion mutants, resulting in substantial nuclear accumulation. It was suggested that the NES in SENP2 functions in the protein especially when NLS was deleted.

Survival of *Senp2*$^{dua/dua}$ OT-I CD8 T cells, but not their +/+ counterparts, was enhanced by retroviral expression of full-length *Senp2* cDNA. This provides further evidence that the *Senp2*$^{dua/dua}$ exon 11 mutation is the causal mutation responsible for the CD8 T cell lymphopenia phenotype. The analysis of *Senp2*$^{dua/-}$ compound heterozygous mice that were generated from outcross of the '*dua'* mutation to *Senp2*$^{+/-}$ knockout mice showed reduced naïve CD8 T cells frequency and number in spleen. The failure of the *Senp2* null allele to complement the *dua* allele proved that Senp2 was the causal mutation.

The *Senp2* null mutation is embryonic lethal at embryonic day 10 due to a defect in accumulation of SUMOylated Pc2/CBX4 resulting in a defect in embryonic cardiac development (Kang, X., et al., 2010). SENP2 has been previously shown to be highly expressed in trophoblast cells and is indispensible for modulating the p53- *Mdm2* pathway during trophoblast development (Chiu et al., 2008). Further study showed SENP2 can co-localize and associate with SUMO conjugated MDM2 in PML bodies where it catalyzes the desumoylation step of SUMO conjugated MDM2 (Jiang et al., 2010). The desumoylated Mdm2 binds to p53 and promotes its degradation. Their study proposes a negative regulation of SENP2 in the MDM2-p53 circuit that is important for genotoxic stresses (Jiang et al., 2010). By contrast homozygous *duan* mice are born normally without any physical abnormalities, indicating that the essential embryonic functions of *Senp2* are preserved by the point mutant allele.

SENP1, a closely related member of SENP2 in the Sentrin-specific protease family, has been studied extensively in mice. Inactivation of the mouse *SENP1* gene leads to embryonic lethality due to placental defects (Yamaguchi et al., 2005). The mutant SENP1 causes an increase in the overall levels of SUMO-1 conjugation but not the levels of SUMO-2 or SUMO-3 conjugation revealing a role for SENP1 in both conjugation and deconjugation of SUMO-1. SENP1 also has an indispensable role in the immune system. Conditional knockout mice have shown that SENP1 is essential in the early development of B and T cells (Nguyen et al., 2012). In SENP1$^{-/-}$ B and T cells, the SUMOylated form of STAT5

accumulates and sumoylated STAT5 remains inactive and unable to form dimers or translocate to the nucleus to activate transcription. STAT5 signalling in developing B and T cells is critical for transmitting survival signals from the cytokine, IL-7. It is interesting that CD127, the alpha chain of the IL-7 receptor, is decreased on the surface of *dua/dua* CD8 T cells, raising the possibility that both SENP proteins contribute in distinct ways to regulate IL-7 signalling for lymphocyte survival.

SENP3 and SENP5 are members of the second SENP subfamily. SENP5 localizes mainly to the nucleolus and nucleus (Gong and Yeh, 2006). Sequences in the N terminus of SENP5 are responsible for nucleolar localization. It has been shown that SENP5 has C-terninal hydrolapse activity against SUMO-3 and isopeptidase acitivity against SUMO-2 and SUMO-3 conjugates. As a closely related member of SENP5, SENP3 also shows similar subcellular localization and substrate specificity.

As most divergent members of the SUMO protease family, SENP6 and SENP7 catalyze the deconjugation of SUMO-2 and SUMO-3 and the di-SUMO chains composed of SUMO-2 and SUMO-3. However, they have a lower preference for processing SUMO precursors (Lima and Reverter, 2008).

It has been shown by Itahana et al that the protease function of SENP2 is not affected by the induction of mutations of two essential leucine residues in the NES (Itahana et al., 2006). To answer if *duan* mutation affects the protease function of the protein different from the mutant form in other studies, an *in vivo* sumoylation assay could be performed to determine the desumoylation activity of mutant protein. Moreover, quantitative PCR and protein half-life assay would also be useful to understand the causal mutation at mRNA and protein level.

Currently there is no known point mutation reported in SENP2 protein in mice or human. The *duan* mice offer us a unique resource to understand how a mutation in a Sentrin-specific protease affects T cell homeostasis, and appear to reveal a novel

control over peripheral CD8 T cell survival. This issue is explored in more detail in the following chapter.

Chapter 5: Functional analysis of CD8 T cells in *duan* mice

5.1 Aim

The aim of the experiments in this chapter were to understand the role of SENP2 in the survival of naïve CD8 T cells and persistence of activated/memory CD8 T cells. First of all, I wanted to know if the naïve *Senp2*$^{dua/dua}$ CD8 T cells could survive in the periphery (section 5.2). Then, I studied whether the *Senp2*$^{dua/dua}$ CD8 T cells could undergo activation and proliferation *in vivo* (section 5.4). I also investigated the possible causes of the survival defects by analyzing IL-7 and TCR signaling pathway *in vivo* and *in vitro* (section 5.3).

5.2 *Senp2*$^{dua/dua}$ mice have normal thymic development

T cells originate from common lymphoid progenitor cells (LPC) and migrate into the thymus for further maturation. To understand if the reduced CD8 T cell phenotype in the periphery was caused by a developmental defect of T cells in the thymus or a survival defect of mature T cells in the periphery, thymocyte subsets from wild type and homozygous mutant mice were assessed by flow cytometry. The CD4 and CD8 double negative (DN) thymocytes can be divided into four developmental stages based on their expression of CD44 and CD25: DN1 ($CD25^-$ $CD44^+$), DN2 ($CD25^+CD44^+$), DN3 ($CD25^+CD44^-$) and DN4 ($CD25^-CD44^-$) (Godfrey et al., 1993). From Figure 5.1A (bottom panel), there was a similar percentage of wild type and *Senp2*$^{dua/dua}$ cells in each developmental stage: 13% vs 16% in DN1, 5% vs 5% in DN2, 50% vs 47% in DN3 and 32% vs 32% in DN4 respectively. There was also a normal percentage of double positive (DP) and CD4 and CD8 single positive T cells present in *senp2*$^{dua/dua}$ thymocytes (Figure 5.1A upper panel). The absolute numbers of thymic subsets from both groups were also analysed (Figure 5.1B). The *dua/dua* mice had comparable numbers of total thymocytes compared with wild-type mice. There was no significant difference in the cell number of DN1-4, DP and CD4 and CD8 SP cells between both groups. Therefore, the *duan* mutation has no discernable effect on T cell development in the thymus.

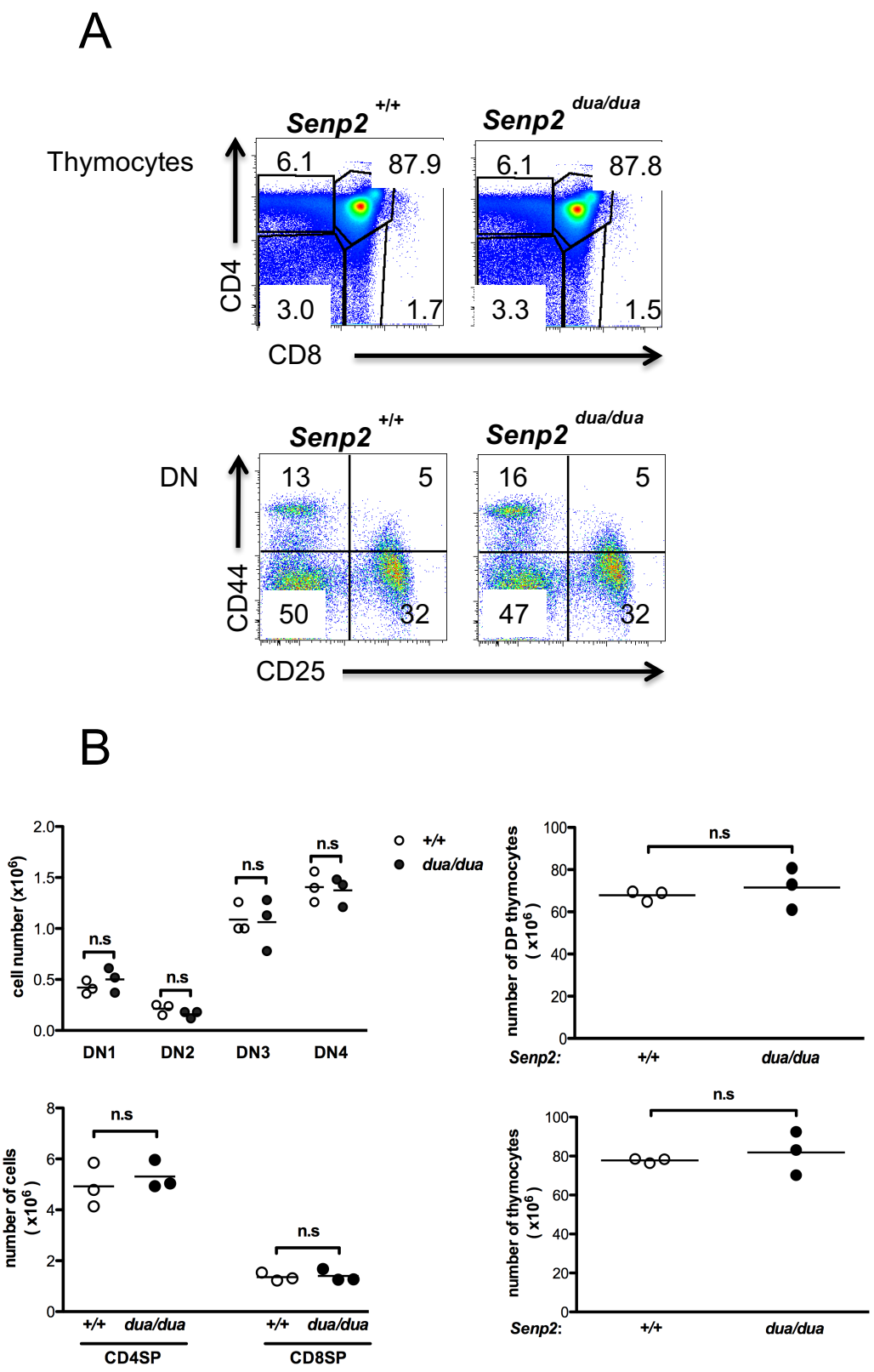

Figure 5.1: The *Senp2*$^{dua/dua}$ mutation does not affect T cell development in the thymus. (A) Representative FACS plots of

thymocytes from wild type and *dua/dua* mice showing (upper panels) CD4 versus CD8 and the gates and percentage of DN, DP, CD4SP and CD8SP subsets, and (lower panels) CD44 versus CD25 gated on CD4- CD8- thymocytes, showing gates and percentage of DN1 ($CD25^{-}CD44^{+}$), DN2 ($CD25^{+}CD44^{+}$), DN3 ($CD25^{+}CD44^{-}$) and DN4 ($CD25^{-}CD44^{-}$) subsets. B) Absolute number of different subsets in thymus of individual wild-type (white circles) or homozygous mutant mice (black circles). Dots represent single mice and the bars represent the arithmetic mean. Statistical analysis by unpaired t-test: n.s., not significant $p>0.05$. This experiment has been repeated twice with 3 mice in each group.

5.2.1 SENP2 mutant mice have reduced CD8 T cells in spleen

Spleen cells from *dua/dua* homozygous mice were compared with age-matched wild-type controls as shown in Figure 5.2. Wild-type and *duan* mice had comparable percentages of $CD4^{+}$ T cells and there was no significant difference when group analysis was performed (Figure 5.2B). The absolute numbers of $CD4^{+}$ T cells for both groups was also calculated and there was no significant difference between the groups (Figure 5.2C middle panel). The analysis of percentage of splenic B cells is also shown in 5.2B, compared with wild-type controls, *dua/dua* mice have slightly increased percentages of B cells which is likely due to a decrease in the $CD8^{+}$ T cell subsets. There was no significant difference in the absolute number of total B cell between the groups.

CD8 T cell numbers in the *duan* mice were significantly lower compared to wild-type mice (Figure 5.2B). When the T cell populations were subdivided into naïve ($CD44^{lo}$) and effector ($CD44^{hi}$) cells, there was no difference in the numbers of both naïve and memory CD4 T cells or in memory CD8 T cells between wild type and *duan* mice. By contrast, the mutant mice had significantly fewer naïve CD8 T cells ($p<0.0055$) (Figure 5.2C bottom panel). CD4 and CD8 T cells were stained for the surface markers CD44, KLRG1 and CD62L. CD44 expression was

comparable on wild type and *senp2*$^{dua/dua}$ CD4 T cells but the *duan* mice had a diminished peak of CD44^{lo} naïve CD8 T cells and a higher peak of CD44^{hi} cells due to the selective decrease in CD44^{lo} CD8 cell numbers.

A

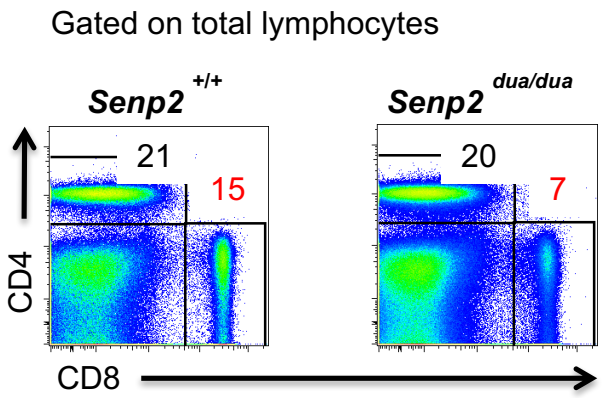

B

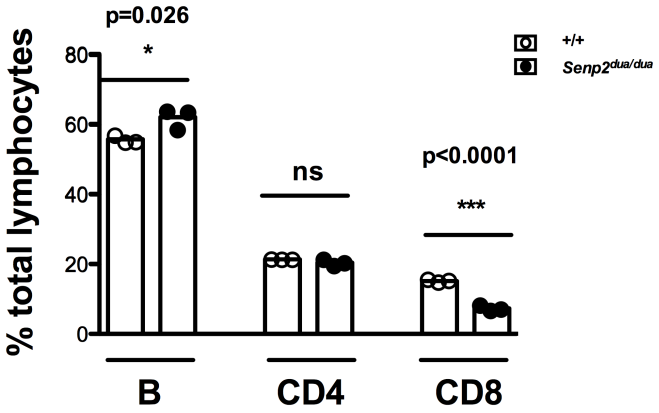

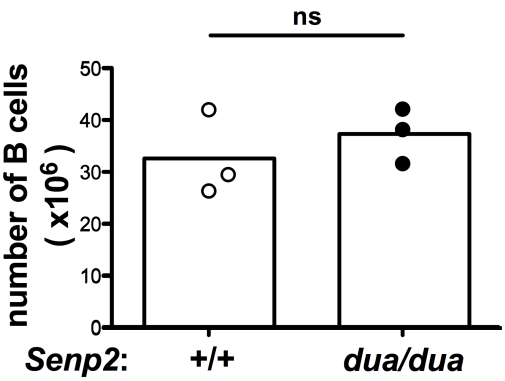
ns
number of B cells
(x10^6)
50
40
30
20
10
0
Senp2:
+/+
dua/dua

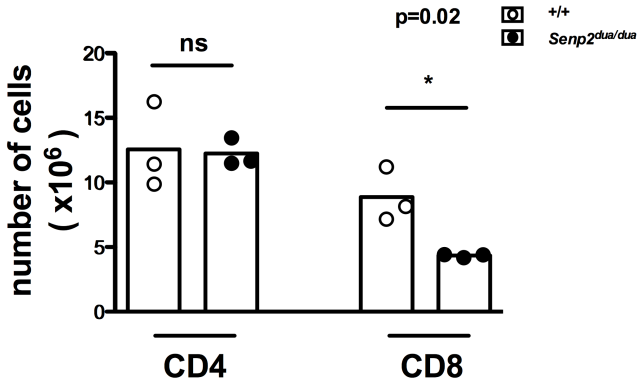
p=0.02
+/+
Senp2dua/dua
ns
*
number of cells
(x10^6)
20
15
10
5
0
CD4
CD8

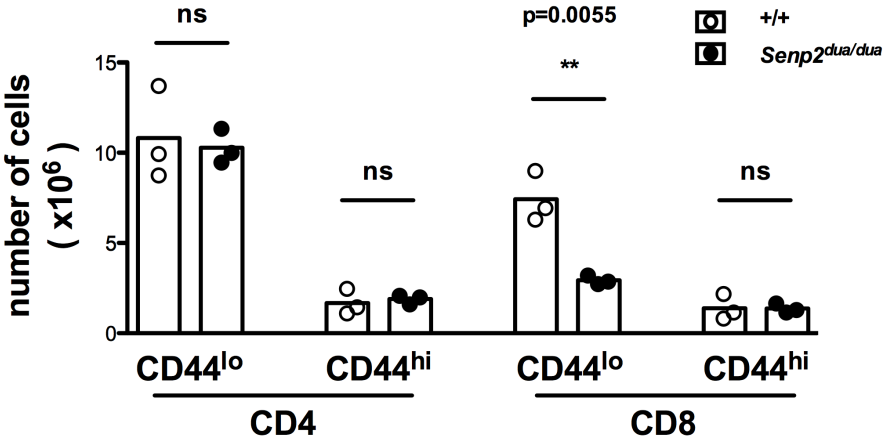
ns
p=0.0055
+/+
Senp2dua/dua
**
ns
ns
number of cells
(x10^6)
15
10
5
0
CD44lo
CD44hi
CD44lo
CD44hi
CD4
CD8

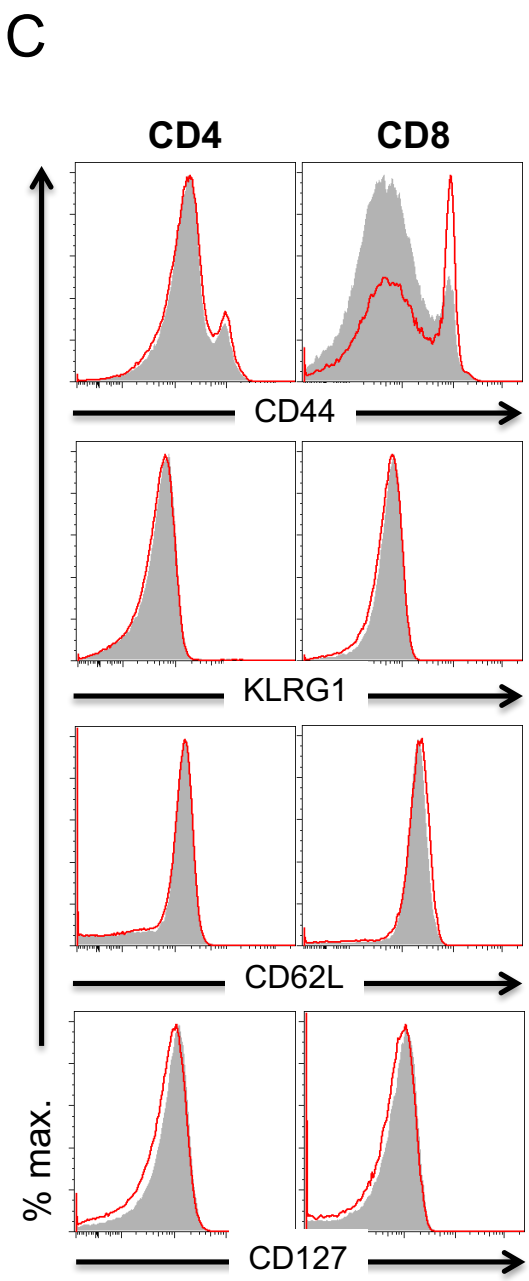

Figure 5.2: Analysis of lymphocyte populations in the spleen. (A) Representative flow cytometry plots of splenic lymphocytes. The plots in A show gates and percentage of CD4+ and CD8+ cells in one representative SENP2 wild-type (left) and one SENP2 mutant (right) mouse. (B) Percentage of different subsets among lymphocytes (top row), and the absolute number of B cells (medium row, left), CD4 and CD8 T cells

(medium row, right), and activated/memory and naïve CD4 and CD8 T cells (bottom row) in the spleen of individual wild-type (white circles) and homozygous mice (black circles). Dots represent single mice and the bars are the arithmetic mean. Statistical analyses by unpaired t-test: ns, not significant p>0.05. (C) Representative flow cytometry plots of different surface markers gated on spleen CD4 or CD8 T cells from dua/dua (red) or +/+ (grey) mice.

The expression of CD127 (IL-7Rα) was measured on T cell subsets in spleen, since this receptor is essential for naïve T cell survival. As shown in figure 5.3A, naïve *Senp2*$^{dua/dua}$ CD8 T cells (CD44^{lo}CD8^{+}) had lower CD127 expression compared to naïve WT CD8 T cells, as was also documented in blood T cells in chapter 4. The difference was not apparent in the activated/memory CD8 T cells (CD44^{hi}CD8^{+}) of the two groups, nor in naïve or activated/effector subsets of CD4 T cells between *Senp2*$^{dua/dua}$ and WT mice (Figure 5.3B).

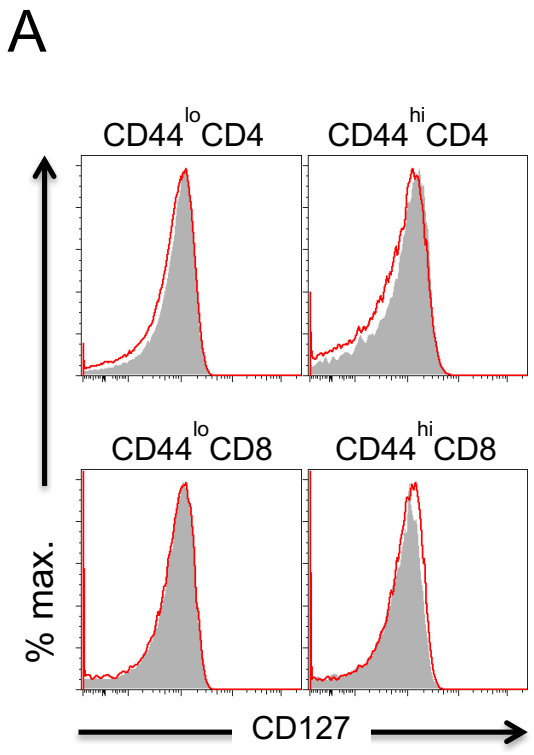

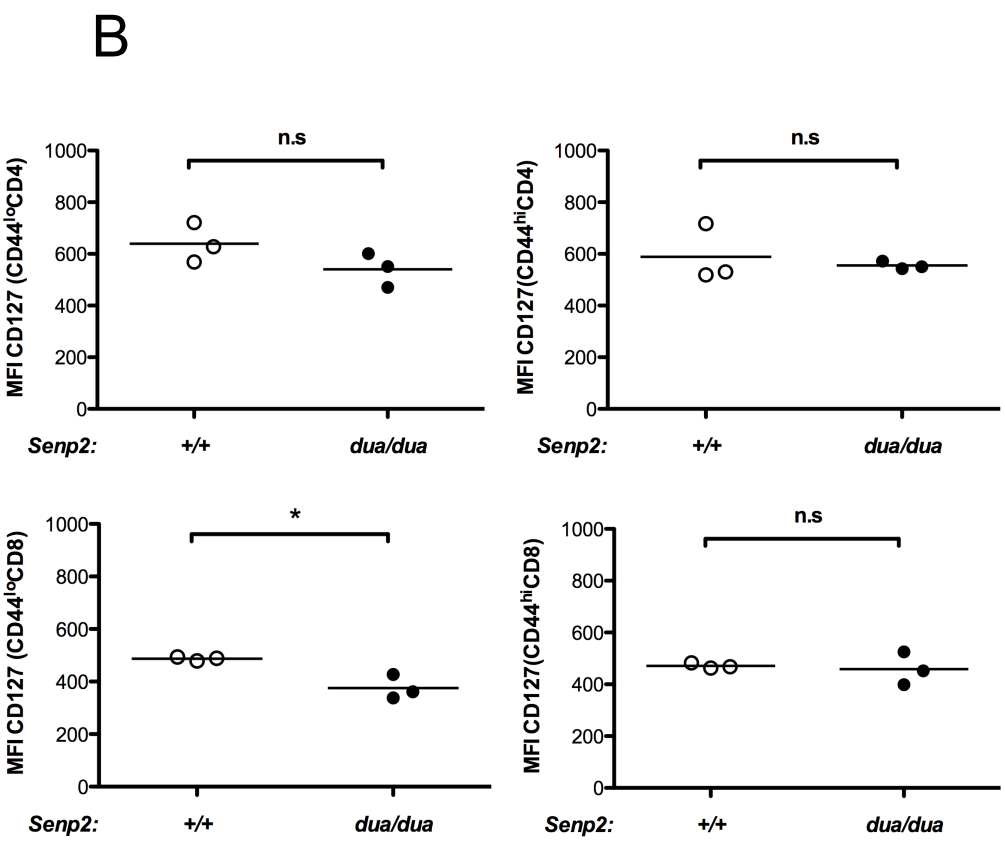

Figure 5.3: Expression of IL-7R on *Senp2*$^{dua/dua}$ T subsets in spleen. (A) Representative flow cytometry plots of CD127 staining gated on spleen CD4+ CD44^{lo}, CD4+CD44^{hi}, CD8+ CD44^{lo} or CD8+CD44^{hi} T cells from *dua/dua* (red) or +/+ (grey) mice. (B) Geometric mean fluorescence intensity (MFI) of CD127 on naïve (CD44^{lo}) CD4 T cells and effector/memory (CD44^{hi}) CD4 T cells (upper panels), or naïve (CD44^{lo}) CD8 T cells and effector/memory (CD44^{hi}) CD8 T cells (lower panels), in individual wild-type (white circles) or homozygous mutant mice (black circles). Dots represent single mice and the bars represent the arithmetic mean. Statistical analysis by unpaired t-test: *, P<0.05; n.s., not significant.

5.3 Naïve CD8 T cell deficit is cell intrinsic (Bone marrow chimeras)

From experiments in Chapter 4, transplantation of T cells from *duan* or wildtype OT-I TCR-transgenic mice revealed a survival defect in *dua/dua* naïve CD8 T cells. The lower expression of IL-7R on the surface of $Senp2^{dua/dua}$ naïve CD8 T cell could be an intrinsic property of mutant T cells contributing to their poor survival in transplantation, or it could be a cell extrinsic secondary effect of elevated IL-7 levels in the lymphopenic environment of *dua/dua* mice. To find out if the survival defect and decreased IL-7R on $Senp2^{dua/dua}$ CD8 T cells was cell autonomous or secondary to other cells, we generated mixed bone marrow chimeras by reconstituting irradiated $Rag1^{-/-}$ recipient mice with a 50:50 mix of wild-type CD45.1 marked bone marrow and either wild-type or mutant CD45.2 marked bone marrow (Figure 5.4A). At the same time, two groups of mice were reconstituted with 100% wild type BM cells and 100% $Senp2^{dua/dua}$ BM cells to serve as controls. The irradiated recipients were bled 6 weeks after the reconstitution and every 2 weeks after, and flow cytometry performed to check the proportions of CD8 T cells in the peripheral blood and the IL-7Rα expression on CD8 T cells. The percent of CD8 T cells derived from 100% wild type BM cells was comparable to normal mice. The recipients with 100% mutant BM cells displayed the same phenotype of lower percentage of CD8 T cells as observed in unmanipulated mutant mice (Figure 5.4B). Mice that received a mix of 50% wild-type CD45.1 and 50% *dua/dua* mutant CD45.2 bone marrow showed equal reconstitution of the splenic B cells by the CD45.2 positive mutant cells, ranging between 40% and 60% of B cells in individual chimeric animals (numbered 1 through 5, Figure 5.4C). By contrast, in the CD8 T cells in each chimeric mouse CD45.2+ *dua/dua* cells accounted for approximately half the percentage observed in the B cells, ranging between 7% and 30% of CD8 T cells. In control mixed chimeras where the CD45.2+ cells were wild type, CD45.2+ cells accounted for 40-60% of CD8 T cells and mirrored the contribution of CD45.2 cells to the B cell compartment. The failure of mutant cells to contribute to the CD8 T cell compartment equally to WT cells indicates that the effect of the *Senp2* mutation was cell intrinsic.

A

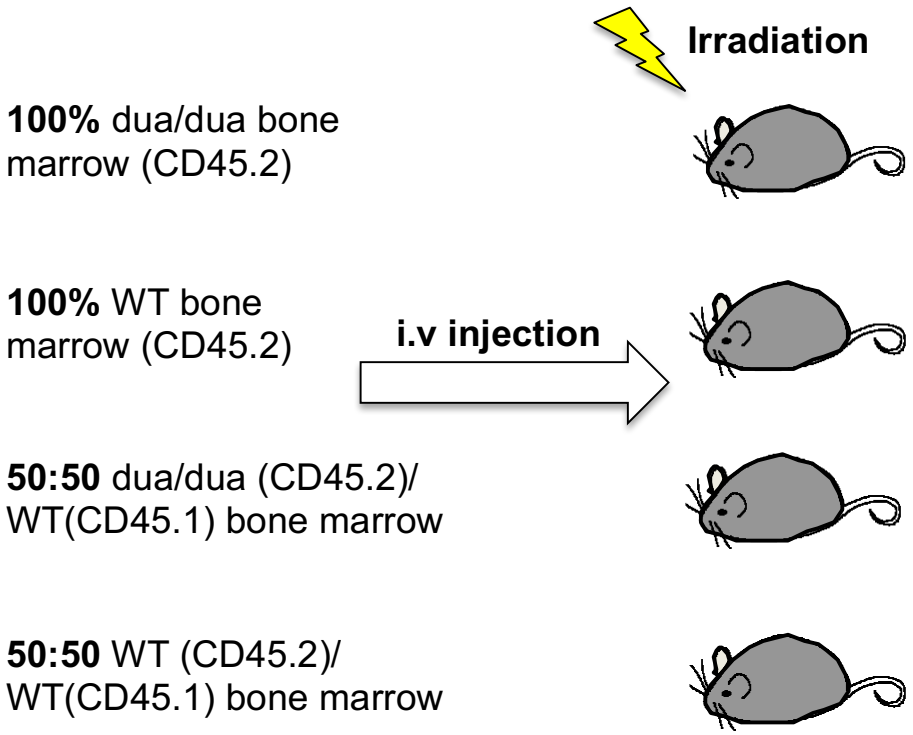
Irradiation
100% dua/dua bone marrow (CD45.2)
100% WT bone marrow (CD45.2)
i.v injection
50:50 dua/dua (CD45.2)/ WT(CD45.1) bone marrow
50:50 WT (CD45.2)/ WT(CD45.1) bone marrow

B

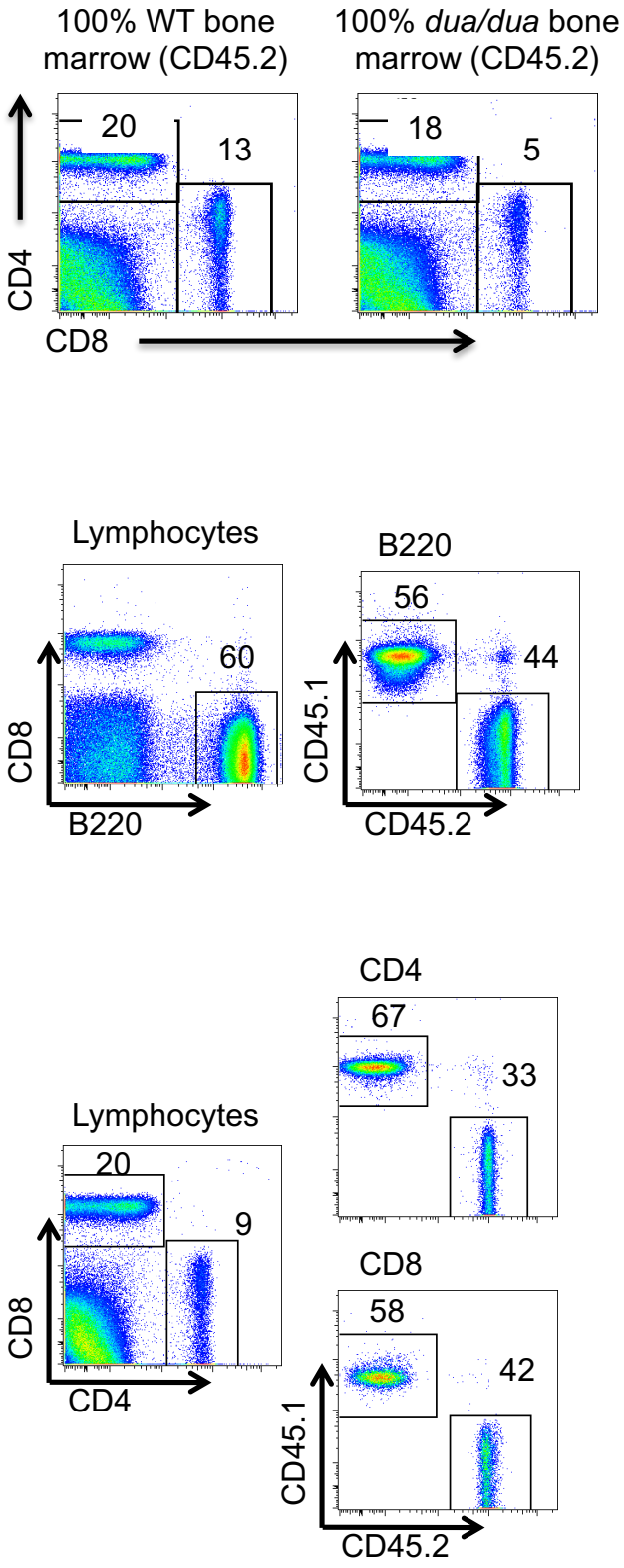
100% WT bone marrow (CD45.2)
100% dua/dua bone marrow (CD45.2)
20
13
18
5
CD4
CD8
Lymphocytes
60
CD8
B220
B220
56
44
CD45.1
CD45.2
CD4
67
33
Lymphocytes
20
9
CD8
CD4
CD8
58
42
CD45.1
CD45.2

C

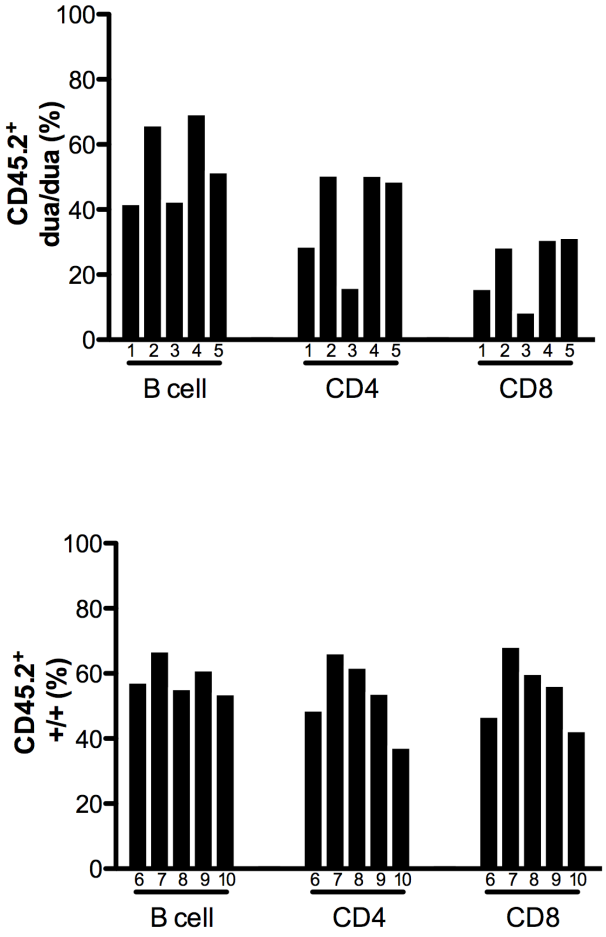
CD45.2+ dua/dua (%)
100
80
60
40
20
0
1 2 3 4 5
B cell
1 2 3 4 5
CD4
1 2 3 4 5
CD8
CD45.2+ +/+ (%)
100
80
60
40
20
0
6 7 8 9 10
B cell
6 7 8 9 10
CD4
6 7 8 9 10
CD8

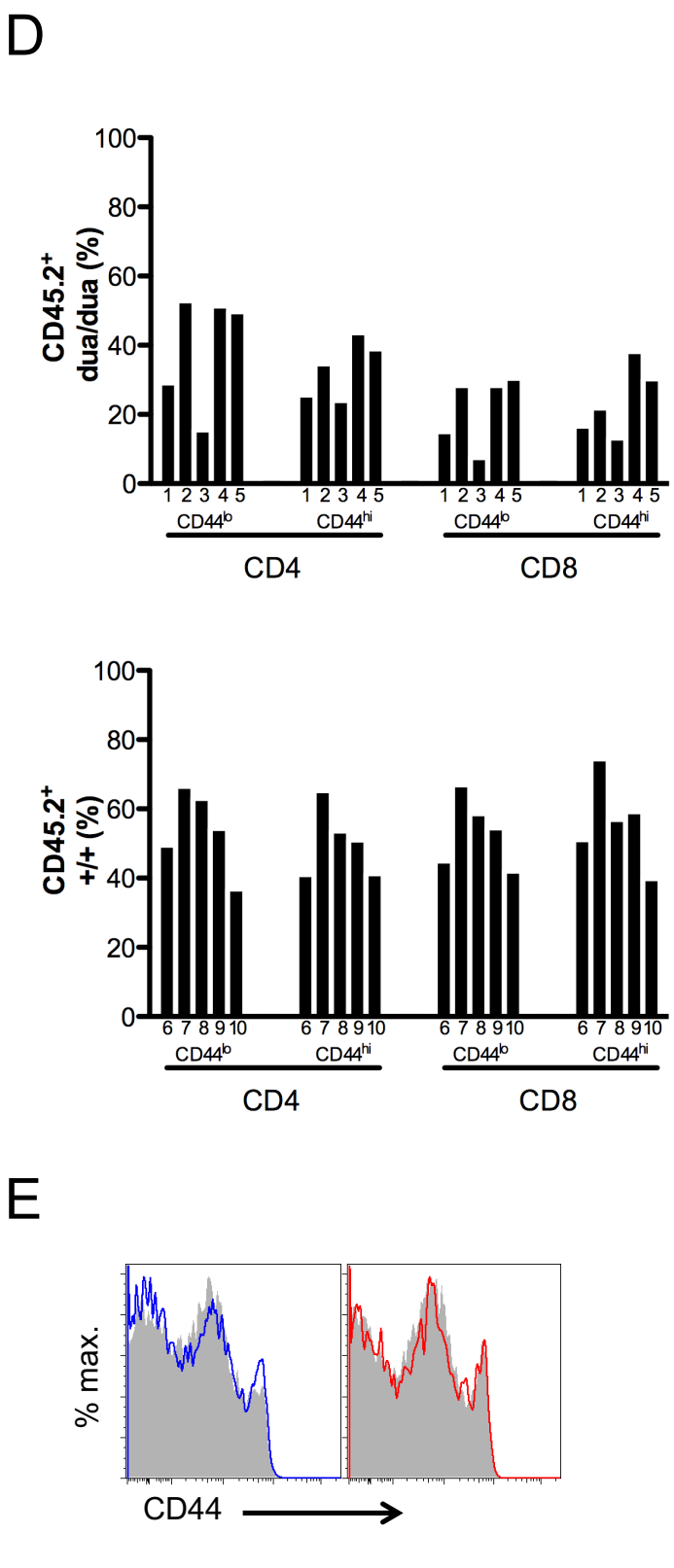

Figure 5.4: The defect in *dua/dua* CD8 T cell accumulation was cell intrinsic in bone marrow chimera experiments. (A) Experimental

design of bone marrow chimera experiments. Bone marrow either 100% marked with congenic marker CD45.2 or 50:50 CD45.2/CD45.1 was injected into irradiated *Rag1*$^{-/-}$ recipient mice. (B) Representative analysis of mice receiving 100% WT bone marrow (left) or 100% mutant bone marrow (right) (top panel). Representative flow cytometry plots of gating strategies for CD45.1+ and CD45.2 B cells (middle panel) and CD45.1+ and CD45.2+ CD4 and CD8 T cells (bottom panel). (C, D) Each column indicates the percentage of CD45.2+ cells in the indicated cell subsets in the peripheral blood of an individual 50:50 chimera mouse constructed as in part A. Each bar is the percent reconstitution of a cell subset in an individual mouse (indicated by the number below the bar). In the upper panels of C and D the CD45.2+ cell are *dua/dua*, while in the lower panels the CD45.2+ cells are wild-type. (E) Representative flow cytometry histograms of CD44 on WT and mutant CD45.2+ CD8+ cells in 50:50 mixed chimeras (CD45.1 +/+ (grey); CD45.2 +/+ (blue) and CD45.2 dua/dua (red)).

The longitudinal analysis of CD45.2+ CD8 T cells in each of the 50:50 bone marrow chimeras is shown in Figure 5.5. From Figure 5.5A, the percentage of CD45.1 and CD45.2 CD8 T cells raised from WT bone marrow cells remained stable over time after the first 6 week bleed, with *Senp2*$^{+/+}$ CD45.2 cells accounting for 40-60% of CD8 T cells even 30 weeks after marrow transplantation. As shown by the red triangles and lines in Figure 5.4B, *Senp2*$^{dua/dua}$ CD45.2 cells accounted for 40% and 55% of CD8 T cells 6 weeks after transplantation in mice 3 and 4, respectively, but decreased to 20% and 35% by 10 weeks after bone marrow transplantation, and further decreased to 4% and 15% 30 weeks after transplantation. In the other three mixed chimeras in this group, *dua/dua* CD45.2+ cells were already decreased to 20-28% of CD8 T cells at 6 weeks and further decreased or remained at similar low proportions at 30 weeks. These results are consistent with the T cell transfer experiments in Chapter 4 indicating a cell autonomous shortening of CD8 T cell peripheral lifespan.

A

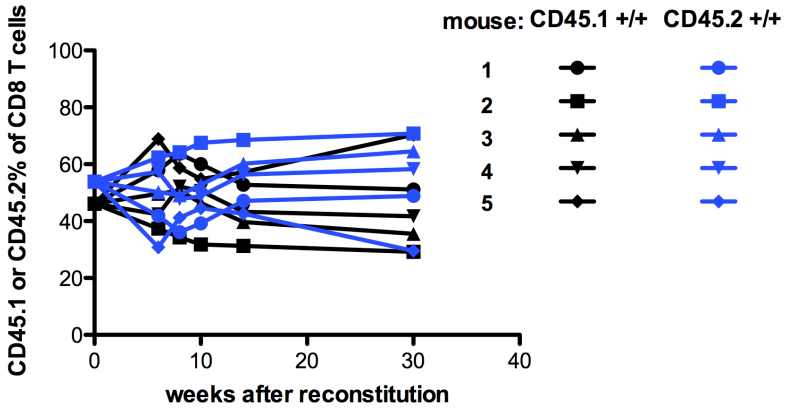

B

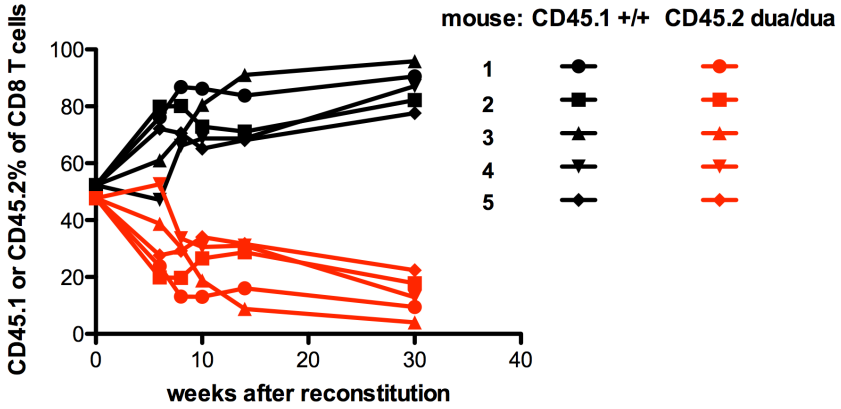

Figure 5.5: CD8 T cell autonomous defects of *duan* mice. Two groups of mixed bone marrow chimeras were generated as shown in Figure 5.4A, with CD45.2 marrow from either (A) +/+ or (B) *dua/dua* donors mixed with CD45.1 marrow from +/+ donors. The percentage of CD45.2+ and CD45.1+ cells among peripheral CD8 T cells from each recipient mouse was analysed in sequential blood samples collected 6, 8, 10, 14 and 30 weeks after marrow transplantation. The day 0 data represents the % of Ly5a/jLy5b cells in the injected BM.

The longitudinal data for B cells and CD4 T cells in the same chimeric animals are shown in Figure 5.6. CD45.2+ cells ranged between 40-60% of B cells at 6 weeks but then tended to increase gradually by 30 weeks after marrow transplantation, regardless of whether the CD45.2 cells were mutant or wild-type. This may reflect a subtle difference between the CD45.1 and CD45.2 congenic C57BL/6 strains, but indicates no discernable effect of the *duan* mutation within B cells. By contrast, *dua/dua* CD45.2 cells accounted for a lower percentage of CD4 T cells at the 6, 8 and 10 week timepoints, ranging between 15% and 50%, but by 30 weeks after reconstitution the percentage of *dua/dua* CD45.2 cells was comparable to +/+ CD45.2 cells among CD4 T cells. Thus, while there may be subtle and transient effects intrinsically within CD4 T cells, the long-term survival defect intrinsic to *dua/dua* CD8 T cells was not apparent in the other lymphocyte subsets.

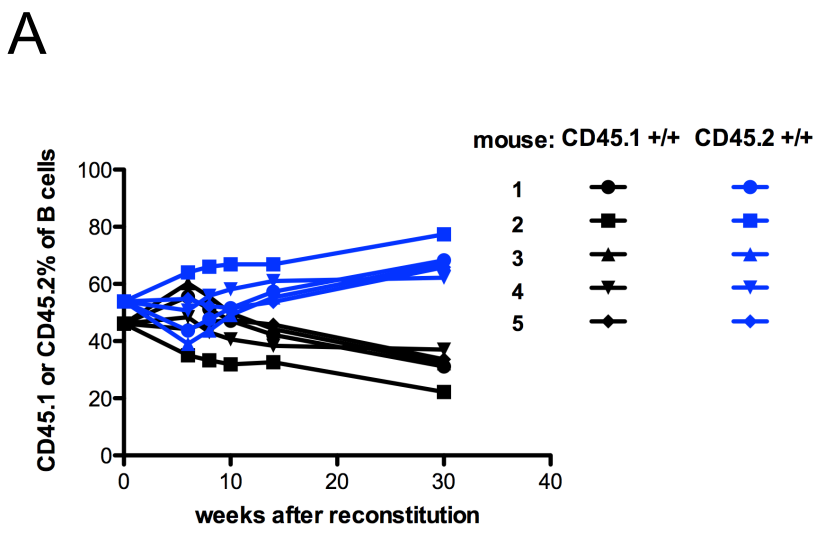

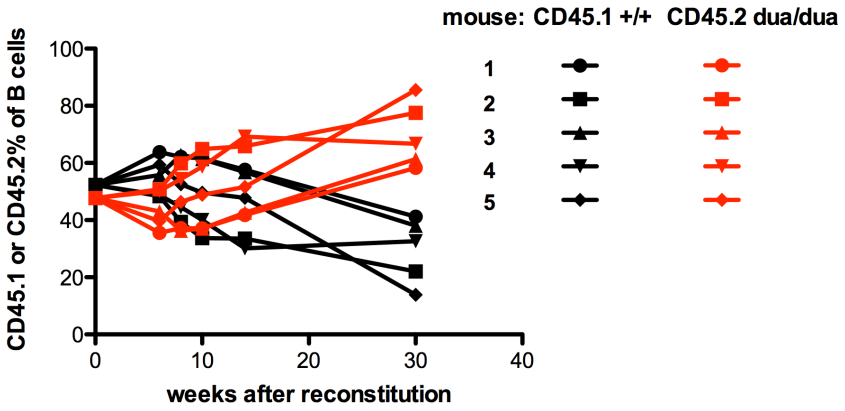

B

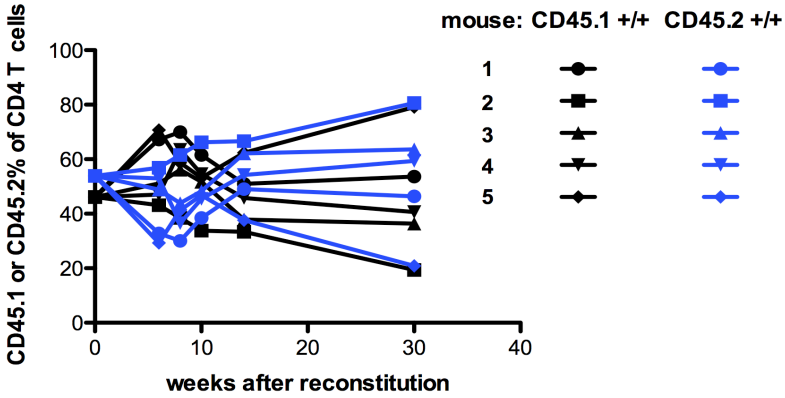

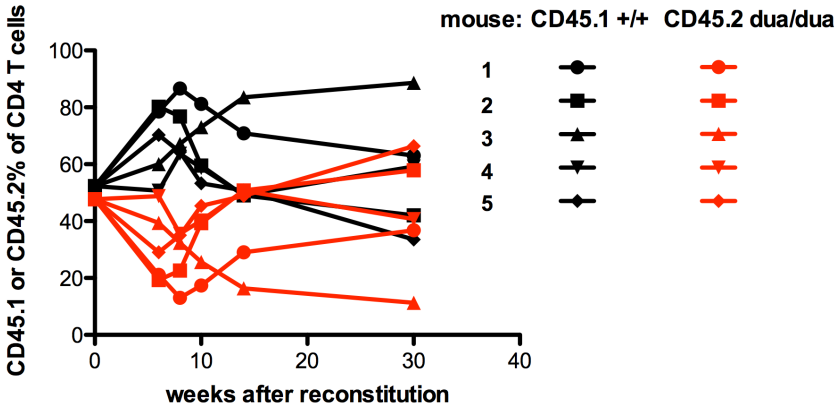

Figure 5.6: Effect of the *duan* mutation on CD4 T cells and B cells in 50:50 mixed bone marrow chimeras. Analysis of the same chimeric

animals as Figure 5.5, showing results of sequential blood samples analyzing (A) B cells, and (B) CD4 T cells.

CD127 (IL-7Rα) expression on the $CD44^{lo}$ CD8 cells derived from the CD45.1 and CD45.2 marrow donors was also measured in the same two groups of mixed chimeras at each time point after marrow transplantation. In the control mixed chimeras, there was no significant difference in the geometric mean of CD127 between the CD45.1 WT or CD45.2 WT derived naïve ($CD44^{lo}$) CD8 T cells at any time after marrow transplantation (Figure 5.7A). In the test group of mixed chimeras (Figure 5.7B), however, the naive ($CD44^{lo}$) CD8 T cells derived from CD45.2 $Senp2^{dua/dua}$ BM cells showed a comparable level of CD127 expression to their wild-type counterparts at 6, 8 and 10 weeks after marrow transplantation, but CD127 was slightly decreased at 14 weeks and a dramatic decrease 30 weeks after transplantation (Figure 5.5B). The relative CD127 on CD45.2+ cells between the +/+ and dua/dua group of chimeras at each timepoint (divide MFI CD45.2 CD8+ by MFI CD45.1+ CD8 cells in the same chimera) is also calculated in Figure 5.7C. The difference in the relative CD127 between the +/+ and dua/dua groups after 10 weeks further showed *duan* mutation results in a cell-autonomous decrease in CD127. In conclusion, the results showed that the $Senp2^{dua/dua}$ mutation acts cell autonomously to lower expression of IL-7R. Interestingly, this phenotype developed later than the decrease in naïve CD8 T cell numbers following bone marrow transplantation, making it unlikely that decreased IL-7R expression is the cause of poor T cell survival.

A

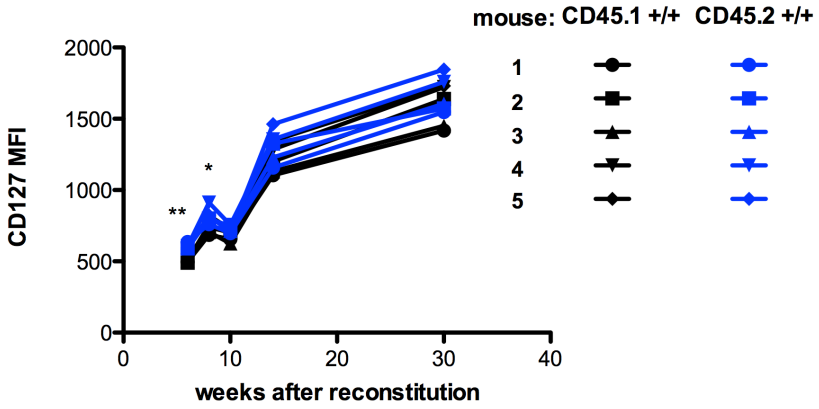
mouse: CD45.1 +/+ CD45.2 +/+
1
2
3
4
5
CD127 MFI
2000
1500
1000
500
0
0
10
20
30
40
weeks after reconstitution
**
*

B

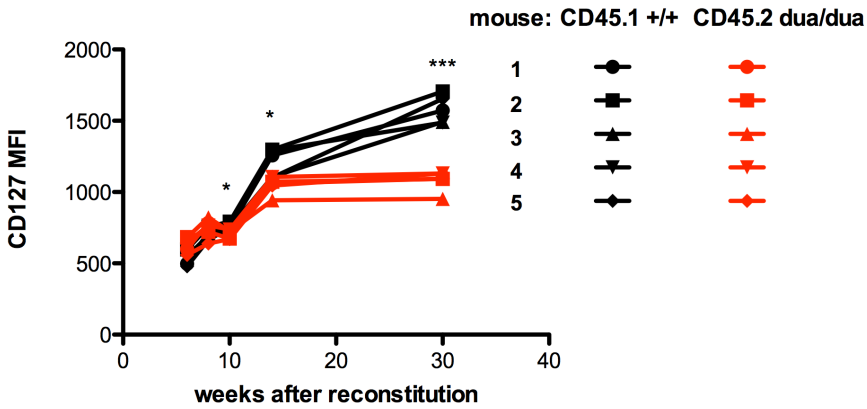
mouse: CD45.1 +/+ CD45.2 dua/dua
1
2
3
4
5
CD127 MFI
2000
1500
1000
500
0
0
10
20
30
40
weeks after reconstitution
***
*
*

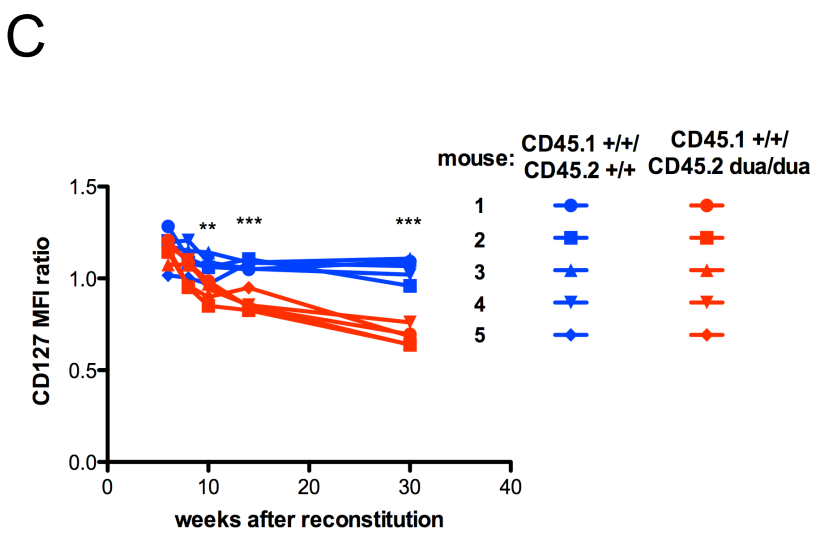

Figure 5.7: Lower IL-7Rα expression on *Senp2*$^{dua/dua}$ naïve CD8 T cells. Analysis of CD127 on the CD45.2+ and CD45.1+ subsets of CD44^{low} CD8+ T cells in sequential bleeds from each of the mixed bone marrow chimeras analysed in Figure 5.5. (A, B) CD127 mean fluorescence intensity (MFI) values for CD45.2+ and CD45.1+ cells in each animal. These were compared by unpaired t-test at each time-point: * p<0.05; ** p<0.01, ***p<0.0005. (C) The relative CD127 on CD45.2+ cells in each chimera at each timepoint expressed relative to the MFI of CD45.1+ CD8 cells in the same chimera. Statistical analysis by unpaired t-test at each timepoint: * p<0.05; ** p<0.01, ***p<0.0005.

5.4 Poor survival of naïve *Senp2*$^{dua/dua}$ OT-I cells in lymphopenic hosts

Transplantation of *Senp2* mutant OT-I T cells into *Rag1* (recombination activation gene 1) deficient recipients was performed to study survival of antigen-naïve peripheral CD8 T cells without ongoing thymic output as existed in the mixed chimeras above and without competition by an established repertoire of T cells as occurred in the OT-I T cell transplant experiments in Chapter 4. RAG1 is an essential enzyme subunit for V(D)J recombination, and *Rag1*-deficient mice lack

mature B and T lymphocytes due to the absence of immunoglobulin or TCR gene rearrangement (Mombaerts *et al*, 1992). The *Rag1*-deficient recipients provide transplanted donor OT-I T cells with increased availability of cytokines and growth factors and empty peripheral "niches" to undergo lymphopenia-induced proliferation. 10 million splenocytes, comprising a 50:50 mixture of congenically marked wild type and *Senp2*$^{dua/dua}$ OT-I spleen cells, were adoptively co-transferred into *Rag1*-deficient recipients. The blood from recipient mice was analysed at multiple time points.

Figure 5.8 shows representative flow cytometry plots and the gating strategy applied to identify wild type and *Senp2*$^{dua/dua}$ OT-I CD8 T cells. I used CD8^{+}Vα2^{+} to measure the percentage of OT-I donor-derived T cells among blood lymphocytes, and then applied CD45.1 and CD45.2 to measure the percentage of wild type (CD45.1/CD45.2 heterozygous) and *Senp2*$^{dua/dua}$ (CD45.1/CD45.1 homozygous) cells among the donor-derived OT-I CD8 T cells. OT-I CD8 T cells were only 1-2% of blood lymphocytes 1 day after transplantation, but progressively increased to (15-30%) by day 69 and remained at these frequencies on day 157 (Figure 5.8B). Among the OT-1 CD8 T cells, the percentage of CD45.1/CD45.1 *Senp2*$^{dua/dua}$ cells declined from a mean of 54% at day 1 to a mean of 31% on day 157 (Figure 5.8C). Compared to the percentages on day 1, the percentage of *dua/dua* cells among OT-I cells was significantly decreased on day 18, 32, 69 and 157 (Figure 5.8C). CD44 expression did not differ between wildtype and mutant OT-I T cells any any of the timepoints from days 1 and 157.

As the survival defect of *Senp2*$^{dua/dua}$ OT-I CD8 T cells in Rag1-deficient mice were not as pronounced as they were in lymphoreplete mice, the mice were observed up to day 490 to see if there was a dramatic difference in longer term. Two mice were ethically culled and one mouse was excluded from the data as it developed lymphoma. The two remaining mice were euthanised and the splenocytes were analysed, revealing that the percent of *Senp2*$^{dua/dua}$ OT-I CD8 T cells had declined to 15% and 17% (Figure 5.8D). CD44 expression was slightly higher on the *Senp2*$^{dua/dua}$ OT-I CD8 T cells at this timepoint.

A

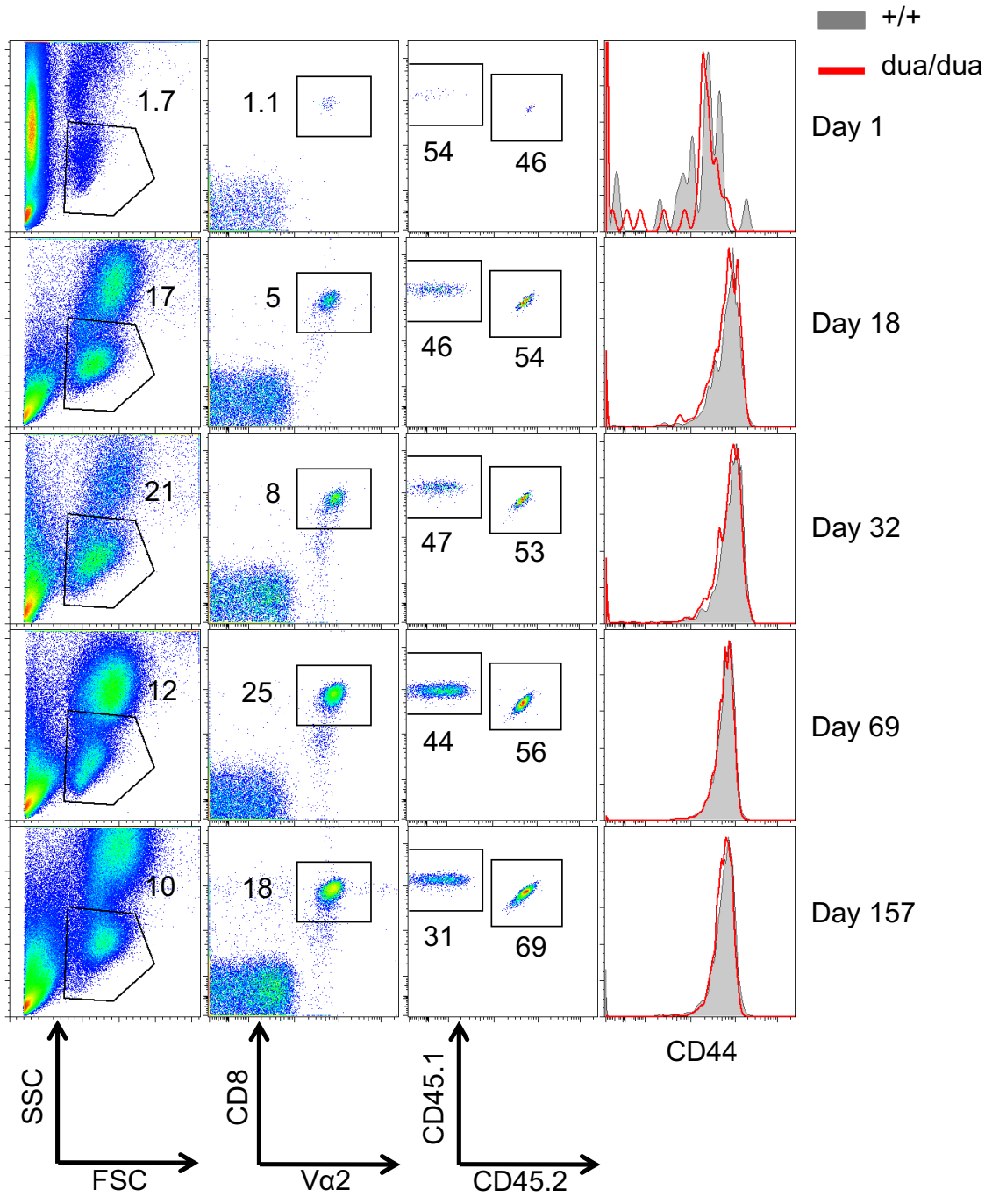
+/+
dua/dua
1.7
1.1
54
46
Day 1
17
5
46
54
Day 18
21
8
47
53
Day 32
12
25
44
56
Day 69
10
18
31
69
Day 157
SSC
FSC
CD8
Vα2
CD45.1
CD45.2
CD44

B

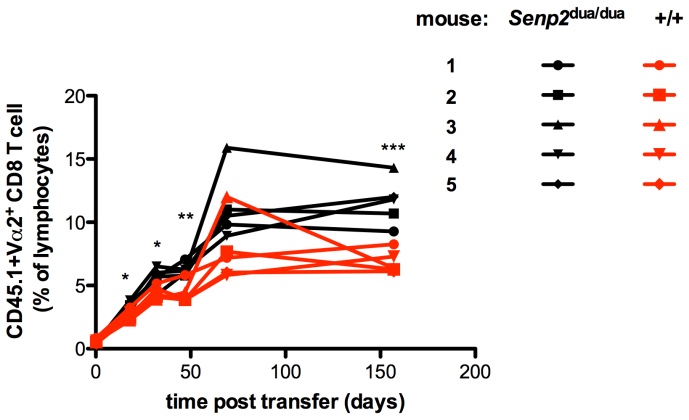
mouse:
Senp2dua/dua
+/+
1
2
3
4
5
CD45.1+Vα2+ CD8 T cell
(% of lymphocytes)
20
15
10
5
0
0
50
100
150
200
time post transfer (days)
*
*
**
***

C

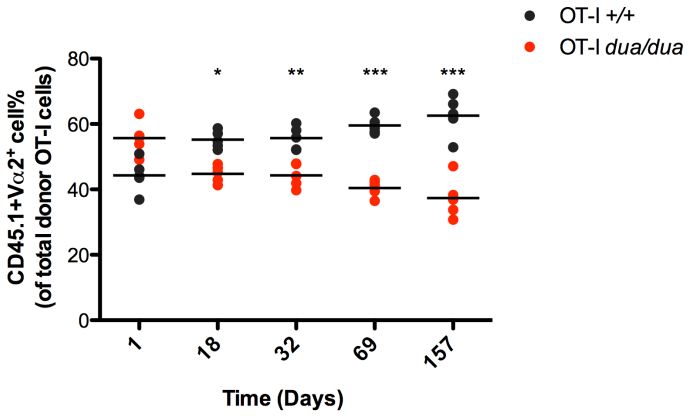
OT-I +/+
OT-I dua/dua
CD45.1+Vα2+ cell%
(of total donor OT-I cells)
80
60
40
20
0
*
**
***
***
1
18
32
69
157
Time (Days)

D

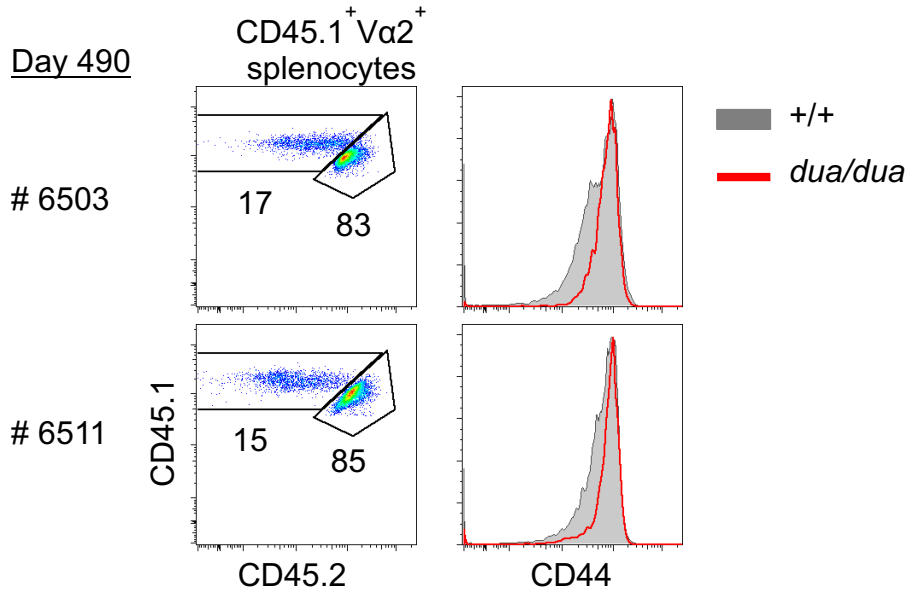

Figure 5.8 Accumulation and persistence of *Senp2*$^{dua/dua}$ OT-I CD8 T cells in *Rag1*-deficient recipients. *Rag1*-deficient mice were intravenously injected on day 0 with an equal mixture of spleen cells from Senp2 mutant and wild-type CD45-marked OT-I TCR transgenic mice. (A) Representative flow cytometry plots of blood on the indicated days after transplanting the T cells, showing the gating strategy applied to identify lymphocytes (left column), and within lymphocytes to identify donor OT-I T cells (middle left column), and within the OT-I T cells to distinguish *Senp2*$^{+/+}$ wild-type (+/+, CD45.1/CD45.2 heterozygous) or *Senp2*$^{dua/dua}$ mutant (*dua/dua*, CD45.1 homozygous) cells (middle right column). The right-most column shows expression of CD44 on the wildtype and mutant OT-I T cells. (B) Percentage of CD8^{+}Vα2^{+} OT-I cells among lymphocytes in individual recipients on the indicated days after transplantation. These were compared by unpaired t-test at each time-point: * $p<0.05$; ** $p<0.01$, ***$p<0.0005$. (C) Percentage of wild type (close circles) or *Senp2*$^{dua/dua}$ (red close circles) cells among OT-I CD8 T cells in individual mice. Lines

show arithmetic mean. These were compared by paired t-test compare percentage of *dua/dua* cells among OT-1 cells at each later timepoint with the percentage of *dua/dua* cells at day 1 at each time-point: * $p<0.05$; ** $p<0.01$, ***$p<0.0005$. (D) Percentage of wild type and *Senp2*$^{dua/dua}$ cells among donor OT-I CD8 T in the spleen of two individual *Rag1*-deficient recipients 490 days after transplantation, and their expression of CD44.

5.5 Effect of SENP2 deficiency on survival of naïve CD8 T cell: TCR and IL-7 signaling pathways

As discussed in the introduction chapter, TCR signaling and IL-7 signaling are both required for naïve CD8 T cell survival. These pathways were investigated separately in *Senp2*$^{dua/dua}$ CD8 T cells to determine whether either is affected.

5.5.1 TCR signaling

Firstly, the TCR signaling pathway was tested by transplanting a 50:50 mixture of CD45.1/CD45.2 wild type and CD45.2/CD45.2 *Senp2*$^{dua/dua}$ OT-I CD8 T cells into TAP1 deficient recipients. TAP1 deficient mice express very little cell surface MHC class-I, depriving transplanted naïve CD8 T cells of survival signals from MHC-self peptide TCR interaction. Consequently transplanted CD8 T cells only survive approximately one week and do not undergo lymphopenia induced proliferation despite the deficiency of CD8 T cells in the TAP1-deficient recipients (Tanchot et al., 1997; Murali-Krishna et al., 1999). Recipient mice were bled on the next day post transfer and sacrificed for spleen cell analysis on day 4. As shown in Figure 5.9A, 1 days after transfer, there were slightly fewer mutant OT-I CD8 T cells than wild-type OT-I cells in each recipient which may simply reflect slight differences in their ratio in the injected inoculum. After 4 days, the percentages of both OT-I populations among lymphocytes had dropped to half due to the lack of MHC survival signals. However the relative ratio between WT

and *Senp2*$^{dua/dua}$ OT-I CD8 T cells remained similar (Figure 5.9B). CD44, CD127, KLRG1 and CD5 (spleen) markers were compared between WT and *Senp2*$^{dua/dua}$ OT-I CD8 T cells and no difference were seen between the two populations at two time points (Figure 5.9C) These experiments indicate that mutant naïve CD8 T cells appear neither more nor less short-lived than their wild-type counterparts when deprived of self pMHC I stimulation, although this does not shed light on their poor long-term survival when self pMHC I is present.

A

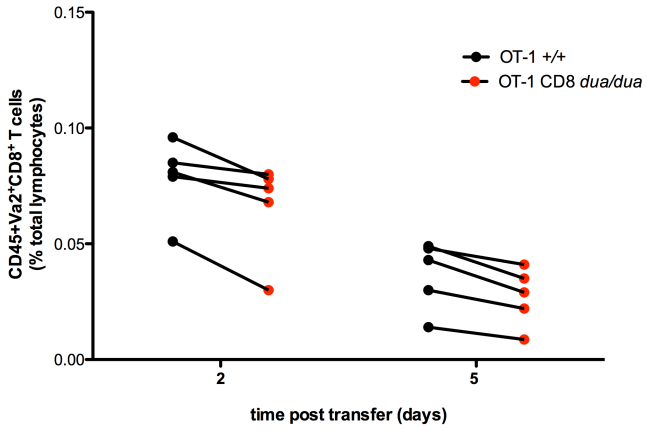

B

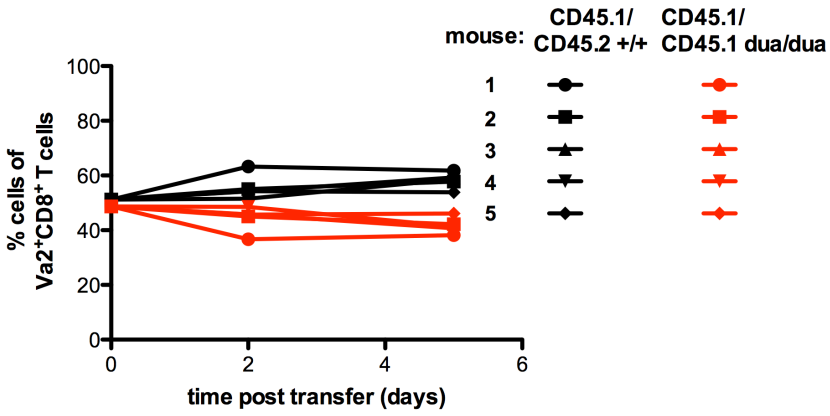

C

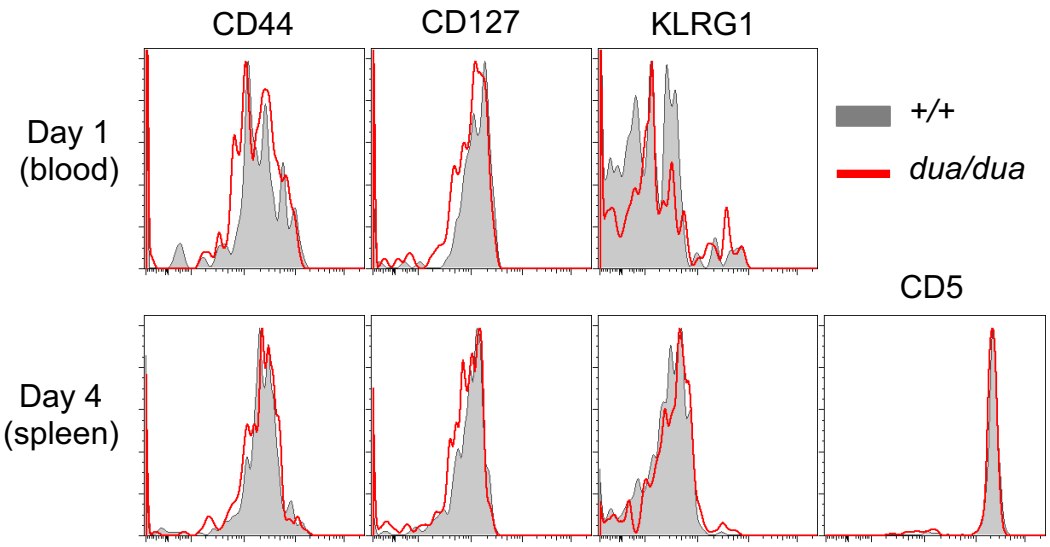

Figure 5.9 Persistence of naïve *Senp2*$^{dua/dua}$ and wild-type OT-I CD8 T cells transplanted into TAP1 deficient recipients. An equal mixture of spleen cells from CD45.1/CD45.2 *Senp2*$^{+/+}$ and CD45.2/CD45.2 *Senp2*$^{dua/dua}$ OT-I TCR transgenic mice was injected into the tail vein of *Tap1*$^{-/-}$ C57BL/6 mice, and the donor Vα2+ CD8+ subsets enumerated in the blood on day 2 and in spleen on day 4 after transfer by flow cytometry. (A) Frequency of wild type (+/+) OT-I CD8 T cells (black circles) and *Senp2*$^{dua/dua}$ *(dua/dua)* OT-I CD8 T cells (red circle) expressed as a percentage of total lymphocytes in individual mice (linked by line). Two-way ANOVA and Bonferroni post-tests were performed to compare statistical differences in +/+ and *dua/dua* at the indicated time points: at D2 (ns), D4 (ns). 5 animals were analysed per time point. The experiment was performed three times. (B) The percentage of OT1 +/+ and *dua/dua* cells in each mouse at both time points. Paired t-test was performed to compare statistical differences in percentage of OT-I *dua/dua* cells of total donor cells at D2 and D4(ns). (C) Representative histograms of CD44, CD127 and KLRG1 at each timepoint, gated on dua/dua OT-I CD8 cells (red) and

+/+ OT-I CD8 cells (grey).

5.5.2 IL-7 signaling

The IL-7 signaling pathway was tested by measuring the ability of *Senp2*$^{dua/dua}$ OT-I CD8 T cells to induce phospho-STAT5 (pSTAT5) upon IL-7 stimulation. STAT5 is a key signaling molecule downstream of the IL-7 receptor (Mazzucchelli and Durum, 2007). There are two STAT5 isoforms: STAT5a and STAT5b. Upon IL-7 stimulation, both isoforms can be phosphorylated and form homo- or heterodimers. The activated STAT5 dimer then translocates to the nucleus and induces the expression of Bcl-2 and Mcl-1 to inhibit the mitochondrial pathway of apoptosis (Surh and Sprent, 2008). It has been shown that mice carrying a deficiency in either Stat5a or Stat5b alone do not have a severe lymphopenic phenotype. However, the combined deficiency of both STAT5A and STAT5B can lead to severe early developmental defects of B and T lymphocytes.

pSTAT5 levels were measured by cytoplasmic staining and flow cytometry and expressed as the mean fluorescent intensity (MFI) at 1 min, 15min, 30min, 60min and 180min with different IL-7 concentrations. pSTAT5 MFI progressively increased with increasing IL-7 concentrations, peaking at 15min followed by a rapid decline, with no discernable difference between the wild type and *Senp2*$^{dua/dua}$ CD8 OT-1 T cells.

A

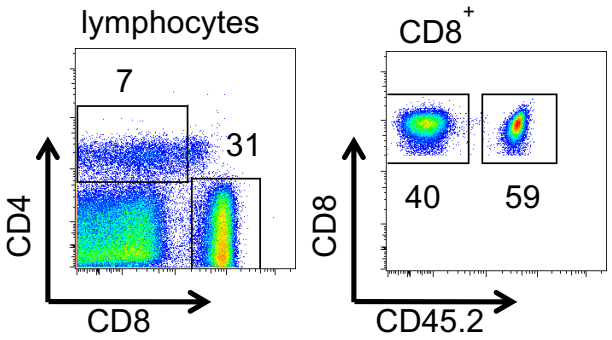
lymphocytes
7
31
CD4
CD8
CD8+
40
59
CD8
CD45.2

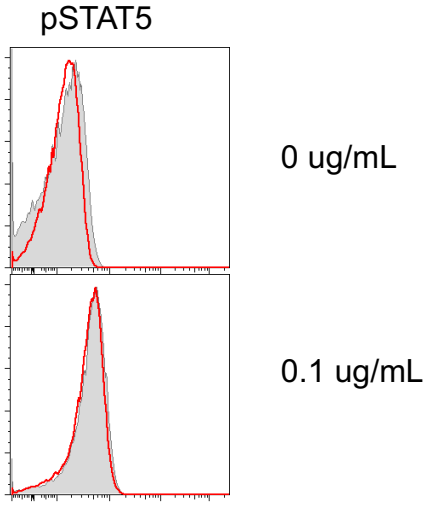
pSTAT5
0 ug/mL
0.1 ug/mL

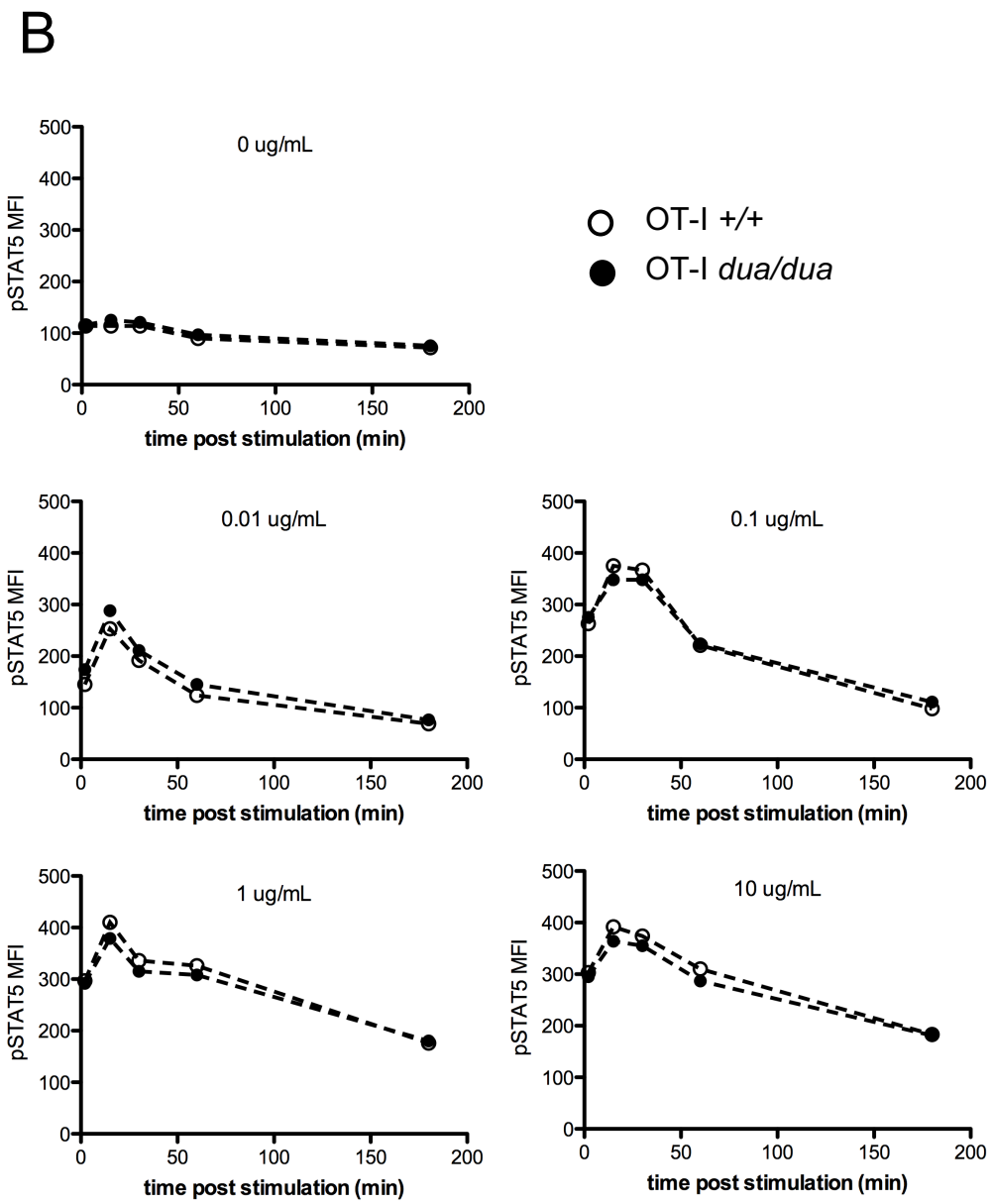

Figure 5.10 IL-7 induction of Stat5 phosphorylation in wild type and *Senp2*$^{dua/dua}$ OT-I CD8 T cells. A 50:50 mixture comprising 2 million cells of *Senp2*$^{+/+}$ wild type (CD45.1/CD45.2) and *Senp2*$^{dua/dua}$ (CD45.1/CD45.1) OT-I spleen cells were co-cultured. The indicated concentrations of IL-7 or no IL-7 (unstimulated) were added for the indicated times prior to fixing the cells, performing immunofluorescent staining for pSTAT5, CD8, and CD45.1/CD45.2, and analysis by flow cytometry. (A) Gating strategy used to measure pSTAT5, and representative overlay histograms of +/+ (grey)

and dua/dua (red) OT-I T cells at 15 minutes with 0 or 0.1 ng/ml IL-7. (B) Graphs show the mean fluorescent intensity (MFI) of phospho-STAT5 in wild type (+/+) or *Senp2*$^{dua/dua}$ (*dua/dua*) OT-I CD8 T cells at each time point.

In naïve T cells, IL-7 stimulation can suppress cell-surface expression of its own receptor to allow unsignaled T cells access to IL-7 (Park et al, 2004). To study whether *Senp2*$^{dua/dua}$ CD8 T cells could up-regulate IL-7R in absence of IL-7 stimulation and down-regulate IL-7R in response to IL-7 stimulation, we next measured surface expression of CD127 (IL-7Rα). One million *Senp2*$^{+/+}$ wild type splenocytes (CD45.1/CD45.2) and one million *Senp2*$^{dua/dua}$ splenocytes (CD45.2/CD45.2) were co-cultured on day -1 with 1ng/mL of IL-7 (Figure 5.11A). On day 0, half of the wells were washed and cultured without IL-7 and the other half remained stimulated with 1ng/ml IL-7. Cell surface CD127 was analysed at 2, 24, and 48 hours and 6 days by flow cytometry.

The expression of CD127 on naïve *Senp2*$^{dua/dua}$ CD8 T cells at 2h of continued IL-7 stimulation was lower than on the co-cultured wild type naïve T cells, and CD127 remained lower on mutant naïve T cells at all the subsequent timepoints (Figure 5.11B). In parallel cultures where IL-7 had been removed, CD127 was remained lower on mutant naïve CD8 T cells than on wild-type naive cells 2 hours after IL-7 removal. However 24 hours after IL-7 removal, naïve CD8 cells had recovered high levels of surface CD127 that were indistinguishable between mutant and wild type cells, and this remained the case 48 hrs and 6 days after IL-7 removal (Figure 5.11C). The exaggerated downregulation of surface CD127 on mutant naïve CD8 cells during continued IL-7 stimulation was not observed in CD44hi CD8 cells (Figure 5.11B, C).

A

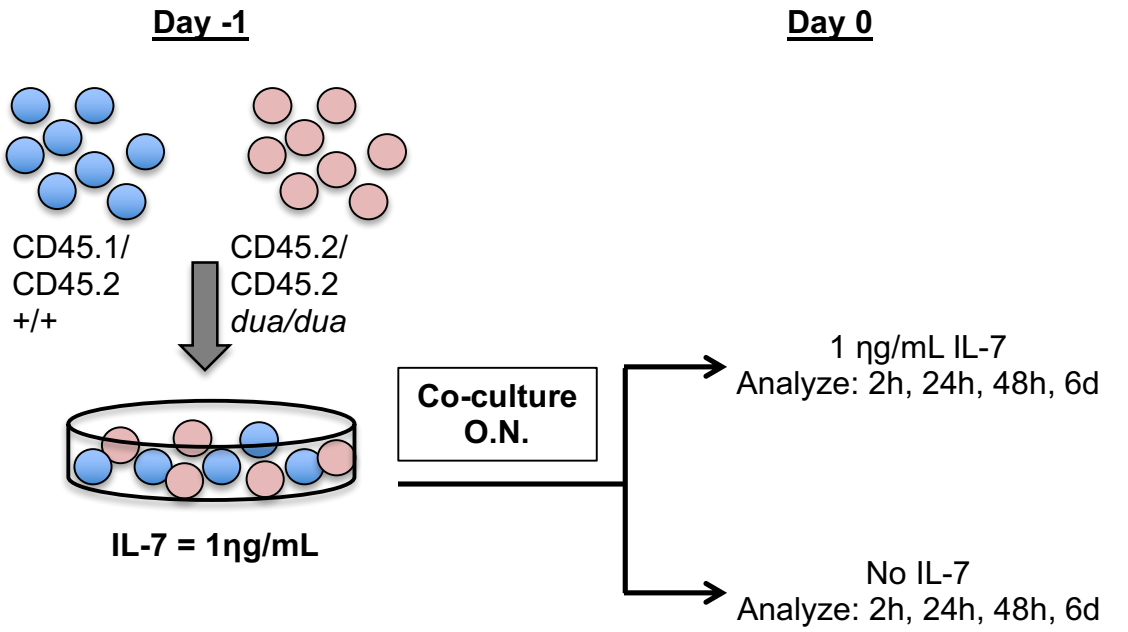
Day -1
Day 0
CD45.1/
CD45.2
+/+
CD45.2/
CD45.2
dua/dua
Co-culture
O.N.
IL-7 = 1ηg/mL
1 ηg/mL IL-7
Analyze: 2h, 24h, 48h, 6d
No IL-7
Analyze: 2h, 24h, 48h, 6d

B

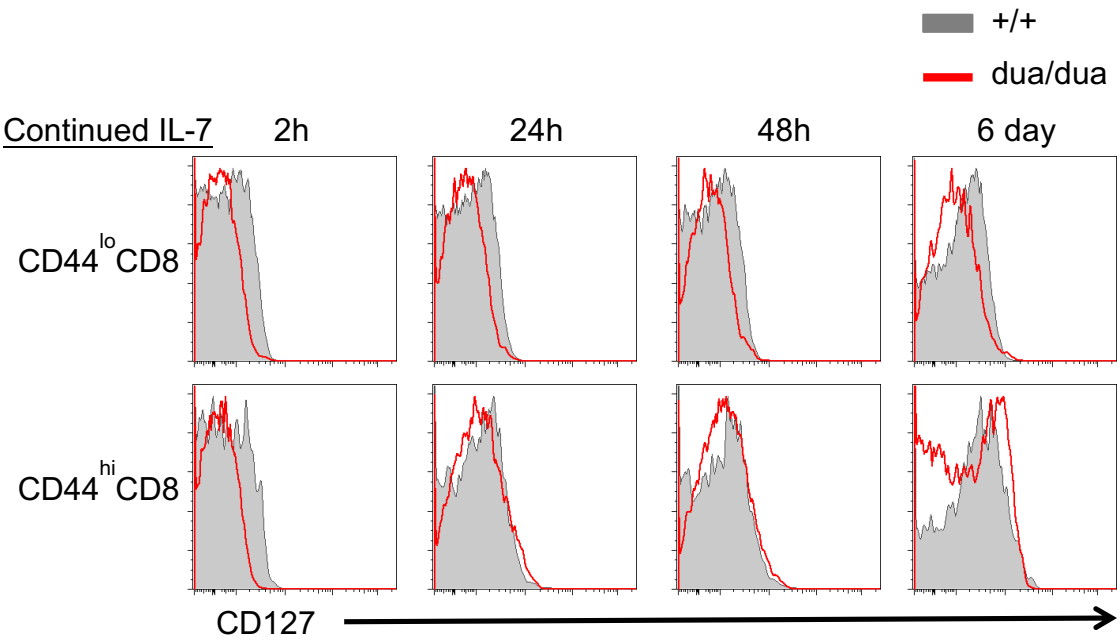
+/+
dua/dua
Continued IL-7
2h
24h
48h
6 day
CD44loCD8
CD44hiCD8
CD127

C

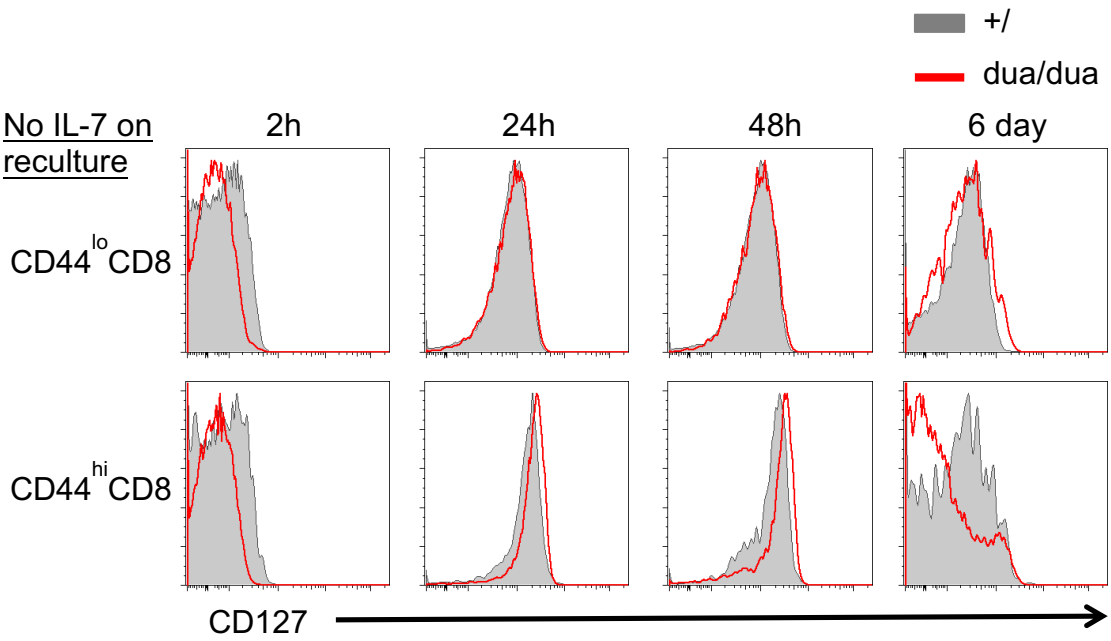

Figure 5.11 Up-regulation of IL-7Rα on wild type and *Senp2*$^{dua/dua}$ CD8 T cells after IL-7 exposure withdrawal. (A) Experimental design to investigate the up-regulation of IL-7 receptor after an initial period of IL-7 exposure in vitro. Wild type (CD45.1/CD45.2) and *Senp2*$^{dua/dua}$ (CD45.2/CD45.2) splenocytes were co-cultured on day -1 with 1ng/mL IL-7. On day 0, cells in half the wells continued to be cultured in IL-7 and cells in the rest of the wells were washed and cultured without IL-7, and all the cells were analysed for cell surface CD127 by flow cytometry at the indicated subsequent times. (B, C) Representative histograms of CD127 staining on co-cultured mutant and wild-type naïve (CD44^{lo}) and activated (CD44^{hi}) CD8 T cells cultured with continued exposure to IL-7 (B), or cultured without further stimulation by IL-7 (C), at the indicated time points.

As *Senp2*$^{dua/dua}$ CD8 T cells had lower CD127 expression during continuous IL-7 stimulation in vitro, I modified the experiment to observe the kinetics of CD127

down-regulation following acute IL-7 exposure (Figure 5.12A). One million *Senp2*$^{dua/dua}$ splenocytes (CD45.2/CD45.2) and one million wild type cells (CD45.1/CD45.2) were co-cultured overnight without IL-7 in 24 well plates to fully up-regulate IL-7 receptor expression. The cells were then cultured with 1ng/mL IL-7 and analysed by flow cytometry at different time points, subdivided into naïve CD44^{lo} CD8 cells and activated CD44^{hi} CD8 cells. Two hours after IL-7 exposure, the CD127 expression was decreased on mutant and wild-type naïve CD8 cells (Figure 5.12B, D) when compared to the CD127 expression on naïve CD8 cells at the same timepoint cultured without IL-7 (Figure 5.12C, D). However a distinct subset of *Senp2*$^{dua/dua}$ naïve CD8 T cells had much more dramatically down-regulated CD127 by 2 hrs (Figure 5.12B). After 4 hrs IL-7, the CD127 expression was further decreased on wild-type naïve CD8 cells but it was now 5-fold lower on mutant naïve CD8 cells in the same culture (Figure 5.12B, D). The exaggerated CD127 downregulation on mutant naïve CD8 cells persisted after 6 and 8 hrs IL-7 exposure, although the difference became smaller because the CD127 expression continued to decrease on the wild-type cells at the later times. Exaggerated CD127 on Senp2 mutant cells was limited to naïve CD8 cells and was not apparent in comparison of mutant and wildtype CD44^{hi} CD8 T cells. This experiment was repeated once, a similar trend of CD127 down-regulation was also observed in later time point (6 hrs) (Figure 5.12E). Collectively, the experiments in Figures 5.11 and 5.12 show that the *Senp2* mutation selectively exaggerates IL7RA downregulation on naïve CD8 T cells in response to acute or chronic IL-7 exposure, explaining the lower IL7RA on mutant naïve CD8 cells *in vivo*.

A

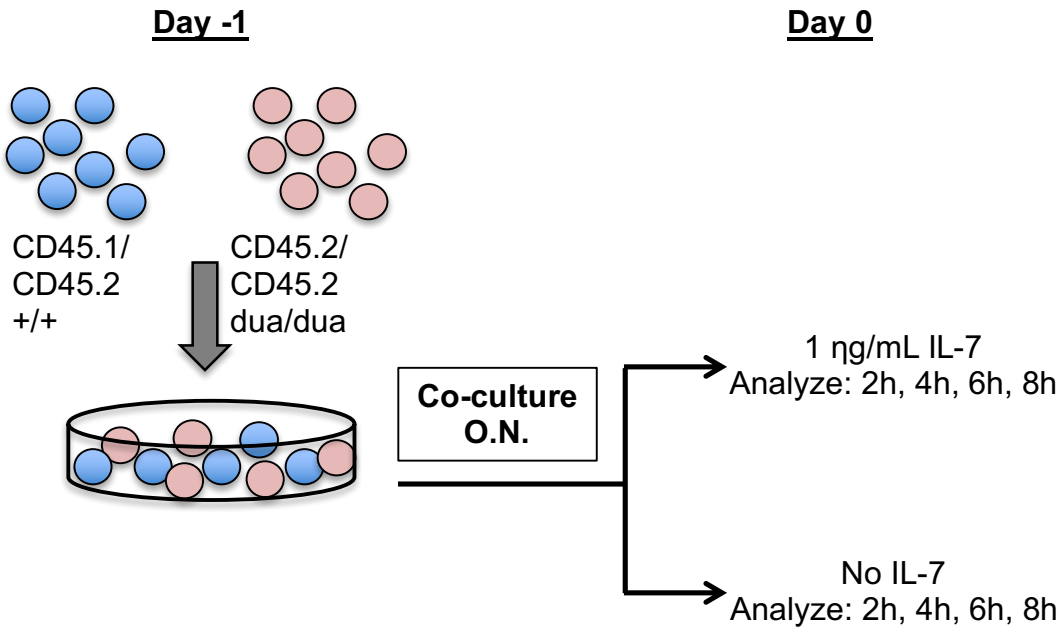
Day -1
Day 0
CD45.1/
CD45.2
+/+
CD45.2/
CD45.2
dua/dua
Co-culture
O.N.
1 ηg/mL IL-7
Analyze: 2h, 4h, 6h, 8h
No IL-7
Analyze: 2h, 4h, 6h, 8h

B

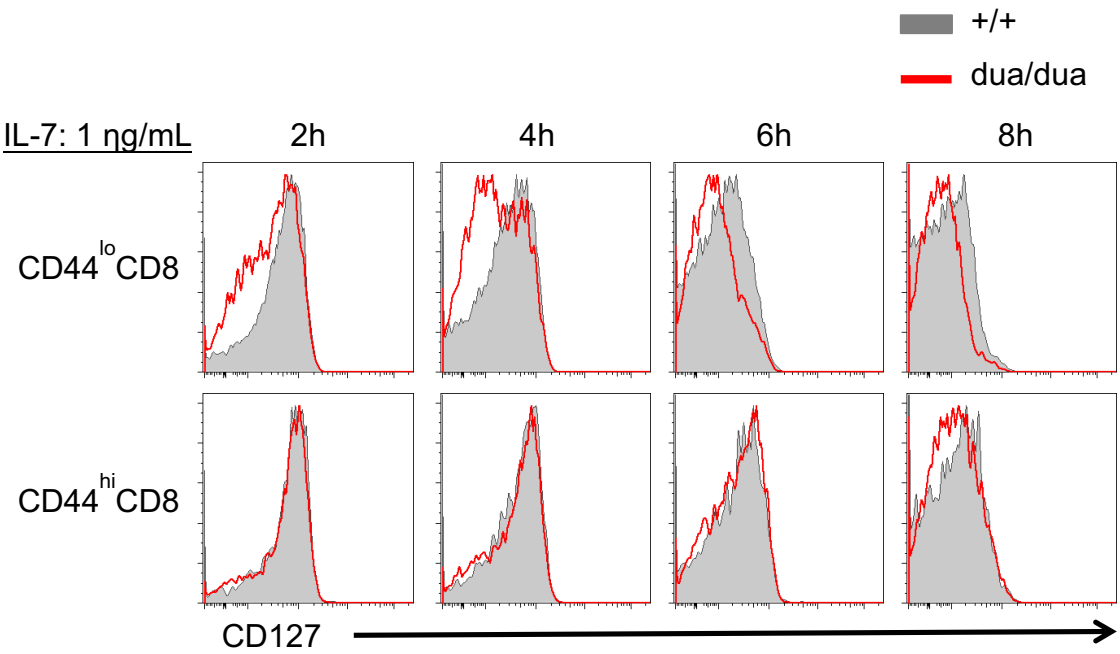
+/+
dua/dua
IL-7: 1 ηg/mL
2h
4h
6h
8h
CD44loCD8
CD44hiCD8
CD127

C

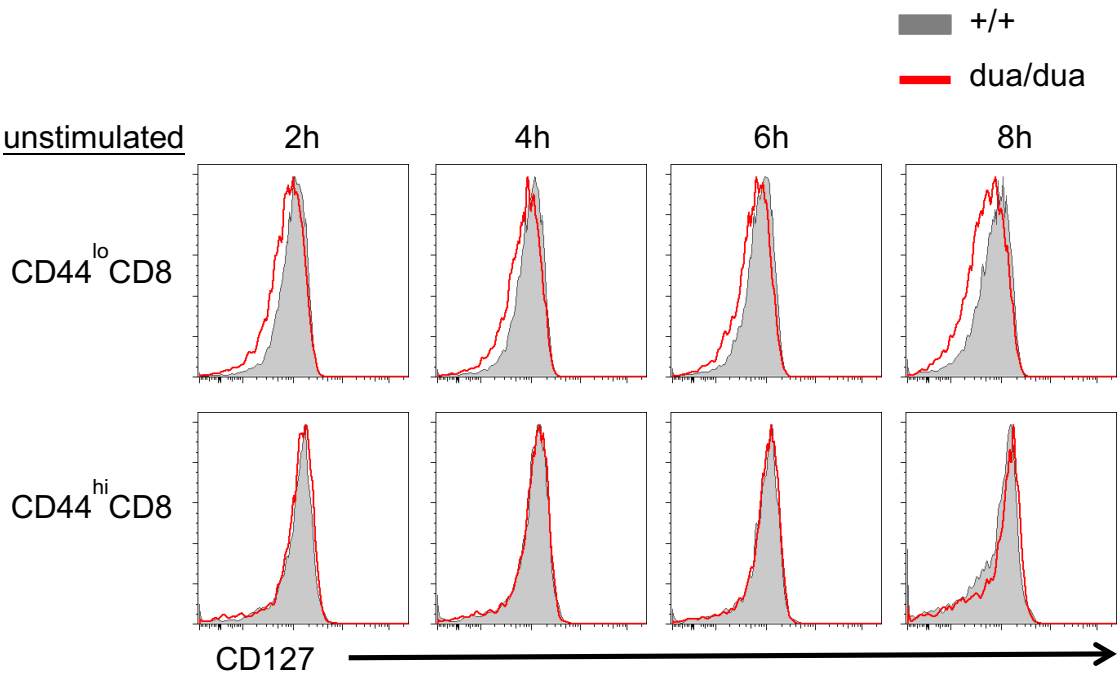
+/+
dua/dua
unstimulated
2h
4h
6h
8h
CD44lo CD8
CD44hi CD8
CD127

D

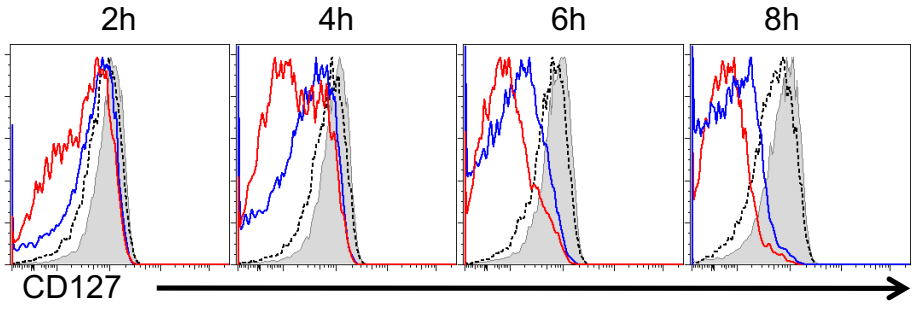
2h
4h
6h
8h
CD127

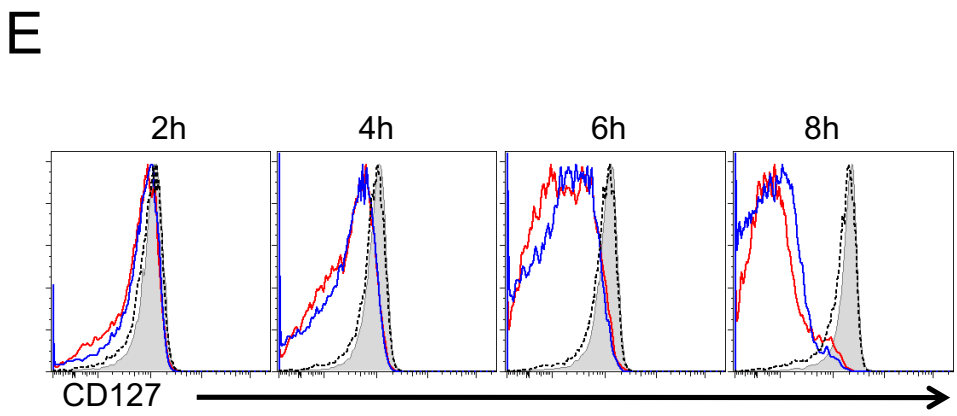

Figure 5.12 Down-regulation of IL-7Rα on wild type and *Senp2*$^{dua/dua}$ CD8 T cells after IL-7 stimulation. (A) Experimental design to investigate the downregulation of IL-7 receptor. Wild type (CD45.1/CD45.2) and *Senp2*$^{dua/dua}$ (CD45.2/CD45.2) splenocytes were co-cultured on day -1 without IL-7 to recover from any IL-7 exposure received *in vivo*. On day 0, half the wells were cultured with 1ng/mL of IL-7 and the rest of the wells were cultured without IL-7. (B, C) Histograms showing CD127 expression on mutant and wild-type naïve (CD44^{lo}) and activated (CD44^{hi}) CD8 T cells with 1ng/mL IL-7 (B) or without IL-7 stimulation for the indicated times. (D) 4 line graphs showing peak CD127 on naïve CD8 dua/dua (red line) and +/+ cells (blue line) with IL-7 stimulation and naïve CD8 dua/dua (black dash line) and +/+ cells (grey shade) without IL-7 stimulation at each time. (E) This experiment was repeated once and 4 line graphs showing peak CD127 on naïve CD8 dua/dua (red line) and +/+ cells (blue line) with IL-7 stimulation and naïve CD8 dua/dua (black dash line) and +/+ cells (grey shade) without IL-7 stimulation at each time.

5.6 Effect of *Senp2*$^{dua/dua}$ mutation on the activation of T cells and persistence of memory T cells with antigenic challenge

In the previous chapter, naïve *Senp2*$^{dua/dua}$ OT-I CD8 T cells were shown to have a

survival defect in vivo but proliferated normally *in vitro* when stimulated with anti-CD3 antibody. We therefore wished to extend these studies to analyse the response of naïve *Senp2*$^{dua/dua}$ OT-I CD8 T cells to antigen *in vivo*, including clonal expansion and persistence of antigen-specific memory CD8 T cells. A mixture of 1000 FACS sorted (B220^{-}CD4^{-}) *Senp2*$^{+/+}$ wild type and *Senp2*$^{dua/dua}$ OT-I CD8 T cells, congenically marked as CD45.1 heterozygous or homozygous respectively, were injected into the circulation of wild type B6 (CD45.2) recipient mice. Six hours later, the recipient mice were challenged intraperitoneally with recombinant H3N2 Influenza A virus expressing OVA peptide (amino acid sequence SIINFEKL; HKx31-OVA). The recipient mice were first bled at day 7 post primary challenge to measure the expansion of *Senp2*$^{dua/dua}$ OT-I CD8 T cells at the peak of the primary immune response. The second bleed was done at day 70 post challenge to measure antigen-specific memory CD8 T cells. Lastly, the recipient mice were received a second challenge on day 77 with H1N1 Influenza A virus expressing OVA (PR8-OVA), which carried serologically non-crossreactive surface haemagglutinin and neuraminidase but expressed the same OVA epitope as HKx31-OVA. The recipient mice were bled 7 days after the secondary challenge (day 84 post primary challenge) to measure the recall response of *Senp2*$^{dua/dua}$ OT-I CD8 T cells upon secondary challenge.

Flow cytometry showed that wild type OT-I cells (CD45.1^{+} CD45.2^{+}) comprised 55% and *Senp2*$^{dua/dua}$ OT-I cells (CD45.1^{+} CD45.2^{-}) comprised 45% of the donor CD8 T cell mixture injected into recipient mice, and there was no difference in their expression of CD44 (Figure 5.13A). Seven days after the recipients received the primary HKx31-OVA virus challenge both wild type and *Senp2*$^{dua/dua}$ OT-I CD8 T cells had undergone dramatic clonal expansion, accounting for 2-7% of all blood lymphocytes. Within individual recipients, the *Senp2*$^{dua/dua}$ OT-I CD8 T cells had expanded to equal or slightly lower percentages than the wild type OT-I CD8 T cells in the same recipient (Fig 5.13C). At day 70 post primary challenge, the virus-expanded wild type OT1 cells had contracted to 0.1-0.3% of blood lymphocytes while *Senp2*$^{dua/dua}$ OT-I cells in the same recipients had contracted much more dramatically to one tenth the frequency of their wild type OT1

counterparts. A second PR8-OVA virus challenge given i.p. on day 77 elicited a recall response in the OT-I memory CD8 T cells, measured at day 84. Wild-type OT-1 cells increased to 8% of blood lymphocytes while mutant OT-1 cells increased to less than 1% of lymphocytes. As there were less memory *Senp2*$^{dua/dua}$ OT-I CD8 T cells surviving at day 70 prior to the second virus administration, a smaller pool of mutant memory CD8 cells may account for the smaller number of *Senp2*$^{dua/dua}$ OT-I CD8 T cell progeny formed 7 days after secondary challenge.

In summary, *Senp2*$^{dua/dua}$ OT-I CD8 T cells could undergo clonal expansion similar to wild type cells. However Ag-specific *Senp2*$^{dua/dua}$ OT-I CD8 T cells had poor survival during the memory phase of the response. The cells remaining were able to recall to approximately the same extent as wild type however due to the poor survival at day 70 post primary challenge, *Senp2*$^{dua/dua}$ OT-I CD8 T cells led to a lower recall response after the secondary challenge.

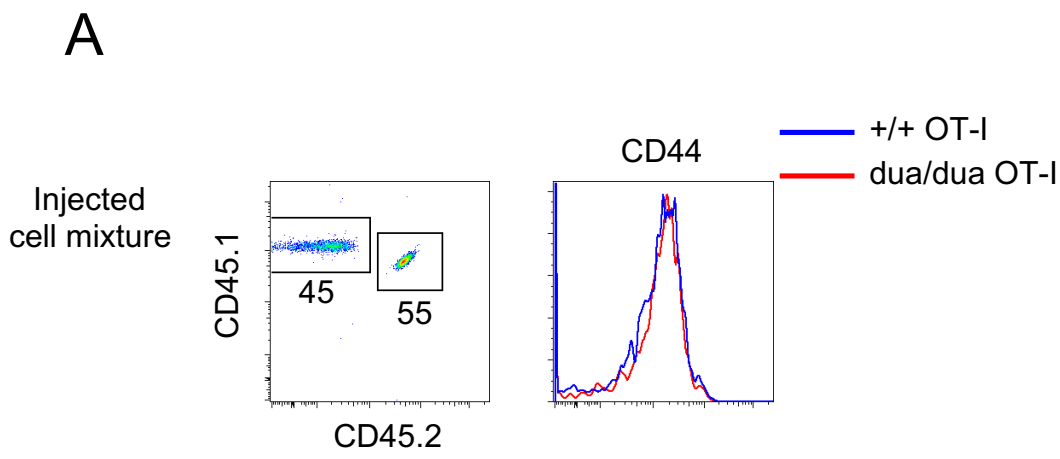

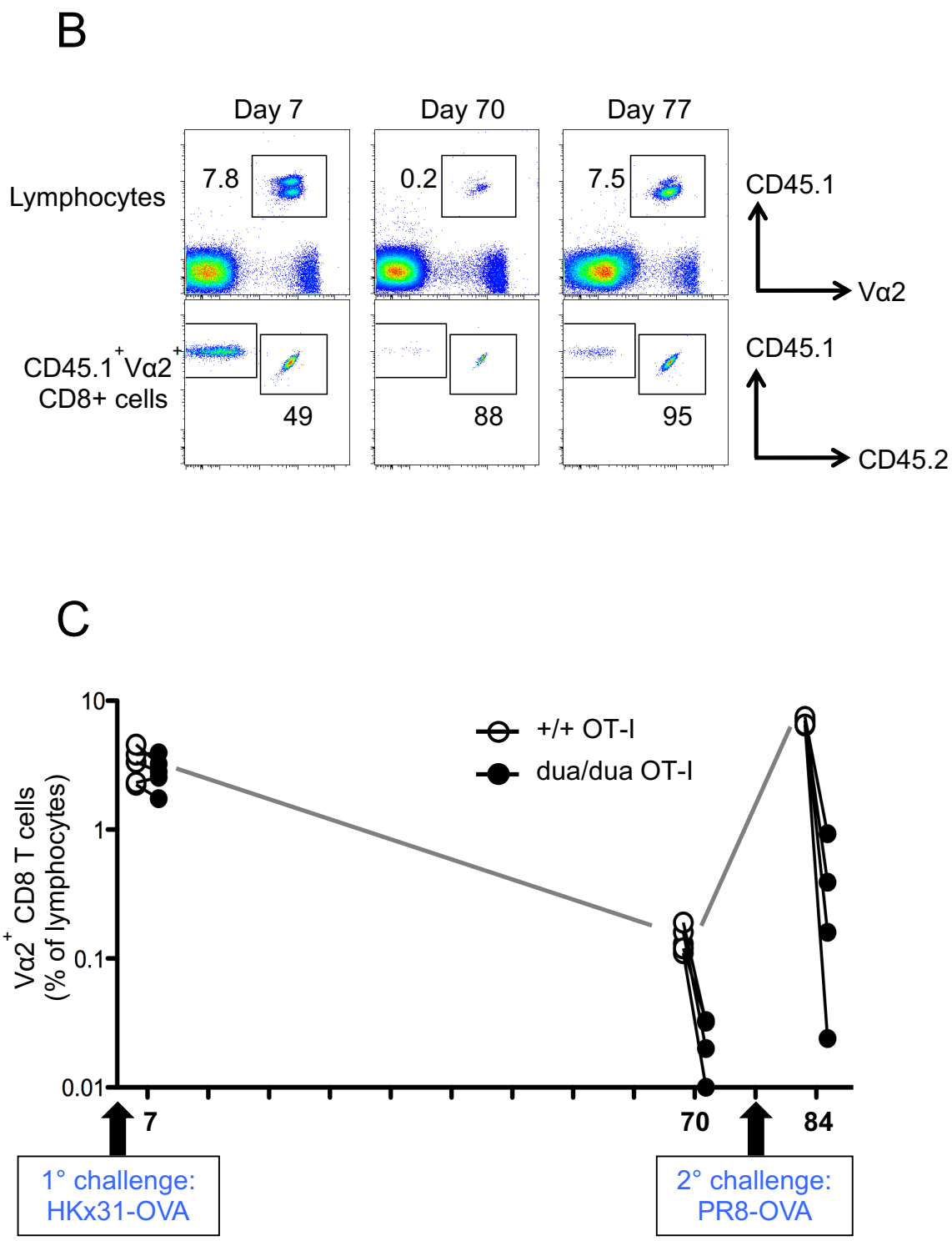

Figure 5.13. Analysis of antigen-specific *Senp2*$^{mut/mut}$ CD8 T cells for persistence and recall response after viral challenge. Congenically marked OT-I T cells with either wild-type SENP2 (CD45.1/CD45.2

heterozygous) or mutant SENP2 (CD45.1 homozygous) were mixed in a 50:50 ratio and 1000 cells were injected into the tail vein of normal C57BL/6 recipients, which were then injected i.p. with recombinant HKx31-OVA influenza virus. (A) Analysis of cells in the donor inoculum at the time of adoptive transfer. (B) Representative flow cytometry plots show the gating strategy applied to distinguish the two donor T cell populations on days 7, 70 and 77. (C) Percentages of wild-type (open) and *Senp2*$^{dua/dua}$ (closed) OT-I CD8 T cells in blood lymphocytes at the indicated time points, with lines connecting data from the same recipient mouse.

To understand whether the effector *Senp2*$^{dua/dua}$ OT-I CD8 T cells could undergo normal differentiation and generate memory cells, expression of CD44, CD62L, CD127 (IL-7Rα) and KLRG1 on *Senp2*$^{dua/dua}$ OT-I CD8 T cells and their wild type OT-1 counterparts was examined at various time points (Figure 5.14). At the peak of the primary immune response (day 7 post challenge), there were no differences in the expression of CD44, CD62L, CD127 and KLRG1. Examination of the cells on day 70 were inconclusive due to the low numbers of cells to assay. At the peak of the recall response (day 84, 7 days post secondary challenge), the expression of all the markers was similar on both donor populations. These results showed that the survival defect caused by the *Senp2*$^{dua/dua}$ mutation was not due to a preferential formation of short-lived effector cells.

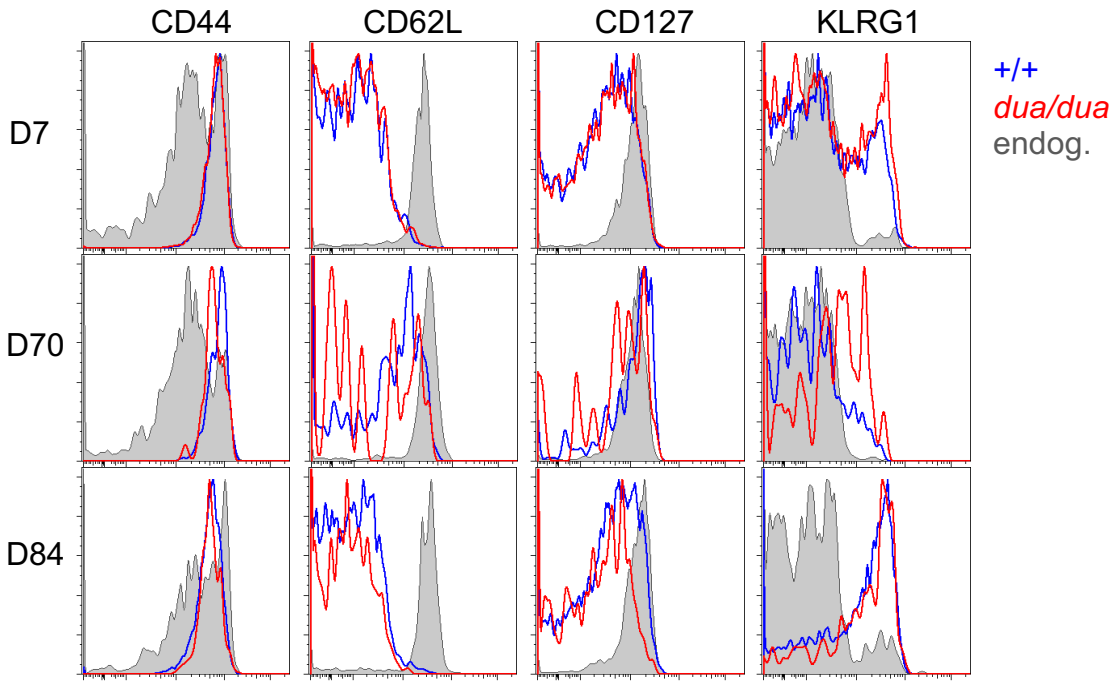

Figure 5.14 Expression of surface markers on OT-1 CD8 T cells during *in vivo* activation, differentiation and survival. Donor-derived *Senp2*$^{+/+}$ wild type and *Senp2*$^{dua/dua}$ OT-I CD8 T cells in the experiment in Figure 5.13 were stained for the cell surface markers CD44, CD62L, CD127 and KLRG1. Representative histograms from a single mouse show wild type (+/+) and *Senp2*$^{dua/dua}$ (*dua/dua*) OT-I CD8 T cells and endogenous (endog.) CD8 T cells.

5.7 Effect of *Senp2*$^{dua/dua}$ mutation on *in vitro* T cell proliferation

In the previous section, *Senp2*$^{dua/dua}$ OT-I CD8 T cells had almost normal expansion upon antigen challenge but the memory cells could not survive longer term like the wild type cells. I next tested the ability of *Senp2*$^{dua/dua}$ OT-I CD8 T cells to proliferate *in vitro* to anti-CD3. CFSE-labeled and CD45-marked wild type and *Senp2*$^{dua/dua}$ OT-I CD8 T cells were co-cultured with 0 (unstimulated), 0.1ug/mL, 1ug/mL and 10ug/mL anti-CD3 antibody, and cell division measured

by flow cytometric analysis of CFSE dilution 3 days later. As shown in Figure 5.15, *Senp2*$^{dua/dua}$ OT-I CD8 T cells diluted CFSE comparably to wild type OT-I CD8 T cells at each of the doses of anti-CD3 tested which indicates *Senp2*$^{dua/dua}$ OT-I CD8 T cells have normal T cell proliferation in *vitro*.

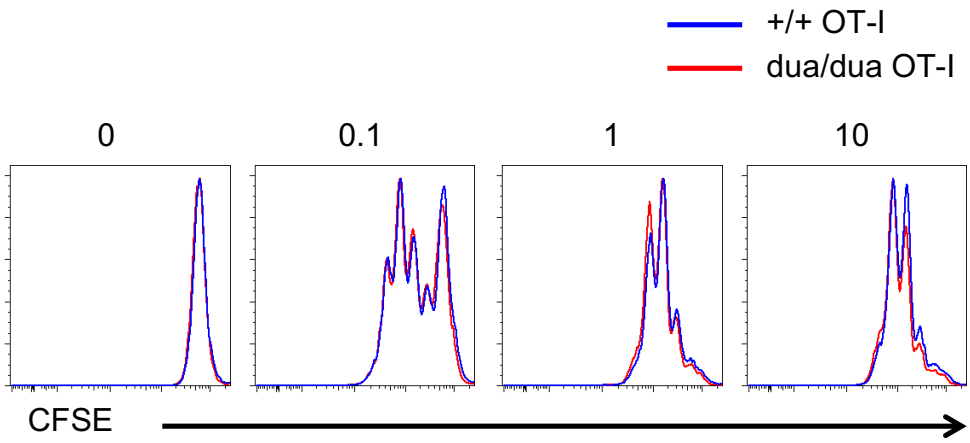

Figure 5.15 *In vitro* division of wild type and *Senp2*$^{dua/dua}$ OT-I CD8 T cells in response to anti-CD3 antibody. CD45.1/CD45.2 wild type OT-I CD8 T cells and CD45.1/CD45.1 *Senp2*$^{dua/dua}$ OT-I CD8 T cells were mixed, labeled with CFSE, and co-cultured with 0, 0.1, 1, 10 μg/mL of anti-CD3. CFSE dilution was measured by flow cytometry after 3 days in wild type (blue), and *Senp2*$^{dua/dua}$ (red) CD8 T cells.

5.8 Discussion

This chapter examined the consequences of the *Senp2 duan* mutation for CD8 T development and response to TCR and IL7RA stimulation. Homozygous *Senp2 duan* mice were found to undergo normal T cell development in the thymus. The mutant mice had normal thymocyte cell percentages and absolute number at different stages of thymic development. However, there was a significant reduction in naive CD8 T cell numbers in the spleen, consistent with the decrease

in blood demonstrated in Chapter 4. These data indicate that the *Senp2* mutation does not affect T cell development but disrupts the accumulation of mature naïve CD8 T cells in the periphery. However memory CD8 T cell numbers were not affected. The *duan* strain was first identified by a lower percentage of CD8 T cell in the peripheral blood and most CD8 T cells carried $CD44^{hi}$ phenotype. This could be explained by decreased numbers of CD8 T cells in the naïve compartment but normal numbers of $CD44^{hi}$ CD8 T cells. The numbers of mutant $CD44^{hi}$ CD8 T cells were likely to be maintained by lymphopenia induced proliferation, which was shown to be normal in T cell transfers.

The peripheral naïve CD8 T cell pool is maintained for long periods in cell cycle interphase by TCR:self-pMHC interactions and IL-7 signaling (Kirberg et al., 1997; Nesic, D. and Vukmanovic,S., 1998; Schluns, K.S., et al., 2000; Benoist, C. and Mathis, D., 2001). After being transplanted into lymphoreplete recipients, naïve donor CD8 T cells compete with host T cells for survival signals from pMHC I and IL-7. The transfer experiments in Chapter 4 showed $Senp2^{dua/dua}$ OT-I CD8 T cells decreased rapidly with a half-life of less than 10 days under these conditions, whereas co-transferred wild type OT-I CD8 T cells declined with a half-life of ~50 days.

Diminished persistence of the *Senp2* mutant CD8 T cells could theoretically reflect abnormalities in either TCR/pMHC I or IL-7/IL7RA signals. It has been shown that naive CD8 T cells decline rapidly after induction of TCR deletion, with a half life about 16 days after induction of TCR deletion compared to l62 days for WT CD8 T cells (Polic et al., 2001). The actual time of CD8 T cells survival after TCR is eliminated is believed to be shorter because of the time delay for loss of TCR. Brown et al. also demonstrated that CD8 T cells could not survive longer than 2 weeks after adoptively transfer into recipients without appropriate MHC-TCR signals (Brown, E., et al., 2005).

When naïve CD8 T cells were adoptively transferred into $IL\text{-}7^{-/-}$ mice, donor cells decreased dramatically and were undetectable at 30 days after cell transfer (Tan et

al., 2001). It has been shown that combination of a deficiency in IL-7 signaling with impairment of TCR signaling causes a more rapid decline of T cell numbers (Seddon and Zamoyska, 2002).

We tested the role of pMHC I in the poor survival of Senp2 mutant naïve CD8 T cells by transferring OT-I CD8 cells into TAP-1 deficient mice, which are unable to load peptides into MHC-I and consequently have very low MHC-I on cell surfaces. There was no obvious survival disadvantage for *Senp2*$^{dua/dua}$ CD8 T cells compared to wild type cells in TAP1-deficient recipients. A confounding factor in this experiment is that the transplanted wild-type and mutant CD8 T cells declined much more rapidly in the absence of pMHC-I than the T cell decline caused by *Senp2* mutation in wild type B6 recipients. Since OT-I transgenic mice have a high affinity TCR for self peptide MHC but still have survival defects, this suggests the *Senp2*^{duan} survival defect was not due to a problem with TCR signaling, although the results are ambiguous on this point.

Additional evidence that TCR signaling was not affected by the mutation comes from the finding that *Senp2*$^{dua/dua}$ OT-I CD8 T cells were able to divide normally when stimulated with anti-CD3 *in vitro*, and undergo normal primary clonal expansion upon viral antigen stimulation *in vivo*. After the viral antigen was cleared, however, the memory *Senp2*$^{dua/dua}$ OT-I CD8 T cells persisted at ten-fold lower frequencies than their wild type OT-I counterparts. It has been shown that IL-2, IL-7 and IL-15 are non-dispensable for memory CD8 T cell persistence or recall. IL-2 during primary infection provides important signals for CD8 memory T cells to mount a full recall response (Williams et al., 2006). IL-15 was required for primary expansion of CD8 T cells challenged with vesicular stomatitis virus (VSV) and also indispensable for the generation and maintenance of memory CD8 T cells (Schluns et al., 2002). Without IL7RA activity, CTL could convert to memory cells but cannot persist (Carrio et al., 2007). It was shown that the IL7RA deficient cells decreased to undetectable levels between 14 and 28 days after adoptive transfer into the B6 mice while wild type cells still persisted.

The CD8 T cell defects caused by the SENP2 *duan* mutation resemble those in 'Thunder' mice carrying a point mutation in the *Hnrpll* gene that destabilizes one of three RNA-binding domains of the hnRNPLL protein. Thunder mice have selectively diminished peripheral CD4 and CD8 T cell accumulation and peripheral survival without affecting proliferation by Wu et al., 2008. The *Hnrpll*$^{thu/thu}$ mice undergo normal T cell development in the thymus. The reduced T cell numbers are restricted to naïve (CD44^{lo}) CD4 and CD8 T cells while activated/memory (CD44^{hi}) T cells numbers are normal. Transfers into lymphoreplete recipients established that *Hnrpll*$^{thu/thu}$ CD8 T cells had a greatly shortened lifespan compared to wild type cells. Also like *Senp2* mutant OT-1 T cells, Randall et al. showed *Hnrpll*$^{thu/thu}$ OT-I CD8 T cells could undergo normal *in vitro* proliferation and *in vivo* clonal expansion on day 7 after viral challenge, but persistence of *Hnrpll*$^{thu/thu}$ memory cells after the contraction phase was greatly decreased 4 weeks post challenge (Randall et al., 2011). hnRNPLL is a memory-induced RNA-binding protein that regulates mRNA splicing. In *Hnrpll*$^{thu/thu}$ mice, mutant hnRNPLL fails to exclude exons 4, 5 and 6 of the T cell *Ptprc* mRNA.

Recently, RNA-seq was performed to study hnRNPLL-dependent splicing events in the *Hnrpll*$^{thu/thu}$ OT-I CD8 T cells. Remarkably, splicing of *Senp2* exon 10 to exon 11 was one of the highest ranked targets of hnRNPLL, with defective hnRNPLL causing retention of parts of the intron and decreasing the formation of exon 10-11 spliced products (Cho et al., 2014). The transduction of *Hnrpll*$^{thu/thu}$ OT-I CD8 T cells with normally spliced *Senp2* cDNA could restore the survival of the *Hnrpll*$^{thu/thu}$ T cell indicating that inefficient splicing of exon 11 in *Senp2* is responsible for the CD8 T cells survival defect in the *Hnrpll*$^{thu/thu}$ mice.

CD127 IL-7Rα chain is displayed at lower levels on naïve CD8 T cells in *Senp2*$^{dua/dua}$ and *Hnrpll*$^{thu/thu}$ mouse mutants. In *Hnrpll* mutant T cells low cell surface protein was accompanied by low *Il7ra* mRNA (Wu et al., 2008). Here I showed low IL-7Rα expression on *Senp*$^{dua/dua}$ naïve CD8 T cells was a cell autonomous trait in mixed bone marrow chimeras, albeit one that developed

relatively late in the reconstitution of these chimeras. IL-7 nevertheless induced acute STAT5 phosphorylation at indistinguishable levels and with identical kinetics in mutant and wild type naïve CD8 T cells exposed to sub-saturating and saturating IL-7 concentrations. Likewise, there was no effect of the *Senp2* mutation on up-regulation of IL-7Rα after IL-7 withdrawal in vitro. However, the *Senp2* mutation caused markedly exaggerated IL-7Rα downregulation within 2 hrs of IL-7 exposure *in vitro*, again selectively on naïve and not on $CD44^{hi}$ activated/memory CD8 T cells. Provided IL-7 stimulation continued, the exaggerated IL-7Rα downregulation on mutant naïve CD8 T cells persisted for at least 6 days *in vitro*. Collectively, these results identify a specific or rate-limiting role for SENP2 in opposing IL-7Rα downregulation selectively on naïve CD8 T cells.

IL-7 is a prosurvival cytokine constitutively produced by stromal cells, monocytes and some epithelial cells (Jiang, Q et al., 2005). IL-7 signaling initiates expression of anti-apoptotic genes such as Bcl-2 in T cells. Once signaling from IL-7 is initiated, transcription of the *Il7ra* gene is inhibited in T cells as a negative feedback mechanism (Park, et al, 2004). Park et al (2007) also demonstrated that transcription of CD8 coreceptor can be activated by IL-7 signaling. Moreover, IL-7 signaling is negatively regulated by TCR signaling stimulated by self pMHC-I and results in a reduction of CD8 expression. Hence, they identified a dynamic feedback loop that promotes CD8 T cell survival through modulating IL-7 receptor and CD8 coreceptor expression.

Negative regulation of IL-7Rα by its cognate ligand IL-7 is mediated by the transcriptional repressor, growth factor independent 1 (GFI-1), in CD8 T cells but not in CD4 T cells (Park, et al., 2004). The selective effect of *Senp2* and *Gfi1* mutations on CD8 T cells and not CD4 T cells raises the hypothesis that sumoylation enhances the effect of GFI-1, so that GFI-1 has an exaggerated inhibitory effect on IL7RA expression when less SENP2 is available to remove SUMO. There is no published evidence that GFI-1 itself is SUMOylated, but GFI-1 interacts with the STAT3 inhibitor and Sumo-specific ligase, PIAS3 (Rodel et

al., 2000). In Tarik Moroy's recent review (Moroy and Khandanpour, 2011), he states: "It remains open, whether the activity of PIAS proteins as E3 ligases for SUMO residues plays a role in this interaction, but it is attractive to speculate that GFI1, which has so far not been shown to be sumoylated, may serve as a docking site for other proteins that are to be sumoylated. This function although highly speculative may be enabled by an interaction with proteins such as PIAS3." To test this hypothesis, western blotting or mass spectrometry could be used to determine the levels of GFI-1 protein and SUMOylation of GFI1 and other proteins in resting and IL-7 stimulated *Senp2*$^{dua/dua}$ cells. A genetic test for a role of GFI1 in mediating the effects of *Senp2* mutation would be to breed *Senp2*$^{dua/dua}$ mice with one *Gfi1* allele inactivated, and measure whether the decreased *Gfi1* gene dose could restore normal IL7RA expression on *Senp2* mutant CD8 T cells.

While the experiments here point to abnormal response to IL-7 signalling as the explanation for poor survival of SENP2 mutant naïve CD8 T cells, other signaling pathways could also be affected by the mutation. The Wnt signalling pathway is involved in various cellular activities including cell fate determination, differentiation, and proliferation (Logan et al., 2004). In the absence of Wnt signal, β-catenin is phosphorylated after binding to a 'destruction complex' that consists of Axin, APC and the protein kinase GSK-3, and degraded after polyubiquitination. Once exposed to Wnt signals, the complex is disrupted and the degradation of β-catenin is inhibited. Zhao et al. found constitutive activation of Wnt signalling pathway can stabilize β-catenin and favors the formation of antigen-specific memory CD8 T cells (Zhao et al., 2010). Sumoylation is also involved in the regulation of the Wnt signaling pathway (Kadoya et al, 2002). Axam (Axin-associating molecule) has a similar C-terminal sequence to SENP1 and has been shown to function as a desumoylation enzyme and remove SUMO-1 molecule from target proteins. The desumoylation activity of Axam is involved in downregulation of β-catenin. Therefore, it could negatively regulate the Wnt signaling pathway. Since *duan* mice have less antigen-specific memory CD8 T cells compared to wild type mice, it could be hypothesized that the loss of exon 11 caused by the *duan* mutation results in a gain function mutation with increased

desumoylation activity against β-catenin. This over activity of desumoylation could downregulate β-catenin and shrink the antigen-specific memory CD8 T cell pool by suppressing the Wnt signaling pathway. However, the results in Chapter 4 establish that the effects of the *duan* mutation on CD8 T cells were recessive and equally severe when a single copy of the *duan* allele was present along with a null allele, arguing against a gain-of-function hypothesis.

Chapter 6: Discussion

ENU-mutagenesis: a non-biased approach to identify novel genes in immune system

ENU mutagenesis screen is a powerful tool to identify novel genes involved in immune system in a nonbiased manner. The Goodnow group has been using ENU mutagenesis screens to identify genes important in adaptive immune cell development, function and homeostasis (Miosge et al., 2002; Jun et al., 2003; Vinuesa et al., 2005, Wu et al., 2010, Randall et al., 2009).

Although ENU mutagenesis is a widely applied phenotype-driven approach to understand gene function, it is inevitable to isolate additional alleles of genes that are already well characterised by knockout mice, like DOCK2. My studies of the *dockland* mouse strain have led to the discovery of a mutation in exon 23 of *Dock2* gene that produced a premature stop codon. Because the mutation 775E to stop codon is right after DHR-1 domain (Figure 3.4), any remaining protein product lacks the DHR-2 domain. Like all the DOCK family proteins, the DHR-2 domain of DOCK2 binds to Rho-family G proteins and promotes GTP-GDP exchange to activate local cytoskeletal changes, cell migration and polarization (Meller et al., 2005; Cote and Vuori, 2007). All these cell activities are abolished with the loss of the DHR-2 domain. The results in Chapter III suggest that our *dockland* mutation is probably equivalent to the knockout allele first described by Fukui (Fukui et al. 2001) and to recessive alleles recently discovered in children with severe combined immunodeficiency (Dobbs et al., 2015).

The powerful ENU mutagenesis can also lead us to discover novel genes. The critical immunological role of another DOCK family protein, DOCK8, was discovered by Randall et al, 2009 through isolation of a missense mutation that changes a conserved serine in the Rac/Cdc42 binding site of the DHR2 domain (Randall et al., 2009). Before the discovery of *primurus* mutation, the in vivo function of DOCK8 had remained unknown, and a human DOCK8 immunodeficiency syndrome was discovered independently and after the mouse mutant was identified.

Moreover, the strength of ENU mutagenesis is that by starting with an abnormal immune system phenotype we can identify entirely new genetic elements of adaptive immunity. For genes where complete loss of function mutations are embryonically lethal, like *Senp2*, discovering their immune function by the gene knockout approach is confound by the absence of viable progeny. The SENP2 protein and gene have been already well studied at molecular level, but knockout mice are lethal at very early stage in development. The discovery of '*duan'* mutation in *Senp2*, with a subtle loss of function allele, revealed an apparently rate-limiting role for SENP2 in peripheral CD8 T cell survival.

In summary *Dock2*$^{doc/doc}$ mice has:

DOCK2-deficient summary	Reference	*Dock2*$^{doc/doc}$
reduced total number of spleen cells	Fukui et al., 2001	✔
atrophic lymphoid follicles	Fukui et al., 2001	
Markly reduced MZ B cells	Fukui et al., 2001	✔
reduced thymocyte number	Fukui et al., 2001	✔
defect mature thymocyte egress from thymus	Fukui et al., 2001	
abnormal thymic architecture	Fukui et al., 2001	
peripheral blood T lymphocytopenia	Fukui et al., 2001	✔
disrupted lymphocyte migration in response to chemokine and S1P	Fukui et al., 2001; Nombela-Arrieta et al., 2007	
normal B-lymphopoiesis	Fukui et al., 2001	✔
Impaired immunological synapse formaiton in T cells	Sanui et al., 2003	
reduction of NKT in thymus and spleen		✔
reduction in pDC; defective IFN-α production	Gotoh et al.,2008	
normal antigens-specific CD8 T cell immune response		✔
surival advantage in innate immune response		✔

The study and analysis in the first part of this thesis showed that the characteristics of our *dockland* mutation in DOCK2 have no difference from DOCK2-deficient mouse (Fukui et al., 2001). The mutation causes a stop codon instead of Glutamic acid after DHR-1 domain. If the protein can be made, there is no functional domain for GEF activity. Western blotting has not been done successfully.

The dedicator of cytokinesis (DOCK) family proteins belong to guanine nucleotide exchange factors (GEFs) that regulate the activation of Rho GTPases. There are more than 20 Rho GTPases that act as molecular switch by cycling between GDP-bound inactive and GTP-bound active states and their GTP-GDP exchange is mediated by GEFs. Rho GTPases like Rho, Rac, Cdc42 are well known for their ability to regulate the actin cytoskeleton and variety of cellular processes. There are 11 members of DOCK proteins. DOCK2 is a member of the DOCK-A family and it has been studied extensively in mice during last decade. DOCK2 is predominantly expressed in hematopoietic cells and has been shown to be indispensable for lymphocyte migration in response to chemokine (Fukui et al., 2001; Sanui et al., 2003) DOCK2 knockout mice display T lymphopenia, atrophy of lymphoid follicles and loss of marginal zone B cells. Homozygous DOCK2 knockout mice leads to B and T cell migration defect in response to chemokines, T cell lymphopenia and absence of marginal zone B cells.

Migration of lymphocytes is of central importance for effective adaptive immune response. T cells need to actively migrate out of the thymus medulla and into the bloodstream, attracted by the sphingosine metabolite S1P acting upon the receptor S1P1 (Allende et al., 2004; Schwab and Cyster, 2007). T and B cells continually actively migrate from the blood into specialized subcompartments of secondary lymphoid organs to survey the antigen, returning to the blood by active migration into the lymphatic vessels, and then via the blood into another lymph node or into tissues to survey for the pathogens if fail to encounter their antigen. This trafficking of lymphocytes into and within secondary lymphoid organs is guided by two families of G protein-coupled receptors: chemokines such as CCL21,

CCL19, CXCL12, and CXCL13, while egress to lymphatics is guided by the sphingosine S1P1 receptor system (Cyster, 2005; Von Andrian et al., 2003). Activated T cells will transit into tissues to survey for pathogens only when they are really activated, otherwise, they will transit back into circulation then back to lymph nodes.

Although normal cells could migrate efficiently to these chemokines in a dose dependent manner, DOCK2 deficient lymphocytes have severe defects responding to these chemokines (Fukui et al., 2001). Surprisingly, the small white pulp in DOCK2-deficient mice has normal segregation of lymphocytes into T and B cell areas which was not seen in mice lacking chemokines CCL19, CCL21 or CXCL13 (Fukui et al., 2001; Reif and Cyster, 2002). It also has been shown in DOCK2-deficient mice that there is still some residual chemotaxis (cell migration ~10% normal level). This evidence may suggest the existence of an independent chemotaxis pathway operating in the presence of DOCK2 or there is a pathway becomes active in the absence of DOCK2. Nombela-Arrieta et al. showed that there is a phosphoinositide-3-kinase (PI3K)-dependent cell migration in DOCK2 deficient lymphocytes (Nombela-Arrieta et al., 2004). Lymphocyte migration is mediated by a largely DOCK2-dependent manner. However, a minor PI3K-dependent pathway is also observed in DOCK2-deficient lymphocytes (Nombela-Arrieta et al., 2004). It is also suggested that PI3K-dependent T cell chemotaxis depends on PI3Kγ, whereas B cell migration depends on other PI3K isoform (Nombela-Arrieta et al., 2004). In the absence of both DOCK2 and PI3Kγ, T cell migration to chemokines is totally abolished in vitro and the homing capacity towards SLOs is further reduced (Nombela-Arrieta et al., 2004).

The other subfamilies of lymphocyte-expressed G protein-coupled receptors (GPCRs), S1P receptor 1 ($S1P_1$) also plays an essential role in thymic emigration and lymphocyte recirculation through the secondary lymphoid organ (Matloubian et al., 2004; Shiow et al., 2006; Cyster, 2005). T-cell-specific deletion of $S1P_1$ receptor results in reduction of total numbers of T cells in peripheral blood and peripheral lymphoid organ (Allende, et al., 2004). DOCK2 is required for efficient

interstitial T and B cell motility and DOCK2-deficient T and B cells displayed markedly reduced $S1P_1$-mediated migration (Nombela-Arrieta et al., 2006) It is suggested that DOCK2 has a central role during T and B cell intertitial migration with a minor but significant role of PI3Kγ specifically in $S1P_1$-mediated T cell migration (Nombela-Arrieta et al., 2006).

$S1P_1$-deficient thymocytes are unable to egress from the thymus and mature $S1P_1$-deficient thymocytes fail to exit SLO (Allende et al., 2004). CD69 can inhibit $S1P_1$ and lymphocytes egress by acting downstream of interferon-a/b (IFN-a/b) (Shiow et al., 2006). As shown in Chapter III, *Dock2*$^{doc/doc}$ mice have reduced DP and mature SP thymocytes. The CD69 expression was reduced on both CD4 and CD8 SP thymocytes from our data. CD69 involves in the generation of mature SP thymocytes and has a potential/putative role in thymic emigration (Feng et al., 2002; Nakayama et al., 2002). The blockade of CD69 can cause a reduction in the number of SP and increased number of DP (Nakayama et al., 2002). Although lack of CD62L marker, there was no significant difference in the number of the CD69low CD4 and CD8 SP thymocytes between our *Dock2*$^{doc/doc}$ and wild type mice. Although there is only 5% normal efficacy of thymic emigration in DOCK2-deficient thymocytes (Fukui et al., 2001; Allende, et al., 2004), our data suggested that the recent mature *Dock2*$^{doc/doc}$ SP thymocytes did not accumulate in the thymus. Combined with above, DOCK2 has been shown to have a dominant role in lymphocytes recirculation like homing, interstitial migration and egress.

DOCK2 also has a role in TCR signaling. Sustained TCR interaction with MHC-peptide complexes in the immunological synapse (IS) at the interface of T cell and antigen-presenting cells (APCs) is required for T cell activation (Paul and Seder, 1994; Norcross, 1984). The mature IS has been defined by the formation of a bull's eye pattern with supramolecular activation clusters (SMACs) whose center (cSMAC) is enriched with for TCR and MHC-peptide complexes. The peripheral SMAC (pSMAC) contains a ring of the cognate integrin LFA-1 (lymphocyte function-associated antigen 1) and its immunoglobulin superfamily ligand ICAM-I (intercellular adhesion molecule 1) (Grakoui et al., 1999; Monks et al., 1998 and

Wulfing and Davis, 1998). The signaling molecules like protein kinase C θ (PKC-θ) and the src family kinase Lck are also in the cSMAC on the cytoplasmic side of the IS.

In DOCK2$^{-/-}$ T cells, TCR-mediated Rac activation is totally abolished (Fukui et al., 2001; Sanui et al., 2003). During the formation of immunological synapse, the signaling molecule PKC-θ and adhesion molecule LFA-1 are not affected in DOCK2 deficient T cells and can still polarize to the cell surface. However, TCR and lipid raft can accumulate at the interface during formation of IS in wild-type T cells, and this clustering is not seen in DOCK2$^{-/-}$ T cells (Sanui et al., 2003).

DOCK2 deficiency also affects antigen-specific T cell proliferation. The proliferative response of 2B4αβ Tg T cells decreased to less than 25% in Dock2 deficient mice compared to wild-type level (Sanui et al., 2003). From our *in vitro* proliferation experiment, naïve (CD44^{lo}) *Dock2*$^{doc/doc}$ CD4 and CD8 T cells could proliferate as well as wild type controls with 1ng/ml αCD3 stimulation. More studies have been shown that the antigen-specific T cell proliferation still occurs in DOCK2 deficient mice (Sanui et al., 2003). However, they required higher concentrations of antigenic peptides to reach the similar proliferative response as wild type (Sanui et al., 2003). As our in vitro proliferation was done under a single concentration condition, different results might be seen with lower concentration of αCD3 condition. Defective TCR polarization and lipid raft clustering may affect the threshold for T cell proliferation (Sanui et al., 2003). Different gangliosides, the major components of lipid raft are presented in CD4 and CD8 T cells, may contribute to different effector response following TCR stimulation (Nagafuku et al., 2011). There is no data has been shown on DOCK2 deficiency on cytotoxic function of CD8 T cells. From our mix bone marrow chimeras' data, DOCK2 has been shown to have a cell-autonomous role in CD8 T cells. The number of circulating naïve CD8 T cells was decreased in *Dock2*$^{doc/doc}$ homozygous mutants. As shown in Chapter III, *Dock2*$^{doc/doc}$ NP-binding CD8 cells accumulated at approximately normal percentage of all CD8 cells during influenza infection. Since most DOCK2 proliferation studies were done in vitro,

the reasonable explanation can be that there might be other costimulatory signals were available in vivo to compensates for the DOCK2 deficiency and allow relatively normal T cell activation and proliferation (Marchingo et al., 2014) than simple in vitro condition.

Unlike naïve CD8 T cells continually recirculating in the lymphoid organs to survey antigen, activated lymphocytes retained within the lymphoid organ and undergoes clonal expansion and exit with the effector function. It is still obscure whether DOCK2 affects the exit of antigen-specific lymphocytes to the infection sites.

Recently biallelic mutations in human *DOCK2* has been identified as molecular cause of combined immunodeficiency found in patients with early-onset, invasive bacterial and viral infections (Dobbs et al., 2015). All patients have T-cell lymphopenia and impaired in vitro T-cell activation, defective T, B and NK cell functions. 3 out of 5 patients have markedly reduced proportion of naïve (CD45RA+CCR7+) CD4 and CD8 T cells which were associated with an increased proportion of effector memory (CD45RA-CCR7-) CD4 T cell and effector memory or CD45RA-CCR7-T_{EMRA} CD8 T cells. 2 out of 5 patients have B cell lymphopenia. And 3 out of 5 patients have defective T-cell dependent immunization antibody production. Consist with finding in mouse, RAC1 activation was impaired in the T cells, the phenotypes shown in DOCK2 deficient patients are very similar as we have seen in mouse. It is noted that Patient 4 had a F744Cfs*27 mutation truncating DOCK2 at a similar position to the *dockland* E775X nonsense mutation which lacks the DHR-2 domain. Moreover, the study of DOCK2 in human also suggested a role in antiviral interferon production in nonhematopoietic cells. DOCK2 deficient mice have a severe reduction of pDCs in the spleen (Gotoh et al., 2008) Further studies showed that DOCK2 has an essential role of mediating interferon-α production in plasmacytoid dendritic cells, the major source of type I IFNs for antiviral immunity (Gotoh et al, 2010). When *Dock2*$^{doc/doc}$ homozygous mice were intranasally infected with influenza virus, they showed less weight loss and had a trend of better survival compared to

heterozygous and wild type mice. It may suggest the existence of a protective mechanism in the *Dock2*$^{doc/doc}$ mice. pDCs are known for contribution to the pathogenesis of some autoimmune disease like systemic lupus erythematosus (SLE), human psoriasis by production of IFN-α (Blanco et al., 2001; Nestle et al., 2005; Lande et al., 2007). Together with our immunization experiments, DOCK2 may serve as a therapeutic target for pDCs/type I IFN-related autoimmune disease.

Another DOCK family member, DOCK8, has been studied extensively in mice and humans and shown to play an indispensable role in immune system function. DOCK8 is DOCK-C family member that functions as a GEF for Cdc42 via its DHR2 domain. *DOCK8* mutation has been first discovered to cause a combined immunodeficiency syndrome in humans (Zhang, Q., et al., 2009; Engelhardt, K.R., et al., 2009). DOCK8 deficient patients also have hyper IgE and severe viral infections. Recently DOCK8 has been shown to have a crucial role in CD8 T cells survival and function (Randall, et al., 2011). *Dock8*$^{pri/pri}$ mutation causes a subtle decrease in the primary response but severely compromised the long-term persistence of memory T cell and the recall response. T and NK cells from DOCK8 deficient mice develop cell shape and nuclear deformation abnormalities that result to a new form of cell death named 'cytothripsis' (Zhang et al., 2014). The defect in DOCK8 prevents the generation of long-lived skin-resident memory CD8 T cells and impairs the control of herpesvirus skin infection. DOCK8-deficient mice have impaired clearance of Herpes simplex virus (HSV) and lead to increased disease and decreased CD4 T cell infiltration into HSV-infected skin (Flesch, I., et al., 2015). This finding may give a hint for the loss of control of HSV in DOCK8-deficient patients.

As two family members that have been studied intensively, DOCK2 and DOCK8 shared some similarities and also have different properties in T cell IS formation. DOCK2 and DOCK8 are indispensible for T cell IS formation but functional differently. In DOCK2-deficient T cells, antigen-induced translocation of TCR and lipid rafts were severely impaired without affecting PKC-θ and LFA-1. On the other hand, DOCK8 affects LFA-1 actin polarization with intact PKC-θ. From

our preliminary data of *Dock2*$^{doc/doc}$ *Dock8*$^{pri/pri}$ double deficient mice, there is a further reduction of spleen T cells number especially CD8 T cell number in the double deficient mice. Since DOCK2 and DOCK8 have different role in T cell synapse formation, they might have an additive effect on T cell survival, activation, and migration. To further address the migration defect in DOCK2 and double deficient mice, analysis of thymocytes with mature and egress marker is necessary to find out whether there is a further block of recent mature SP thymocytes to egress from thymus. Chemotactic assay with the mature SP thymocytes is also useful to answer this question. More functional studies can be done to understand how the double mutant can affect the activation, survival of antigen-specific CD8 T cells.

Table 6.1: Comparison of Dock2 and Dock8 mutation in mouse and human

Gene	Family	Mutation	Mouse phenotype	Human mutation	Associated disease
Dock2	DOCK-A	*doc/doc* and KO	lymphocyte migration in response to chemokines; TCR-mediated Rac activation; IS formation in T cell; IL-4Rα internlization in T_H2 cells; MZ B cells; NKT cell development; NK cell-mediated cytotoxicity	biallelic mutations	Combined immunodeficiencies; Early-onset and invasive infections
Dock8	DOCK-C	*pri/pri*	IS formation, long-term humoral immunity; survival of memory CD8 T cells; viral control and CD4 T cell infiltration of herpes simplex virus infection; MZ B cells; survival and function of NKT cells	homozygous mutations	Autosomal recessive hyper IgE syndrome

In summary *Senp2* is required for:

Persistence of naïve OT-I CD8 T cells in lymphoreplete host
Persistence of long-term memory OT-I CD8 T cells
Survival of naïve CD8 T cells
Attenuate IL-7 induced downregulation of IL7RA

My studies of the *duan* mouse strain reveal a role for *Senp2* in the CD8 T cell survival, offering a new insight into a known gene with no previous known function in immune system. In particular, my studies show that *Senp2* has an indispensible role in survival of naïve CD8 T cells and long-term survival of antigen-specific memory CD8 T cells. However, the mechanism by which *Senp2* regulates naïve and memory T cell survival is still unknown.

SENP2 is ubiquitously expressed in multiple tissues, increasing the difficulty to study its specific role in immune cell subset *in vivo*. A targeted null mutation in *Senp2* causes embryonic lethal phenotypes about E10 (Kang et al., 2010). Consequently most studies of SENP2 function are in transfected cell lines expressing the mutant form of protein *in vitro*.

Although the SENP2-null homozygous mice are embryonic lethal (Chiu et al., 2008), the mice carrying the *duan* mutation in *Senp2* gene are physically normal and can be bred to propagate the mutation. It is still obscure exactly how the *duan* mutation disrupts the function of SENP2 protein. From our PCR data, the *duan* mutation caused exon 11 skipped in at least 50% of remaining SENP2 mRNA transcripts. One possibility is that loss of the exon 11 from the SENP2 protein may cause the CD8 T cell phenotype. Western blot has not been done successfully to show whether the variant mRNA lacking exon 11 makes protein, either because there is no good SENP2 antibody available or there is low expression of SENP2 in T cells as suggested by the bioGPS microarray data in Chapter 4. If the exon 11 skipped protein can be made and detected, it is critical to determine the proportion of full protein versus truncated protein presented in *duan* homozygous CD8 T

cells. It is also possible that there is reduction of normal mRNA or protein in the overall amount of mRNA and protein. The CD8 T cell phenotype in *duan* mice may not be caused by the increased amount of truncated protein (if protein can be made). The main effect of the *duan* mutation is to lower the efficiency of splicing so that there is a substantial decrease in the correctly spliced *Senp2* mRNA, which may be by as much as 90%. As shown in Chapter IV, mice carrying heterozygous null allele or heterozygous for *duan* mutation do not cause the CD8 T cell phenotype which implies that a 50% decrease in SENP2 protein is insufficient. In order to understand the underlying mechanism, future studies should quantify and compare the spliced *Senp2* polyA+ mRNA and protein level in *dua*/*dua*, +/-, and +/+ CD8 T cells.

Duan **mutation affects the persistence of CD8 T cell**

Duan mice have normal thymic development and T cell maturation. However, their naive CD8 T cells were markedly reduced in the periphery. When transferred into secondary hosts with a full T cell repertoire, the homozygous mutant CD8 T cells survived for a much shorter period than co-transferred wild type CD8 T cells. *Duan* CD8 T cells were nevertheless able to survive and compete successfully during homeostatic proliferation with wild-type CD8 T cells when the cell mixture was co-transferred into lymphopaenic host. Their competitive disadvantage was only seen once the T cell compartment began to be repopulated. These *in vivo* experiments suggested that $Senp2^{dua/dua}$ naïve CD8 T cells can proliferate normally in response to pMHC and IL-7, but have a specific survival defect and cannot persist normally once the repertoire has been repopulated.

IL-7 has been shown to have a critical role in the thymic T cell development and in peripheral naïve T cell survival, as reviewed in the introductory chapter. We examined IL-7/IL-7R signaling in $Senp2^{dua/dua}$ T cells. We found that $Senp2^{dua/dua}$ naïve CD8 T cells had consistently lower IL7RA (CD127) receptor expression on the cell surface. Moreover, in mixed bone marrow chimeras experiment, the CD8

T cells derived from *Senp2*$^{dua/dua}$ bone marrow had lower IL-7RA expression, establishing that the lower expression of IL-7R is a cell intrinsic phenotype rather than a secondary effect to the altruistic inhibition of excess IL-7. In vitro culture with IL-7 showed *Senp2*$^{dua/dua}$ naïve CD8 T cells had a normal STAT5 phosphorylation response, but exaggerated downregulation of surface IL7RA expression. These results imply that the *duan* mutation affects naïve CD8 T cell survival by exaggerating the downregulation of *Il7ra* mRNA following IL-7 signalling.

Although how IL-7 protects cells from death is not fully understood, it may involve the regulation of Bcl-2 family members. Bcl-2 is an anti-apoptosis protein and can protect T cell against apoptotic signals. Enforced expression of Bcl-2 in IL-7Rα-deficient mice improves the survival of T lymphocytes (Akashi et al., 1997). It has not been tested whether Bcl-2 expression is affected in *duan* naïve CD8 T cells, and this would be a useful future experiment.

A possible clue to the action of SENP2 comes from the finding that the *duan* mutation primarily affects CD8 T cell survival and IL7RA expression, with little or no diminution of naïve CD4 T cell numbers or IL7RA expression on these cells. In response to IL-7, IL-7R expression is tightly regulated at transcriptional level by various nuclear factors and is downregulated by suppressing IL-7Rα transcription to allow other cells receive IL-7-mediated survival signal. Different molecular mechanism in CD4 and CD8 T cells cytokine-mediated suppression of IL-7Ra transcription. The transcriptional repressor Growth Factor Independence-1 (GFI1) is utilized in CD8 T cells but not CD4 T cells (Park et al., 2004, Ligons et al., 2012). IL7Rα expression was dramatically increased on GFI1-deficient CD8 T cells but not on CD4 T cells from the same *Gfi1*$^{-/-}$ mice (Park et al., 2004). When a *Gfi1* transgene was constitutively expressed in either wild type or *Gfi1*$^{-/-}$ mice, IL7Rα expression was markedly suppressed on CD8 T cells without significantly affecting IL7Rα expression on CD4 T cells (Park et al., 2004, Ligons et al., 2012). Binding of GFI1 to DNA is insufficient in itself and it needs to specifically interact with other nuclear proteins to repress transcription (Grimes et al., 1996).

Another Group A member, SENP1, has been shown to play a crucial permissive role in STAT5 signalling during early T and B lymphocyte development in the thymus and bone marrow (Van Nguyen et al. 2012). The sumo-specific protein ligase family, Protein Inhibitor of Activated STAT (PIAS), was discovered as a negative regulator of STAT signaling (Schmidt and Muller, 2003). PIAS3 has been shown to attach SUMO-2 to phosphorylated STAT5, inhibiting its transcriptional activity and preventing further rounds of phosphorylation until the SUMO group is removed by SENP1 (Rycyzyn and Clevenger, 2002; Dagvadorj et al., 2010 and Van Nguyen et al., 2012). Consequently a homozygous null *Senp1* mutation resulted in greatly diminished IL-7 induced STAT5 phosphorylation in immature T cells, and in thymic lymphopenia in fetal liver transplant recipients that resembles IL7RA deficiency (Van Nguyen et al., 2012). This mechanism does not appear to explain the effects of the *Senp2 duan* mutation, because I found there is normal thymopoiesis and normal STAT5 phosphorylation in response to IL-7 in *duan* homozygous T cells.

Il7ra transcription is specifically inhibited in CD8 T cells in response to IL-7 STAT5 signalling by the DNA binding protein, growth-factor independent 1 (GFI-1) (Park et al., 2004). Given CD8-specific downregulation of IL7RA and exaggerated downregulation in response to IL-7 caused by the *duan* mutation, an attractive hypothesis is that unchecked sumoylation enhances the inhibitory effect of GFI-1 on IL7RA expression. There is no published evidence that GFI-1 itself is SUMOylated, but GFI-1 interacts with the STAT3 inhibitor and Sumo-specific ligase, PIAS3 (Rodel et al., 2000). In Tarik Moroy's recent review (Moroy and Khandanpour, 2011), he states: "It remains open, whether the activity of PIAS proteins as E3 ligases for SUMO residues plays a role in this interaction, but it is attractive to speculate that GFI1, which has so far not been shown to be sumoylated, may serve as a docking site for other proteins that are to be sumoylated. This function although highly speculative may be enabled by an interaction with proteins such as PIAS3." To test this hypothesis, western blotting or mass spectrometry could be used to determine the levels of GFI-1 protein and

SUMOylation of GFI1 and other proteins in resting and IL-7 stimulated *Senp2*$^{dua/dua}$ cells. A genetic test for a role of GFI1 in mediating the effects of *Senp2* mutation would be to breed *Senp2*$^{dua/dua}$ mice with one *Gfi1* allele inactivated, and measure whether the decreased *Gfi1* gene dose could restore normal IL7RA expression on *Senp2* mutant CD8 T cells.

The loss of naïve CD8 T cells in the *Senp2*$^{dua/dua}$ mice may not be the result of a single gene defect and it could due to the combined effect of multiple genes. Besides IL-7 signals, naïve T cells require signals from TCR contact with self-peptide/MHC complexes for long-term survival (Surh, and Sprent, 2005; Dorfman, and Germain, 2002). There is evidence that there could be an interplay between TCR signaling and IL-7 signaling pathway in peripheral T cells. It has been shown that TCR-mediated activation can up-regulate IL-2R expression but down-regulate the IL-7R expression (Franchimont et al., 2002) Down-regulated IL-7R expression on *Senp2*$^{dua/dua}$ naïve CD8 T cells has been observed. Although the TCR complex signals, co-receptor expression and CD5 expression still need to further testing on *duan* CD8 T cells, it is possible that lower expression of IL7Rα in *Senp2*$^{dua/dua}$ naïve CD8 T cells reflects the increased TCR signaling under resting conditions. It is hypothesized that *duan* mutation may affect downstream molecules in TCR signaling pathway that augment TCR signaling and cause the resting T cells to become hyper-activation.

SENP2 is the downstream target of Hnrpll

SENP2 has been shown as an important functional target of HnRNPLL for regulating T-cell survival. The heterogeneous nuclear ribonucleoproteins (hnRNP) bind pre-mRNAs in the nucleus to regulate alternative splicing (Dreyfuss et al., 1993). There are more than 20 hnRNP proteins and hnRNPLL is one member of hnRNP proteins that involves in memory T cell RNA rearrangement. hnRNPLL has 3 RNA recognition motifs (RRM) and the *Hnrpll*$^{thu/thu}$ mutation occurs in the first RRM of *Hnrpll* which substitutes a valine residue to a aspartic acid.

hnRNPLL is required for normal alternative splicing target genes, therefore the mutation affects the alternative splicing of target genes and subsequently affect the expression target protein. CD45 (*Ptprc*) is the most defined mRNA target of hnRNPLL, and *thunder* mice with mutant hnRNPLL constitutively express isoform CD45RA, RB and RC and fail to express the lower isoform CD45RO.

The thunder (*Hrnpll*^{thu}) CD8 T cells showed defect in CD8 T cells survival and lower IL-7R expression on naïve CD8 T cells but not in the memory CD8 T cells (Wu et al, 2008). Exon assay experiments showed that there was a dramatic decrease of IL-7Rα mRNA in naïve *Hrnpll*^{thu} CD8 T cells compared to their wild-type counterparts which suggested that the IL-7R expression is decreased in *Hrnpll*^{thu} naïve CD8 T cells at both levels of protein and mRNA (Wu et al, 2008). From RNA-sequencing of *Hnrpll* mutant and wild-type CD8 OT-I T cells, *Senp2* is one of the highly ranked candidate of hnRNPLL targets. By transducing normally spliced *Senp2*, it restored the survival of *Hrnpll*^{thu} CD8 T cells (Cho et al., 2014). Therefore, *Senp2* exon 10-exon 11 splicing is an important target for *Hnrpll*-dependent T cell survival.

Conclusion

CD8 T cells play a major role in controlling infection by intracellular pathogens. Based on the complexity of possible targets of SENP2, it is very hard to identify a regulatory pathway that is responsible for the T cell survival defect in *duan* mice. The lower IL-7R expression could contribute to the survival defect seen in mutant CD8 T cells. The proliferation of *Senp2*$^{dua/dua}$ CD8 T cell is normal upon influenza virus challenge while long-term memory CD8 T cells fail to persistence.

Dockland mutation has been generated through ENU-mutagenesis screening of splenocytes. The DOCK2 mutant strain has T and B cell lymphopenia with absence of marginal zone B cells. The phenotypes of *Dockland* mice match to the DOCK2 knockout mice. *Dock2*$^{doc/doc}$ CD8 T cells have a cell-intrinsic defect in

50:50 mix bone marrow experiment. The significance of how the mutation affects the CD8 T cell cytotoxic function has not been studied.

Dockland and *duan* are two different examples of mutations that affect the survival or function of CD8 T cells. DOCK2 works downstream of various receptors and affect different pathways in different type of cells. On the other hand, SENP2 has been shown to have a restricted effect only on CD8 T cells. Both mutations could help us to understand the complexity of pathways regulating CD8 T cells.

With the help of high-throughput next generation sequencing, more novel genes involved in regulating of the immune system could be discovered. Understanding of their roles may help us to understand many immune disorders and also to generate new therapeutics.

Chapter 7: References

Alfonso, C., Mcheyzer-Williams, M.G. and Rosen, H. (2006) CD69 down-modulation and inhibition of thymic egress by short- and long-term selective chemical agonism of sphingosine 1-phosphate receptors. European Journal of Immunology *36*: 149-159

Allende, M.L., Dreier, J.L., Mandala, S. and Proia, R.L. (2004) Expression of the sphingosine 1-phosphate receptor, S1P1, on T-cells controls thymic emigration. The Journal of Biological Chemistry *279*: 15396-15401

Almeida, A.R., Rocha, B., Freitas, A.A., and Tanchot, C. (2005) Homeostasis of T cell numbers: From thymus production to peripheral compartmentalization and the indexation of regulatory T cells. Seminars in Immunology *17*: 239-249

Anderson, D.M., Kumaki, S., Ahdieh, M., Bertles, J., Tometsko, M., Loomis, A., Giri, J., Copeland, N.G., Gilbert, D.J., Jenkins, N.A., Valentine, V., Shapiro, D.N., Morris, S.W., Park, L.S., and Cosman, D. (1995) Functional characterization of the human interleukin-15 receptor α chain and close linkage of IL15RA and IL2RA genes. The Journal of Biological Chemistry *270*: 29862-29869

Arnon, T.I., and Cyster, J.G. (2014) Blood, sphingosine-1-phosphate and lymphocyte migration dynamics in the spleen. Current topics in microbiology and immunology *378*: 107-128

Asao, H., Okuyama, C., Kumaki, S., Ishii, N., Tsuchiya, S., Foster, D., and Sugamura, K. (2001) The common γ-chain is an indispensable subunit of the IL-21 receptor complex. The Journal of Immunology *167*: 1-5

Babbitt, B.P., Allen, P.M., Matsueda, G., Haber, E., and Unanue, E.R. (1985) Binding of immunogenic peptides to Ia histocompatibility molecules. Nature *317*: 359-361

Bankovich, A.J., Shiow, L.R. and Cyster, J.G. (2010) CD69 supresses sphingosine 1-phosophate receptor-1 (S1P1) function through interaction with membrane helix 4. The Journal of Biological Chemistry *285*: 22328-22337

Bayer, P., Arndt, A., Metzger, S., Mahajan, R., Melchior, F., Jaenicke, R., and Becker, J. (1998) Structure determination of the small ubiquitin-related modifier SUMO-1. Journal of Molecular Biology *280*: 275-286

Beier, D.R. (2000) Sequence-based analysis of mutagenized mice. Mammalian Genome *11*: 594-597

Bell, E.B., and Sparshott, S.M. (1997) The peripheral T-cell pool: regulation by non-antigen induced proliferation? Seminars in Immunology *9*:347-353

Benoist, C., and Mathis, D. (2001) T lymphocytes need IL-7 but not IL-4 or IL-6 to survive in vivo. International Immunology *13*: 763-768

Bertram, E.M., Dawicki, W., and Watts, T.H. (2004) Role of T cell costimulation in anti-viral immunity. Seminars in Immunology *16*: 185-196

Beutner, U., and MacDonald, H.R. (1998) TCR-MHC class II interation is required for peripheral expansion of CD4 cells in a T cell-deficient host. International Immunology 10: 305-310

Bjorkman, P.J., Saper, M.A., Samraoui, B., Bennett, W.S., Strominger, J.L., and Wiley, D.C. (1987) Structure of the human class I histocompatibility antigen, HLA-A2. Nature *329*: 506-512

Bjorkman, P.J., Saper, M.A., Samraoui, B., Bennett, W.S., Strominger, J.L., and Wiley, D.C. (1987) The foreign antigen binding site and T cell recognition regions of class I histocompatibility antigens. Nature *329*: 512-518

Blanco, P., Palucka, A.K., Gill, M., Pascual, V. and Banchereau, J. (2001) Induction of dendritic cell differentiation by IFN-α in systemic lupus erythematosus. Science *294*: 1540-1543

Boise, L.H., Minn, A.J., June, C.H., Lindsten, T., and Thompson, C.B. (1995) Growth factors can enhance lymphocyte survival without committing the cell to undergo cell division. Proceedings of the National Academy of Sciences of the United states of Amierica *92*: 5491–5495.

Bouneaud, C., Garcia, Z., Kourilsky, P., and Pannetier, C. (2005) Lineage relationships, homeostasis, and recall capacities of central- and effector-memory CD8 T cells in vivo. The Journal of Experimental Medicine *201*: 579-590

Brinkmann, V., Davis, M.D., Heise, C.E., Albert, R., Cottens, S., Hof, R., Bruns, C., Preschl, E., Baumruker, T., Hiestand, P., Foster, C.A., Zollinger, M., and Lynch, K.R. (2002) The immune modulator FTY720 targets sphingosine 1-phosphate receptors. The Journal of Biological Chemistry *277*: 21453-21437

Brown, E., Mashayekhi, M., Markiewicz, M., Alegre, M. L., and Gajewski, T. F. (2005) Peripheral survival of naïve $CD8^+$ T cells. Apoptosis *10*: 5-11

Cao, X., Shores, E.W., Hu-Li, J., Anver, M.R., Kelsall, B.L., Russel, S.M., Drago, J., Noguchi, M., Grinberg, A., Bloom, E.T., Paul, W.E., Katz, S.I., Love, P.E., and Leonard, W.J. (1995) Defective lymphoid development in mice lacking expression of the common cytokine receptor γ chain. Immunity *2*: 223-238

Carbone, F.R. (2015) Tissue-Resident memory T cells and fixed immune surveillance in nonlymphoid organs. The Journal of Immunology *195*: 17-22

Carrette, F., and Surh, C.D. (2012) IL-7 signaling and CD127 receptor regulation in the control of T cell homeostasis. Seminars in Immunology *24*: 209-217

Chen, A., Mannen, H., and Li, S.S. (1998) Characterization of mouse ubiquitin-like SMT3A and SMT3B cDNAs and gene/pseudogenes. Biochemistry and Molecular Biology International *46*: 1161-1174

Chiu, S.Y., Asai, N., Costantini, F. and Hsu, W. (2008) SUMO-Specific protease 2 is essential for modulating p53-Mdm2 in development of trophoblast stem cell niches and lineages. PLoS Biology *6*: e310

Cho, V., Mei, Y., Sanny, A., Chan, S., Enders, A., Bertram, E., Tan, A., Goodnow, C.C., and Andrews, T.D. (2014) The RNA-binding protein hnRNPLL induces a T cell alternative splicing program delineated by differential intron retention in polyadenylated RNA. Genome Biology *15*: R26

Clarke, S. R., and Rudensky, A. Y. (2000) Survival and homeostatic proliferation of naive peripheral CD4+ T cells in the absence of self peptide:MHC complexes. The Journal of Immunology *165*: 2458-2464

Coghill, E.L., Hugill, A., Parkinson, N., Davison, C., Glenister, P., Clements, S., Hunter, J., Cox, R.D., and Brown, S.D.M. (2002). A gene-driven approach to the identification of ENU mutants in the mouse. Nature Genetics *30*: 255-256.

Collins, A., Littman, D.R., and Taniuchi, I. (2009) RUNX proteins in transcription factor networks that regulate T-cell lineage choice. Nature Reviews Immunology *9*: 106-115

Cote, J.F., and Vuori, K. (2007) GEF what? DOCK180 and related proteins help Rac to polarize cells in new ways. Trends in Cell Biology *17*:383-393

Coom, H.A., Denton, A.E., Valkenburg, S.A., Swan, N.G., Olson, M.R., Turner, S.J., Doherty, P.C., and Kedzierska, K. (2011) Memory precursor phenotype of CD8+ T cells reflects early antigenic experience rather than memory numbers in a model of localized acute influenza infection. European Journal of Immunology *41*:

682-693

Cui, W., Liu, Y., Weinstein, J.S., Craft, J., and Kaech, S.M. (2011) An interleukin-21-interleukin-10-STAT3 pathway is critical for functional maturation of memory CD8+ T cells. Immunity *35*: 792-805

Curtsinger, J.M., Schmidt, C.S., Mondino, A., Lins, D.C., Kedl, R.M., Jenkins, M.K., and Mescher, M.F. (1998) Inflammatory cytokines provide a third signal for actiation of naïve CD4+ and CD8+ T cells. The Journal of Immunology *162*: 3256-3262

Cyster, J.G. (2005) Chemokines, Sphingosine-1-Phosphate, and cell migration in secondary lymphoid organs. Annual Review of Immunology *23*:127-159

Dagvadorj, A., Tan, S.H., Liao, Z., Xie, J., Nurmi, M., Alanen, K., Rui, H., Mirtti, T., and Nevalainen, M.T. (2010) N-terminal truncation of Stat5a/b circumvents PIAS3-mediated transcriptional inhibition of Stat5 in prostate cancer cells. The International Journal of Biochemistry& Cell Biology *42*:2037-2046

Daley, S.R., Hu, D.Y., and Goodnow, C.C. (2013) Helios marks strongly autoreactive CD4+ T cells in two major waves of thymic deletion distinguished by induction of PD01 of NF-kB. The Journal of Experimental Medicine 210: 269-285

Davis, M.M., and Bjorkman, P.J. (1988). T-cell antigen receptor genes and T-cell recognition. Nature *334*: 395-402.

Desterro, J.M., Rodriguez, M.S., Kemp, G.D., and Hay R.T. (1999) Identification of the enzyme required for activation of the small ubiquitin-like protein SUMO-1. Journal of Biological Chemistry *274*: 10618-10624

Desterro, J.M., Thomson, J., and Hay, R.T. (1997) Ubch9 conjugates SUMO but

not ubiquitin. FEBS letters *417*: 297-300

Di Santo, J.P., and Rodewald, H.R. (1998) In vivo roles of receptor tyrosine kinases and cytokine receptors in early thymocyte development. Current Opinion in Immunology *10*: 196-207

Dobbs, K., Dominguez Conde, C., Zhang, S.Y., Parolini, S., Audry, M., Chou, J., Haapaniemi, E., Keles, S., Bilic, I., Okada, S., Massaad, M.J., Rounioja, S., Alwahadneh, A.M., Serwas, N.K., Capuder, K., Ciftci, E., Felgentreff, K., Ohsumi, T.K., Pedergnana, V., Boisson, B., Haskologlu, S., Ensari, A., Schuster, M., Moretta, A., Itan, Y., Patrizi, O., Rozenberg, F., lebon, P., Saarela, J., Knip, M., Petrovski, S., Goldstein, D.B., Parrott, R.E., Savas, B., Schambach, A., Tabellini, G., Bock, C., Chatila, T.A., Comeau, A.M., Geha, R.S., Abel, L., Buckley, R.H., Ikinciogullari, A., Al-Herz, W., Helminen, M., Dogu, F., Casanova, J.L., Boztug, K., and Notarangelo, L.D. (2015) Inherited DOCK2 deficiency in patients with early-onset invasive infections. The New England Journal of Medicine *372*: 2409-2422

Dorfman, J.R., Stefanova, I., Yasutomo, K., and Germain, R.N. (2000). CD4+ T cells survival is not directly linked to self-MHC-induced TCR signaling. Nature Immunology *1*: 329-335.

Egawa, T. (2009) RUNX and ThPOK: A balancing act to regulate thymocyte lineage commitment. Journal of Cellular Biochemistry *107*: 1037-1045

Ernst, B., Lee, D.S., Chang, J.M., Sprent, J., and Surh, C.D. (1999) The peptide ligands mediating positive selection in the thymus control T cell survival and homeostatic proliferation in the periphery. Immunity *11*: 173-181

Feng, C., Woodside, K.J., Vance, B.A., El-Khoury, D., Canelles, M., Lee, J., Gress, R., Fowlkes, B.J., Shores, E.W. and Love, P.E. (2002) A potential role for CD69 in thymocyte emigration. International Immunology *14*: 535-544

Foxwell, B.J., Beadling, C., Guschin, D., Kerr, I., and Cantrell, D. (1995). Interleukin-7 can induce the activation of Jak1, Jak3 and STAT5 proteins in murine T cells. European Journal of Immunology *25*: 3041-3046

Freitas, A.A., and Rocha, B.B. (1993) Lymphocyte lifespans: homeostasis, selection and competition. Immunology today *14*: 25-29

Freitas, A.A., and Rocha, B. (2000) Population biology of lymphocytes: The flight for survival. Annual Review of Immunology *18*: 83-111

Fry, T.J., Connick, E., Falloon, J., Lederman, M.M., Liewehr, D.J., Spritzler, J., Steinberg, S.M., Wood, L.V., Yarchoan, R., Zuckerman, J., Landay, A., and Mackall, C.L. (2001) A potential role for interleukin-7 in T-cell homeostasis. Blood *97*: 2983-2990

Gebhardt, T., Wakim, L.M., Eidsmo, L., Reading, P.C., Heath, W.R., and Carbone, F.R. (2009) Memory T cells in nonlymphoid tissue that proved enhanced local immunity during infection with herpes simplex virus. Nature Immunology *10*: 524-530

Gilks, C.B., Bear, S.E., Grimes, H.L., and Tsichlis, P.N. (1993) Progression of interleukin-2 (IL-2)-dependent rat T cell lymphoma lines to IL-2-independent growth following activation of a gene (Gfi-1) encoding a novel zinc finger protein. Molecular and Cellular Biology *13*: 1759-1768

Giri, J.G., Ahdleh, M., Eisenman, J., Sharnebeck, K., Grabstein, K., Kumaki, S., Namen, A., Park, L.S., Cosman, D., and Anderson, D. (1994). Utilization of the β and γ chains of the IL-2 receptor by the novel cytokine IL-25. The EMBO Journal *13*:2822-2830

Giri, J. G., Kumaki, S., Ahdieh, M., Friend, D.J., Loomis, A., Shanebeck, K., DuBose, R., Cosman, D., Park, L.S., and Anderson, D.M. (1995) Identification

and cloning of a novel IL-15 binding protein that is structurally related to the α chain of the IL-2 receptor. The EMBO Journal *14*: 3654-3663

Gottschalk, R.A., Corse, E., and Allison, J.P. (2012) Expression of Helios in peripherally induced Foxp3+ regulatory T cells. The Journal of immunology *188*: 976-980

Grabstein, K. H., Eisenman, J., Shanebeck, K., Rauch, C., Srinivasan, S., Fung, V., Beers, C., Richardson, J., Schoenborn, M.A., Ahdieh, M., Johnson, L., Alderson, M.R., Watson, J.D., Anderson, D.M., and Giri, J.G. (1994) Cloning of a T cell growth factor that interacts with the β chain of the interleukin-2 receptor. Science *264*: 965-968

Godfrey, D.I., Kennedy, J., Suda, T., and Zlotnik, A. (1993). A developmental pathway
involving four phenotypically and functionally distinct subsets of CD3-CD4-CD8-
triple-negative adult mouse thymocytes defined by CD44 and CD25 expression. The Journal of Immunology *150*, 4244-4252.

Godfrey, D.I., and Zlotnik, A. (1993) Control points in early T-cell development. Immunology Today *14*: 547-553

Goldrath, A.W., and Bevan, M.J. (1999) Low-affinity ligands for the TCR drive proliferation of mature CD8+ T cells in lymphopenic host. Immunity *11*: 183-190

Goldrath, A.W., Bogatzki, L.Y., and Bevan, M.J. (1999) Naïve T cells transiently acquire a memory-like phenotype during homeostasis-driven proliferation. The Journal of Experimental Medicine *192*: 557-564

Gong, L., and Yeh, E.T.H (2006) Characterization of a family of nucleolar SUMO-specific proteases with preference for SUMO-2 or SUMO-3. The Journal of Biological Chemistry *281*:15869-15877

Gong, L., Li, B., Millas, S., and Yeh, E.T. (1999) Molecular cloning and characterization of human AOS1 and UBA2, components of the sentrin-activating enzyme complex. FEBS letters *448*: 185-189

Gong, L., Millas, G., Maul, G., and Yeh, E.T.H (2000) Differential regulation of sentrinized proteins by a sentrin-specific protease. Journal of Biological Chemistry *275*: 3355-3359

Gonzalo, J.A., Delaney, T., Corcoran, J., Goodearl, A., Gutierrez-Ramos, J.C., and Coyle, A.J. (2001) Cutting edge: the related molecules CD28 and inducible costimulator deliver both unique and complementary signals required for optimal T cell activation. The Journal of Immunology *166*: 1-5

Grandjean, I., Duban, L., Bonney, E.A., Corcuff, E., Di Santo, J.P., Matzinger, P., and Lantz, O. (2003). Are major histocompatibility complex molecules involved in the survival of naive CD4+ T cells? The Journal of Experimental Medicine *198*: 1089-1102

Grimes, H.L., Chan, T.O., Zweidler-McKay, P.A., Tong, B., and Tsichlis, P.N. (1996) The Gfi-1 proto-oncoprotein contains a novel transcriptional repressor domain SNAG, and inhibits G1 arrest induced by interleukin-2 withdrawal. Molecular and Cellular Biology *16*: 6263-6272

Haluszczak, C., Akue, A.D., Hamilton, S.E., Johnson, L.D.S., Pujanauski, L., Teodorovic, L., Jameson, S.C., and Kedl, R.M. (2009) The antigen-specific CD8+ T cell repertoire in unimmunized mice includes memory phenotype cells bearing markers of homeostatic expansion. The Journal of Experimental Medicine *206*: 435-448

Hataye, J., Moon, J.J., Khoruts, A., Reilly, C. and Jenkins, M.K. (2006) Naïve and memory CD4+ T cell survival controlled by clonal abundance. Science *312*: 114-

He, Y.W., and Malek, T.R. (1996) Interleukin-7 receptor alpha is essential for the development of gamma delta+ T cells, but not nature killer cells. The Journal of Experimental Medicine 184: 289-293

He, X., He, X., Dave, V.P., Zhang, Y., Hua, X., Nicolas, E., Xu, W., Roe, B.A., and Kappes, D.J. (2005) Nature *433*: 826-833

Hershko, A., and Ciechanover, A. (1998) The ubiquitin system. Annual Review of Biochemistry *67*: 425-479

Hla, T., and Maciag, T. (1990) An abundant transcript induced in differentiation human endothelial cells encodes a polypeptide with structural similarities to G-protein-coupled receptors. The Journal of Biological Chemistry *265*: 9308-9313

Im, D.S.*,* Heise, C.E.*,* Ancellin, N.*,* O'Dowd, B.F.*,* Shei, G.J.*,* Heavens, R.P.*,* Rigby, M.R.*,* Hla, T.*,* Mandala, S.*,* McAllister, G.*,* George, S.R.*, and* Lynch, K.R. *(*2000*)* Characterization of a novel sphingosine 1-phosphate receptor, EDG-8. *The* Journal of Biological Chemistry *275:*14281–14286

Itahana, P., Yeh, E.T.H., and Zhang, Y. (2006) Nucleocytoplasmic shuttling modulates activity and ubiquitination-dependent turnover of SUMO-specific protease 2. Molecular and cellular biology *26*: 4675-4689

Jameson, S.C. (2002) Maintaining the norm: T-cell homeostasis. Nature Reviews Immunology *2*: 547-556

Jafar-Nejad, H., and Bellen, H.J. (2004) Gfi/Pag-3/senseless zinc finger proteins: a unifying theme? Molecular and Cellular Biology *24*: 8803-8812

Jenkins,M.R., Webby, R., Doherty, P.C., and Turner, S.J. (2006) Addition of a prominent epitope affects Influenza A virus-specific CD8+ T cell immunodominance hierarchies when antigen is limiting. The Journal of Immunology *177*: 2917-2925

Jiang, Q., Li, W.Q., Aiello, F.B., Mazzucchelli, R., Asefa, B., Khaled, A.R., and Durum, S. K. (2005) Cell biology of IL-7, a key lymphotrophin. Cytokine Growth Factor Reviews *16*:513-533

Johnson, E.S., and Blobel, G. (1997) Ubc9p is the conjugating enzyme for the ubiquitin-like protein Smt3p. Journal of Biological Chemistry *272*: 26799-26802

Johnson, E.S., and Gupta, A.A. (2001) An E3-like factor that promotes SUMO conjugation to the yeast septins. Cell *106*: 735-744

Johnson, E.S., Schwienhorst, I., Dohmen, R.J., and Blobel, G. (1997) The ubiquitin-like protein Smt3p is activated for conjugation to other proteins by an Aos1p/Uba2p heterodimer. The EMBO Journal *16*: 5509-5519

Joshi, N.S., Cui, W., Chandele, A., Lee, H.K., Urso, D.R., Hagman, J., Gapin, L., and Kaech, S.M. (2007) Inflammation directs memory precursor and short-lived effector CD8+ T cell fates via the graded expression of T-bet transcription factor. Immunity *27*: 281-295

Joshi, N.S., and Kaech, S.M. (2008) Effector CD8 T cell development: a balancing act between memory cell potential and terminal differentiation. Journal of Immunology *180*: 1309-1315

Kaech, S.M., Tan, J.T., Wherry, E.J., Konieczny, B.T., Surh, C.D., and Ahmed, R. (2003) Selective expression of the interleukin 7 receptor identifies effector CD8 T cells that give rise to long-lived memory cells. Nature Immunology *4*:1191-1198

Kaech, S.M., and Wherry, E.J. (2007) Heterogeneity and cell-fate decisions in effector and memory CD8+ T cells differentiation during viral infection. Immunity *27*: 393-405

Kang, X., Qi, Y., Zuo, Y., Wang, Q., Zou, Y., Schwartz, R.J., Cheng, J., and Yeh, E.T.H. (2010) SUMO-Specific protease 2 is essential for suppression of polycomb group proteins mediated gene silencing during embryonic development. Molecular Cell *38*:157-159

Kappes, D.J., He, X., and He, X. (2006) Role of the transcription factor Th-POK in CD4:CD8 lineage commitment. Immunological Reviews *209*: 237-252

Kieper, W.C., Burghardt, J.T., and Surh, C.D. (2004) A role for TCR affinity in regulating naïve T cell homeostasis. The Journal of Immunology *172*: 40-44

Kieper, W.C., and Jameson, S.C. (1999) Homeostatic expansion and phenotypic conversion of naïve T cells in response to self peptide/MHC ligands. Proceedings of the National Academy of Science of the United States of America *96*: 13306-13311

Kirberg, J., Berns, A. and Von Boehmer, H. (1997). Peripheral T cell survival requires continual ligation of the T cell receptor to major histocompatibility complex-encoded molecules. The Journal of experimental Medicine *186*: 1269-1275

Kondo, M., Takeshita, T., Ishii, N., Nakamura, M., Watanabe, S., Arai, K., and Sugamura, K. (1993). Sharing of the interleukin-2 (IL-2) receptor γ chain between receptors for IL-2 and IL-4. Science *262*: 1874-1877

Labrecque, N., Whitfield, L.S., Obst, R., Waltzinger, C., Benoist, C. and Mathis, D. (2001) How much TCR does a T cell need? Immunity *15*: 71-82

Lande, R., Gregorio, J., Facchinetti, V., Chatterjee, B., Wang, Y., Homey, B., Cao, W., Wang, Y., Su, B., Nestle, F.O., Zal, T., Mellman, I., Schroder, J., Liu, Y. and Gilliet, M. Plasmacytoid dendritic cells sense self-DNA coupled with antimicrobial peptide. Nature *449*: 564-569

Lantz, O., Grandjean, I., Matzinger, P., and Di Santo, J.P. (2000) γ chain required for naïve CD4+ T cell survival but not for antigen proliferation. Nature Immunology 1: 54-58

Lau, L.L., Jamieson, B.D., Somasundaram, T., Ahmed, R. (1994) Cytotoxic T-cell memory without antigen. Nature *369*: 648-652

Lee, G.W., Melchior, F., Matunis, M.J., Mahajan, R., Tian, Q., and Anderson, P. (1998) Modification of Ran GTPase-activating protein by the small ubiquitin-related modifier SUMO-1 requires Ubc9, an E2-type ubiquitin-conjugating enzyme homologue. Journal of Biological Chemistry *273*: 6503-6507

Ligons, D.L., Tuncer, C., Linowes, B.A., Akcay, I.M., Kurtulus, S., Deniz, E., Atasever Arslan, B., Cevik, S.I., Keller, H.R., Luckey, M.A., Feigenbaum, L., Moroy, T., Erasahin, T., Atalay, R., Erman, B., and Park, J.H. (2012) CD8-lineage-specific regulation of interleukin-7 receptor expression by the transcriptional repressor Gfi1. The Journal of Biological Chemistry *287*: 34386-34399

Lima, C.D., and Reverter, D. (2008) Structure of the human SENP7 catalytic domain and poly-SUMO deconjugation activities for SENP6 and SENP7. The Journal of Biological Chemistry *283*: 32045-32055

Macchi, P., Villa, A., Giliani, S., Sacco, M.G., Frattini, A., Porta, F., Ugazio, A.G., Johnston, J.A., Candotti, F., O'Shea, J.J., Vezzoni, P., and Notarangelo, L.D. (1995) Mutations of Jak-3 gene in patients with autosomal severe combined

immune deficiency (SCID). Nature *377*: 65-68

Mahajan, R., Delphin, C., Guan, T., Gerace, L., and Melchior, F. (1997) A small ubiquitin-related polypeptide involved in targeting RanGAP1 to nuclear pore complex protein RanBP2. Cell *88*: 97-107

Mannen, H., Tseng, H.M., Cho, C.L., and Li S.S. (1996) Cloning and expression of human homolog HSMT3 to yeast SMT3 suppressor of MIF mutations in a centromere protein gene. Biochemical and Biophysical Research Communications *222*: 178-180

Marchingo, J.M., Kan, A., Sutherland, R.M., Duffy, K.R., Wellard, C.J., Belz, G.T., Lew, A.M., Dowling, M.R., Heinzel, S. and Hodgkin, P.D. (2014) Antigen affinity, costimulation, and cytokine inputs sum linearly to amplify T cell expansion. Science *346*: 1123-1127

Masopust, D., Vezys, V., Marzo, A.L., and Lefrancois, L. (2001) Preferential localization of effector memory cells in nonlymphoid tissue. Science *291*: 2413-2417

Matunis, M.J., Coutavas, E., and Blobel, G. (1996) A novel ubiquitin-like modification modulates the partitioning of the Ran-GTPase-activating protein RanGAP1 between the cytosol and the nuclear pore complex. The Journal of Cell Biology *135*: 1457-1470

Mazo, I.B., Honczarenko, M., Leung, H., Cavanagh, L.L., Bonasio, R., Weninger, W., Engelke, K., Xia, L., McEver, R.P., Koni, P.A., Silberstein, L.E., and Von Andrian, U.H. (2005) Bone marrow is a major reservoir and site of recruitment for central memory CD8+ T cells. Immunity *22*: 259-270

Mazzucchelli, R. and Durum, S.K. (2007) Interleukin-7 receptor expression: intelligent design. Nature Reviews Immunology *7*:144-154

Meller, N., Merlot, S., and Guda, C. (2005) CZH proteins: a new family of Rho-GEFs. Journal of Cell Science *118*:4937-4946

Meluh, P.B., and Koshland, D. (1995) Evidence that the MIF2 gene of *Saccharomyces cerevisiae* encodes a centromere protein with homology to the mammalian centromere protein CENP-C. Molecular Biology of The Cell *6*: 793-807

Miller, J.F. (1959). Role of the thymus in murine leukaemia. Nature *183*: 1069.

Miller, J.F. (1961). Immunological function of the thymus. Lancet *2*: 748-749.

Min, B., McHugh, R., Sempowski, G.D., Mackall, C., Foucras, G., and Paul, W.E. (2003) Neonates support lymphopenia-induced proliferation. Immunity *18*: 131-140

Mombaerts, P., Iacomini, J., Johnson, R.S., Herrup, K., Tonegawa, S., and Papaioannou, V.E. (1992) RAG-1-deficient mice have no mature B and T lymphocytes. Cell *68*: 869-877

Moon, J.J., Chu, H.H., Pepper, M., McSorley, S.J., Jameson, S.C., Kedl, R.M. and Jenkins, M.K. (2007) Naïve CD4(+) T cell frequency varies for different epitopes and predicts repertoire diversity and response magnitude. Immunity *27*: 203-213

Moroy, T., and Khandanpour, C. (2011) Growth factor independence 1 (Gfi1) as a regulator of lymphocyte development and activation. Seminars in Immunology *23*: 368-378

Moses, C.T., Thorstenson, K.M., Jameson, S.C., and Khoruts, A. (2003) Competition for self ligands restrains homeostatic proliferation of naïve CD4 T cells. Proceedings of the National Academy of Science of the United States of

America *100*: 1185-1190

Mosley, C.J. March, D. Urdal, S. Gillis, et al. 1988. Stimulation of B-cell progenitors by cloned murine interleukin-7. Nature *333*:571-573.

Munitic, I., Williams, J.A., Yang, Y., Dong, B., Lucas, P.J., El Kassar, N., Gress, R.E., and Ashwell, J.D. (2004) Dynamic regulation of IL-7 receptor expression is required for normal thymopoiesis. Blood *104*: 4165-4172

Murali-Krishna, K., Lau, L.L., Sambhara, S., Lemonnier, F., Altman, J., and Ahmed, R. (1999) Persistence of memory CD8 T cells in MHC class I-deficient mice. Science *286*: 1377-1381

Nagafuku, M., Okuyama, K., Onimaru, Y., Suzuki, A., Odagiri, Y., Yamashita, T., Iwasaki, K., Fujiwara, M., Takayanagi, M., Ohno, I., and Inokuchi, J. (2011) CD4 and CD8 T cells require different membrane gangliosides for activation. PNAS 109: 336-342

Nakayama, T., Kasprowivz, D.J., Yamashita, M., Schubert, L.A., Gillard, G., Kimura, M., Didierlaurent, A., Koseki, H. and Ziegler, S.F. (2002) The generation of mature, single-positive thymocytes in vivo is dysregulated by CD69 blockade or overexpression. The Journal of Immunology *168*: 87-94

Namen, A.E., S. Lupton, K. Hjerrild, J. Wignall, D.Y. Mochizuki, A. Schmierer, B., Nesic, D. and Vukmanovic, S. 1998 MHC class I is required for peripheral accumulation of $CD8^+$ thymic emigrants. The Journal of Immunology *160*: 3705-3712

Nesic, D., and Vukmanovic, S. (1998) MHC Class I is required for peripheral accumulation of CD8+ thymic emigrants. The Journal of Immunology *160*: 3705-3712

Nestle, F.O., Conrad, C., Tun-kyi, A., Homey, B., Gombert, M., Boyman, O., Burg, G., Liu, Y. and Gilliet, M. (2005) Plasmacytoid predendritic cells initiate psoriasis through interferon-α production. The Journal of Experimental Medicine *202*: 135-143

Nishikimi, A., Kukimoto-Niino, M., Yokoyama, S., and Fukui, Y. (2013) Immune regulatory functions of DOCK family proteins in health and disease. Experimental Cell Research *319*: 2343-2349

Noguchi, M., Nakamura, Y., Russel, S.M., Ziegler, S.F., Tsang, M., Cao, X., and Leonard, W.J. (1993). Interleukin-2 receptor γ chain: a functional component of the interleukin-7 receptor. Science *262*: 1877-1880

Noguchi, M., Yi, H., Rosenblatt, H.M., Filipovich, A.H., Adelstein, S., Modi, W.S., McBride, O.W., Leonard, W.J. (1993) Interleukin-2 receptor chain mutation results in X-linked severe combined immunodeficiency in humans. Cell *73*:147-157

Nombela-Arrieta, C., Mempel, T.R., Soriano, S.F., Mazo, I., Wymann, M.P., Hirsch, E., Martinez-A, C., Fukui, Y., von Andrian, U.H., and Stein, J.V. (2007) A central role for DOCK2 during interstitial lymphocyte motility and sphingosine-1-phosphate-mediated egress. The Journal of Experimental Medicine *204*: 497-510

Obar, J.J., Khanna, K.M. and Lefrancois, L. (2008) Endogenous naïve CD8+ T cell precursor frequency regulates primary and memory responses to infection. Immunity *28*: 859-869

Obar, J.J., Jellison, E.R., Sheridan, B.S., Blair, D.A., Pham, Q.M., Zickovich, J.M., and Lefrancois, L. (2011) Pathogen-induced inflammatory environment controls effector and memory CD8+ T cell differentiation. Journal of Immunology *187*: 4967-4978

Okazaki, H., Ishizaka, N., Sakurai, T., Kurokawa, K., Goto, K., Kumada, M., Takuwa, Y. (1993) Molecular cloning of a novel putative G protein-coupled receptor expressed in the cardiovascular system. Biochemical and Biophysical Research Communications *190:* 1104-1109

Okuma, T., Honda, R., Ichikawa, G., Tsumagari, N., and Yasuda, H. (1999) In vitro SUMO-1 modification requires two enzymatic steps, E1 and E2. Biochemical and Biophysical Research Communications *254*: 693-698

Okura, T., Gong, L., Kamitani, T., Wada, T., Okura, I., Wei, C.F., Chang, H.M., and Yeh, E.T. (1996) Protection against Fas/APO-1 and tumor necrosis factor-mediated cell death by a novel protein, sentrin. The Journal of Immunology *157*: 4277-4281

Pante, N., Bastos, R., McMorrow, I., Burke, B., and Aebi, U. (1994) Interactions and three-dimensional localization of a group of nuclear pore complex proteins. The Journal of cell biology *126*: 603-617

Park, L.S., Friend, D.J., Schmierer, A.E., Dower, S.K., and Namen, A.E. (1990) Murine interleukin 7 (IL-7) receptor. Characterization on an IL-7-dependent cell line. The Journal of Experimental Medicine *171*:1073-1089

Park, J.H., Adoro, S., Lucas, P.J., Sarafova, S.D., Alag, A.S., Doan, L.L, Erman, B., Liu, X., Ellmeier, W., Bosselut, R., Feigenbaum, L., and Singer, A. (2007) 'Coreceptor tuning': cytokine signals transcriptionally tailor CD8 coreceptor expression to the self-specificity of the TCR. Nature Immunology *8*:1049-1059

Park, J.H., Yu, Q., Erman, B., Appelbaum, J.S., Montoya-Durango, D., Grimes,H.L., and Singer, A. (2004) Suppression of IL7Rα transcription by IL-7 and other prosurvival cytokines: a novel mechanism for maximizing IL-7-Dependent T cell surivival. Immunity *21*:289-302

Peschon, J.J., Morrissey, P.J., Grabstein, K.H., Ramsdell, F.J., Maraskovesky, E., Gliniak, B.C., Park, L.S., Ziegler, S.F., Williams, D.E., Ware, C.B., Meyer, J.D., Davison, B.L. (1994) Early lymphocyte expansion is severely impaired in interleukin 7 receptor-deficient mice. The Journal of Experimental Medicine 180: 1955-1960

Polic, B., Kunkel, D., Scheffold, A., and Rajewsky, K. 2001 How αβ T cells deal with induced TCRα ablation. Proceedings of the National Academy of Science of the United States of America *98*:15 8744-8749

Puel, A., Ziegler, S.F., Buckley, R.H., and Leonard, W.J. (1998) Defective IL7R expression in T-B+NK+ severe combined immunodeficiency. Nature Genetics. 20: 394-397

Rabellino, A., Andreani, C., and Scaglioni, P.P. (2017) The role of PIAS SUMO E3-ligases in cancer. American Association for Cancer Research *77*: 1542-1547

Radtke, F., Wilson, A., Stark, G., Bauer, M., Van Meerwijk, J., MacDonald, H.R., and Aguet, M. (1999) Deficient T cell fate specification in mice with an induced inactivation of *Notch 1*. Immunity *10*: 547-558

Randall, K.L., Chan, S. Y., Ma, C.S., Fung, I., Mei, Y., Yabas, M., Tan, A., Arkwright, P.D., Wafaa al Suwairi., Saul Oswaldo Lugo Reyes, Yamazaki-Nakashimada, M.A., Maria de la Luz Garcia-Cruz, Smart, J.M., Picard, C., Okada, S., Jouanguy, E., Jean-Laurent Casanova., Lambe, T., Cornall, R.J., Russell, S., Oliaro, J.,Tangye, S.G., Bertram, E.M., and Goodnow, C.C. (2011). DOCK8 deficiency impairs CD8 T cell survival and function in human and mice. The Journal of experimental medicine *208*: 2305-2020

Rathmell, J. C., Farkash, E.A., Gao, W., and Thompson, C.B. (2001) IL-7 enhances the survival and maintains the size of naive T cells. The Journal of Immunology *167*: 6869- 6876

Reif, K., and Cyster, J.G. (2002) The CDM protein DOCK2 in lymphocyte migration. Trends in Cell Biology *12*: 368-373

Russell, S.M., Keegan, A.D., Harada, N., Nakamura, Y., Noguchi, M., Leland, P., Friedmann, M.C., Miyajima, A., Puri, R.K., Paul, W.E., and Leonard, W.J. (1993). Interleukin-2 receptor γ chain: a functional component of the interleukin-4 receptor. Science *262*:1880-1883

Russell, S.M., Tayebi, N., Nakajima, H., Riedy, M.C., Roberts, J.L., Aman, M.J., Migone, T.S., Noguchi, M., Markert, M.L., Buckley, R.H., O'Shea, J.J., and Leonard, W.J. (1995) Mutation of Jak3 in a patient with SCID: essential role of Jak3 in lymphoid development. Science 270: 797-799

Rycyzyn, M.A. and Clevenger, C.V. (2002) The intranuclear prolactin/cyclophilin B complex as a transcriptional inducer. Proceedings of the National Academy of Sciences of the United states of Amierica *99*: 6790-6795

Sallusto, F., Lenig, D., Forster, R., Lipp, M., and Lanzavecchia, A. (1999) Two subsets of memory T lymphocytes with distinct homing potentials and effector functions. Nature *401*: 708-712

Sarkar, S., Kalia, V., Haining, W.N., Konieczny, B.T., Subramaniam, S., and Ahmed, R. (2008) Functional and genomic profiling of effector CD8 T cell subsets with distinct memory fates. The Journal of Experimental Medicine *205*: 625-640

Samaridis, J., Casorati, G., Traunecker, A., Iglesias, A., Gutierrez, J.C., Muller, U., and Palacios, R. (1991). Development of lymphocytes in interleukin 7-

transgenic mice. European Journal of Immunology *21*:453-460

Schluns, K.S., Kieper, W.C., Jameson, S.C. and Lefrancois, L. 2000 Interleukin-7 mediates the homeostasis of naïve and memory CD8 T cells in vivo. Nature Immunology *1*: 426-432

Schluns, K.S., Williams, K., Ma, A., Zheng, X.X., and Lefrancois, L. (2002) Cutting Edge: Requirement for IL-15 in the generation of primary and memory antigen-specific CD8 T clels. The Journal of Immunology *168*: 4827-4831

Schmidt, D., and Muller, S. (2003) PIAS/SUMO: new partners in transcriptional regulation. Cellular and Molecular Life Sciences *60*: 2561–2574

Schwab, S.R., and Cyster, J.G. (2007) Finding a way out: lymphocyte egress from lymphoid organs. Nature Immunology *8*: 1295-1301

Scollay, R.G., Butcher, E.C., and Weissman, I.L. (1980) Thymus cell migration. Quantitative aspects of cellular traffic from the thymus to the periphery in mice. European Journal of Immunology *10*: 210-218

Seddon, B., Tomlinson, P., and Zamoyska, R. (2003) Interleukin 7 and T cell receptor signals regulate homeostasis of CD4 memory cells. Nature Immunology *4*: 680-686

Seddon, B., and Zamoyska, R. (2002) TCR signals mediated by Src family kinases are essential for the survival of naïve T cells. The Journal of Immunology *169*: 2997-3005

Seki, Y., Yang, J., Okamoto, M., Tanaka, S., Goitsuka, R., Farrar, M.A., and Kubo, M. (2007) IL-7/STAT5 cytokine signaling pathway is essential but insufficient for maintenance of naive CD4 T cell survival in peripheral lymphoid organs. Journal of Immunology *178*: 262-270

Sheridan, B.S., and Lefrancois, L. (2011) Regional and mucosal memory T cells. Nature Immunology *12*: 485-491

Shiow, L.R., Rosen, D.B., Brdickova, N., Xu, Y., An, J., Lanier, L.L., Cyster, J.G. and Matloubian, M. (2006) CD69 acts downstream of interferon-alpha/beta to inhibit S1P1 and lymphocyte egress from lymphoid organs. Nature *440*: 540-544

Shortman, K., and Wu, L. (1996) Early T lymphocyte progenitors. Annual Review of Immunology *14*: 29-47

Siegel, A.M., Heimall, J., Freeman, A.F., Hsu, A.P., Brittain, E., Brenchley, J.M., Douek, D.C., Fahle, G.H., Cohen, J.I., Holland, S.M., and Milner, J.D. (2011) A critical role for STAT3 transcription factor signaling in the development and maintenance of human T cell memory. Immunity *35*: 806-818

Sprent, J., and Surh, C.D. (2002) T cell memory. Annual Review of Immunology *20*: 551-579

Stefanova, I., Dorfman, J.R., and Germain, R.N. (2002) Self-recognition promotes the foreign antigen sensitivity of naïve T lymphocytes. Nature *420*: 429-434

Su, H., and Li, S. (2002) Molecular feature of human ubiquitin-like SUMO genes and their encoded proteins. Gene *296*: 65-73

Surh, C.D., and Sprent, J. (2000) Homeostatic T cell proliferation: How far can T cells be activated to self-ligands? The Journal of Experimental Medicine *192*: F9-F14

Surh, C.D. and Sprent, J. (2009) Homeostasis of naïve and memory T cells. Immunity *29*: 848-862

Suzuki, K., Nakajima, H., Saito, Y., Saito, T., Leonard, W.J., Iwamoto, I. (2000)

Janus kinase 3 (Jak3) is essential for common cytokine receptor gamma chain (gamma(c))-dependent signaling: comparative analysis of gamma(c) Jak3, and gamma(c) and Jak3 double-deficient mice. International Immunology *12*: 123–32.

Takada, K., and Jameson, S.C. (2009) Naïve T cell homeostasis: From awareness of space to a sense of place. Nature Reviews Immunology *9*: 823-832

Takahashi, Y., Toh-e, A., and Kikuchi, Y. (2001) A novel factor required for the SUMO1/Smt3 conjugation of yeast septins. Gene *275*: 223-231

Takeda, S., Rodewald, H.R., Arakawa, H., Bluethmann, H., and Shimizu, T. (1996) MHC class II molecules are not required for survival of newly generated CD4+ T cells, but affect their long-term life span. Immunity *5*: 217-228

Takeshita, T., Asao, H., Ohtani, K., Ishii, N., Kumaki, S., Tanaka, N., Munakata, H., Nakamura, M., and Sugamura, K. (1992). Cloning of the γ chain of the human IL-2 receptor. Science *257*:379-382

Tan, J.T., Dudi, E., LeRoy, E., Murray, R., Sprent, J., Weinberg, K. I. and Surh, C. D. (2001) IL-7 is critical for homeostatic proliferation and survival of naïve T cells. Proceedings of the National Academy of Sciences of the United States of Amierica *98*: 8732-8737

Tanchot, C., Lemonnier, F.A., Peranau, B., Freitas, A.A., and Rocha, B. (1997) Differential requirements for survival and proliferation of CD8 naïve or memory T cells. Science *276*: 2057-2062

Thornton, A.M., Korty, P.E., Tran, D.Q., Wohlfert, E.A., Murray, P.E., Belkaid, Y., and Sevach, E.M (2010) Expression of Helios, an Ikaros transcription factor family member, differentiates thymic-derived from peripherally induced Foxp3+ T regulatory cells. The Journal of Immunology *184*: 3433-3441

Townsend, A.R.M., Gotch, F.M., and Davey, J. (1985) Cytotoxic T cells recognize fragments of the influenza nucleoprotein. Cell *42*: 457-467

Townsend, A.R.M., Rothbard, J., Gotch, F.M., Bahadur, G., Wraith, D., and McMichael. A.J. (1986) The epitopes of influenza nucleoprotein recognized by cytotoxic T lymphocytes can be defined with short synthetic peptides. Cell *44*: 959-968

Van Nguyen, T., Angkasekwinai, P., Dou, H., Lin, F., Lu, L., Cheng, J., Chin, Y.E., Dong, C., and Yeh, E.T.H. (2012) SUMO-specific protease 1 is critical for early lymphoid development through regulation of STAT5 activation. Molecular Cell *45*:210--221

Vella, A., Teague, T.K., J.Kappler, J.I., and Marrack, P. (1997) Interleukin4 (IL-4) or IL-7 prevents the death of resting T cells: stat 6 is probably not required for the effect of IL-4. The Journal of Experimental Medicine *186*: 325–330.

Von Andrian, U.H., and Mempel, T.R. (2003) Homing and cellular traffic in lymph nodes. Nature Review of Immunology *3*: 867-878

von Freeden-Jeffry, U., Vieira, P., Lucian, L.A., McNeil, T., Burdach, S.E., and Murray, R. (1995). Lymphopenia in interleukin (IL)-7 genedeleted mice identifies IL-7 as a nonreductant cytokine. The Journal of Experimental Medicine *181*: 1519-1526

Wherry, E., and Ahmed, R. (2004) Memory CD8 T-cell differentiation during viral infection. Journal of Virology *78*: 5535-5545

Willians,M.A., Tyznik, A.J., and Bevan, M.J. (2006) Interleukin-2 signals during priming are required for secondary expansion of CD8 memory T cells. Nature *441*:890-893

Wu, L., Antica, M., Johnson, G.R., Scollay, R., and Shortman, K. (1991) Developmental potential of the earliest precursor cells from the adult mouse thymus. The Journal of Experimental Medicine *174*:1617-1627

Wu, Z., Jia, X., De la Cruz, L., Su, X.C., Marzolf, B., Troisch, P., Zak, D., Hamilton, A., Whittle, B., Yu, D., Sheahan, D., Bertram, E., Aderem, A., Otting, G., Goodnow, C.C., and Hoyne, G.F. (2008) Memory T cell RNA rearrangement programmed by heterogeneous nuclear ribonucleoprotein hnRNPLL. Immunity *29*:863-875

Xu, X., Araki, K., Li, S., Han, J.H., Ye, L., Tan, W.G., Konieczny, B.T., Bruinsma, M.W., Matinez, J., Pearce, E.L., Green, D.R., Jones, D.P., Virgin, H.W., Ahmed, R. (2014) Autophagy is essential for effector CD8(+) T cells survival and memory formation. Nature Immunology *15*: 1152-1161

Yamaguchi, T., Sharma, P., Athanasiou, M., Kumar, A., Yamada, S., and Kuehn, M.R. (2005) Mutation of SENP1/SuPr-2 reveals an essential role for desumoylation in mouse development. Molecular and Cellular Biology *25*: 5171-5182

Yajima, T., Yoshihara, K., Nakazato, K., Kumabe, S., Koyasu, S., Sad, S., Shen, H., Kuwano, H., and Yoshikai, Y. (2006) IL-15 regulates CD8+ T cell contraction during primary infection. The Journal of Immunology 176: 507-515

Yao, Z., Cui, Y., Watford, W.T., Bream, J.H., Yamaoka, K., Hissong, B.D., Li, D., Durum, S.K., Jiang, Q., Bhandoola, A., Hennighausen, L., and O'Shea, J.J. (2006) Stat5a/b are essential for normal lymphoid development and differentiation. Proceedings of the National Academy of Sciences of the United States of America *103*: 1000-1005

Zamoyska, R., Basson, A., Filby, A., Legname, G., Lovatt, M., and Seddon, B. (2003) The influence of the src-family kinases, Lck and Fyn, on T cell

differentiation, survival and activation. Immunological Review *191*:107-118

Zehn, D., Lee, S.Y., and Bevan, M.J. (2009) Complete but curtailed T-cell response to very low-affinity antigen. Nature *458*: 211-214

Zhang, Q., Davis, J.C., Lamborn, I.T., Freeman, A.F., Jing, H., Favreau, A.J., Matthews, H.F., Davis, J., Turner, M.L., Uzel, G., Holland, S.M., Su, H.C. (2009) Combined immunodeficiency associated with DOCK8 mutations. The New England Journal of Medicine *361*: 2046-2055

Zhang, Q., Dove, C.G., Hor, J.L., Murdock, H.M., Strauss-Albee, D.M., Garcia, J.A., Mandl, J.N., Grodick, R.A., Jing, H., Chandler-Brown, D.B., Lenardo, T.E., Crawford, G., Matthews, H.F., Freeman, A.F., Cornall, R.J., Germain, R.N., Mueller, S.N. and Su, H.C. (2014) DOCK8 regulates lymphocyte shape integrity for skin antiviral immunity. The Journal of experimental medicine *211*: 2549-2566

Zhang, X., Sun, S., Hwang, I., Tough, D. F., and Sprent, J. (1998) Potent and selective stimulation of memory-phenotype $CD8^+$ T cells in vivo by IL-15. Immunity 8: 591-599

Zuccolo, M., Alves, A., Galy, V., Bolhy, S., Formstecher, E., Racine, V., Sibarita, J., Fukagawa, T., Shiekhattar, R., Yen, T., and Doye, V. (2007) The human Nup107-160 nuclear pore subcomplex contributes to proper kinetochore functions. The EMBO journal *26*: 1853-1864

Zweidler-Mckay, P.A., Grimes, H.L., Flubacher, M.M., and Tsichlis, P.N. (1996) Gfi1 encodes a nuclear zinc finger protein that binds DNA and functions as a transcriptional repressor. Molecular and Cellular Biology *16*: 4024-4034